THE CENTRAL GREECE EARTHQUAKES OF FEBRUARY-MARCH 1981

A Reconnaissance and Engineering Report

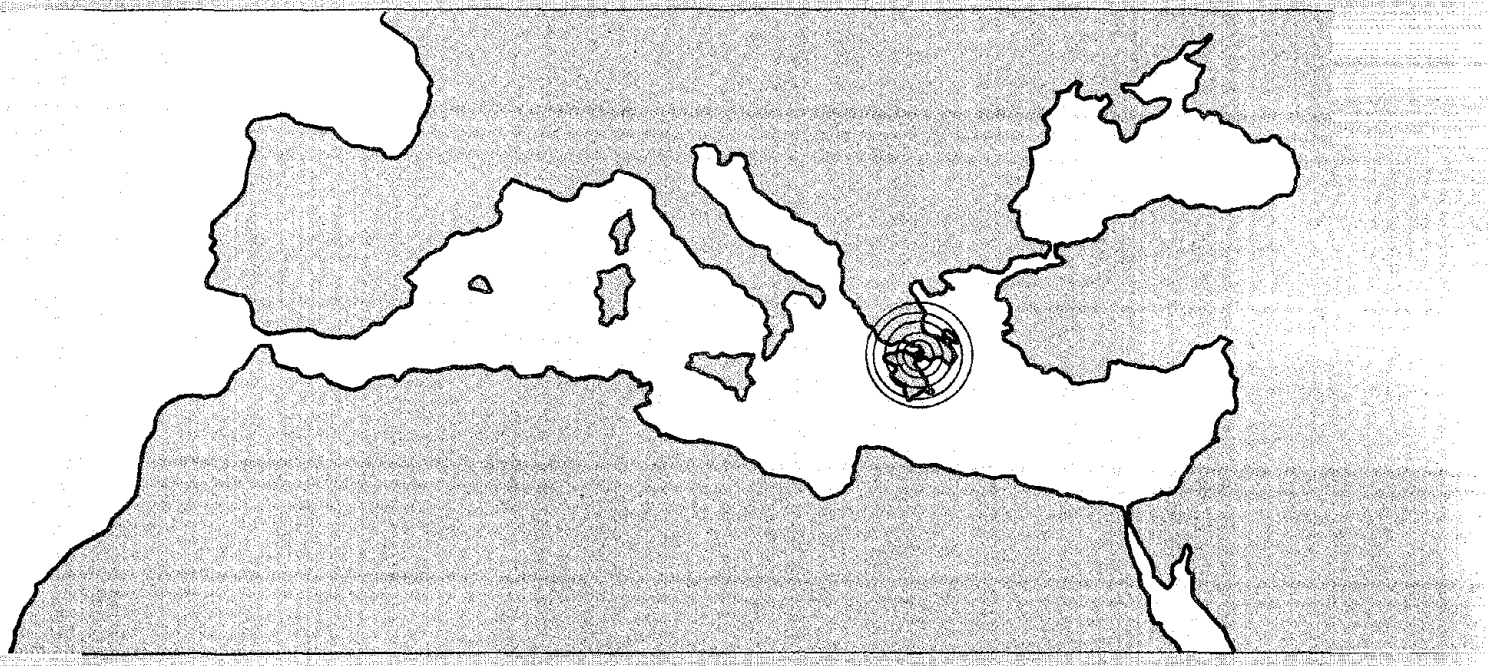

THE CENTRAL GREECE EARTHQUAKES OF FEBRUARY-MARCH 1981

A Reconnaissance and Engineering Report

by

Panayotis G. Carydis, Professor, Chair of Earthquake Engineering, National Technical University, Athens
Norman R. Tilford, Chief Geologist, Ebasco Services, Inc., Greensboro, North Carolina, and Visiting Associate Professor, Texas A&M University, College Station, Texas
Gregg E. Brandow, Structural Engineer, Brandow and Johnston Associates, Los Angeles, California
James O. Jirsa (Team Leader), Professor of Civil Engineering, University of Texas at Austin

Sponsored jointly by:

Committee on Natural Disasters
Commission on Engineering and Technical Systems
National Research Council

and

Earthquake Engineering Research Institute
Berkeley, California

NATIONAL ACADEMY PRESS
Washington, D.C. 1982

NOTICE: The Committee on Natural Disasters project, under which this report was prepared, was approved by the Governing Board of the National Research Council, whose members are drawn from the councils of the National Academy of Sciences, the National Academy of Engineering, and the Institute of Medicine. The members of the committee responsible for the report were chosen for their special competences and with regard for appropriate balance.

This report has been reviewed by a group other than the authors according to procedures approved by a Report Review Committee consisting of members of the National Academy of Sciences, the National Academy of Engineering, and the Institute of Medicine. It has also been reviewed for the Earthquake Engineering Research Institute (EERI) by a group under the procedures approved by the EERI Board of Directors.

The National Research Council was established by the National Academy of Sciences in 1916 to associate the broad community of science and technology with the Academy's purposes of furthering knowledge and of advising the federal government. The Council operates in accordance with general policies determined by the Academy under the authority of its congressional charter of 1863, which establishes the Academy as a private, nonprofit, self-governing membership corporation. The Council has become the principal operating agency of both the National Academy of Sciences and the National Academy of Engineering in the conduct of their services to the government, the public, and the scientific and engineering communities. It is administered jointly by both Academies and the Institute of Medicine. The National Academy of Engineering and the Institute of Medicine were established in 1964 and 1970, respectively, under the charter of the National Academy of Sciences.

The Committee on Natural Disasters of the National Research Council was formed to study the impact of natural disasters such as earthquakes, floods, tornadoes, and hurricanes on engineered structures and systems. Its objectives are to improve protection against disasters by providing factual reports of the consequences of these extreme events of nature and to stimulate the research needed to understand the hazards posed by natural disasters.

The Earthquake Engineering Research Institute was founded in 1949 as an outgrowth of the Advisory Committee on Engineering Seismology of the U.S. Coast and Geodetic Survey. It is a national multidisciplinary society of more than 1,000 engineers, architects, geoscientists, planners, and social scientists whose objective is to advance the science and practice of earthquake engineering and the solution of national earthquake engineering problems. The Institute not only investigates and reports on the effects of destructive earthquakes but sponsors conferences and publishes monographs on earthquake engineering and earthquake hazard reduction.

This study was supported by the National Science Foundation under Grant No. PFR-7810631 to the National Academy of Sciences and under Grant No. PFR-7902990 to the Earthquake Engineering Research Institute.

Any opinions, findings, and conclusions or recommendations expressed in this report are those of the authors and do not necessarily reflect the views of the National Science Foundation, the National Research Council, or the organizations of the authors.

National Technical Information Service
Attention: Document Sales
5285 Port Royal Road
Springfield, Virginia 22161

Report No.: CETS-CND-018
Price Codes: paper A08, mf A01

Committee on Natural Disasters
National Academy of Sciences
2101 Constitution Avenue, N.W.
Washington, D.C. 20418

or

Earthquake Engineering
Research Institute
2620 Telegraph Avenue
Berkeley, California 94704

COMMITTEE ON NATURAL DISASTERS (1981)

Chairman

JACK E. CERMAK, Fluid Dynamics and Diffusion Laboratory, Department of Civil Engineering, Colorado State University

Vice Chairman

ANIL K. CHOPRA, Department of Civil Engineering, University of California, Berkeley

Members

PAUL C. JENNINGS, Division of Engineering and Applied Sciences, California Institute of Technology
JAMES O. JIRSA, Department of Civil Engineering, University of Texas at Austin
JOHN F. KENNEDY, Institute of Hydraulic Research, University of Iowa
EDWIN KESSLER III, National Severe Storms Laboratory, National Oceanic and Atmospheric Administration, Norman, Oklahoma
RICHARD D. MARSHALL, Structural Engineering Group, Center for Building Technology, National Bureau of Standards
KISHOR C. MEHTA, Institute for Disaster Research, Texas Tech University
THOMAS SAARINEN, Department of Geography, University of Arizona
ROBERT V. WHITMAN, Department of Civil Engineering, Massachusetts Institute of Technology

Staff

O. ALLEN ISRAELSEN, Executive Secretary
STEVE OLSON, Consultant Editor
LALLY ANNE ANDERSON, Secretary
JOANN CURRY, Secretary

Liaison Representative

MICHAEL P. GAUS, Program Director, Design Research, Division of Civil and Environmental Engineering, National Science Foundation, Washington, D.C.

BOARD AND OFFICERS OF
EARTHQUAKE ENGINEERING RESEARCH INSTITUTE (1981)

Board of Directors

JOHN A. BLUME, URS/J.A. Blume and Associates, San Francisco
WILLIAM J. HALL, Department of Civil Engineering, University of Illinois
DONALD K. JEPHCOTT, Office of State Architect, Sacramento, California
PAUL C. JENNINGS, Division of Engineering and Applied Sciences, California Institute of Technology
ROY G. JOHNSTON, Brandow and Johnston Associates, Los Angeles
R. B. MATTHIESEN, Seismic Engineering Branch, U.S. Geological Survey, Menlo Park
BRUCE C. OLSEN, Consulting Engineer, Seattle
CHARLES THIEL, Woodward-Clyde Consultants, San Francisco

Executive Committee

President, Paul C. Jennings
Vice President, Roy G. Johnston
Secretary, Christopher Rojahn
Treasurer, R. Gordon Dean

Staff

Association Director, Susan B. Newman
Technical Director, Roger E. Scholl
Newsletter Editor, David J. Leeds

ACKNOWLEDGMENTS

The authors gratefully acknowledge the contributions of many engineers, scientists, and technicians who assisted the team in the field and with analysis of data for this study. Norman Tilford was assisted in preparing Chapter 2 by the Ebasco staff, by Professor John Drakopoulos, Chairman of the Seismological Laboratory, Athens University, and Director of the Seismological Institute, National Observatory of Athens, and by his staff both in the field and with the analysis of seismic data from the Greek National Seismic Network.

The considerable field work, data analysis, and report preparation by the following members of the Ebasco Services geotechnical staff are gratefully acknowledged and appreciated: Samir Khoury, Robert Cannon, Frederic Snider, Sarah Wilkinson, David Amick, and Myron Temchin.

Professor Panayotis Carydis was aided in preparing Chapters 3 and 6 and Appendix B by Demetrius Elias and John Taflambas, Dipl. Civ. Eng., Assistants at the Chair for Earthquake Engineering, National Technical University, Athens.

CONTENTS

OVERVIEW AND SUMMARY

At 10:57 p.m. (local time) on February 24, 1981, an earthquake with a Richter magnitude of 6.7 occurred in the region around the eastern Gulf of Corinth. Initial reports placed the epicenter of this event in the Gulf of Corinth about 70 km west of Athens and 20 km north-northeast of Corinth. A major aftershock with a Richter magnitude of 6.3 occurred at 4:36 a.m. on February 25. Additional aftershocks occurred of Richter magnitude 6.2 at 11:58 p.m. on March 4 and of Richter magnitude 5.9 on March 5. In the period following the March 4 aftershock, 15 to 20 aftershocks of Richter magnitude 5 to 5.7 were monitored. A map of Greece is shown in Figure 1.1. The epicenters of the three main events are shown in Figure 1.2.

The focal depth of the February 24 main event was about 10 km. The focal depth of the first aftershock five and a half hours later was also about 10 km. Evidence indicates that the fault plane initially ruptured by the main event ruptured through to the surface during the aftershock.

These earthquakes offered an unusual opportunity to examine ground deformation caused by tectonic activity. The Corinth region has historically been the location of strong earthquakes, notably in 227 B.C. and in A.D. 77, 551, 1858, and 1928 (see Appendix A). The 1981 surface ruptures occurred along existing faults and were exposed for 1 to 5 km. Vertical offsets of up to 0.7 m and lateral separations of up to 0.5 m were observed. An estimated subsidence of 1.2 m affected some areas along the coast.

DISTRIBUTION OF DAMAGE

The main event produced effects on the modified Mercalli scale of intensity VIII within an estimated area of 1,400 km^2. The most heavily damaged areas from the major earthquake and the first aftershock were concentrated around the southeastern coast of the Gulf of Corinth about 10 to 20 km from the epicenter of the major event. Corinth is the largest city in the immediate area, and damage there appeared to be primarily cracking of unreinforced tile and masonry infill walls in concrete frame buildings. To the north of Corinth a number of modern buildings in Loutraki collapsed or were heavily damaged, and to the west of Corinth a few engineered buildings in Vrahati and Kiato collapsed.

FIGURE 1.1 Epicentral area of central Greece.

Intensity IX effects observed in some villages probably resulted from the shallow magnitude 6.3 aftershock of February 25. Perahora, a small village in the hills north of Corinth, was heavily damaged; however, many of the dwellings were constructed of stone rubble with mud and straw mortar. Similarly, the relatively shallow event of March 4 caused intensity IX effects in some places.

Between Corinth and Athens the region along the coast contains a number of heavy manufacturing facilities--steel mills, refineries, and shipyards. There was little reported damage to these facilities. However, heavy damage to some residential and light commercial structures was observed in Megara and Isthmia.

In Athens, which experienced intensity VII effects, damage occurred primarily to nonstructural walls and facades in residential areas to the west and northwest of the city's center. A few buildings suffered structural damage, but no collapses were observed.

The large aftershock on March 4 produced heavy damage in an area to the north of the Gulf of Corinth, especially in the villages of Plataeae

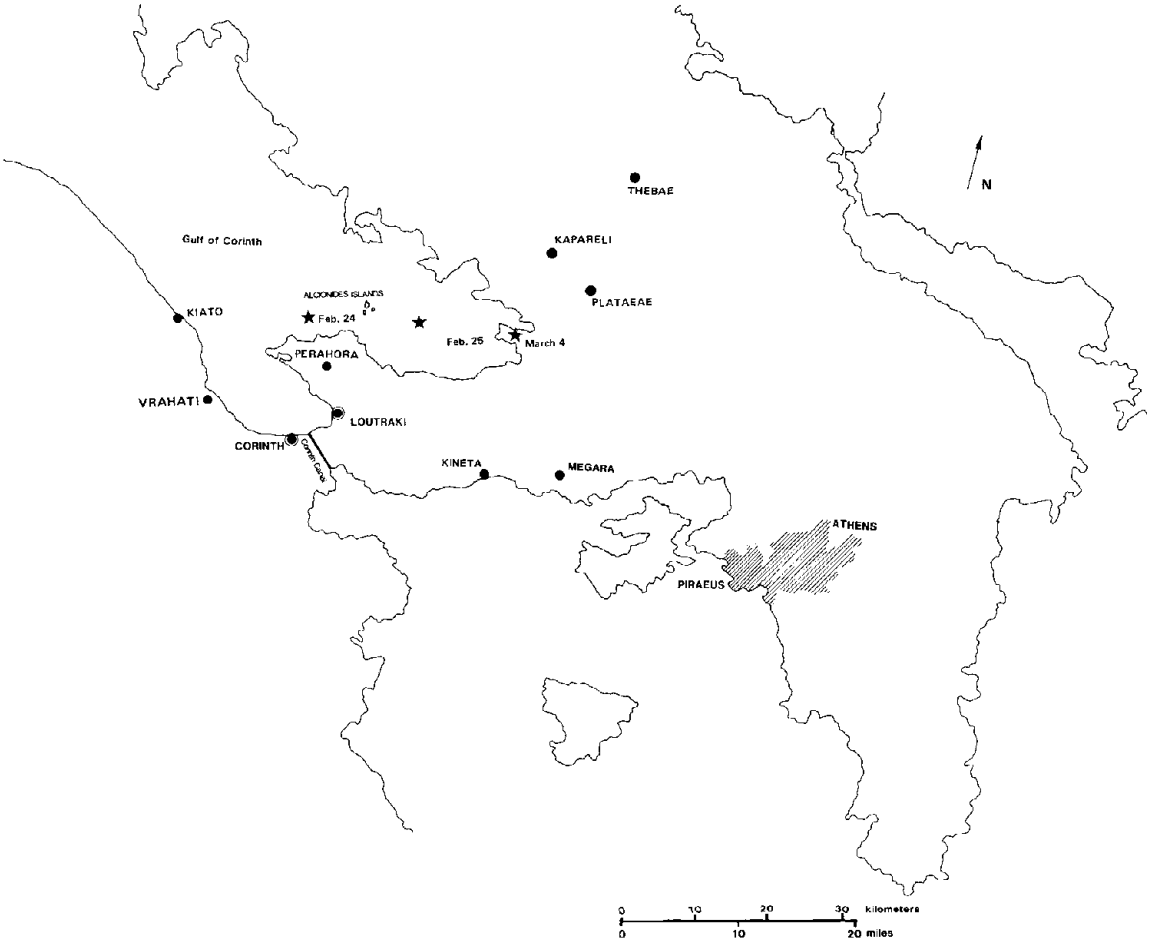

FIGURE 1.2 Epicenters of major shocks.

and Kapareli. Damage was reported to the north as far as Thebae, and additional damage was noted to the south in Megara.

LOSS OF LIFE

Very few lives were lost. Fewer than 20 deaths were caused directly by the earthquakes. This low loss of life can be attributed to the fact that a number of buildings heavily damaged by the main event just before midnight on the twenty-fourth were evacuated and were not occupied when collapse occurred during the first aftershock early the next morning. In addition, many of the tourist and vacation facilities along the coast were closed for the season and were not occupied.

While the loss of life was low, the anxiety in the population was high. The continued aftershocks, some of which were quite strong, caused widespread panic, especially in Athens. Apparently, the populace of Athens was not prepared for the possibility that earthquakes could

affect the city. The last earthquake to affect Athens seriously occurred in 1928, beyond the memory of most Athenians. After experiencing the earthquake, many people were afraid to return to their homes and jobs, even though damage was minimal and lifelines were not interrupted. As a result, open squares and lots in some regions of Athens were filled with tents and cars where people spent the nights to avoid returning to their homes.

STRONG MOTION RECORDS

Records obtained from an instrument (part of the Greek national seismic network) located in the telecommunications center in Corinth indicate a maximum horizontal acceleration of 0.28 g for the February 24 main event and 0.12 g for the February 25 aftershock. Vertical accelerations were less than 40 percent of the horizontal values.

The records from 1981 and those for an earthquake in 1975 of magnitude 5.0 in the same area show very similar characteristics, and there is a nearly constant ratio between maximum values of the horizontal traces. The isoseismals are also similarly shaped. It appears that weak shocks in this area may be extrapolated to describe shocks from stronger events.

CONSTRUCTION PRACTICES IN THE AREA

Masonry buildings have traditionally been common in Greece. Such structures range from those of native rubble stone with timber floors and roofs to structures of fired brick or concrete blocks. Most structures using reinforced concrete frames with masonry infill and partition walls have been constructed in the past 20 years.

Designs generally do not consider the influence of "nonstructural" walls, which can produce eccentricities between the structure's center of mass and its center of lateral resistance. Discontinuities in the walls often abruptly change the lateral resistance.

The quality of construction varies greatly. In nearly all privately owned structures, however, details such as the amount of transverse reinforcement at the ends of columns and anchorage of main reinforcement appeared to be inadequate.

Many frame structures consist of rigid upper stories (with masonry partitions) supported on weak, flexible first floors. Tradition and the law do not consider the first floor habitable space. Also, in many cases builders have added floors to structures without adding lateral resistance at the existing lower levels.

STRUCTURAL DAMAGE

Although many buildings were extensively damaged by the earthquakes, only a few totally collapsed. Where collapse did occur, it could often be attributed to problems with the structural concept. For example, the

Galaxy Hotel was a reinforced concrete frame structure that had three sections separated by expansion joints. Two of the three sections collapsed. The two collapsed sections had discontinuities both in the lateral shear resistance with height (lower floors were higher and had fewer interior partitions and walls) and in the plan (one section was skewed about 60 degrees from the rest of the structure). Further detailed study of this structure is warranted. In other cases, walls were not carefully arranged to ensure symmetry.

Brittle infill walls often changed the anticipated response of a structure. Instead of being ductile the frame was stiff, so that large horizontal forces were imposed on a weak, flexible first story. As might be expected, the performance of these structures during the earthquakes was poor.

Some evidence indicates that several large structures located very near the shore were damaged or collapsed as a result of the foundation conditions at the site. It was observed that in areas where stiff structures were founded on silt or mud, they performed better than did structures of other types.

Finally, attention to detailing was inadequate. In some structures, there was little transverse reinforcement for either shear or confinement. Splices and hooked bar anchorages were often located in critical regions of members and were not enclosed with transverse reinforcement. Also, vertical additions to structures were made without considering the existing lateral capacity or structural continuity.

CONCLUSIONS

From the perspective of the many earthquakes that have been examined in the literature, the Central Greece earthquakes revealed few new problems. The significant point is that the engineering and construction practices in the region have resulted in a large number of structures that can be expected to perform poorly in any future major earthquake. Once again, the importance of the roles of detailing, construction control, and nonstructural walls on response was demonstrated.

Existing codes appear to address the types of problems likely to affect structures in a seismic zone, but they may not be specific enough to prevent some of the detailing and conceptual problems seen after the recent earthquakes. Seismic codes must be continually revised to avoid such problems and engineers must be informed of those revisions. In addition, existing structures need to be systematically evaluated to determine their actual strength and response, as opposed to their anticipated behavior when designed. Where necessary, strengthening procedures will have to be undertaken.

The Central Greece earthquakes demonstrated that loss of life in an earthquake is a function of timing. In this case, the loss was low only because the earthquakes occurred "out of season" when the vacation resort areas were practically vacant. Some deaths were due to panic. To reduce the loss of life in any seismically active area, a preparedness and rescue program should be organized and maintained.

GEOLOGICAL AND SEISMOLOGICAL OBSERVATIONS

The earthquakes of February 24 and 25 generated a 12-km-long, east-west-trending, northward-dipping zone of surface rupture along preexisting faults and caused subsidence along a 9-km-long stretch of shoreline. The March 4 event, and the several magnitude 5.5 to 5.9 aftershocks that followed it in the next four days, generated a second zone of east-west-trending surface ruptures along different preexisting fault scarps. This second zone of faulting is located 15 km northeast of the initial rupture zone; at this second zone, ruptures dip steeply toward the south. The total average vertical surface displacement along the southern rupture zone is on the order of 1 m, while the average vertical displacement along the northern zone is slightly less. Epicenters and surface ruptures are shown in Figure 2.1. During the months following the February 24 and 25 and March 4 events, hundreds of aftershocks were recorded in the region.

To study the effects of these moderately large, shallow earthquakes on man-made structures, and to examine these cases of surface faulting, a comprehensive field program was initiated by Ebasco Services, Inc., on February 25, just hours after the two largest shocks. The field program included detailed mapping of each surface rupture, seismic intensity studies, and the installation and monitoring of a microseismic network, strain gauges, tiltmeters, and a tide gauge.

TECTONIC SETTING

The Gulf of Corinth occupies a zone of crustal extension and rifting that has been seismically active throughout historical times. The city of Corinth has repeatedly been severely damaged, most recently in 1928. The most significant earthquakes to take place in the gulf region in the last 2,500 years occurred in 227 B.C. and in A.D. 77, 521, 1858, and 1928. The seismic history of central Greece is shown in Appendix A. Each of these earthquakes produced effects of at least IX on the modified Mercalli scale in the epicentral region.

The western segment of the gulf connects to the Ionian trench system along a zone of northeast-trending transform faults, while its eastern segment may be a cross fault of the Aegean volcanic arc. Evidence

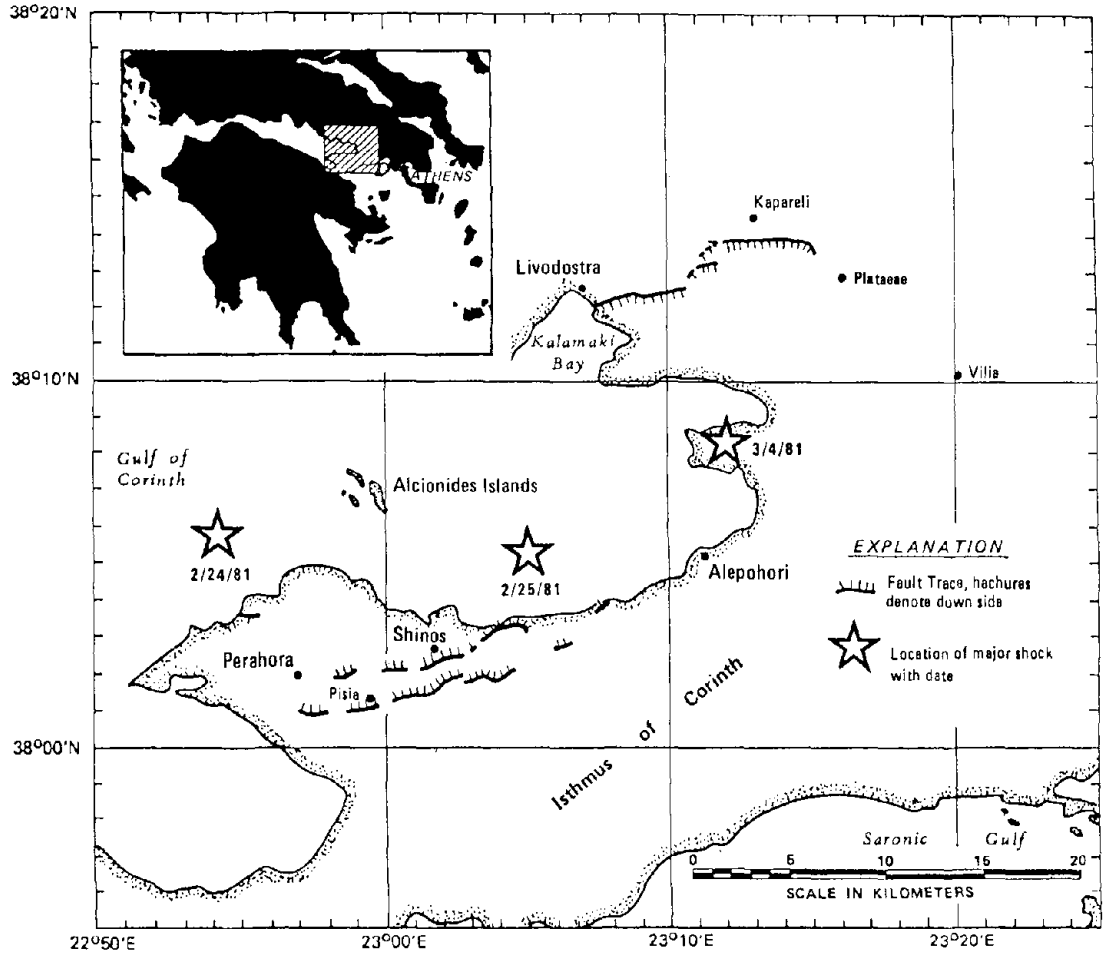

FIGURE 2.1 Location of surface ruptures.

suggests that the area south of the gulf is undergoing uplift at a geologically rapid rate. Over 500 m of uplift has occurred in the last few hundred thousand years. On the other hand, the northern gulf coast has remained relatively stable during the same period. Uplift most probably has taken place due to thermal processes at work in the plastic lower crust and upper mantle. Asymmetric rifting of the cooler, more rigid surface rocks has created the graben or trough known as the Gulf of Corinth.

STRATIGRAPHIC SETTING

The stratigraphy of the area is dominated by the intercalation of huge bodies of massive recrystallized limestone into a pervasive hydrothermally altered suite of extrusive igneous rocks, locally identified as ophiolites. While these altered or metamorphosed rocks

may or may not be classical ophiolites, they certainly were deposited in the sea and contemporaneously altered. The source of much, if not all, of the calcium in the associated limestones may have been the igneous rocks themselves, and the field team believes that the limestone units, with thicknesses ranging from tens to the low hundreds of meters and plan view dimensions of as much as several kilometers, were deposited as discrete accreting bodies alongside and with the igneous rocks. The limestones are presently massive and hard, forming high, abrupt topography where they crop out, while the metamorphics are generally "crushed in place" and can be scratched out of exposures using finger or hand-tool pressures. In locations where they are not being rapidly uplifted, the metamorphics form subdued topography. These widespread rock masses dominate the local topography but are overlain in much of the region by Neogene sedimentary rocks. The Neogene sedimentary rocks surely do not influence seismicity and therefore are not discussed further here.

TIME AND LOCATION OF LARGE SHOCKS

Arrival times and first motion data were obtained from the seismograms of the Greek national seismic network. Hypocenters were then computed by applying the joint epicenter determination relocation technique. The calibration event used in this procedure was the magnitude 5.1 aftershock of 01:49 (GMT) on March 12, 1981, as located by a six-station portable network deployed during this study. In addition, S-accelerograph trigger times obtained from the Corinth and Xylokastro strong motion records were used as additional constraints. Figure 2.1 shows the relocated epicenters for the three main events.

The epicenter of the magnitude 6.7 main shock was located at 38°05.75'N, 22°53.20'E, with a focal depth of 10.5 km. A focal plane solution obtained from short-period data (Figure 2.2) indicates normal faulting. Nodal planes strike N69°E (dipping 45°NW) and N88°W (dipping 46°SE). Based on the field observations of surface rupture, the first plane is the preferred fault plane. The epicenter of the magnitude 6.3 aftershock that occurred at 4:36 a.m. on February 25 was located at 38°03.15'N, 23°04.55'E, with a focal depth of 10.0 km. These two events were located on the downdip extension of the southern surface ruptures.

The epicenter of the magnitude 6.2 event on March 4, 1981, was located approximately 20 km to the northeast of the southern surface ruptures, at 38°07.75'N, 23°11.70'E. The focal depth was 7.0 km.

SEISMIC INTENSITY SURVEY

A survey of earthquake damage in the mesoseismic region was begun on the morning of February 25, only hours after the two large events of the previous night. The purpose of this survey was to gather data for the preparation of isoseismal intensity maps to determine attenuation relations for the region. At each of the towns and villages visited,

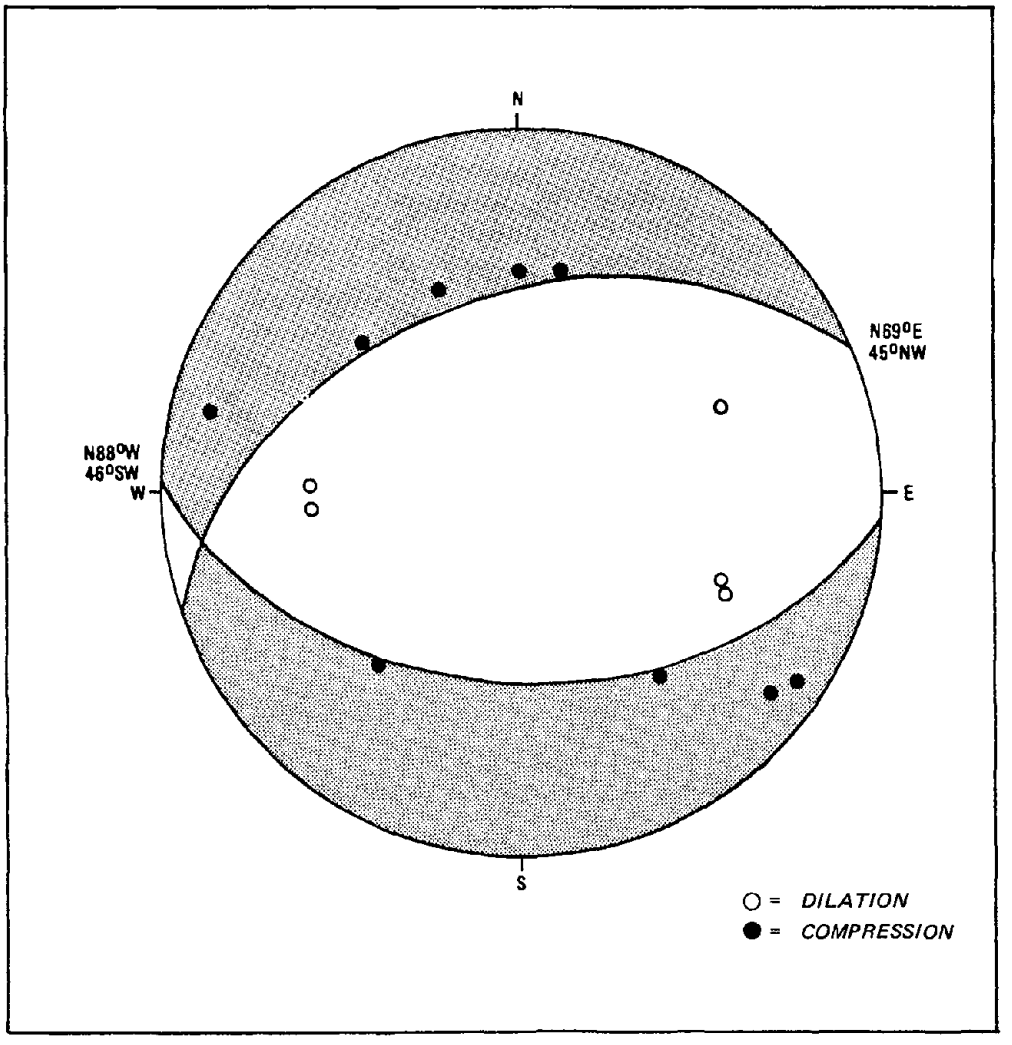

FIGURE 2.2 Focal plane solution for the magnitude 6.7 main shock of February 24, 1981. Lower hemisphere projection. (See Figure 2.1 for location.)

visual inspections of earthquake damage were made and local residents were interviewed to determine which of the two large events caused the observed damage. However, the singular effects of the February 24 main shock and its magnitude 6.3 aftershock were difficult to distinguish even by local residents because both events had occurred at night and were only five and one half hours apart (Figure 2.3). By the time of the magnitude 6.2 event on March 4 (Figure 2.4), field studies had progressed far enough that damage caused by this event could be distinguished from that caused by the February events. During visual inspections of earthquake damage, particular attention was paid to the types and quality of construction, the conditions of foundations at the site, and depths to the water table, since these are major factors

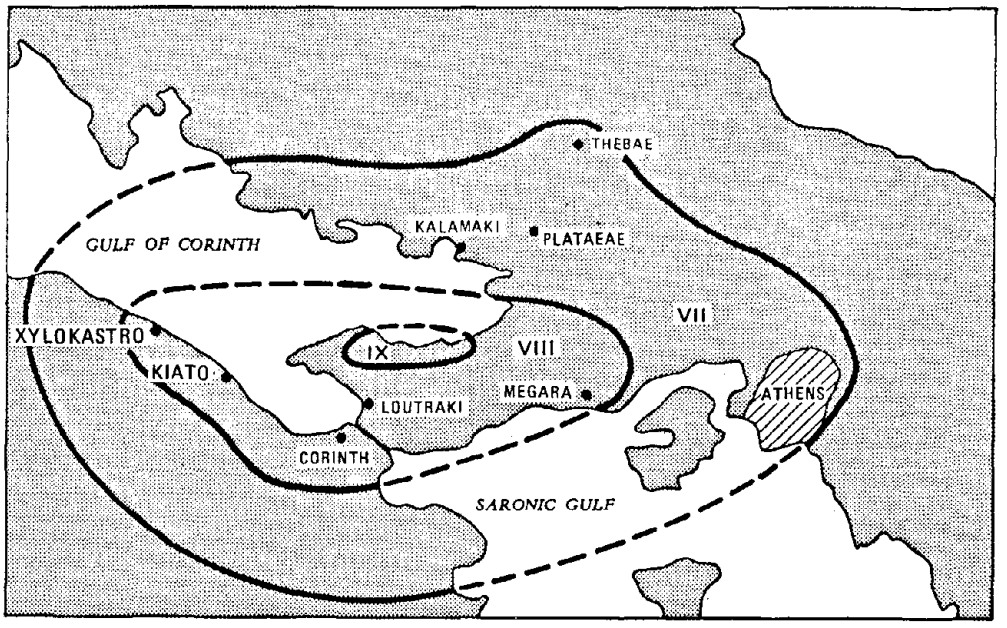

FIGURE 2.3 Isoseismal map for February 24 and 25 events.

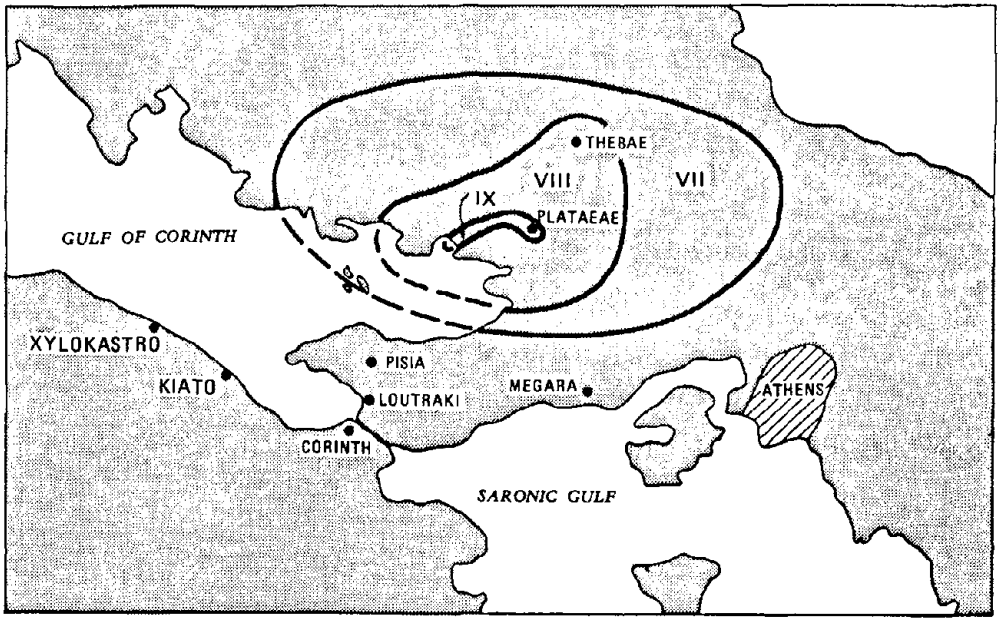

FIGURE 2.4 Isoseismal map for March 4 event.

controlling the degree of damage and must be considered in any analysis of intensity data to obtain a meaningful attenuation relationship.

Based on the information obtained from the survey, intensity values for each of the three largest earthquakes were assigned to each survey site using the Modified Mercalli scale proposed by Tocher (1956). The main shock of the sequence occurred at a depth of about 10 km just west

of the Alcionides Islands in the eastern Gulf of Corinth. This event was felt over an area of approximately 250,000 km^2 and was responsible for generating intensity VIII effects within an area of 1,400 km^2. The city of Corinth, as well as the gulf coast east and west of it, were included within this intensity VIII area. Parts of Athens and Thebae were subjected to intensity VII ground motion. The intensity VII and VIII isoseismals are elongated in an east-west direction by a factor of two. This elongation is parallel to the strike of the causative fault as determined from the focal plane solution of the main shock and from mapping of surface ruptures.

The distribution of observed damage and interviews with local residents suggest that many of the intensity IX effects shown in Figure 2.3 were associated with the magnitude 6.3 aftershock that occurred during the early hours of February 25. This event occurred downdip of the projected strike of the southernmost trace near its eastern end (Figure 2.1). The temporal characteristics of the damages to the towns of Perahora and Pisia suggest, but do not prove, that it was the aftershock that actually ruptured the fault plane through to the ground surface.

The March 4 event generated a maximum epicentral intensity of IX, but its effects were felt over a much smaller area than were those of the February events due to its slightly lower magnitude and shallower focal depth. The orientation of the isoseismals is again roughly parallel to the strike of the causative fault as determined from field mapping of the surface rupture.

GROUND DEFORMATION

The earthquakes of February-March 1981 are significant from a geological standpoint because they offer investigators the opportunity to examine ground deformation caused by tectonic activity. Both surface rupture and tectonic subsidence were observed following these earthquakes.

Nature and Extent of Surface Faulting

Surface ruptures occurred along existing but in some cases unrecognized late-Quaternary faults. Two distinct zones of faulting were found (Figure 2.1): the first associated with the shocks of February 24 and 25, the second with the event of March 4. These zones of surface faulting are not continuous faults at the surface. Each is made up of segments several kilometers in length. Very minor components of both left and right lateral motion were observed. These right and left lateral motions were observed near the ends of individual rupture segments and probably are spurious, representing pull-down separation required geometrically near the end of each normal separation. However, the overall geometry of the east-west-trending rifting systems, which exhibits offset in its initial and secondary stress relief fractures, strongly implies the necessity for lateral components of offset during some of the faulting episodes. Certain field evidence discussed elsewhere supports this interpretation.

The southern surface rupture zone was found during a helicopter overflight on February 27 initiated to search for surface ruptures. It consists of two parallel surface rupture traces (Figure 2.1). Along these traces the surface ruptures are found in soil (Figure 2.5) at or near the base of steep north-facing limestone cliffs (Figure 2.6). Each of the two major traces is segmented, since surface rupture, with a single exception, did not take place in the closely fractured metamorphosed igneous rocks that form the basement throughout the area and intermittently crop out adjacent to and surrounding the massive, largely contemporaneous limestone lenses.

The southernmost surface rupture, hereafter referred to as the Pisia trace, begins 1.5 km west of Perahora and at this location strikes northwest-southeast. South of Perahora the rupture follows the edge of an olive grove, where vertical displacements on the order of 15 cm, with the lower side on the north, were measured. Near Pisia the surface rupture occurs as a vertical offset of up to 50 cm (Figure 2.6) and is located a few meters downslope of a 3-km-long limestone fault plane that dips 45° to the north (Figure 2.7). Along the base of this slope, a lowering of the soil has left a line on the limestone face about 50 cm above the present ground surface. Above the present soil line, a band of soil and leached white limestone proves that at least one additional episode of recent displacement has taken place along this same plane.

At the end of the limestone fault plane slope, the surface rupture trace rises dramatically in elevation and follows very near to the top of the metamorphic ridge line at 800 m elevation. The surface rupture was observed here as fractures in the thin soil cover of the metamorphic rock, with vertical displacements as great as 80 cm (north side down). The surface rupture trace was easily followed by helicopter and on foot until it apparently ended along a very thin ridge of metamorphic rock bounded on both sides by extremely steep faces of closely fractured, metamorphosed igneous rock. Because the surface rupture took place in the metamorphics in this location, to the exclusion of every other possible location in the metamorphic rocks, and because the displacement was commonly large, the field team concluded that this reach of fault exposure was very near to the strongest shaking and greatest rupture at depth. Conversely, the marked lack of evidence of surface and vegetative disturbance or destruction in the metamorphic terrain at this location or elsewhere along the strike of the surface rupture is compelling evidence of the strong damping effect of these closely fractured or "crushed in place" rocks.

The northernmost of the two southern rupture traces, hereafter referred to as the Shinos trace, begins 4 km east of the town of Perahora but cannot be traced along the road from Perahora to Shinos because most of the area was severely affected by rock falls, landslides, and disturbed and destroyed trees and brush. The road was destroyed by slope failure and boulder impacts. However, the surface trace was mapped east of this area along the base of the steep mountain faces 500 m south of Shinos. There it consists of vertical offsets in the soil, lower to the north, with a maximum observed offset of 50 cm. To the east the surface rupture changes strike and curves northward toward the sea. At the coast the trace again turns to the east and

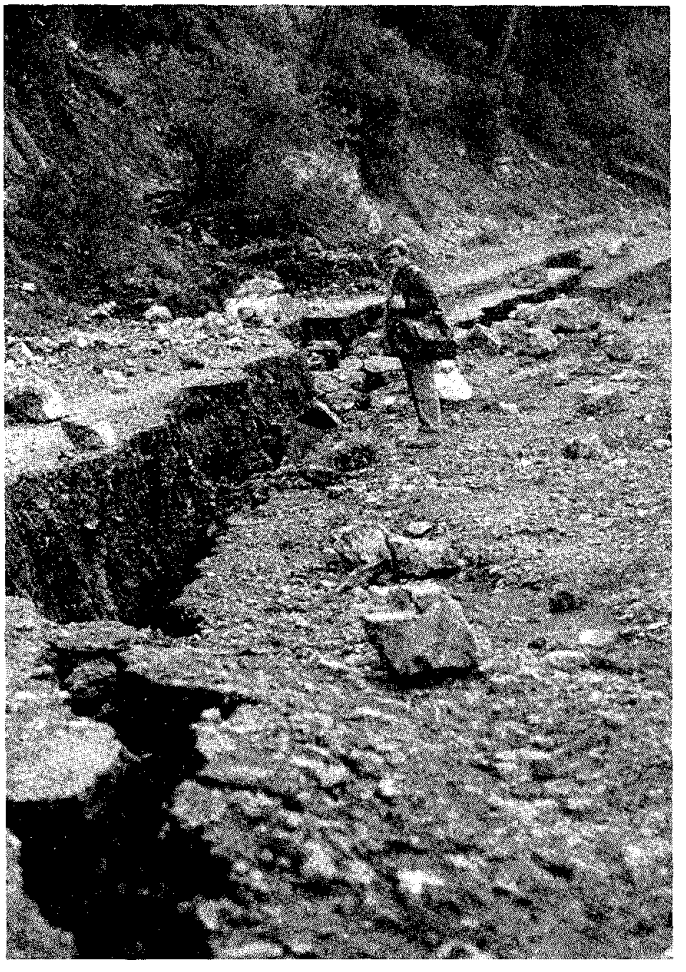

FIGURE 2.5 Ground rupture along the Shinos trace.

follows along the coastal road. In places, large landslides and rockfalls have destroyed the road. Near the foot of an alluvial fan to the east, the surface rupture veers southward and climbs the fan as a series of right-stepping en echelon fractures, each approximately 100 to 300 m long. Maximum vertical displacements of 50 to 60 cm occur at the center of each crack, with the north side down. Toward the end of each fracture, the displacement decreases to zero and other fractures begin upslope to continue the displacement. The total width of the rupture zone is about 70 m. The surface rupture cracks follow old scarps on this alluvial fan, proving that previous surface ruptures have followed the same trace. At the eastern edge of the alluvial fan, the surface rupture ends with a series of small dendritic cracks or fissures. The observed rupture does not cross or go around the ridges of metamorphic rock to the east. The total mapped length of the Shinos trace is 9 km.

The dip of slickensided limestone fault faces along the Shinos trace is steeper (60^{o} to 70^{o}) than the dip (45^{o}) on fault plane outcrops along the Pisia trace. This observation, coupled with the fact that the

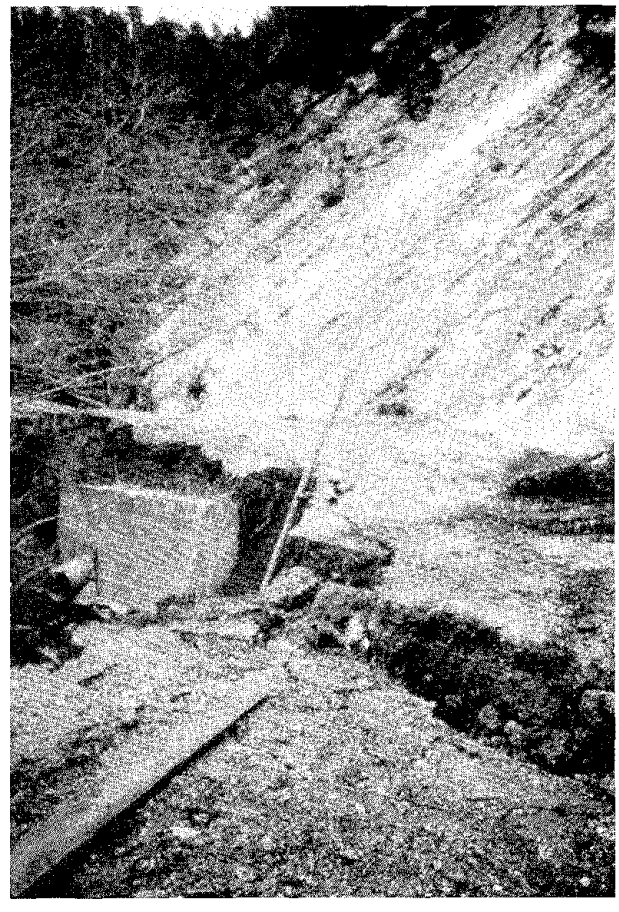

FIGURE 2.6 Ground rupture in alluvium near the base of a limestone fault surface on the Pisia trace.

preferred focal plane solution of the mainshock dips 46°, suggests that the Pisia rupture trace is the main fault and that the Shinos rupture trace is probably the result of splaying of the fault plane.

The northern fault zone, which is associated with the large aftershock of March 4, also consists of two parallel ground ruptures. The southernmost of the two will be referred to as the Kalamaki trace and the other will be referred to as the Kapareli trace (see Figure 2.1).

The Kalamaki fault trace is exposed for a length of approximately 4.5 km. It consists of a series of discontinuous segments with an east-west strike overall and dips 60° to 70° to the south. The fault trace generally is exposed in soil and alluvial material (Figure 2.8). However, in several places the rupture breaks through moderately weathered limestone conglomerate. Maximum vertical offsets ranging up to 70 cm, with the south down, were observed. Although topography often coincides with the rupture trace, in some locations the ground rupture did not follow a definite topographic trend. In fact, at several locations the down-thrown block was upslope of the actual surface rupture. The lateral separation between the hanging wall and the foot wall varies from a few centimeters to over 0.5 m.

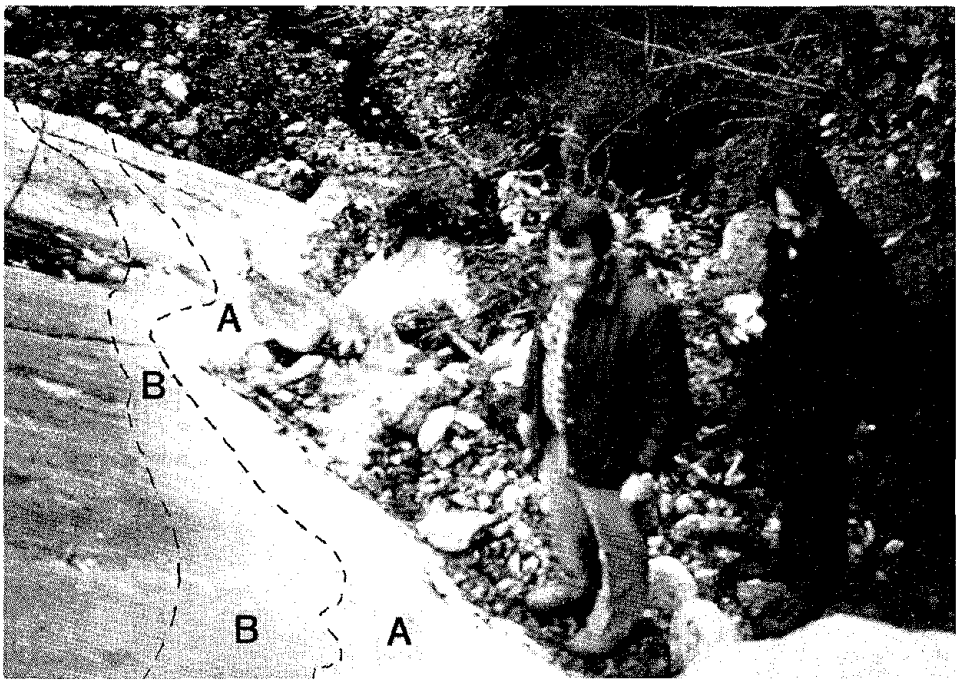

FIGURE 2.7 Dip-slip movement along the base of a limestone fault surface, Pisia trace, prior to the earthquakes of February 24 and 25. The formerly soil-covered part of the rock face is labeled "A." Weathering characteristics in area "B" indicate that at some time in the past the soil covered this area as well. This locality, then, records two recent episodes of surface rupture and dip-slip movement.

At the western extent of the Kalamaki trace, at the Bay of Kalamaki, the vertical offset in the beach gravel was measured to be 25 cm extending into the sea, but this was smoothed by wave action within days of the March 4 event. Extending from the sea inland, the fault rupture follows a canyon for approximately 2 km, sometimes in alluvium along the valley floor and at other times partially up either the north or south slopes (Figure 2.9). Approximately 2.5 km from the coast, the trace cuts across a small plateau and through the north side of a broad saddle. At the eastern end of this trace, the segments become discontinuous and the magnitude of the vertical offset decreases to just a few centimeters until only slightly open fissures could be traced. The overall strike of the Kalamaki trace is east-west; however, the fissures at the eastern end exhibit a northeast trend.

In the area connecting the two fault traces in the northern zone are left-stepping, northeast-trending fissures broken by a short segment of ground rupture. This small segment, about 0.3 km long, strikes east-northeast, has a vertical displacement of 20 cm, and reoccupies a preexisting fault scarp.

The left-stepping zone of open fissures connects to the 6.0-km-long Kapareli trace, so-named because the village of Kapareli is located near the center of the surface rupture. For most of its length, this trace

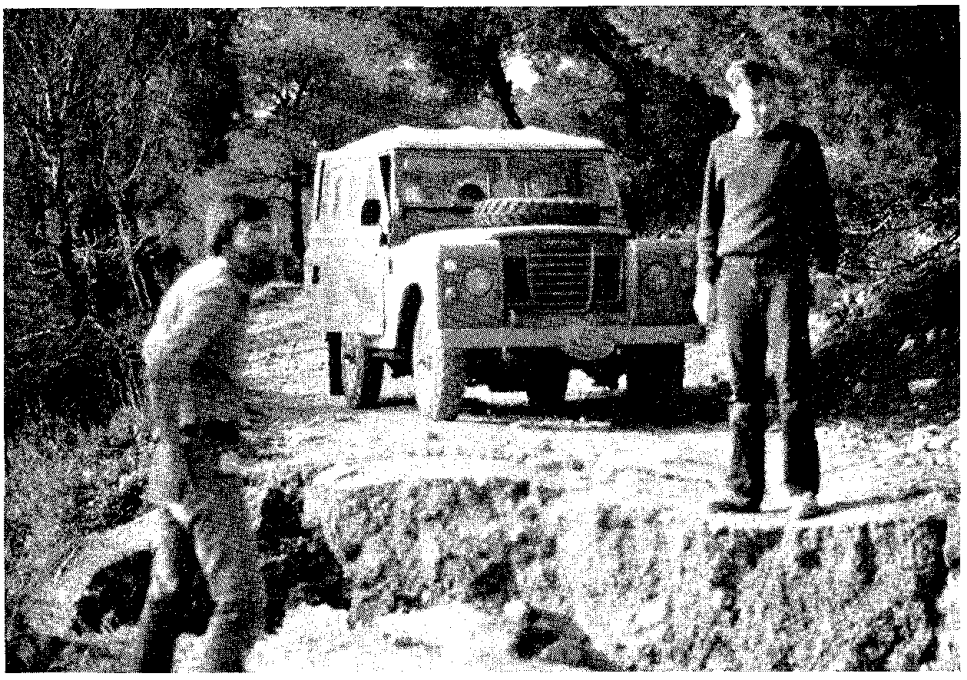

FIGURE 2.8 Vertical offset of road in the central part of the Kalamaki rupture trace.

spectacularly follows the northern side of a wide valley, trending east-west. The surface rupture usually occurs in the soil material either on the side of the hill or just along the base (Figure 2.10). On several steep hills, series of parallel fractures were observed, suggesting that gravity slumping also occurred. The fault plane is nearly vertical, although separation between the hanging wall and the foot wall is common. In some locations a smooth limestone cliff, 1 to 3 m high, marks the fault trace. Offsets vary from 10 cm to 1 m.

At its eastern end the Kapareli rupture trace veers away from this limestone cliff and splays to the southeast across an alluvium-filled valley toward the village of Plataeae. Subtle older scarps in the alluvium and truncations of small hills within the valley indicate that the present faulting reoccupies an older rupture trace. Before reaching Plataeae the vertical offset diminishes to zero, and at the western end of the fault trace the ground rupture becomes a series of parallel fissure segments, approximately 20 to 100 m long.

The nature of the surface expression of the northern ruptures differs strikingly from that of the southern ruptures. The southern fault zone exhibits pure dip-slip motion, with striking dip-slip deformations on the fault surface. The northern surface ruptures characteristically exhibit a rotation of the hanging wall in a direction perpendicular to and away from the foot wall (as shown in Figure 2.11) and lack dip-slip compressive fault surface fractures. This rotation has resulted in the opening of a wedge-shaped fissure along these rupture traces except where slumping along either side of the fault has

FIGURE 2.9 Eastern end of the Kalamaki trace at the location where ground motion was observed during a magnitude 5.7 earthquake on March 7, 1981. The main rupture trace is on left side of the photograph. The smaller rupture on the right is a secondary, near-surface cantilever failure in the soil, which appeared several days after the original surface break. This pattern is analogous to the relation between the southern and northern earthquakes and surface ruptures.

closed it (Figures 2.12 and 2.13). Commonly these wedge-shaped fissures are open to a depth of 7 m or more. Because normal faulting is commonly accompanied by tilting of the blocks on one or both sides of the main fault, the rotational character of the northern surface ruptures may indicate a south-to-southeast tilting of the fault block bounded by the recent surface ruptures. This observation is consistent with a hypothesis that the northern earthquakes, surface rupture, and thousands of aftershocks in the mass of rock between the southern and northern ruptures resulted from failure of a huge cantilevered mass of rock that lost support during extension produced by the earlier southern events.

Strong ground motion in the immediate vicinity of the southern ground ruptures caused disruption of soil, destruction of trees, and massive earth failures on unstable slopes. Damage to vegetation resulted from ground vibrations, liquefaction of soil materials, and falling rocks. Damage from ground vibration was primarily restricted to areas less than 0.5 km wide along sections of the trace or projected trace of the ground ruptures. Landslides and rockfalls were triggered by the earthquake and blocked coastal roads, particularly along the steep limestone cliffs parallel to the Shinos fault trace. Here,

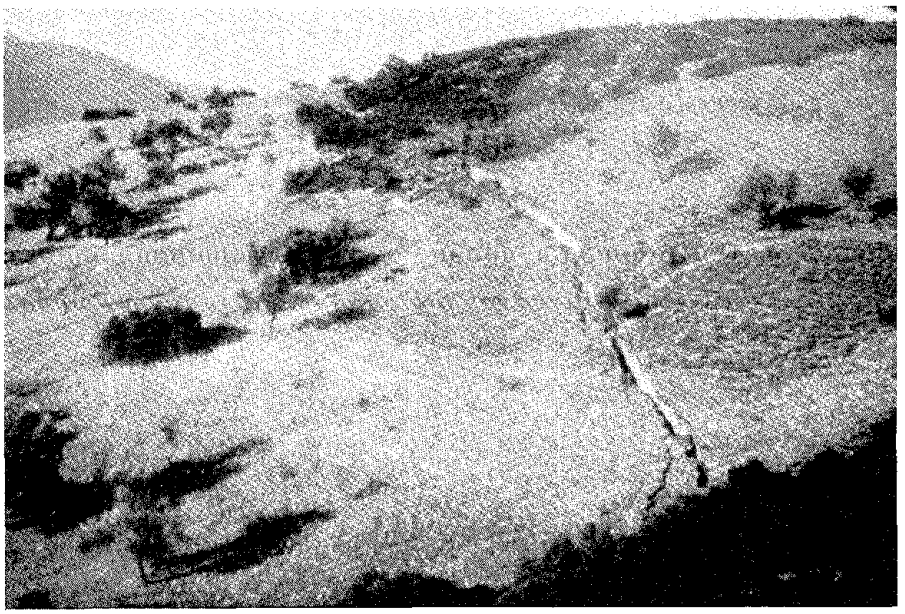

FIGURE 2.10 Ground rupture along the western end of the Kapareli trace, looking west. The average displacement is about 1 m.

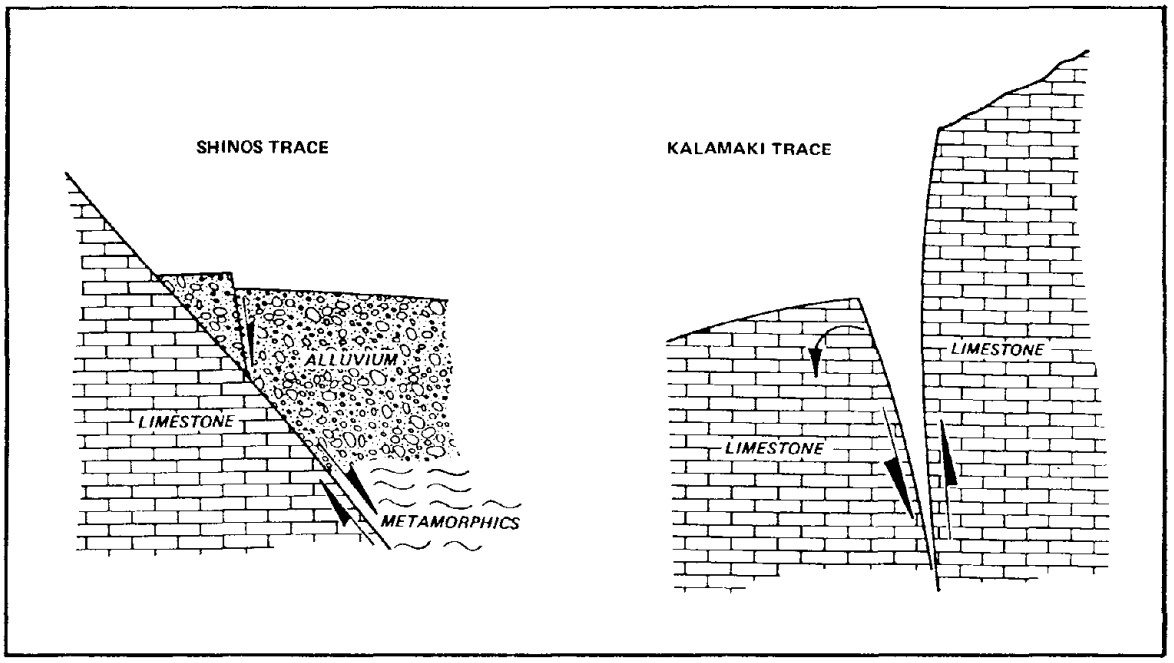

FIGURE 2.11 Close-up schematic cross section illustrating differences in the style of offset between the Shinos/Pisia and Kalamaki/Kapareli traces.

FIGURE 2.12 Typical ground rupture along the Kalamaki and Kapareli traces. At this location there were 60 cm of dip-slip displacement and 50 cm of rotational "opening" displacement.

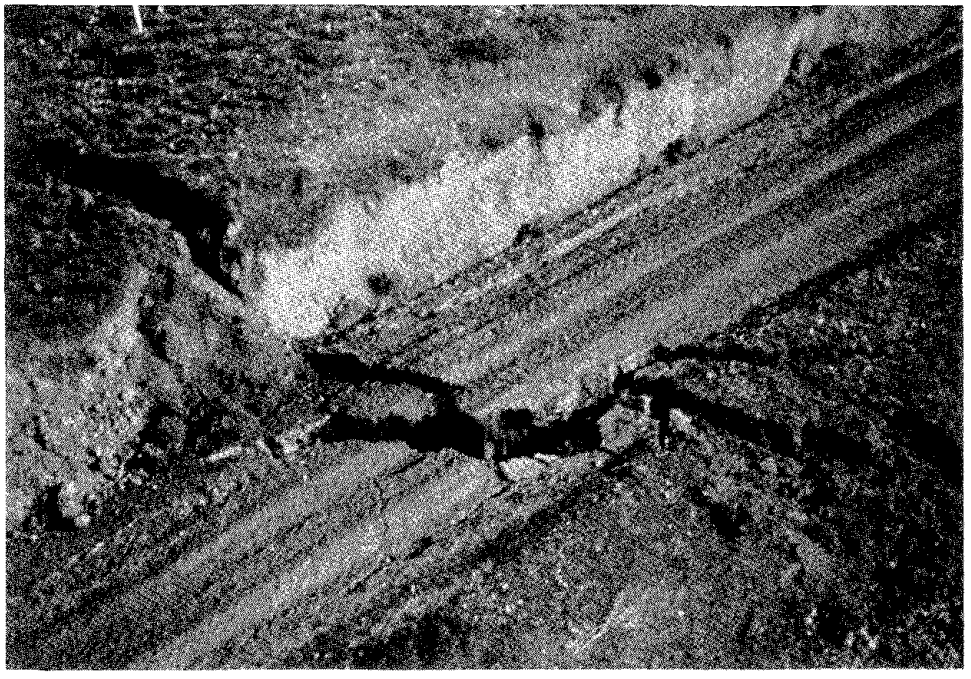

FIGURE 2.13 Part of the Kapareli surface rupture, showing combination of dip-slip and rotational "opening" displacement. In this case the opening displacement exceeded the dip-slip component.

boulders as large as 40 to 50 m^3 rolled downslope, leaving a path of destruction in their wake. The boulders hit trees, walls, and buildings, leaving craters where they struck the ground (Figure 2.14).

Along the northern rupture zones many observations were made of "flipped" stones located within a few hundred meters of the surface rupture but not accompanied by any other surface or vegetative damage (Figure 2.15). In many cases this was observed where there is little or no slope, suggesting that in the very near field the vertical acceleration exceeded 1.0 g but produced no significant ground disturbance.

SUBSIDENCE

Observations and measurement of past and present shoreline levels and reports by local residents indicate that the coast immediately to the north of the Shinos trace has subsided by as much as 1.20 m (Figure 2.16). A few kilometers west, measurements of algal lines on a submerged concrete dock, corrected for tidal fluctuations, indicate subsidence of approximately 1.0 m (Figure 2.17). Other indications of subsidence were observed along the shoreline eastward as far as the eastern extent of the Shinos trace.

Investigations in the coastal areas around the northern traces revealed no discernible subsidence. South of the main traces, however, a substantial number of small offsets, facing both south and north, were located, indicating that the dip-slip motion observed along the main rupture traces was disseminated throughout the mass of rock to the south.

STRAIN GAUGE AND TILTMETER MEASUREMENTS

Strain gauges were installed along the rupture traces immediately after the earthquake events. One strain gauge was installed on the Shinos ground rupture trace on February 28 at a location 3 km east of the town of Shinos. During the months of March and April, no additional movement was observed at this monitoring site.

Strain gauges were installed on March 6 along the Kapareli and Kalamaki traces. These gauges all showed some additional displacement during the 30 days following installation. Most of the movement along the fault traces measured by strain gauges occurred between March 6 and 9, and was probably associated with the magnitude 5.7 event that occurred on March 7. It appears that this event caused an additional displacement of approximately 1 cm along the Kalamaki trace and western end of the Kapareli trace. Small ground movements were also recorded at two of the stations on the western portion of the surface rupture between March 11 and 18, although no movements were noted on the eastern end of the rupture trace during this period.

In mid-March 13 tiltmeter plates were installed along the hanging wall and foot wall blocks of each surface rupture at locations shown in Figure 2.18. Tilt (in this case defined as the rotation down from the horizontal plane) was measured using a Sinco tiltmeter (Model 50322) with a Digitilt indicator (Model 50306) having a sensitivity of 1 part

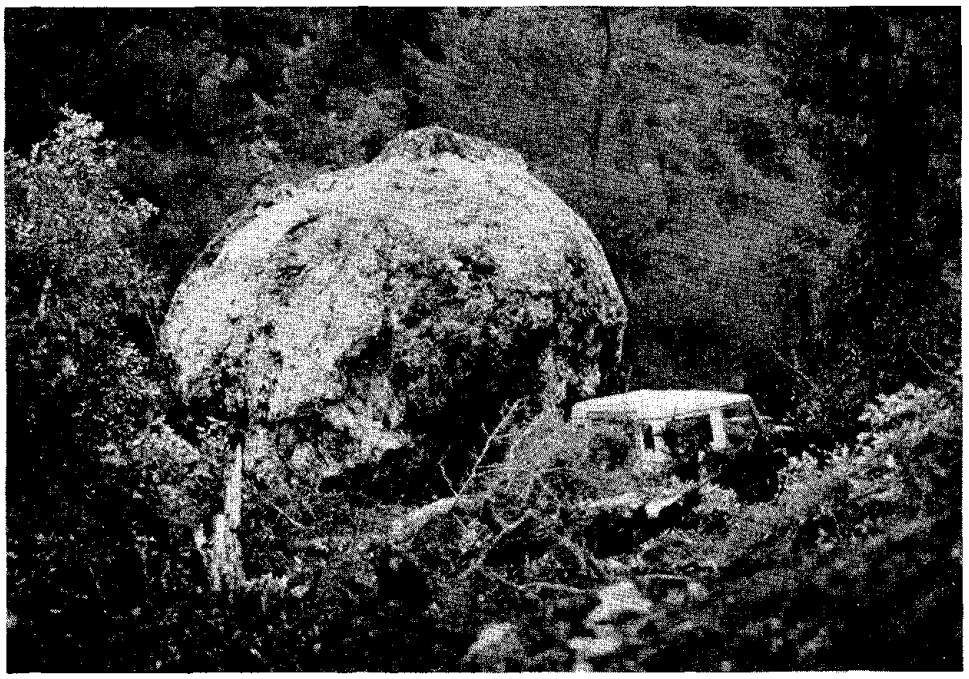

FIGURE 2.14 Large boulder heaved from the side of the mountain south of Shinos. This photograph was taken standing uphill within the swath cut by the rolling, bouncing rock.

FIGURE 2.15 Typical "flipped" rock around the Kapareli and Kalamaki rupture traces. This phenomenon indicates near-field vertical acceleration of over 1.0 g during the March 4 earthquake (magnitude 6.2).

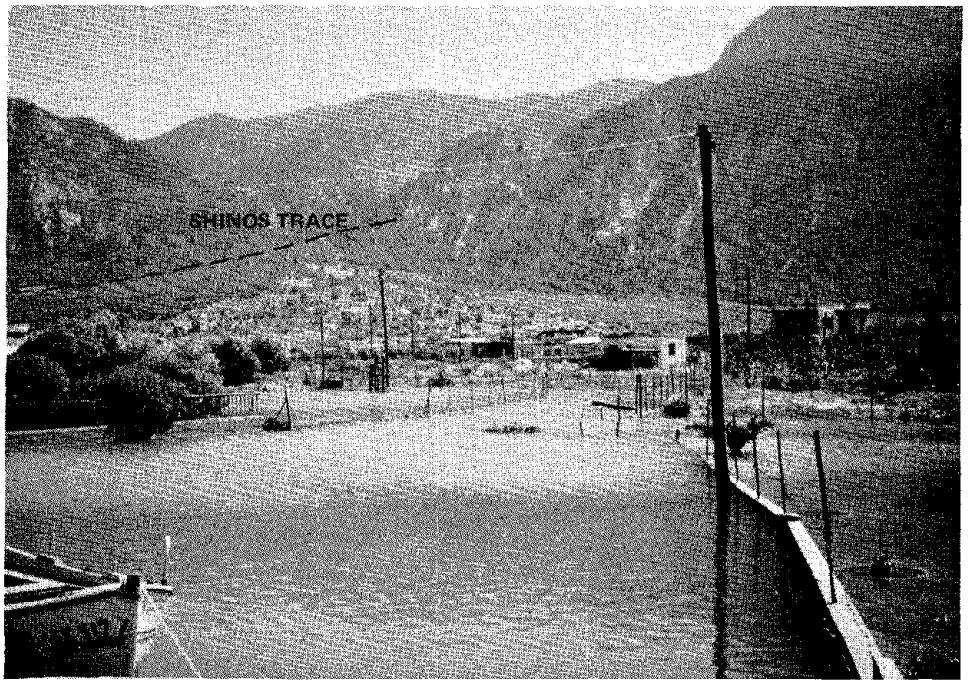

FIGURE 2.16 Subsidence of the ground surface north of the Shinos trace (looking south). A segment of the Shinos trace is shown where it crosses a large alluvial fan.

in 10,000, or about 10 seconds of arc at 0^{o} inclination. Data recorded during March, April, and May of 1981 showed that further or renewed deformation took place in the region. Stations along the southern traces north of the Shinos rupture indicated tilting parallel or subparallel to the faults. The pattern of tilting along the northern traces was significantly different. The foot wall block of the Kalamaki fault and the hanging wall block of the Kapareli faults tilted generally northward, while the opposite blocks tilted east and southeast.

AFTERSHOCK PHENOMENA

The early deployment of a geological team into the epicentral areas following the main shocks gave members of the team several opportunities to observe firsthand various phenomena associated with the aftershocks. Two accounts of these observations are particularly worthy of mention, the first because geologists were able to observe ground motion on an existing surface rupture during a seismic event, and the second because a sequence of observations made preceding an aftershock significantly reflects a precursory phenomenon.

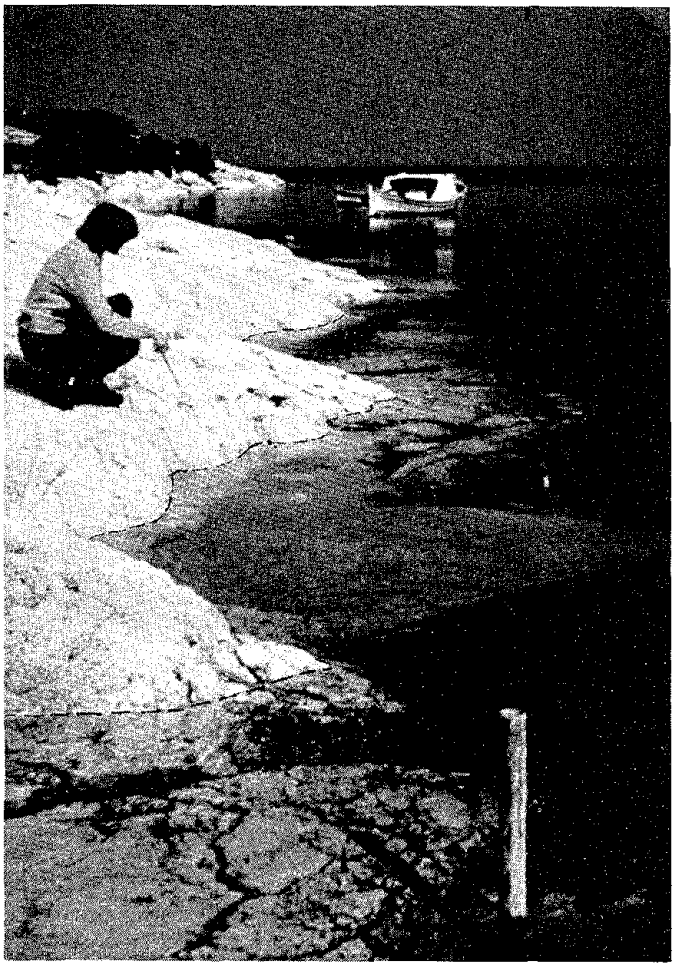

FIGURE 2.17 Submerged concrete docks north of Shinos. The dotted line indicates the present water level. At this site over 1.0 m of subsidence was documented associated with the earthquakes of February 24 and 25, 1981.

Ground Motion

On March 7, 1981, a field party was investigating the Kalamaki rupture trace on the north side of the Gulf of Corinth (see Figure 2.9). In the early afternoon the field crew was mapping the rupture in a recently planted field. At that location the vertical offset generated by the 6.2 magnitude earthquake on March 4 was 35 to 40 cm and the fracture was open 10 to 15 cm, except where wedge-shaped blocks had broken from one side of the fracture to close it up. At 1:35 p.m. an earthquake, reported later to have a Richter magnitude of 5.7, occurred in the region. At the instant of onset, two investigators were standing by the

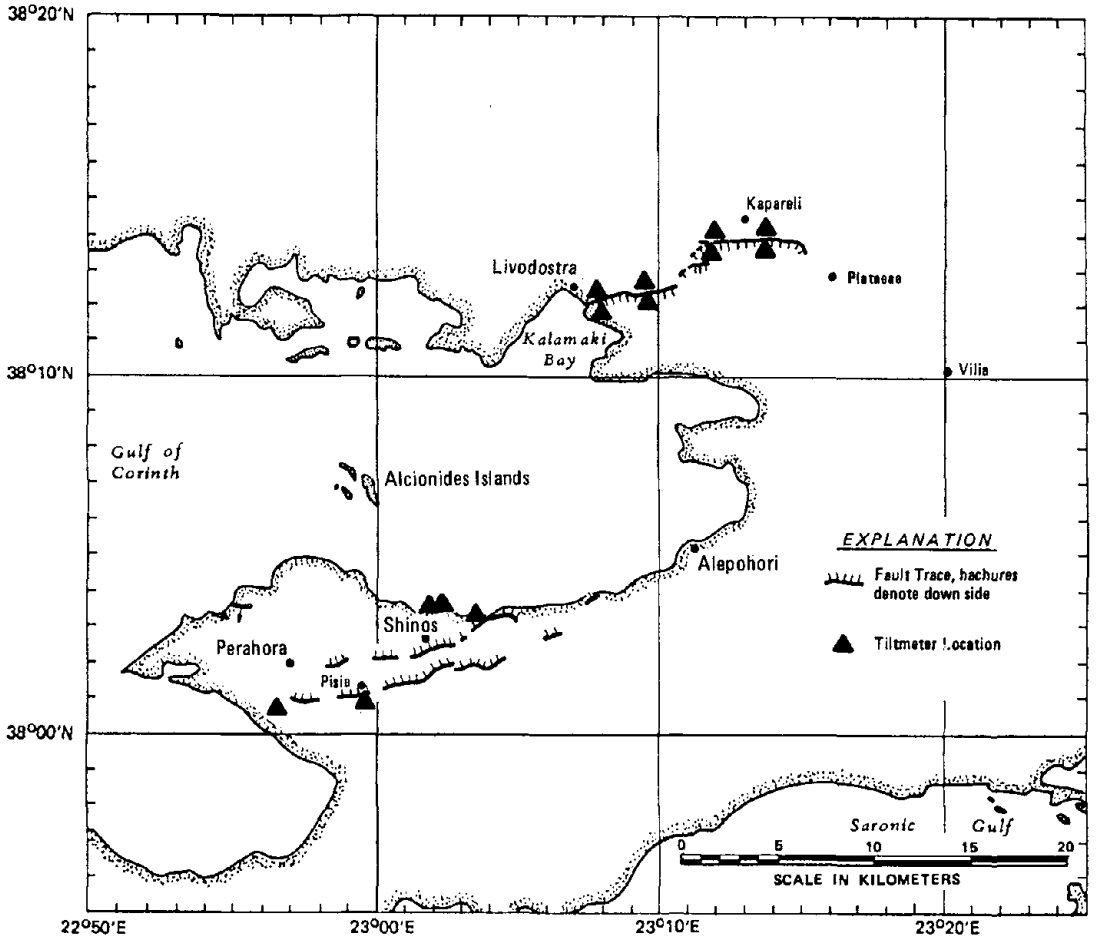

FIGURE 2.18 Location of tiltmeter plates.

open fracture. The first sensation was of motion without sound. It gave the observers the feeling of stumbling while standing in place. The soil underfoot seemed fluid, necessitating a "treading" motion to avoid sinking into the softening soil. The existing fracture was observed to open and shut repeatedly, and within the first second a deep but muffled rumbling noise was heard, accompanied by a slapping sound as the sides of the fracture hammered together. Individual rows of soil that had been plowed parallel to the fracture were seen to heave and roll, so that the entire plowed surface appeared to be in disharmonic motion. Also, small cracks were observed opening parallel to the plowed furrows. The ground shaking lasted 4 to 5 seconds and was followed by two loud "thunderclaps" about 8 to 10 seconds after the commencement of ground motion.

Approximately 20 minutes after the earthquake the two investigators examined the area where the Kalamaki rupture trace intersects the shoreline of the Gulf of Corinth. From a viewpoint overlooking the gulf they observed a newly formed silt plume extending approximately 0.5 km out into the gulf along the projection of the rupture trace. The plume

apparently resulted from pumping of water and bottom sediments as the underwater fracture opened and closed during the earthquake. Reports from local residents indicate that a "geyser" occurred offshore in the area during the earthquake. A crater some 3 m across in alluvium surrounded by ejecta was later observed in low-lying fields at Livodostra. Local residents reported that the crater was formed during the earthquake by explosive geysering.

A Precursory Phenomenon

On the afternoon of March 3, 1981, a field party was inspecting a locality on the south coast of the Gulf of Corinth near Shinos where a road had been submerged below low tide level by subsidence associated with the February 24-25 earthquakes. Seawater from the rising tide was pouring inland over ground where boats had formerly been stored above high tide level. At approximately 3:00 p.m. (local time) the field party was checking the rate of tidal rise, by observing the tide crossing and covering a second road and rising around a stake in the ground, when the water stopped rising and began to recede. The recession continued for about four minutes, by which time the water was about 1 cm lower on the metal stake than before. At 3:04 local time an earthquake of several seconds' duration was felt. Within minutes after the shock, which was reported by the National Observatory as a magnitude 4.6 event, the tide had again risen to its former level and continued to rise and cover the road. The breeze was constant in velocity and direction during these events.

This sequence of events indicates that the land surface rose over a period of a few minutes at a rate greater than that of the rising water level of the incoming tide.

STRONG MOTION RECORDS

This chapter summarizes strong-motion records of the two major events of February 24 and 25, 1981, and associated studies from the work of Carydis, Drakopoulos, and Taflambas (1981). The records were obtained from an instrument (SMA-1) located in Corinth and operated by the Greek National Observatory as part of its instrumentation network. The instrument was placed in the basement of a two-story building that serves as the telecommunications center of Corinth. The building consists of a rather stiff reinforced concrete skeleton with infilled hollow brick walls. The instrument is located about 20 km from the epicenter of both events.

EVENT OF FEBRUARY 24, 1981

Figure 3.1 is a contact copy of the original recording. Figures 3.2, 3.3, and 3.4 show the ground acceleration, velocity, and displacement of the longitudinal, vertical, and transverse components of the seismic motion after instrument, base line, and digitization corrections were made (band pass filter between 0.125 and 25 cycles per second). The traces, which represent the response of the instrument, have been converted to ground components using procedures described by Hudson (1979). The maximum values are for the February 24, 1981, event.

TABLE 3.1 Maximum Values for the February 24 Event

Component	Acceleration (gal)	Velocity (cm/s)	Displacement (cm)
Longitudinal (N35^{o}E)	234	22.5	6.7
Vertical	94	8.0	2.6
Transverse (N55^{o}W)	281	24.6	6.3

Figures 3.5, 3.6, and 3.7 present response spectra for the longitudinal, vertical, and transverse components, respectively, following the methodology described by Nigam and Jennings (1968) and Hudson (1979).

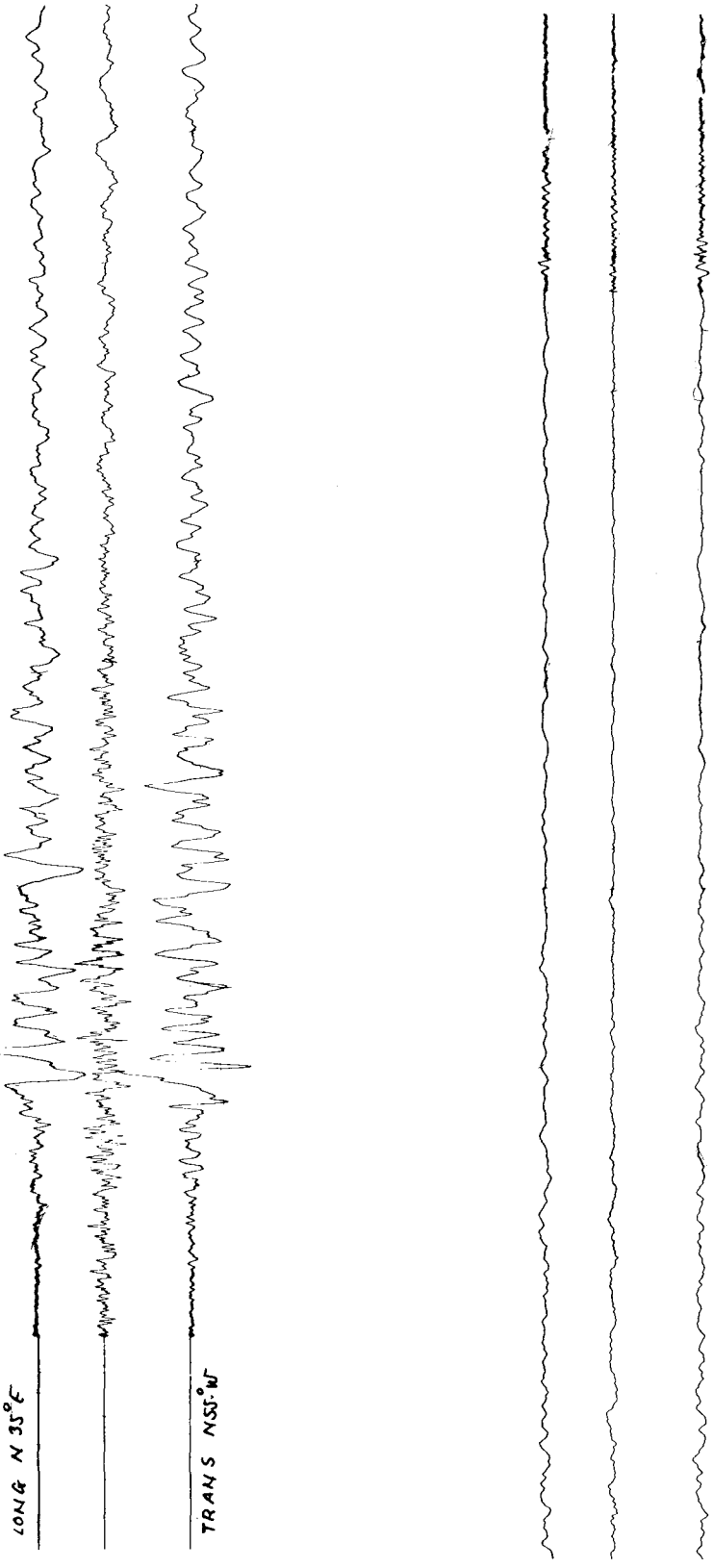

FIGURE 3.1 Contact copy of the February 24, 1981, record, Corinth.

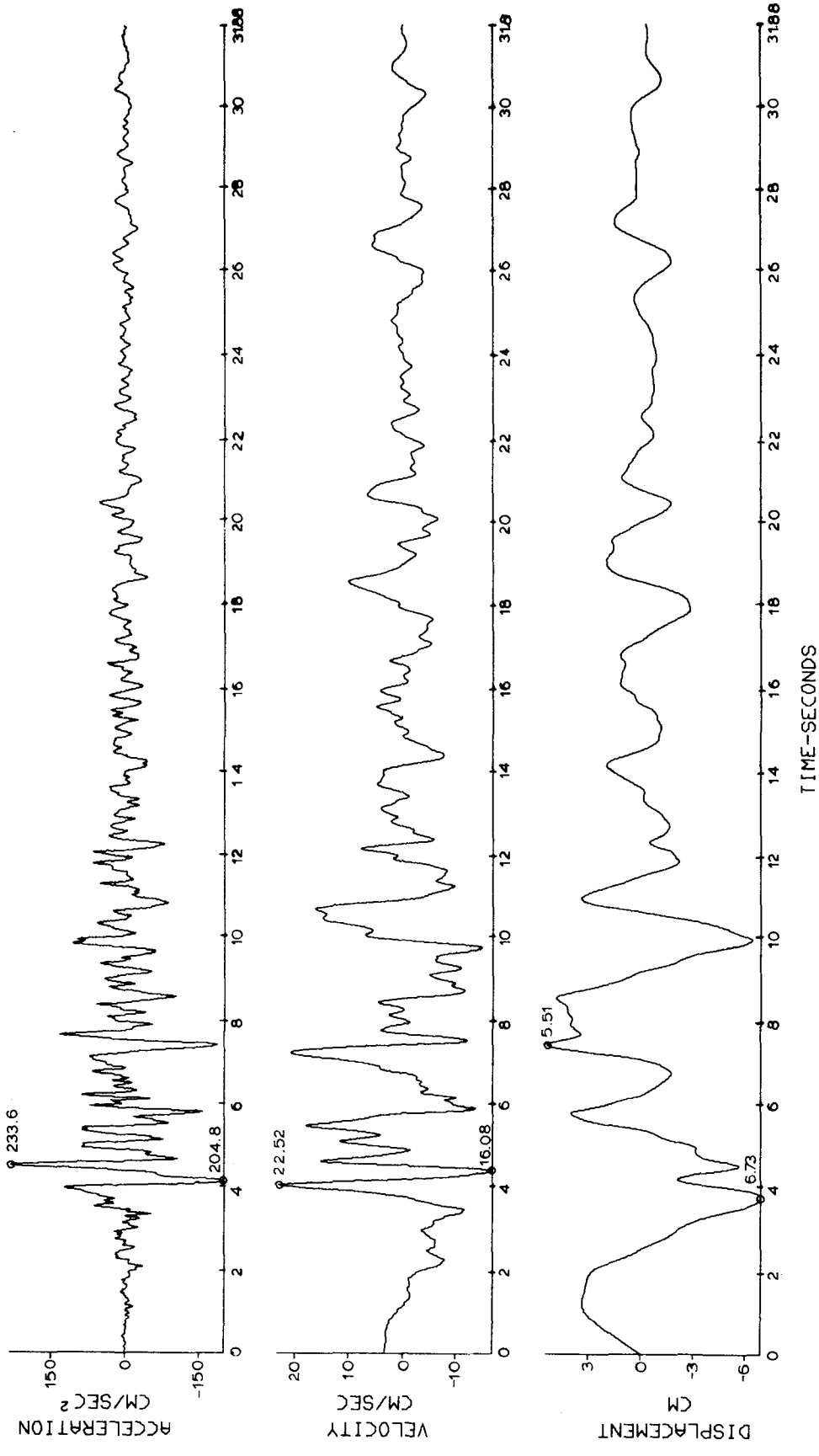

FIGURE 3.2 Longitudinal ground acceleration, velocity, and displacement on February 24, 1981, Corinth.

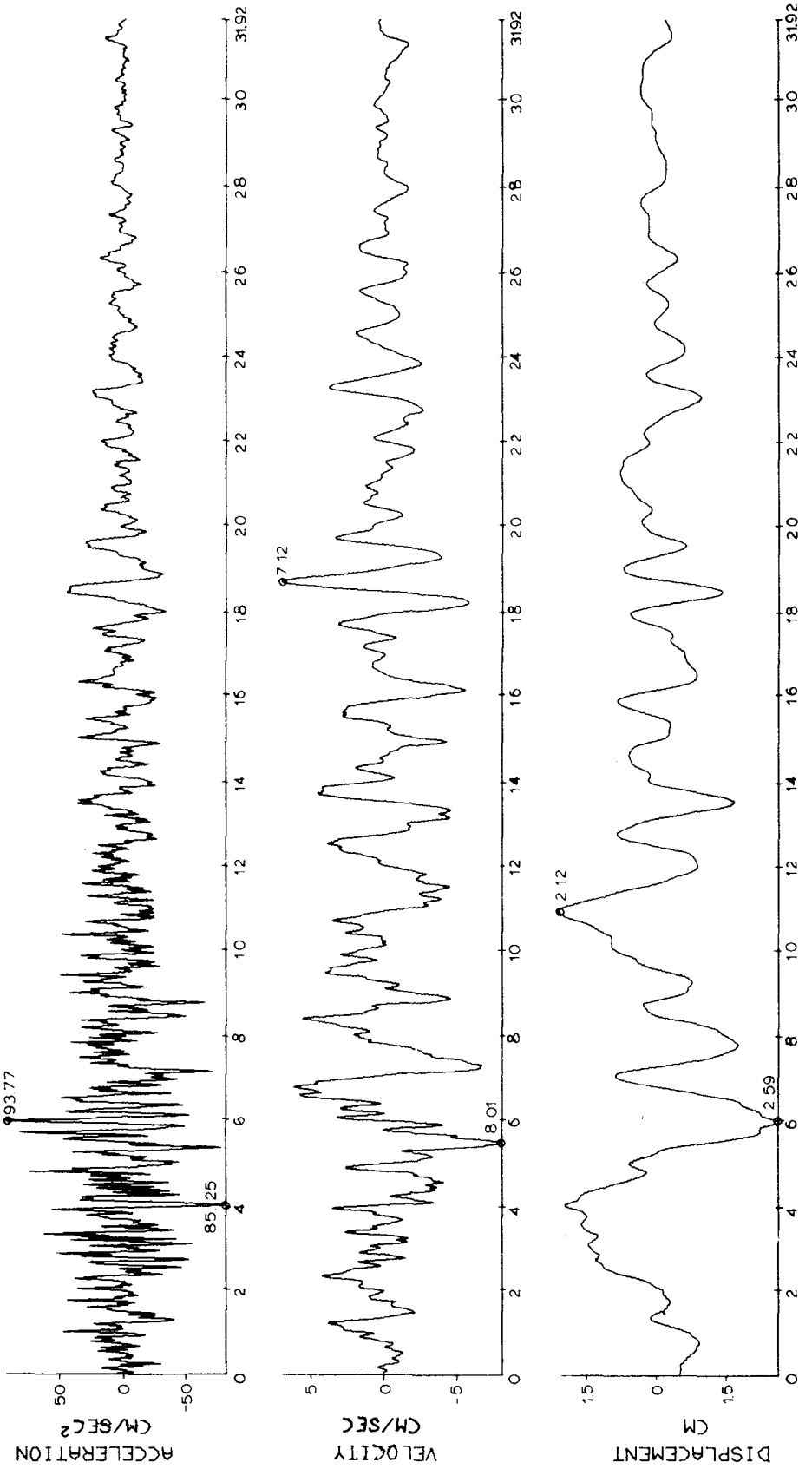

FIGURE 3.3 Vertical ground acceleration, velocity, and displacement on February 24, 1981, Corinth.

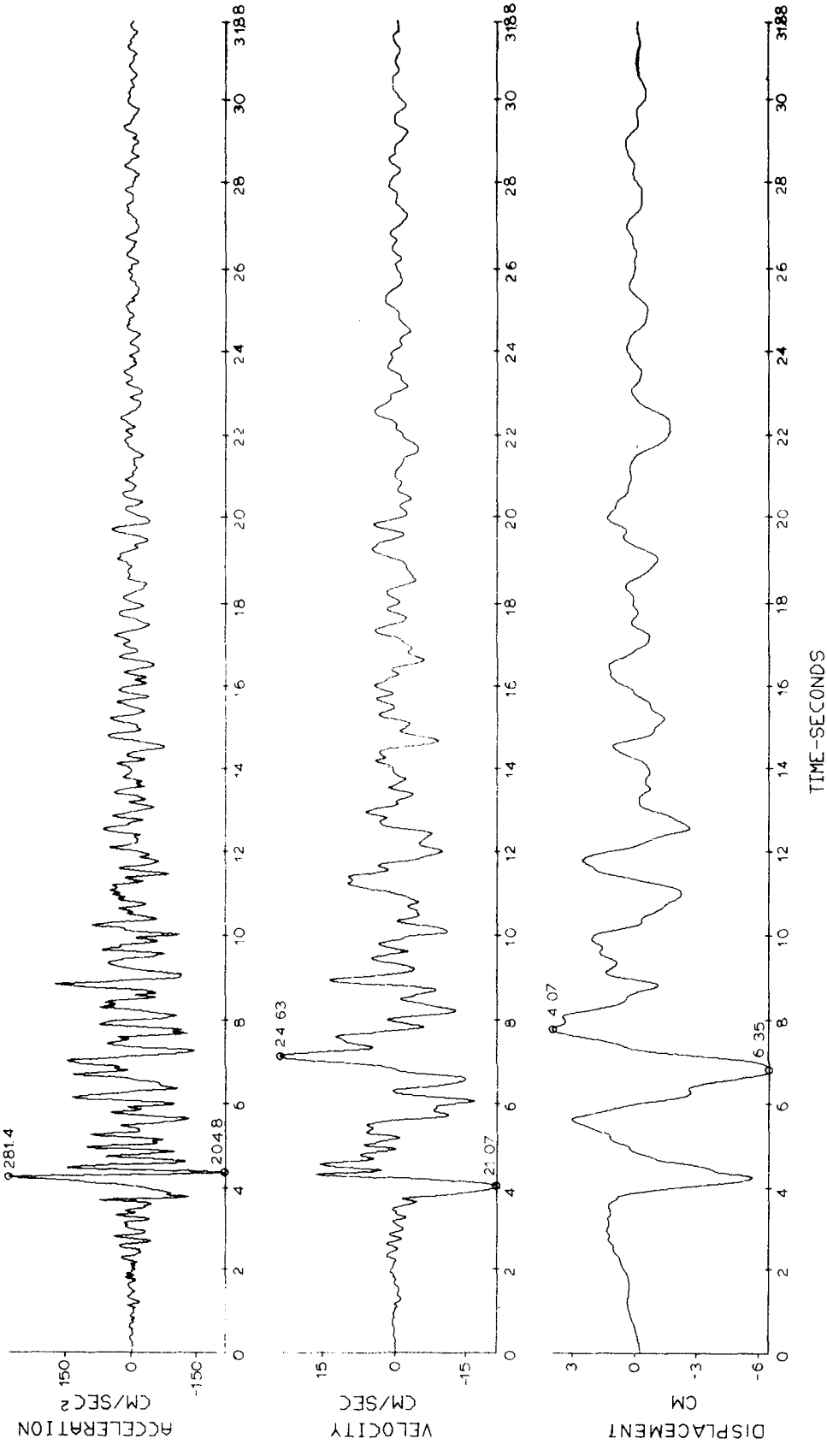

FIGURE 3.4 Transverse ground acceleration, velocity, and displacement on February 24, 1981, Corinth.

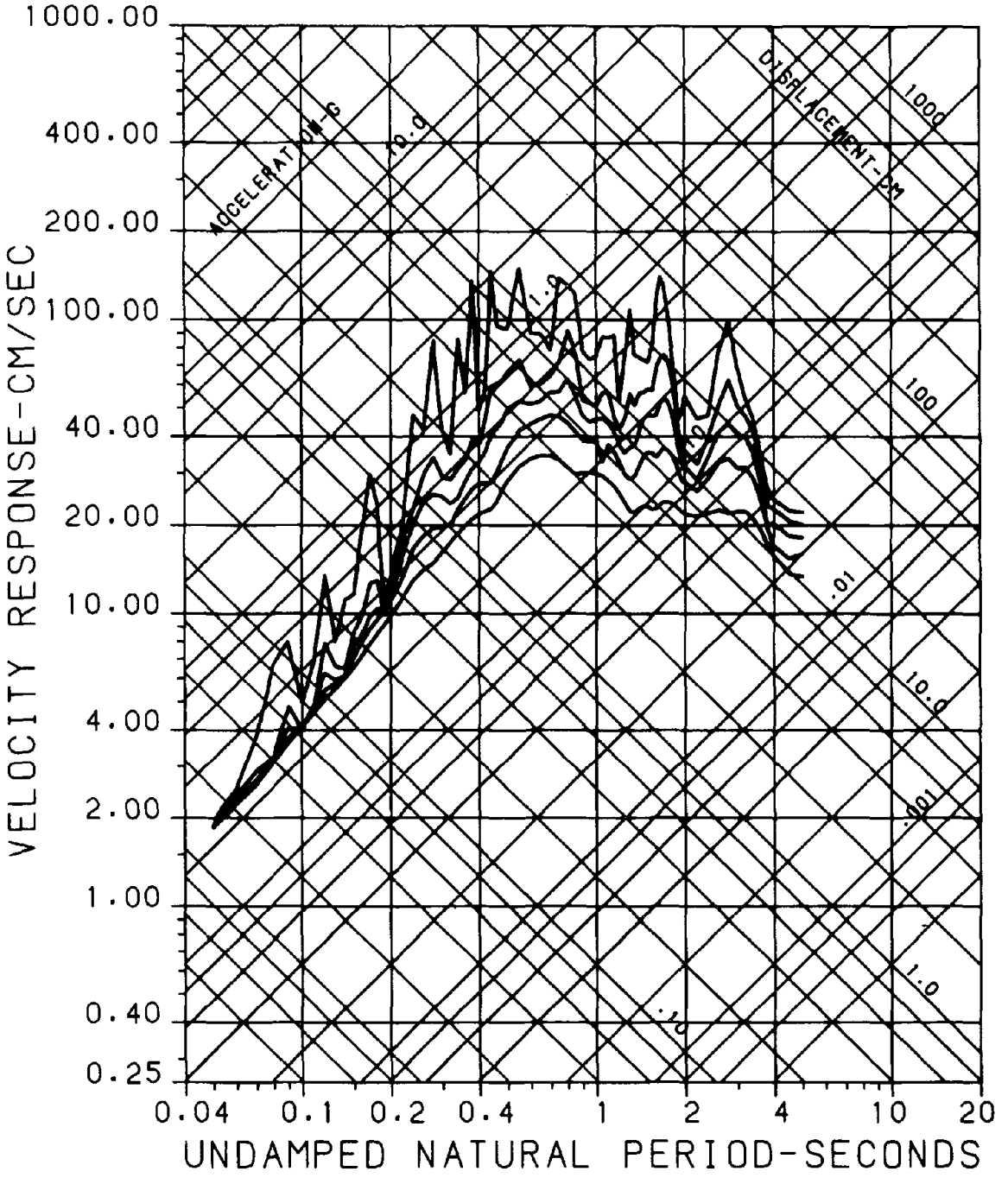

FIGURE 3.5 Longitudinal response spectra on February 24, 1981, Corinth.

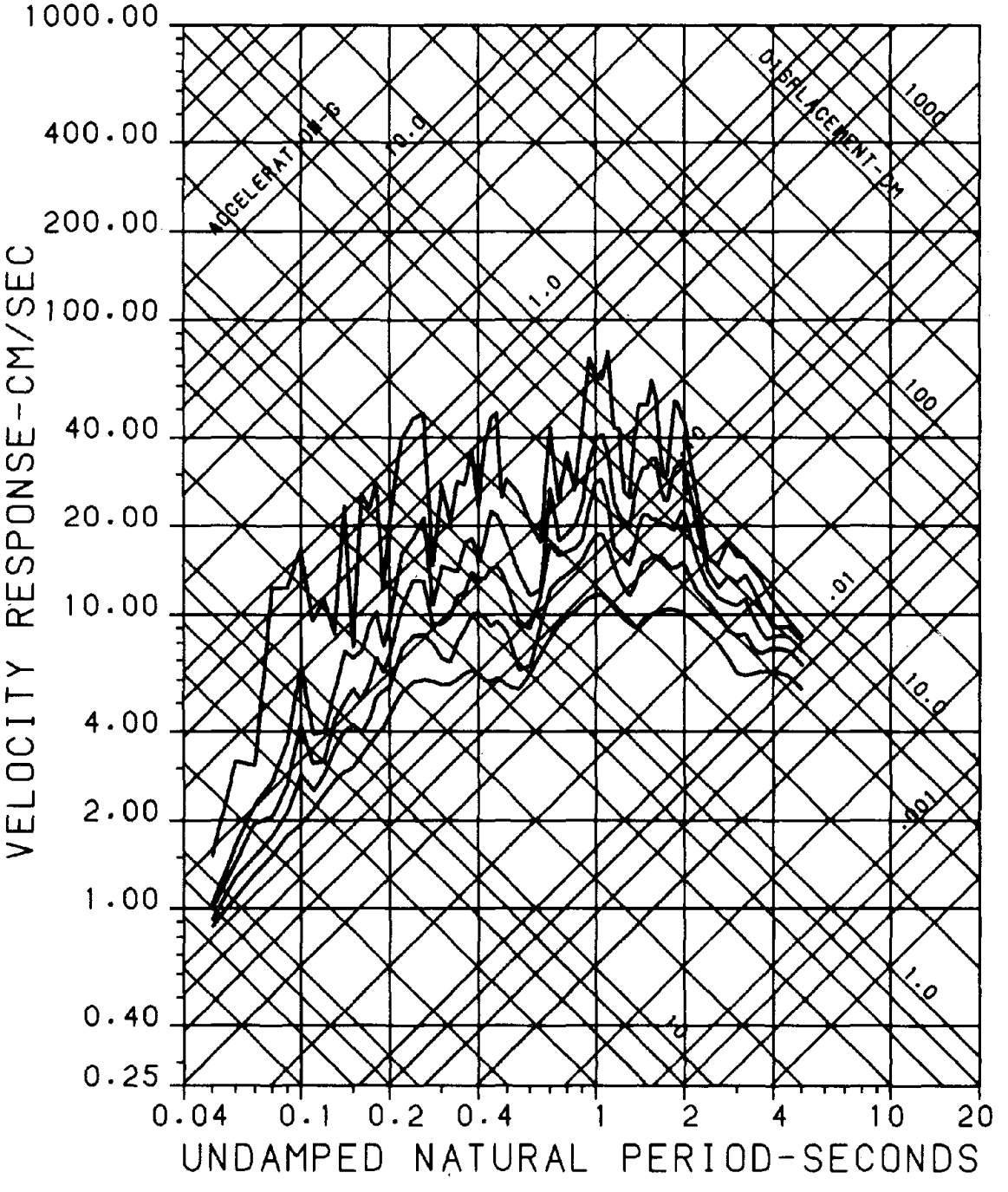

FIGURE 3.6 Vertical response spectra on February 24, 1981, Corinth.

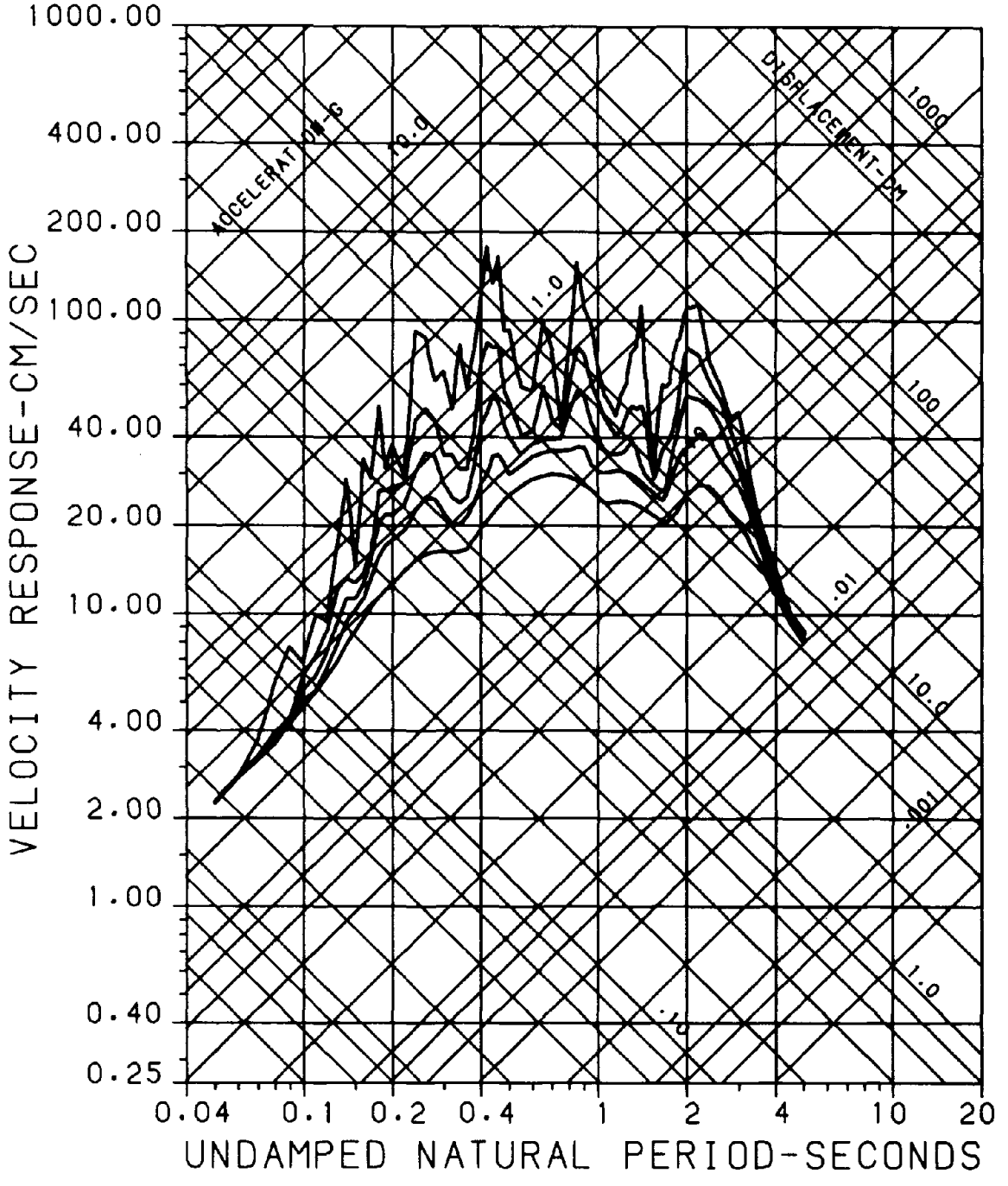

FIGURE 3.7 Transverse response spectra on February 24, 1981, Corinth.

EVENT OF FEBRUARY 25, 1981

Figure 3.8 is a contact copy of the original recording. Figures 3.9, 3.10, and 3.11 show the ground acceleration, velocity, and displacement of the longitudinal, vertical, and transverse components of the seismic motion. Table 3.2 gives the maximum values for the February 25, 1981, event.

TABLE 3.2 Maximum Values for the February 25 Event

Component	Acceleration (gal)	Velocity (cm/s)	Displacement (cm)
Longitudinal (N35°E)	118.5	12.5	4.5
Vertical	39.8	5.3	2.4
Transverse (N55°W)	118.2	14.0	5.8

Figures 3.12, 3.13, and 3.14 present the response spectra for the longitudinal, vertical, and transverse components. The procedure followed was the same as for the record of February 24, 1981.

COMPARISON OF RECORDS OF OCTOBER 12, 1975, WITH 1981 EVENTS

On October 12, 1975, an earthquake of magnitude 5.0 was registered at the same station (Carydis and Sbokos, 1978). The epicenter (about 20 km from Corinth) and isoseismals are shown in Figure 3.15. The same figure shows the epicenter of the February 24, 1981, event. The maximum ground accelerations for the events of October 1975 and February 1981 are indicated. Figure 3.16 gives the pseudo-velocity response spectra for the longitudinal and transverse components of both events for a damping ratio of 5 percent.

The similarities between the two earthquakes are quite interesting. The ratio between the maximum values of the two horizontal traces (0.029/0.025 and 0.28/0.23) are almost constant. The shape and frequency content of the pseudo-velocity response spectra are very similar (compare Figures 3.16a and 3.16b). The isoseismals are elongated in the east-west direction, the pattern that corresponds with the location of damage reported for the 1981 event.

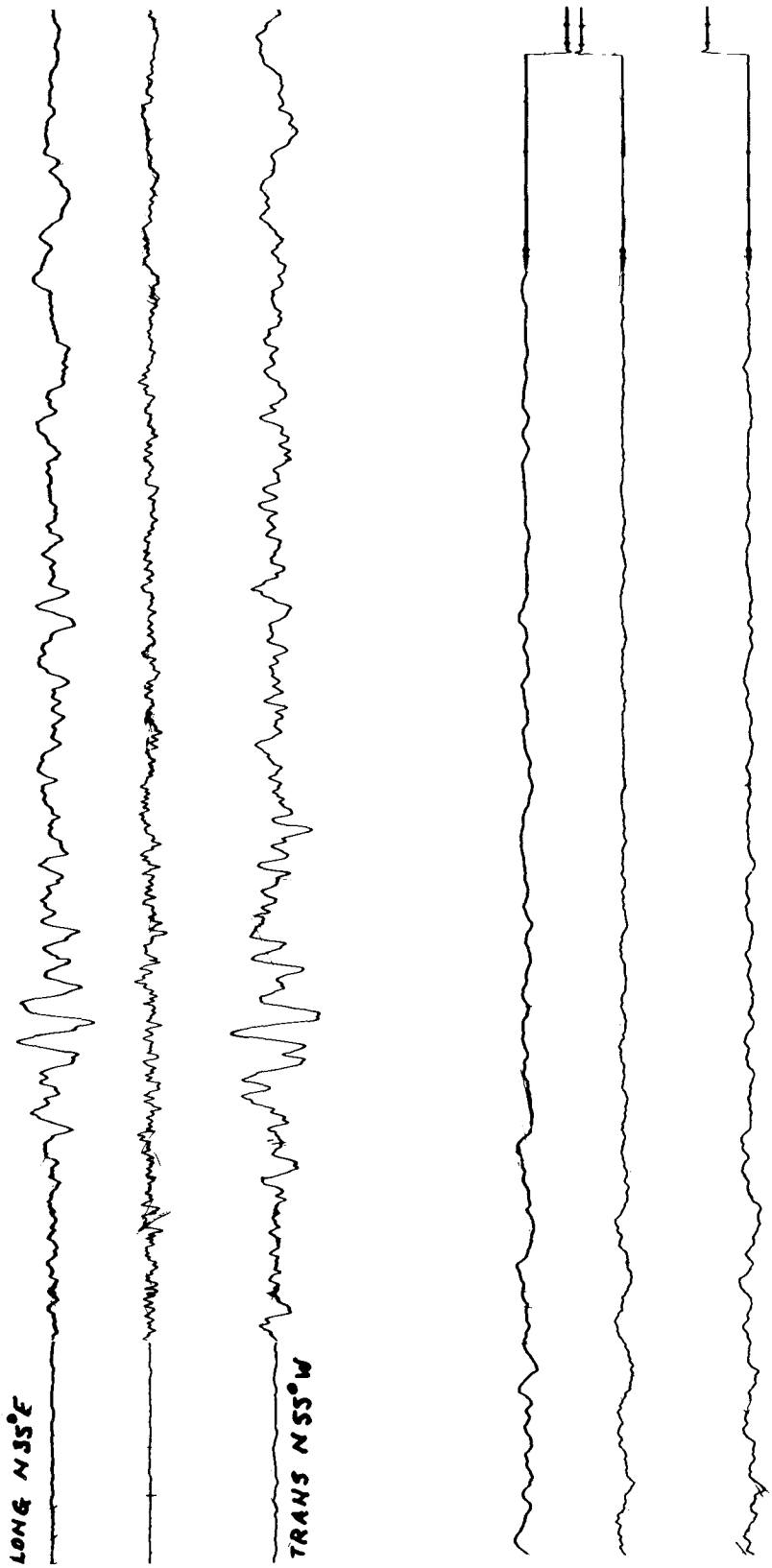

FIGURE 3.8 Contact copy of the February 25, 1981, record, Corinth.

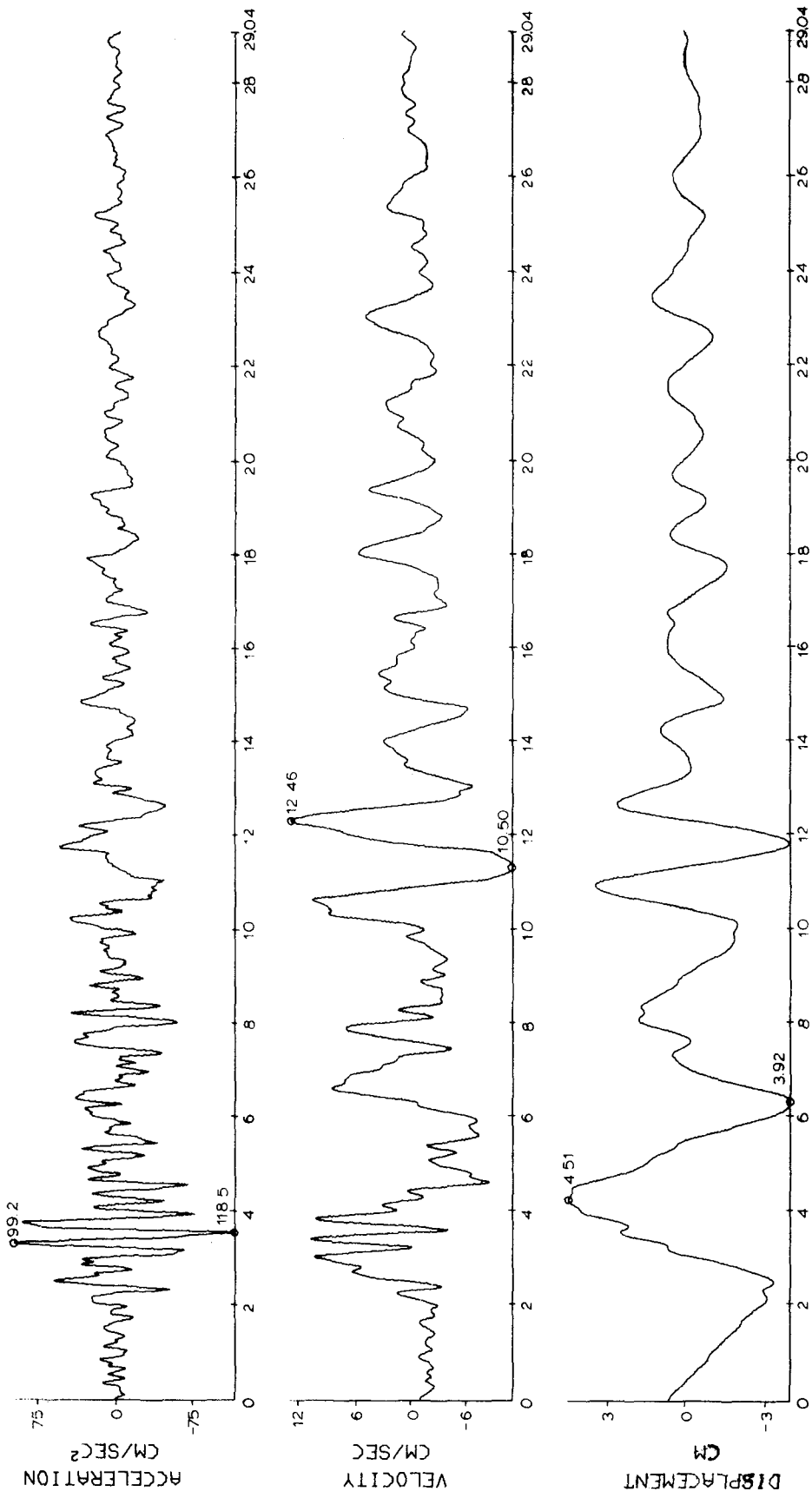

FIGURE 3.9 Longitudinal ground acceleration, velocity, and displacement on February 25, 1981, Corinth.

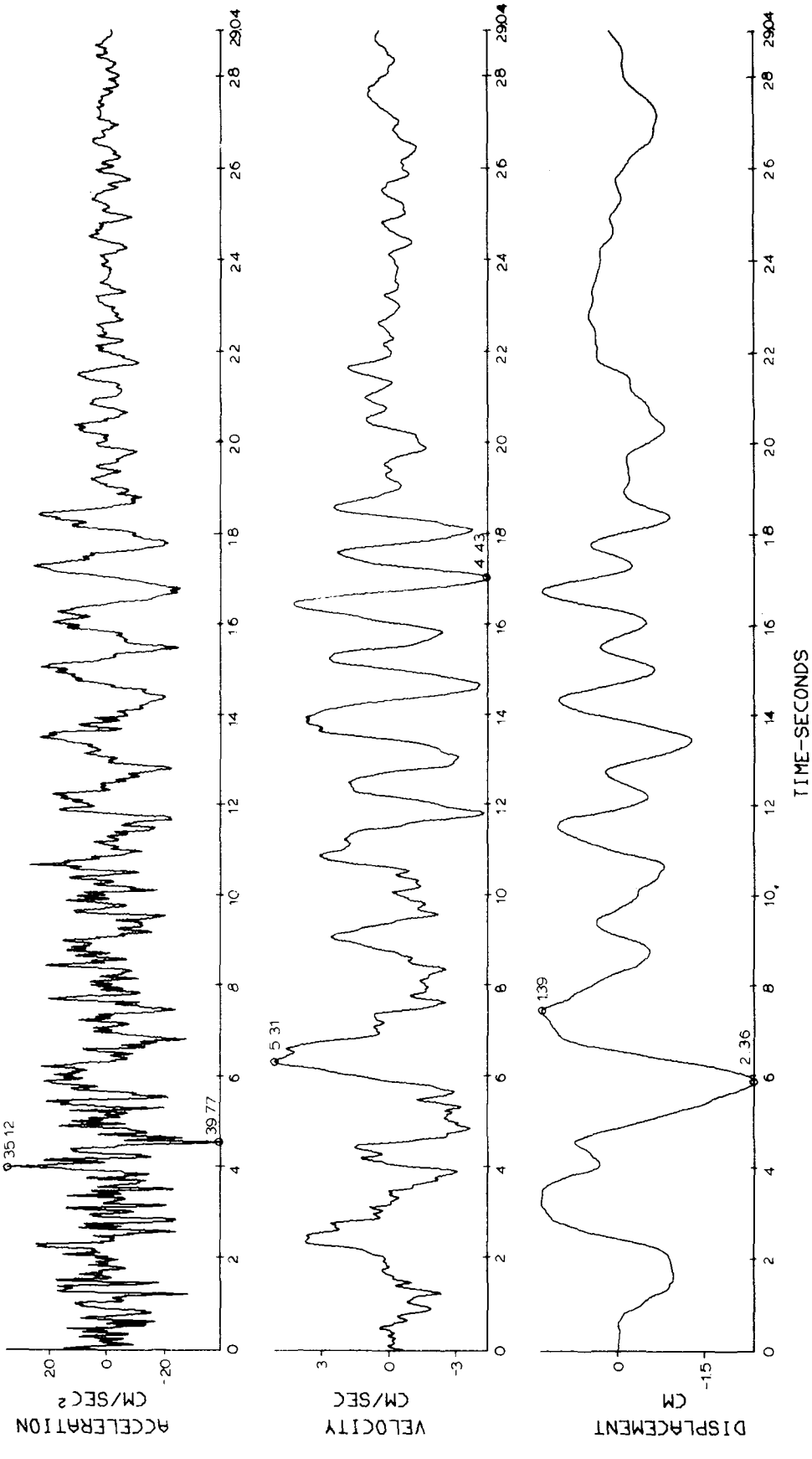

FIGURE 3.10 Vertical acceleration, velocity, and displacement on February 25, 1981, Corinth.

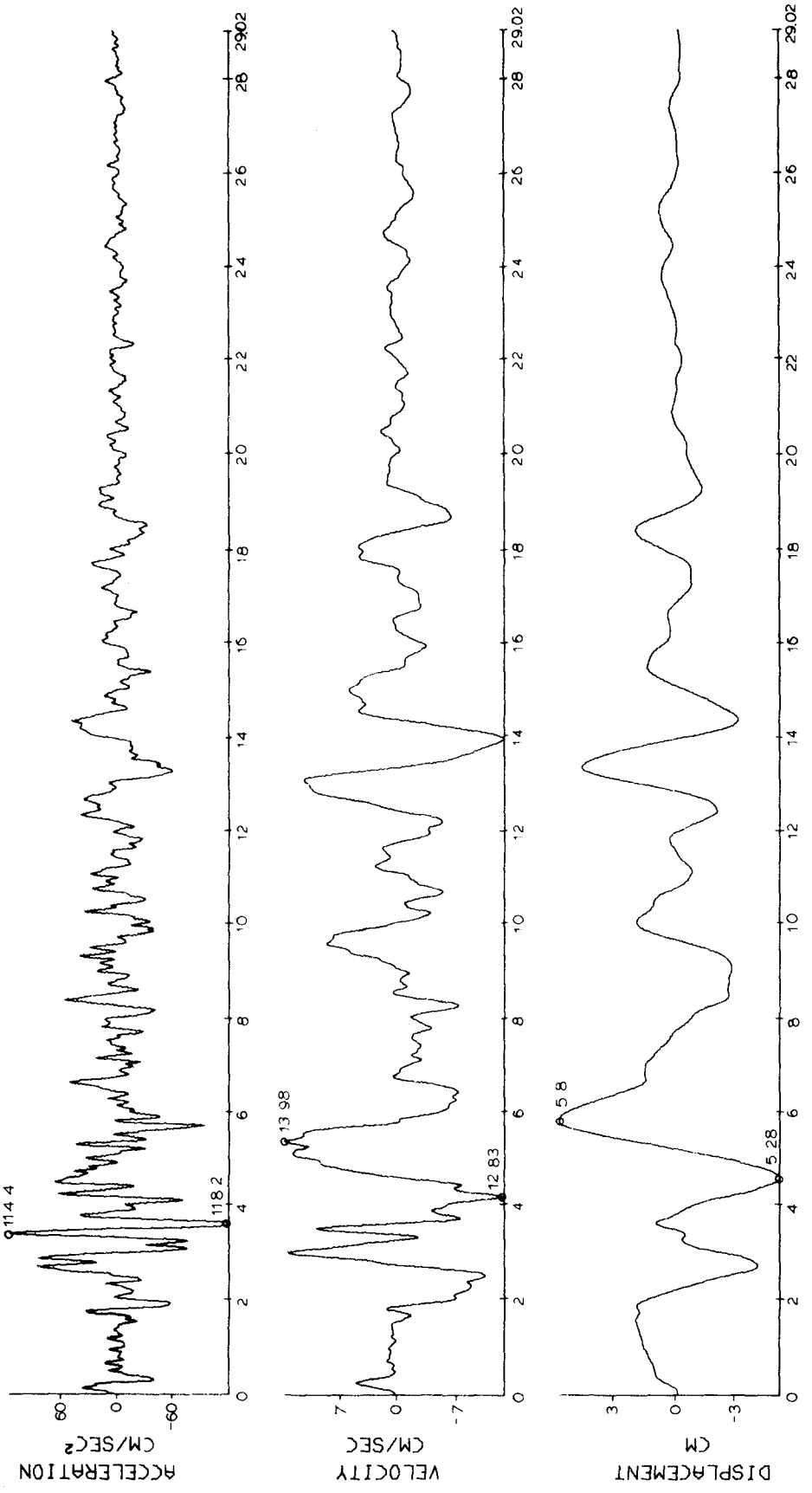

FIGURE 3.11 Transverse ground acceleration, velocity, and displacement on February 25, 1981, Corinth.

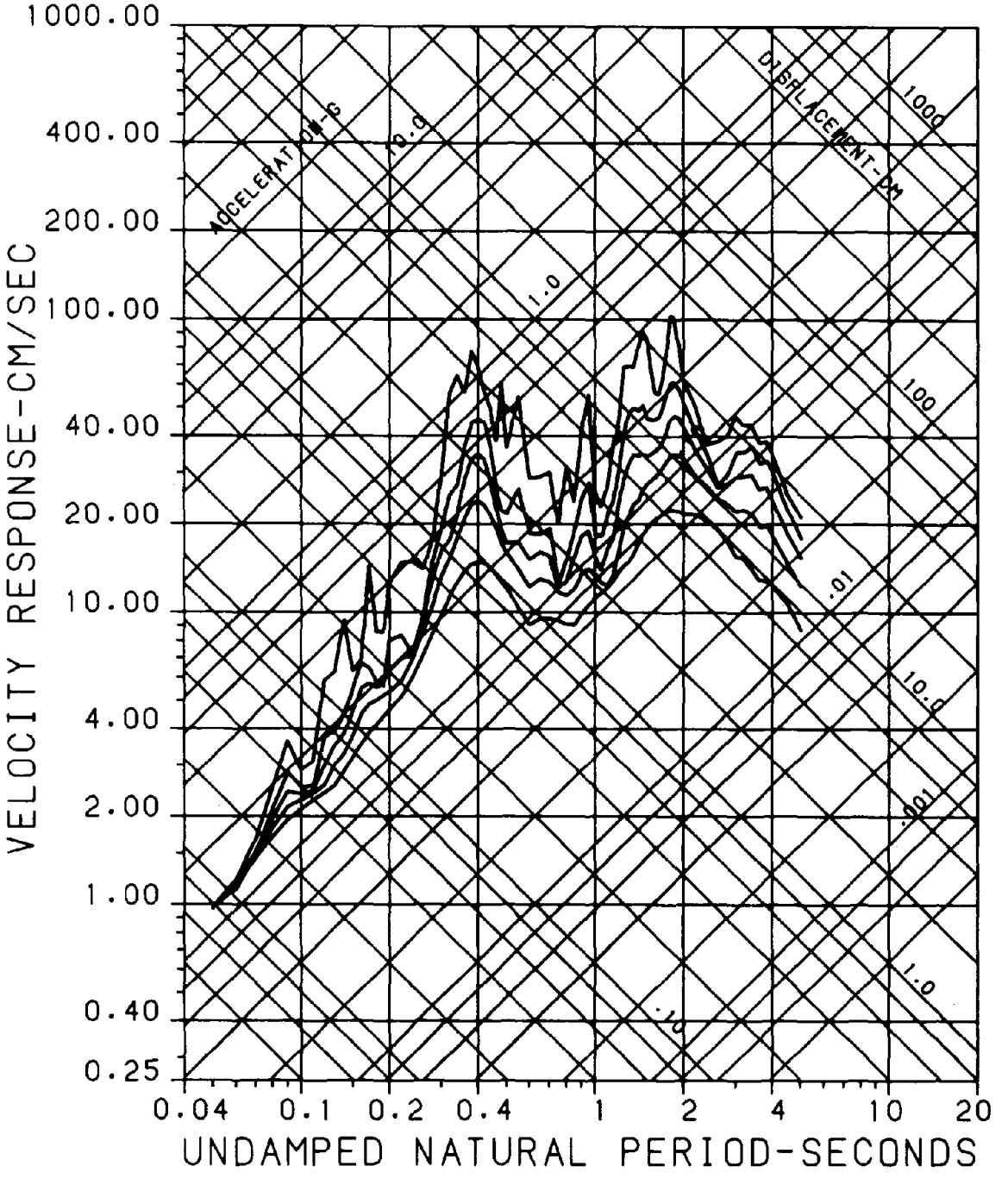

FIGURE 3.12 Longitudinal response spectra on February 25, 1981, Corinth.

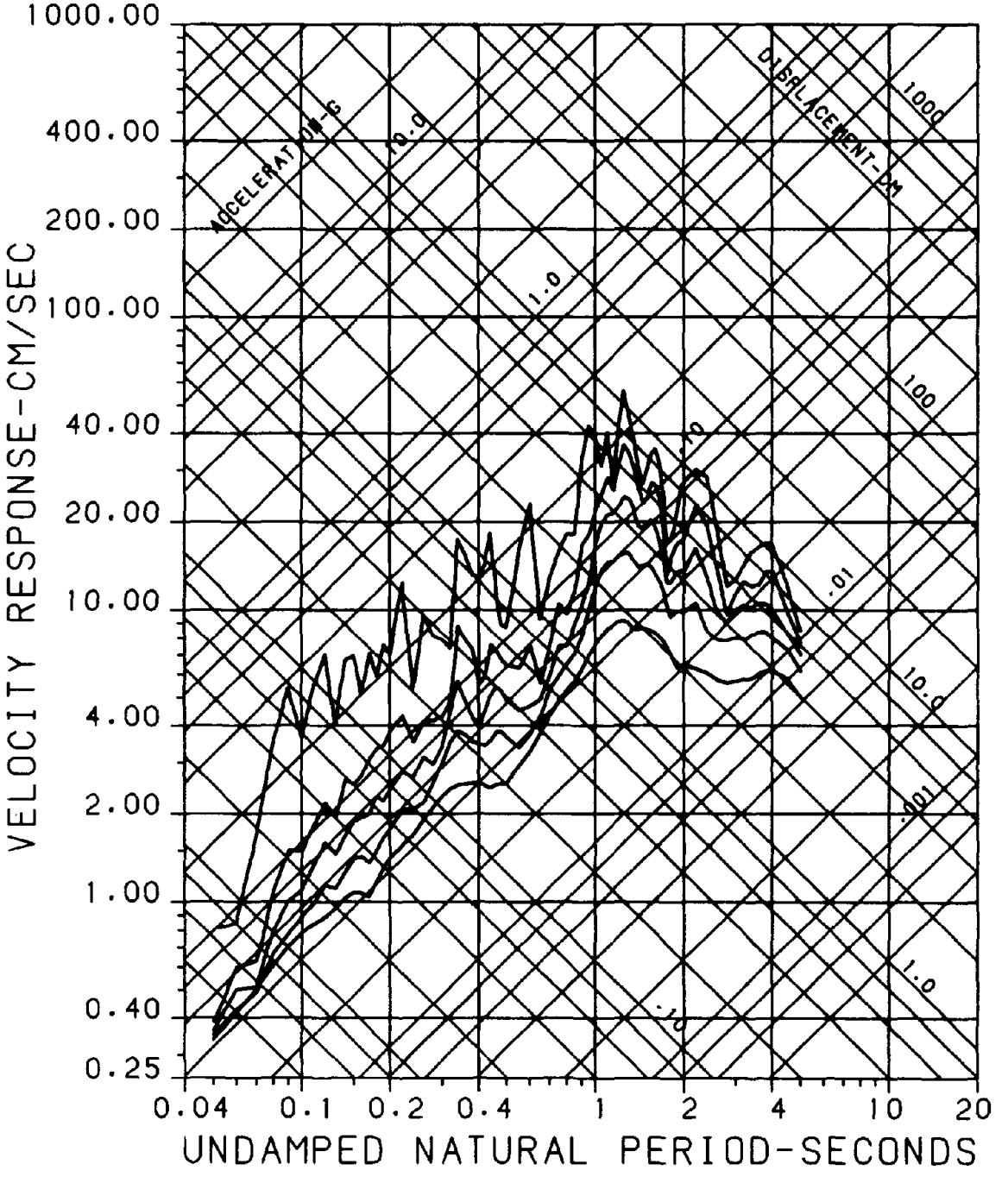

FIGURE 3.13 Vertical response spectra on February 25, 1981, Corinth.

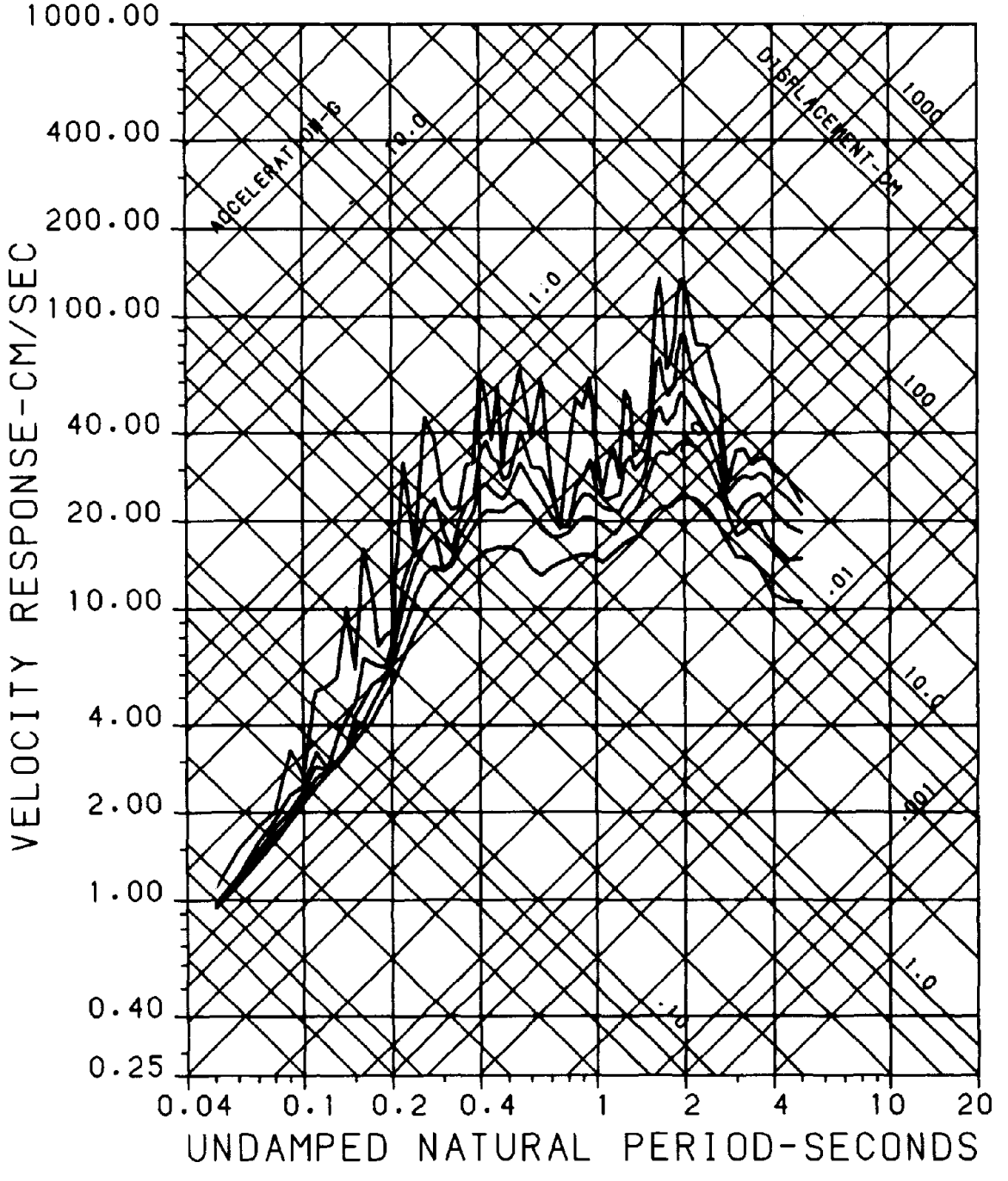

FIGURE 3.14 Transverse response spectra on February 25, 1981, Corinth.

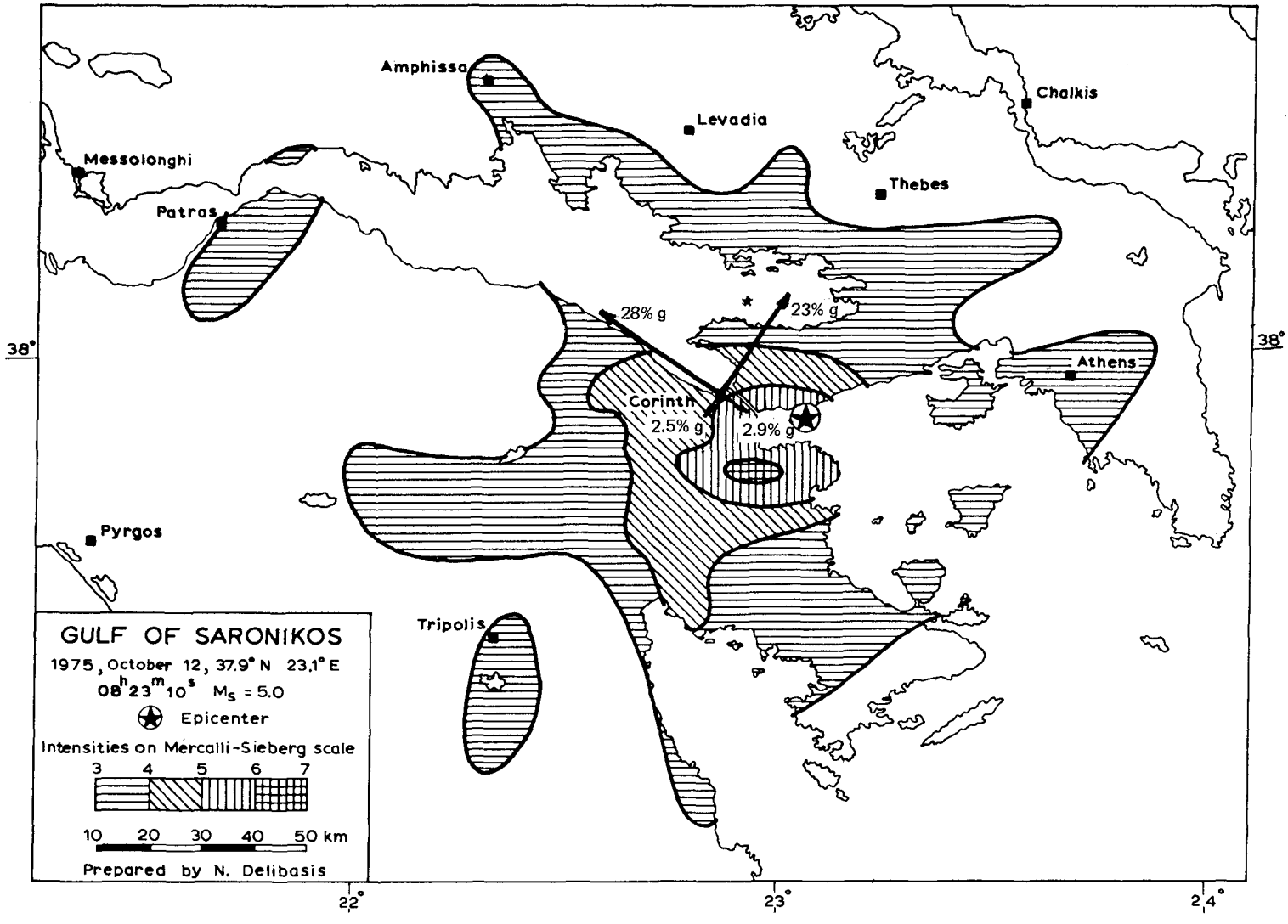

FIGURE 3.15 Isoseismal map for the October 12, 1975, earthquake. The star shows the epicenter of the February 24, 1981, earthquake (N35°E, N55°W). The thick solid line shows the maximum ground accelerations for the February 24, 1981, earthquake. The thin solid line shows the maximum ground accelerations for the October 12, 1975, earthquake. Source: National Observatory of Athens (1975).

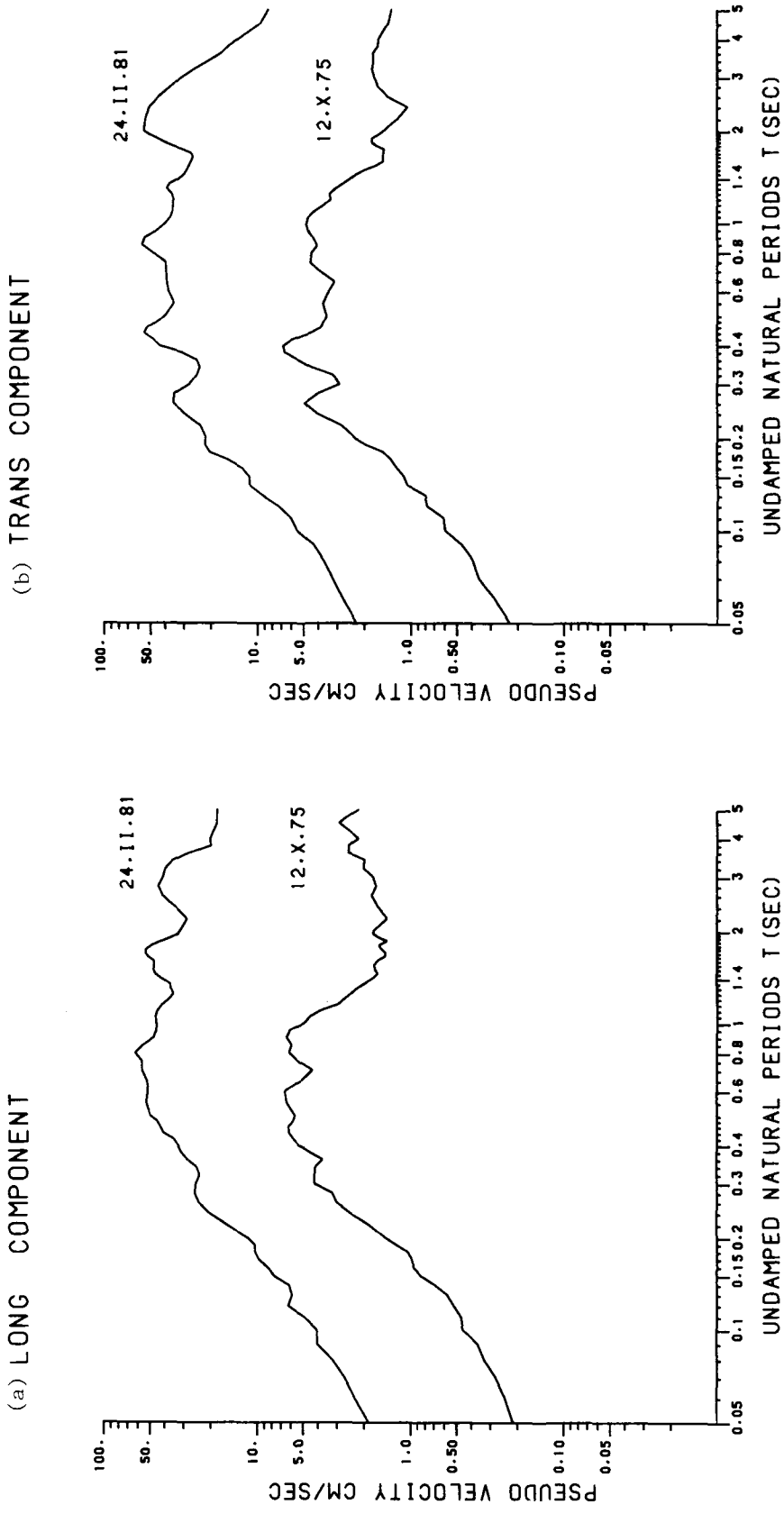

FIGURE 3.16 Comparison of pseudo-velocity response spectra for the 1975 and 1981 earthquakes. The critical damping is 5 percent.

4

GENERAL DESCRIPTION OF CONSTRUCTION PRACTICE IN CENTRAL GREECE

The February-March 1981 earthquakes produced considerable damage in residential structures, including single-family dwellings, apartment blocks, and hotels. To provide background for a better understanding of the kinds of damage observed, this chapter contains a general description of typical construction practice, the condition of the structures, and the behavior of residential structures during the earthquakes. In Chapter 5 specific damage observed in different localities is described and details of several structures are provided. For further background, Appendix B contains a brief description of the Greek building code provisions for seismic design.

MASONRY BUILDINGS

Masonry buildings are constructed of native stone, fired brick, and concrete blocks.

Stone Masonry Structures

Stone masonry buildings and other structures of native stone have been the most common traditional structures in Greece. The floors and roofs generally have been wood. Because the use of many old masonry buildings has changed, they have been renovated with the addition of enclosed space in both plan and height. Until the late 1940s, timber beams were included at various locations in the structure as strengthening elements. Timber beams were placed in window sills, in lintels, at intermediate levels up to and under the roof, and even in corners (Figure 4.1). In some cases steel was used instead of wood. In newer construction, timber or steel beams have been replaced by reinforced concrete beams, as required by recent codes. Timber floors and roofs (Figure 4.2) have now been replaced by reinforced concrete slabs. The partitions of older buildings consist of light wooden frames covered with a plaster called bagdhati.

For earthquake resistance, careful attention must be given to the construction of a stone masonry structure. The entire thickness of the

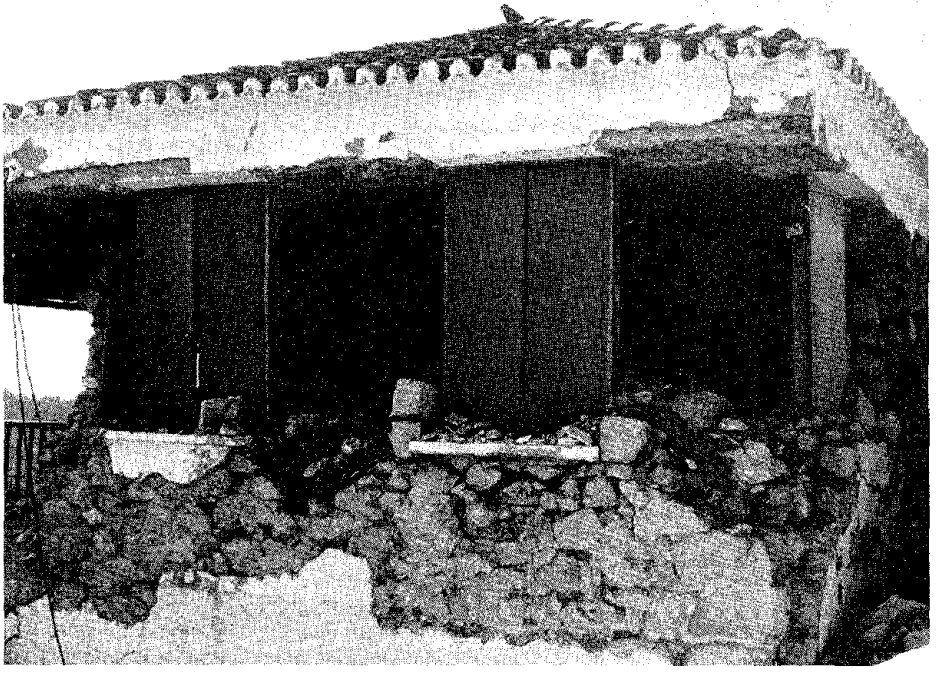

FIGURE 4.1 Tile roof supported by timber frame in Perahora.

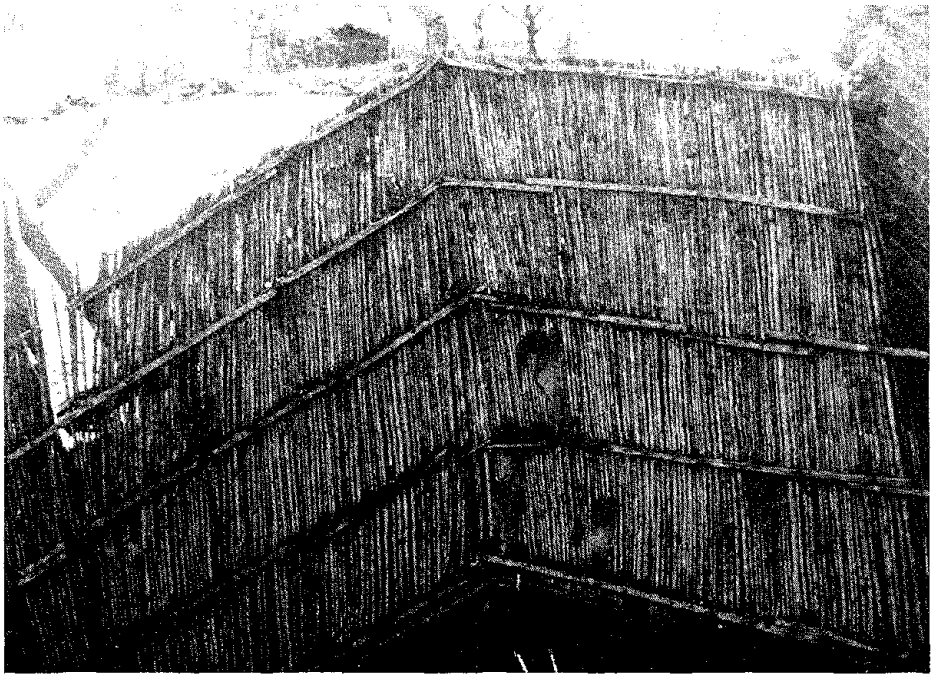

FIGURE 4.2 Timber roof supporting tiles in Perahora.

walls must be constructed carefully, and the mortar must be of good quality. In Perahora many of the masonry walls were constructed as two separate faces without any connection and the cavity was filled with rubble and earth. Earth mortar without any cementing material was used (Figure 4.3).

If a stone masonry building is reinforced with properly located tie beams of good quality, and if the masonry units are dimensionally correct, this type of building displays sufficient earthquake resistance for some to remain in use for 200 to 300 years. The soil plays a very important role in determining the useful life of the structure. Most stone masonry buildings have been erected on slopes, where problems such as differential settlement of the foundation occur even without earthquakes.

During the 1981 earthquakes, stone masonry buildings exhibited various kinds of behavior. In Athens one- or two-story buildings stood very well, as did the buildings of Corinth and Loutraki that were constructed after the 1928 earthquake or were repaired according to the requirements of recent seismic codes. Even though most existing stone masonry structures in Loutraki were founded on good soils, some old hotels and houses suffered damage beyond repair. The damage may be attributed to the various additions of closed space in both plan and height through renovations and alterations carried out over the years, as shown in Figures 4.4 and 4.5. In these additions, different materials like reinforced concrete and steel were used. In order to obtain open space, masonry walls were removed and replaced by slender steel columns. In some cases two or three stories were added on the top of old three-story masonry structures by "planting" slender steel or reinforced concrete columns down to the foundation without any horizontal stiffening elements, as shown in Figure 4.6. In some cases, stiff structures suffered almost no damage in the epicentral region when founded on very soft soil. Figure 4.7 shows such a structure in Vrahati. Note that in both cases the columns from the upper floors are on the exterior of the existing first floor. The old masonry structures, already weakened by the removal of walls explained above, had to withstand increased horizontal loads imposed by the added stories. In many cases the old masonry structures had been exposed previously to several strong earthquakes.

In Megara old masonry structures were heavily damaged. Due to the rapid development of the region, large open spaces and windows for shops and other facilities had to be created in existing structures in the old section of the city. Although Megara is near the epicentral zone of seismic activity near the Gulf of Corinth (see Figure 1.2 and Figure B.1), the seismic code classifies the region as one of weak seismicity.

Fired Brick Masonry Structures

Fired brick masonry structures are generally one or two stories in height. Older traditional units are of solid bricks, with more modern units constructed of hollow bricks. Where massive bricks are used, the structures are reinforced with wood and steel beams as in the stone masonry structures. The floors and roofs are timber and the partitions are bagdhati. In more recent construction using either type of brick,

FIGURE 4.3 Stone and mud walls in Perahora.

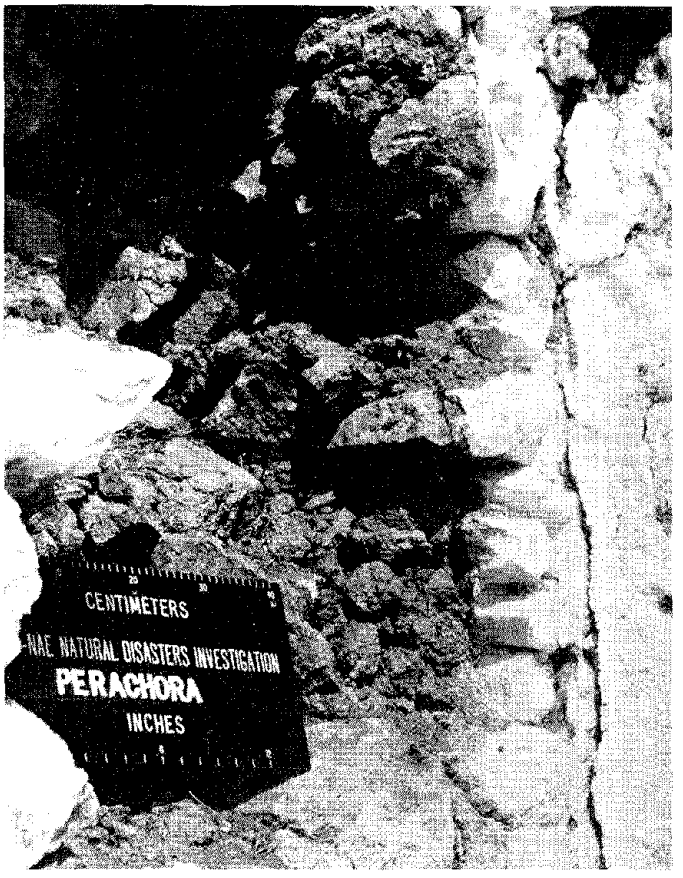

FIGURE 4.4 Additions are very vulnerable, as in this case in Megara. Usually the old building (the lower one) suffers most of the damage.

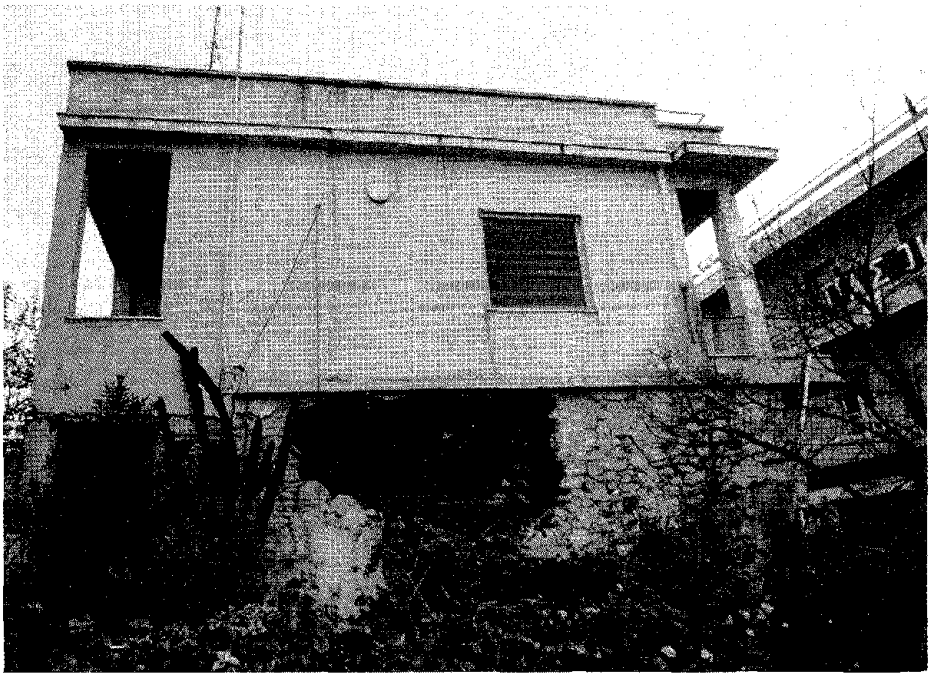

FIGURE 4.5 Addition to an existing stone masonry building (Megara).

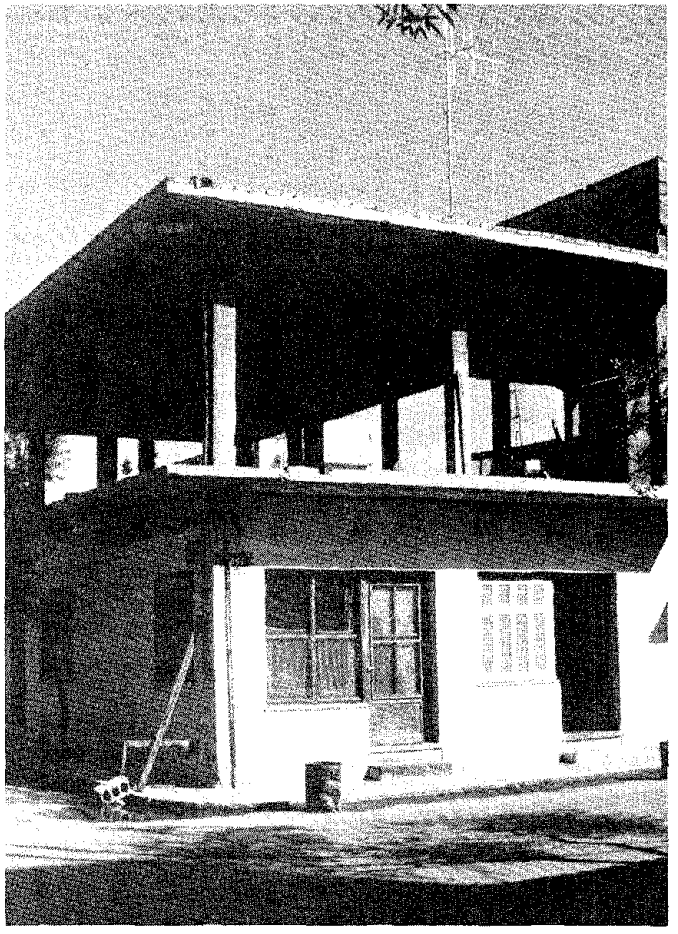

FIGURE 4.6 House with upper floor added.

the reinforcing elements as well as the floors and roofs consist of reinforced concrete. The partitions are thin (7 to 9 cm in thickness) hollow brick walls. As shown in the 1981 earthquake and other earthquakes, the behavior of the structures with solid brick walls (Figure 4.8) was superior to that of the structures with hollow brick walls. The quality of modern bricks generally has been inferior to that of traditional solid bricks, as indicated by the nature of local damage in walls. In some cases the infill walls did not develop typical diagonal cracks (Figures 4.9 and 4.10) but failed by crushing along the reinforcing elements (Figures 4.11 and 4.12).

Concrete Block Structures

Concrete block structures are a recent development. The concrete blocks are hollow and generally of poor-quality material. As a result, concrete blocks are used for secondary structures. Only in cases of squatters' settlements or isolated squatters' houses are concrete blocks used for the construction of dwellings. Dwellings of these blocks are generally one story with a reinforced concrete slab roof. The behavior of such structures during the earthquakes was uniformly poor.

In some cases concrete blocks were used for agricultural buildings or nondwelling additions to existing buildings. With light roof construction and minimal lateral force requirements, these structures performed reasonably well (Figure 4.13).

REINFORCED CONCRETE FRAME STRUCTURES

Configuration

Discussions with Greek engineers indicate that reinforced concrete frame structures have been constructed throughout Greece in all heights. In general, the connections between horizontal and vertical elements are seldom designed to resist moments produced by horizontal forces. The reinforced concrete code permits the beams to be designed for vertical loads assuming simple supports. Typical cases are shown in Figure 4.14. For example, heavy beams (widths up to 30 cm and depths up to 80 cm on 5-m spans) may be supported at ends by walls or columns with a thickness of 30 cm or less. The frame of the structure generally is very flexible since no shear walls are used. If walls are added around an elevator shaft or stairwell, the location and the effect on structural performance generally are not considered in the design. Since the elevator shaft and the stairwell are placed according to architectural needs without considering the eccentricity between the center of mass and the center of lateral resistance, severe torsional problems are usually encountered. An example of such construction is shown in Figure 4.15. Note the walls along the left side of the structure and the change in plan of the top two levels.

Due to architectural and functional reasons (and ignorance of the need for lateral resistance or ductility), the framing system in one direction in most cases is quite rigid and strong. In the perpendicular direction the difference in rigidity and strength may be dramatic

FIGURE 4.7 Undamaged build ing in Vrahati, founded on silty soil and mud. There is a small brook at left. The building is an addition to an old one in height and length. The old one is made of very good quality concrete blocks, produced locally by the owner. The mortar used for the masonry of these concrete blocks is cement and sand.

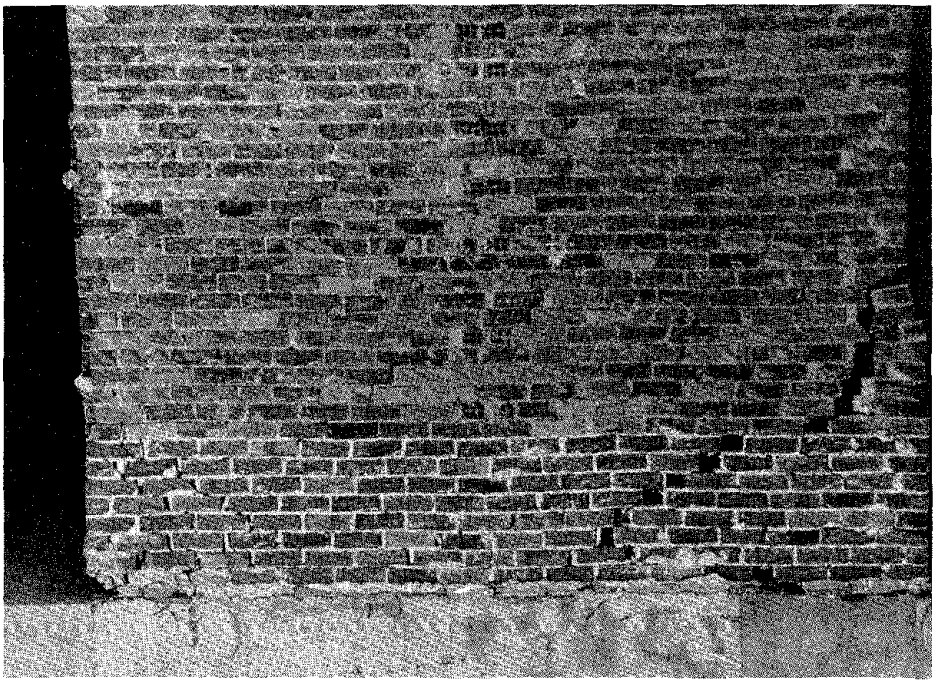

FIGURE 4.8 Solid-brick wall.

FIGURE 4.9 Unreinforced hollow brick wall in an apartment building.

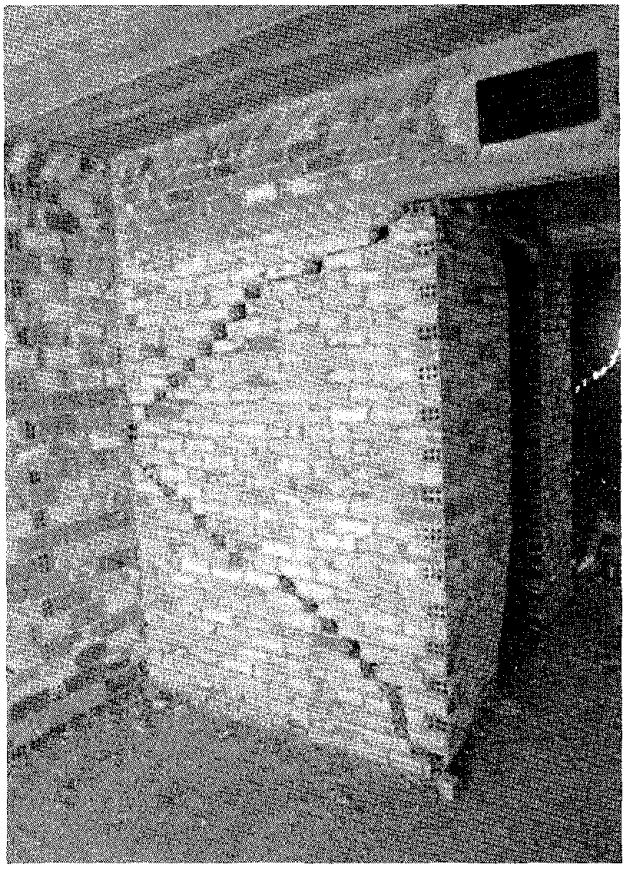

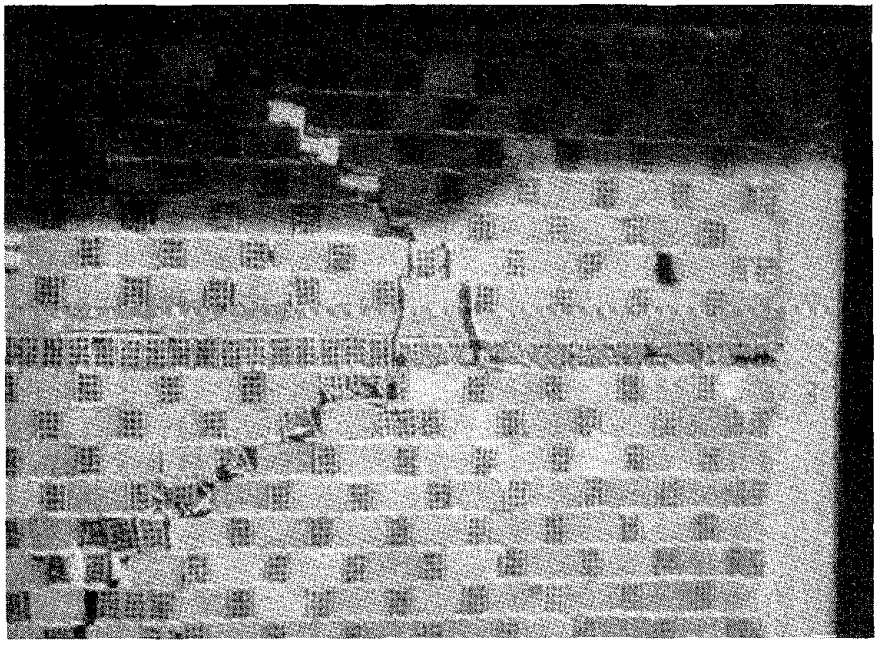

FIGURE 4.10 Hollow-brick wall with a reinforced concrete beam at the midheight of the story.

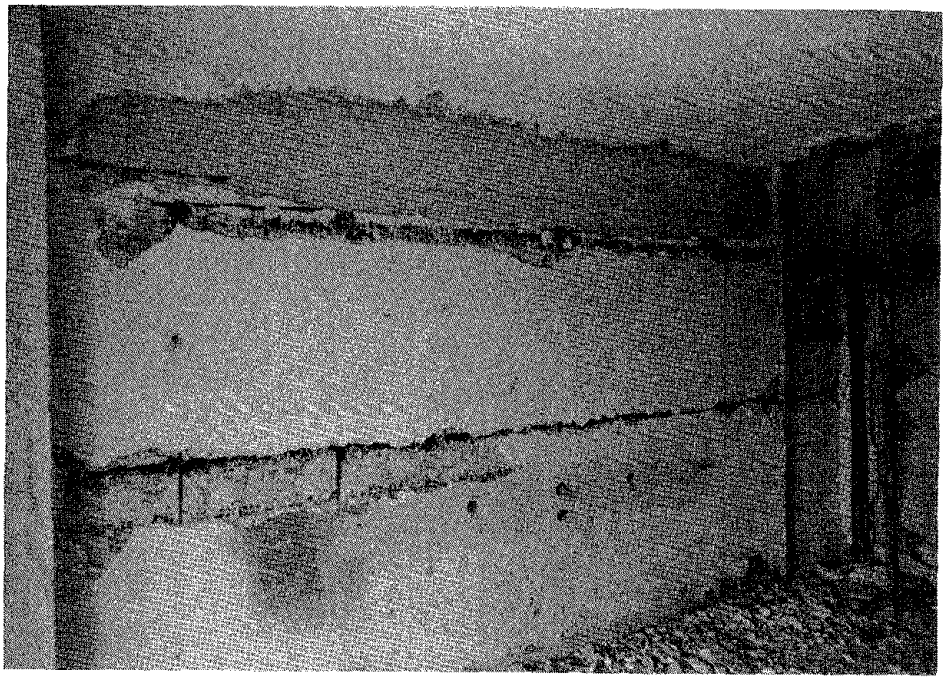

FIGURE 4.11 Brick wall reinforced by a concrete beam. The bricks under and over this beam as well as the ones at the top of the wall are crushed.

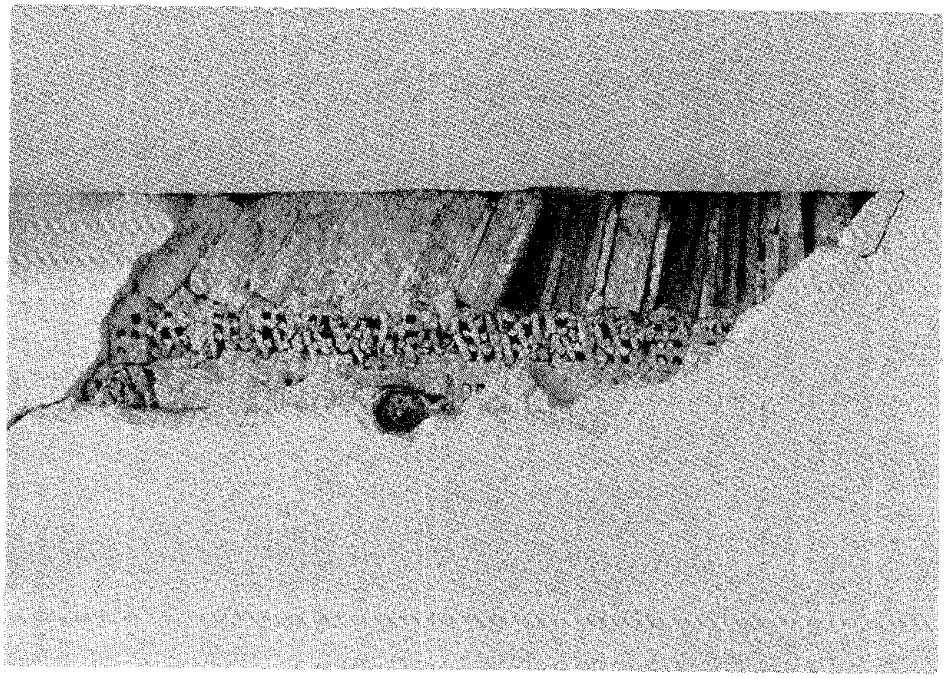

FIGURE 4.12 Detail of failure shown in Figure 4.11. Typical practice calls for the inclined bricks to be wedged under the ceiling beam. The underlying row of bricks are crushed.

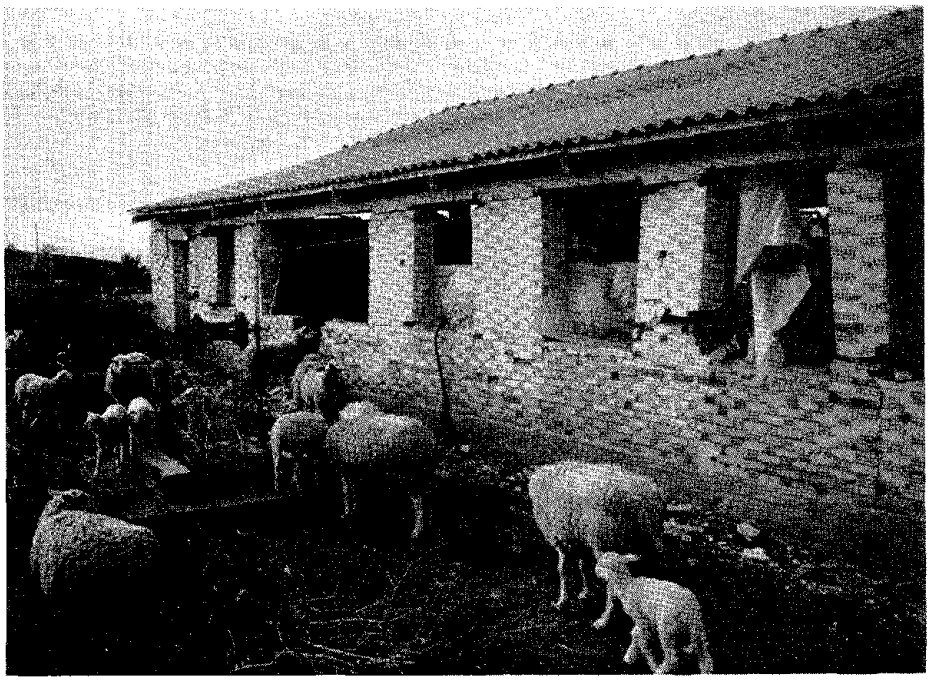

FIGURE 4.13 Farm building of block construction with light metal roof.

(Figure 4.16). For example, there are six- to eight-story buildings with slabs supported by reinforced concrete walls having a thickness of no more than 20 cm. The rigidity of the structure varies drastically in orthogonal directions. Sometimes prestressed concrete beams and slabs are used to achieve large openings without vertical elements. This is done especially in the central areas of cities. The vertical elements are placed on the line separating adjacent properties, with the weak axis parallel to the facade. In some cases flat slab construction is used without walls (Figure 4.17). Serious distress at the slab-column connections of such structures was observed (Figures 4.18 and 4.19).

In the old centers of villages and cities there is no separation between contiguous buildings. Therefore the lateral loads from the more flexible structures within a block are transmitted to the relatively more rigid structures. In a block there may be 3 to 10 buildings. The corner buildings of a block showed more damage than did the inner buildings. Away from the centers of villages and cities, where there are gardens and more free space is allowed, the buildings are separated by an open strip of more than 2 m. In some cases there was also a disparity between floor levels of adjacent structures (Figure 4.17). In such cases, hammering between buildings led to column damage (Figures 4.20 and 4.21).

Foundations

The foundations of the structures are constructed according to the quality of the soil. Generally, isolated footings are used. In regions

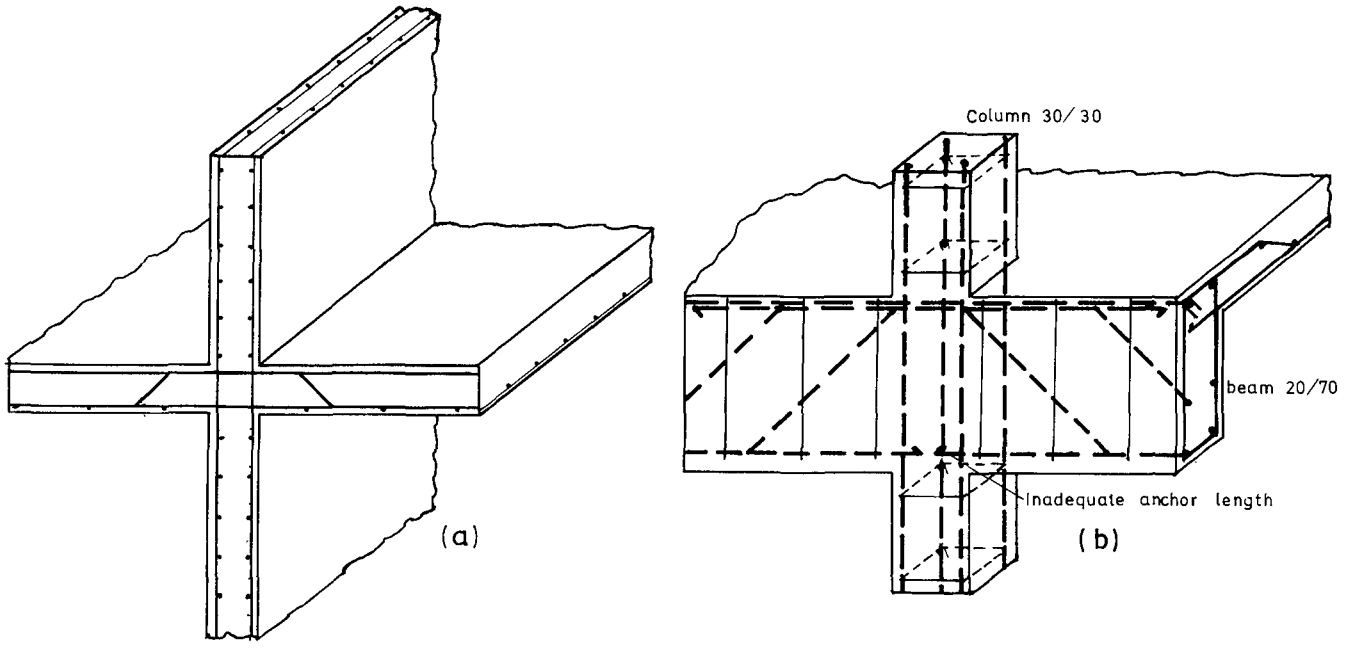

FIGURE 4.14 Typical joint between vertical and horizontal elements as usually constructed in the area. (a) Wall-slab joint. The bottom reinforcement is insufficient to resist the positive moment at the support produced by lateral forces. (b) Column-beam joint. The anchor length is inadequate because the bottom bars are not continuous through the joint.

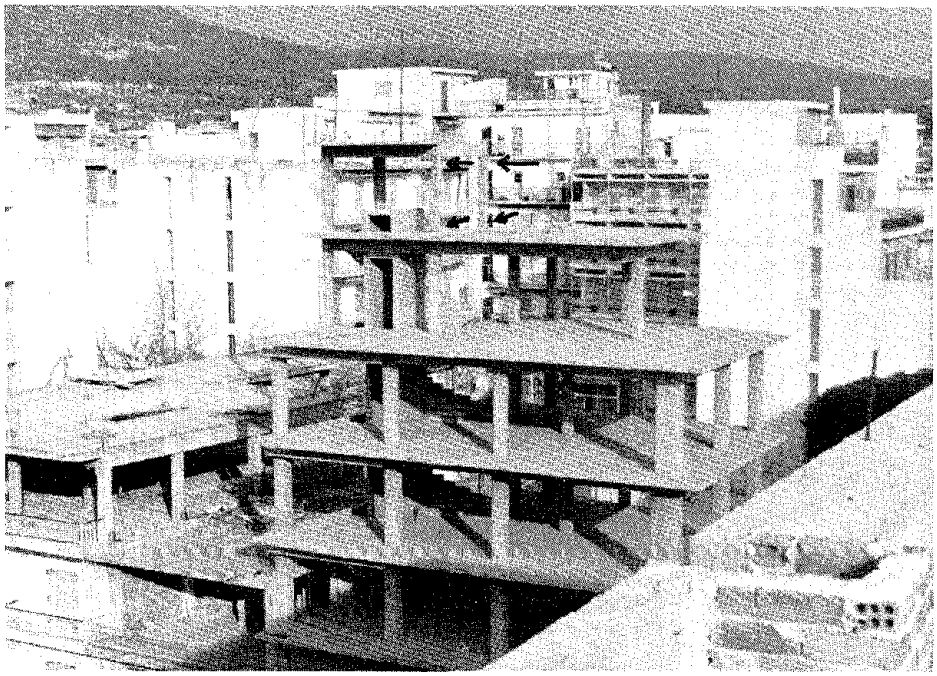

FIGURE 4.15 Eccentrically located walls in reinforced concrete frame under construction. This is a typical example of a drastic change in the plan area in a penthouse. Collapses of such penthouses were reported.

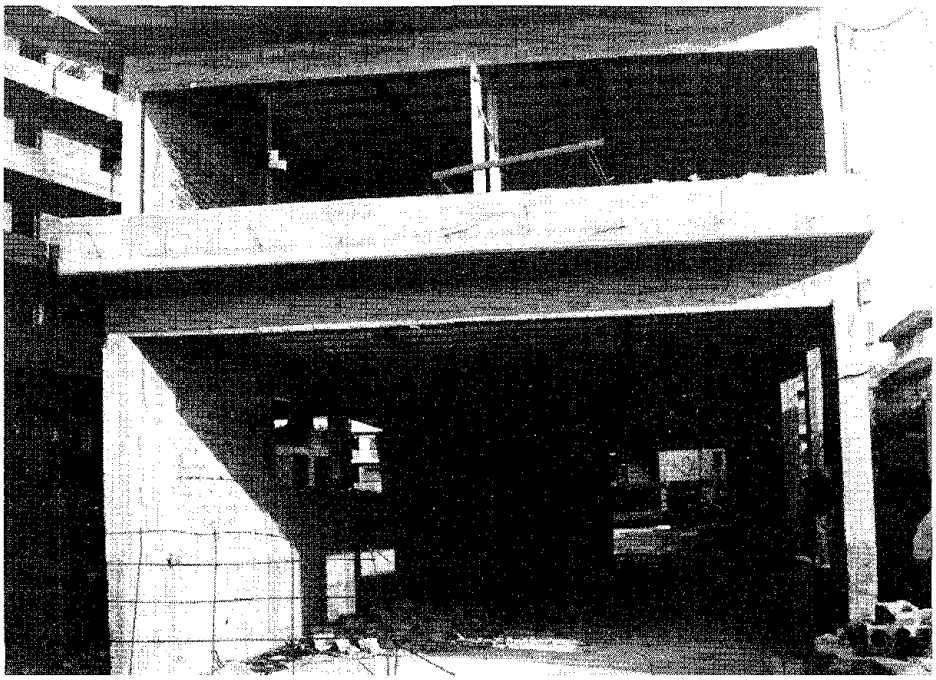

FIGURE 4.16 Difference in stiffness of framing and walls in orthogonal directions. The first story is flexible in one direction.

FIGURE 4.17 Flat slab construction without any stiffening walls in Megara. The brick walls were constructed afterward. The building suffered considerable damage with permanent deformations.

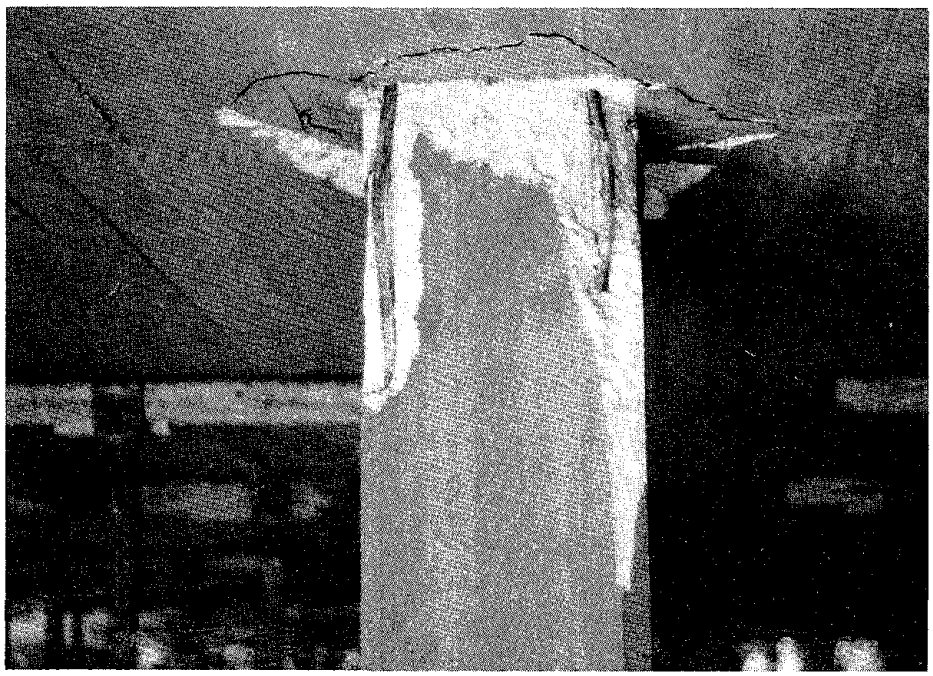

FIGURE 4.18 Typical damage of column-to-slab connections. This shows detail of damage to the building on the left in Figure 4.17.

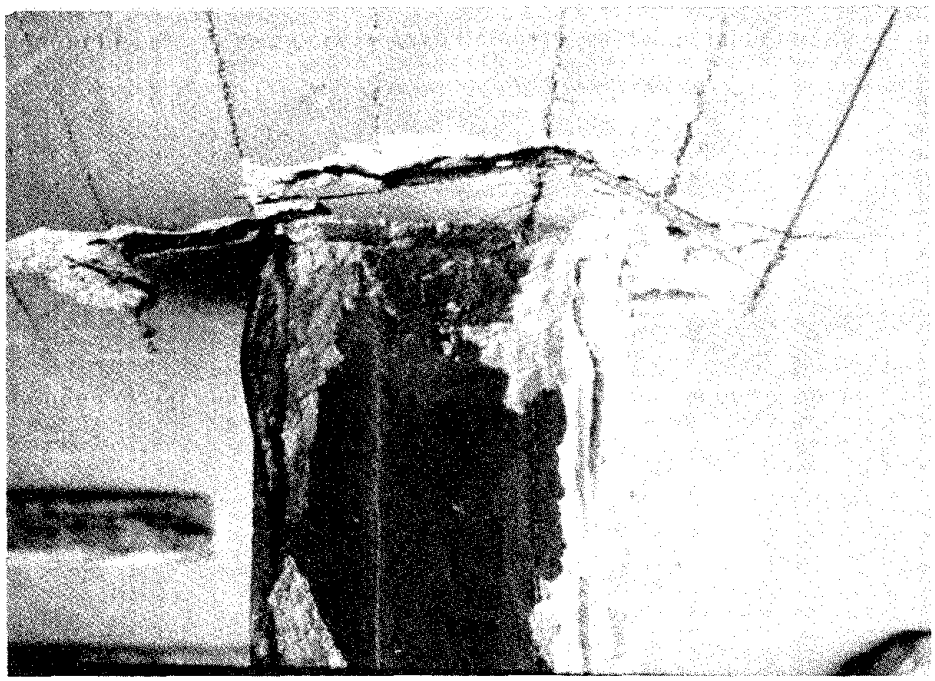

FIGURE 4.19 Typical damage of column-to-slab connections. A steel plate has been fixed at the top of the column to add support.

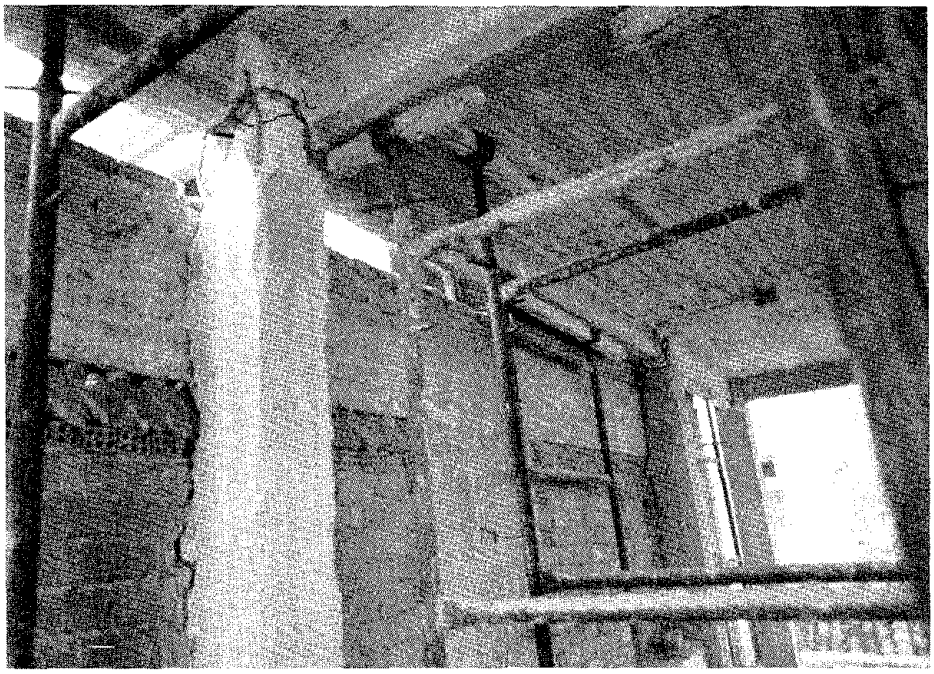

FIGURE 4.20 Hammer effect between two adjacent buildings not separated in Megara.

of high seismicity and poor soils, grade beams between the bottom of the foundation and the lower part of the column at the level of the ground floor are recommended by the code and used in most structures (Figure 4.22).

Materials and Quality of Construction

The quality of the materials used in reinforced concrete structures is specified according to the German Code DIN 1045. Until 1950 to 1960, typical concrete strength was 120 kg/cm^2 (1.7 ksi) and steel yield/ultimate strengths were 2,200/3,400 kg/cm^2 (31/48 ksi). Later the quality of concrete was improved to 160 kg/cm^2 (2.3 ksi), and during the last 10 years 225 kg/cm^2 (3.2 ksi) has been used extensively. Steel strengths of 4,200/5,000 kg/cm^2 (60/71 ksi) are used for all members. Steel mesh with a strength of 5,000/5,500 kg/cm^2 (71/78 ksi) is used for slabs and walls. For walls the mesh is placed in both faces and between the main reinforcement at the corners.

Local failures at the ends of columns and in joints were observed in many structures. These failures can be attributed to poor construction practices--in some cases poor-quality concrete, but in others lack of attention to details. Figure 4.23 shows a failure at the bottom of a column. Note the closely spaced column bars and lack of transverse ties. Figure 4.24 shows a local column failure initiated by an anchorage detail. Columns from the lower story extend through the floor and terminate in hooks when mild steel (22 to 34 kg/mm^2) is used. Under lateral forces the hooked bars opened and caused spalling of the concrete that was not confined by lateral ties. Nearly complete deterioration of column bars due to rust is shown in Figure 4.25. Figure 4.26 shows a construction joint at the middle of a column containing rubbish. The consequences of inadequate transverse reinforcement in the joints of frames is illustrated in Figure 4.27. Figure 4.28 shows the manner in which utilities (electrical conduits) were installed in an infilled frame structure.

Partitions and Infill Walls

Partitions and infill walls are generally of hollow bricks or hollow concrete blocks. The presence of infill walls, their position and extent in the plan, the quality of the walls, and the interaction of infill walls with the frame substantially affect the seismic response of the whole structure.

In the case of the apartment buildings with partitions extending throughout the height of the structure, good-quality infill walls often improve the overall response of the structure. The walls absorb a considerable amount of energy and may act as the primary system for transmitting earthquake forces to the ground. However, the response of the frame and masonry walls combined will not be favorable if the seismic forces exceed the strength of the masonry. Under initial seismic motions, high loads may be developed in the structure due to temporarily high stiffness, as shown in Figure 4.29. When the brittle

FIGURE 4.21 Detail of the damaged column in Figure 4.20. Note the gap between the two buildings after the earthquake.

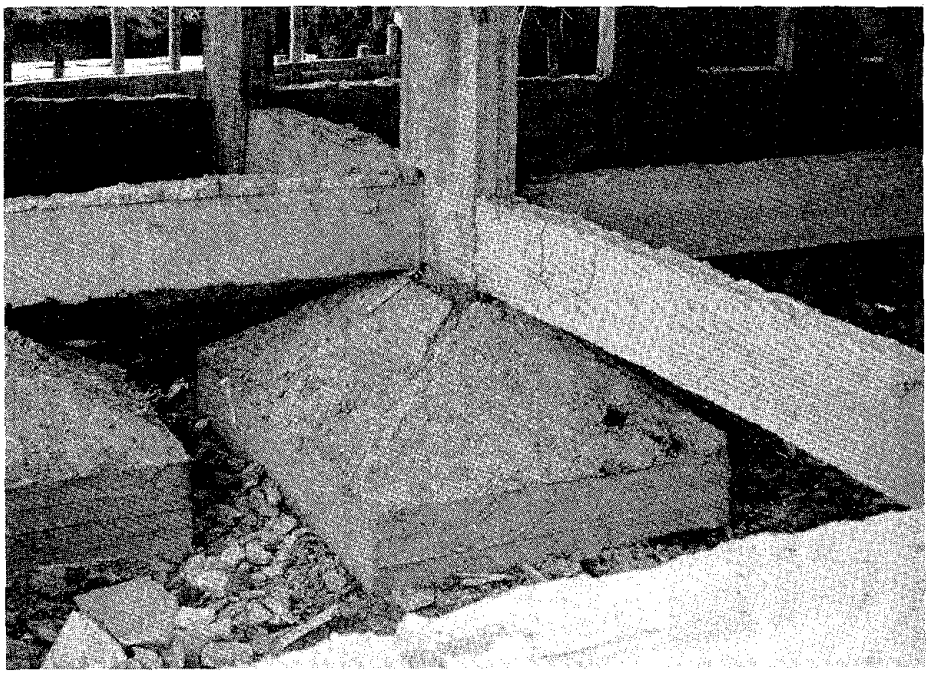

FIGURE 4.22 Spread footings with grade beams.

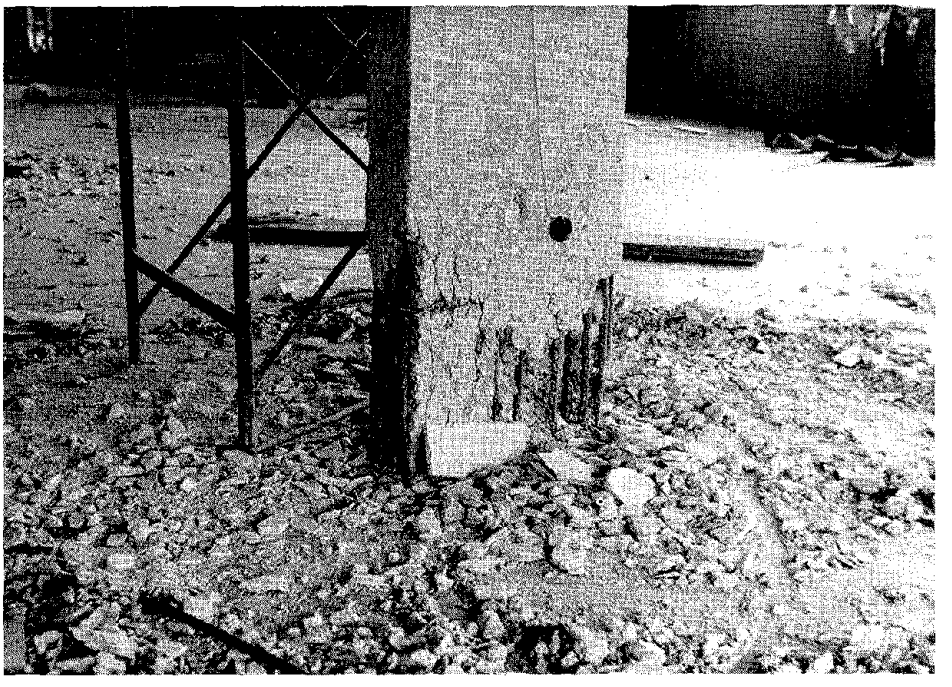

FIGURE 4.23 Poor quality concrete, too many bars, inappropriate aggregate gradation, and poor consolidation.

FIGURE 4.24 Poor detailing--too many steel bars appear in the lower part of the column. Most of the bars are from the lower story. The hooks opened and initiated the damage.

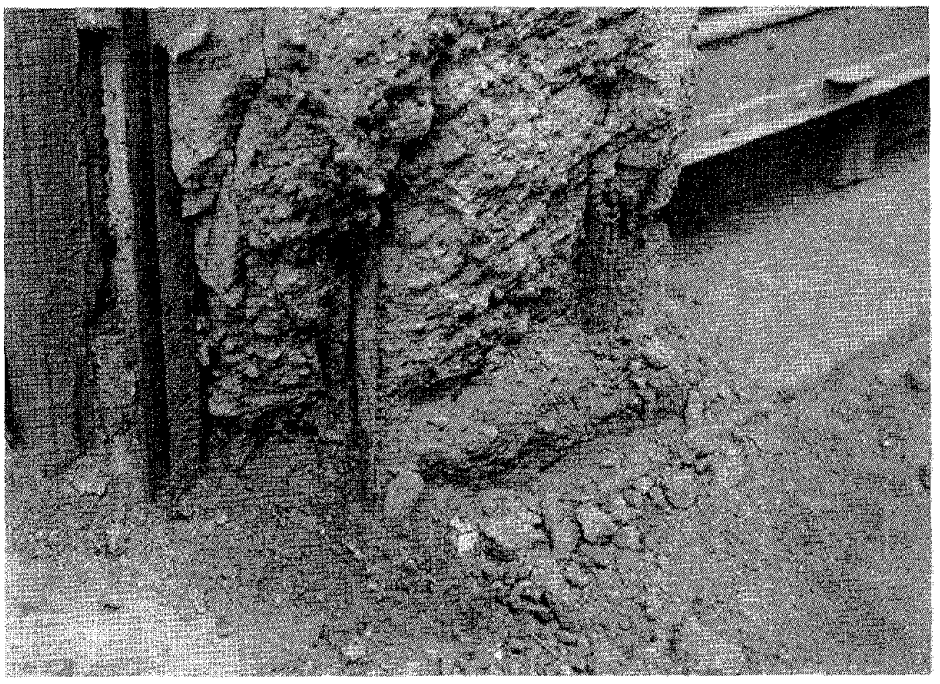

FIGURE 4.25 Nearly complete rusting of reinforcing steel bars at the bottom of a column, due to poor concrete quality.

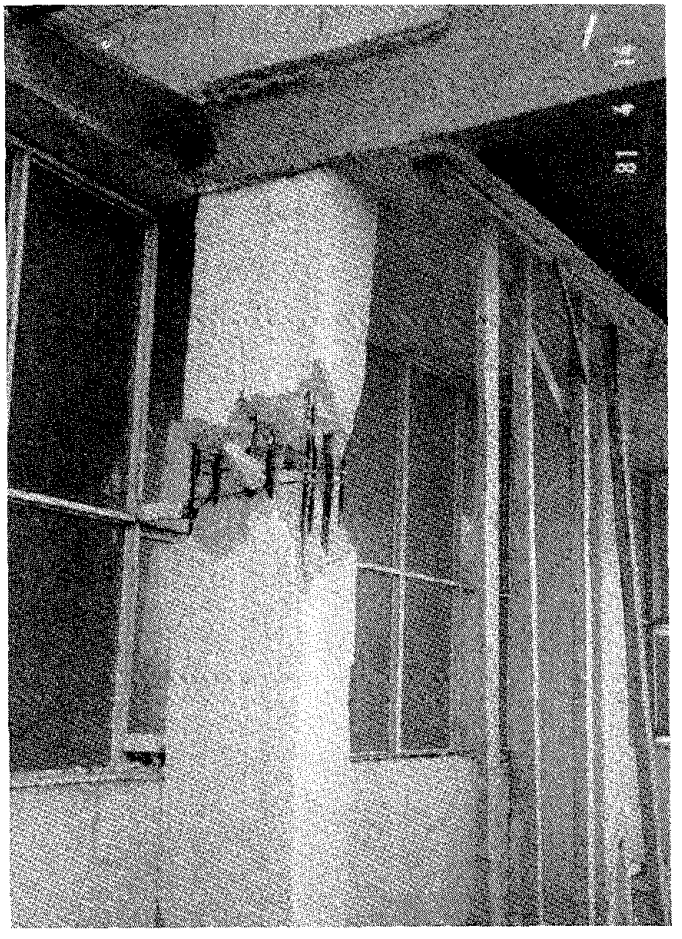

FIGURE 4.26 Typical case of damage to construction joint in the block of flats in Loutraki. Various kinds of rubbish were found in these joints in addition to steel and concrete.

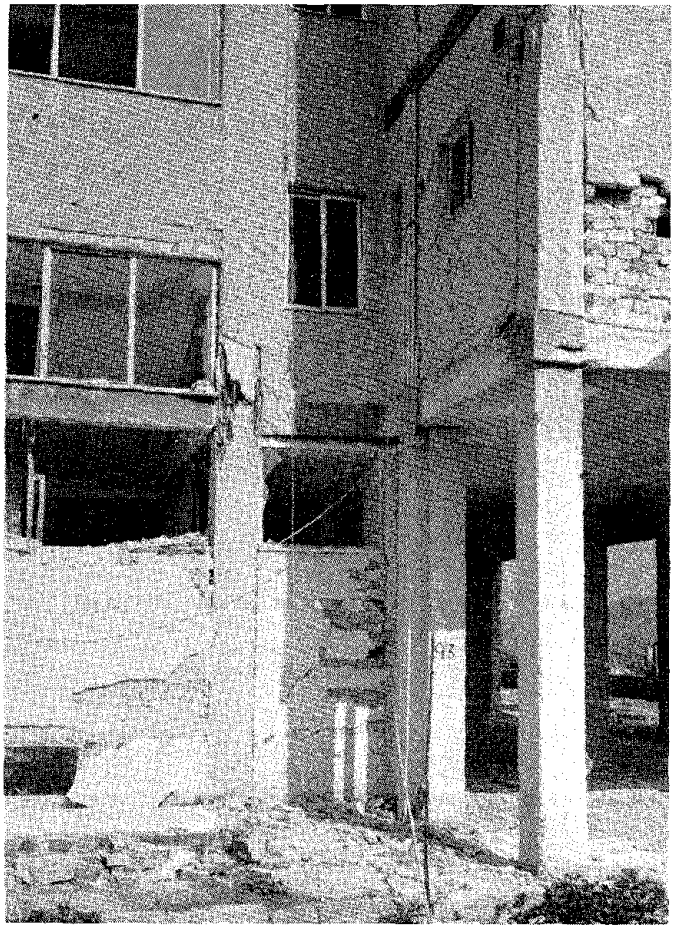

FIGURE 4.27 Typical damage of the column-to-beam connections in the block of flats in Loutraki. The lack of ties at the connections is common.

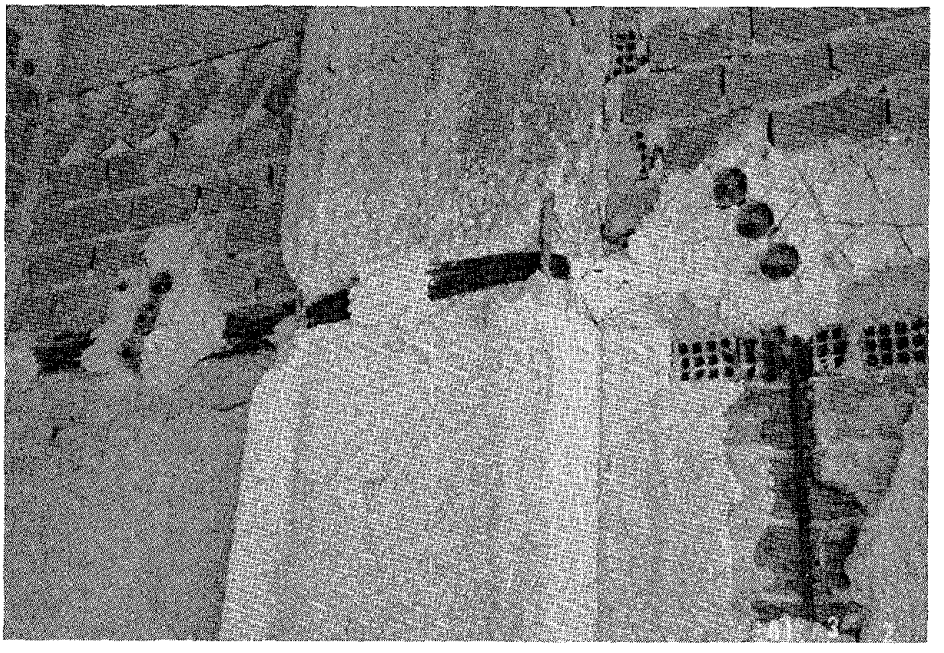

FIGURE 4.28 Conduits for electric cables pass through the column just inside the reinforcing bars and along the brick walls through channels chipped into the column and walls.

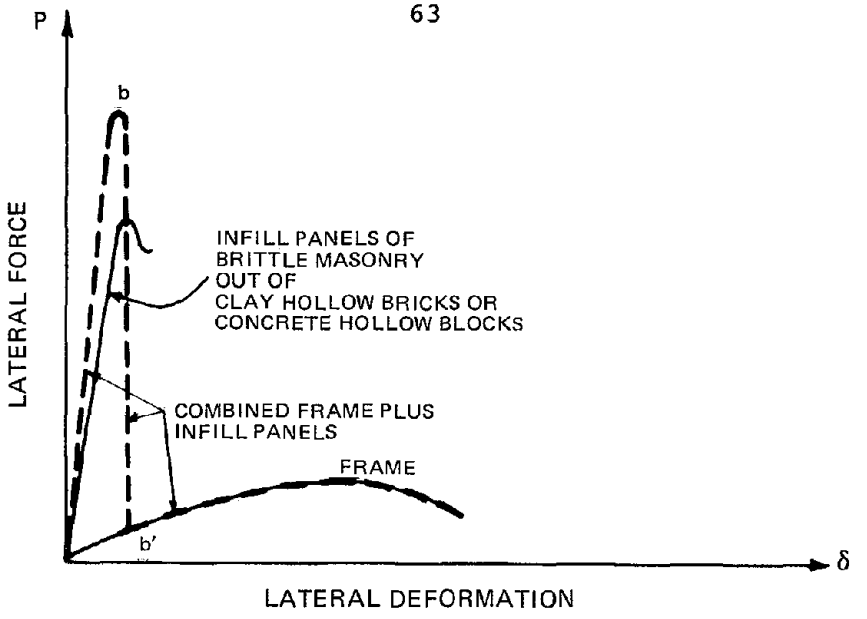

FIGURE 4.29 A combined reinforced concrete flexible frame plus brittle infill panels produces a stiff and brittle structure.

masonry units fail, the frame alone must resist the lateral forces and deformations. The rupture of the masonry wall often extends through the columns, which also fail in shear as shown in Figure 4.30.

The size and quality of the bricks or blocks, the quality of the mortar used, and the manner in which they are joined are of primary consideration. Generally, it was observed that the smaller the size of the bricks or blocks, the better the performance. With small good-quality bricks or blocks, shear cracks followed the mortar along the horizontal and vertical joints instead of forming a diagonal crack through the bricks (Figure 4.31).

Flexible First Story

Many structures in the area consist of a rigid superstructure supported by a very weak and flexible first story, e.g. apartment buildings with a shop or a parking space on the first story. In general, the first floor is not considered suitable for habitation. Such configurations are very popular in Greece, and this type of construction is termed "sur pilotis" after the French terminology. The rigidity of the structure above the first story is due to (1) the existence of many partitions in both directions (Figure 4.32), (2) the relatively low story height, and (3) the presence of many deep beams (Figure 4.33). However, the reinforced concrete or masonry walls existing in the superstructure are discontinued in the first story. The performance of this type of structure during the February-March 1981 earthquakes was generally poor. Large, often inelastic displacements occurred in the first story, leading to considerable damage there (Figure 4.34). The presence of strong beams at the top and bottom of first-story columns produced more serious damage. With weak beams, damage extended to the second story,

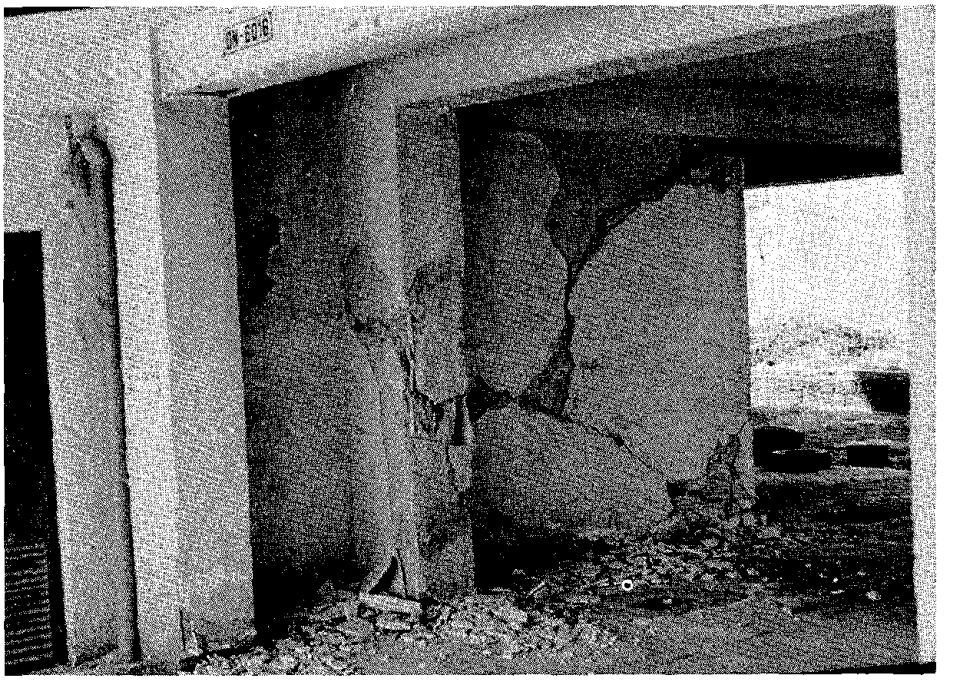

FIGURE 4.30 Typical shear failure of reinforced concrete column confined by a brick wall. The rupture of the masonry extends through the column.

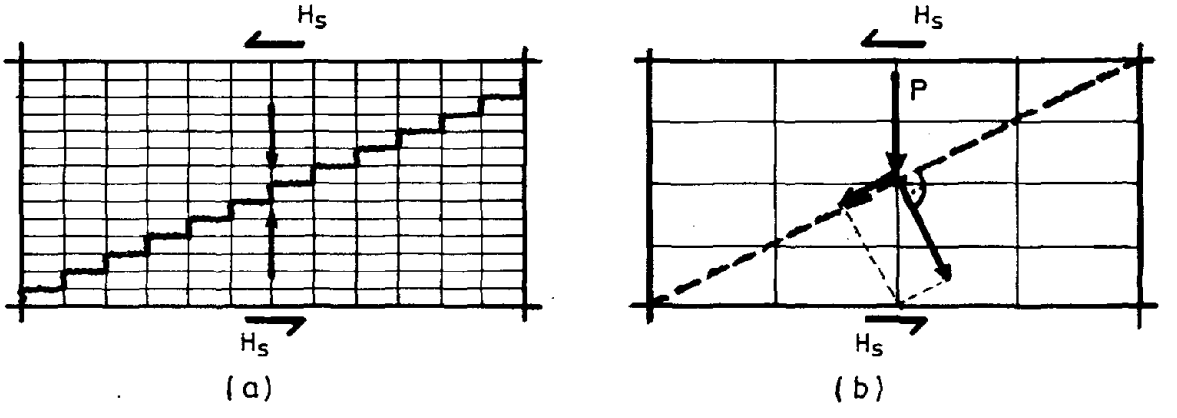

FIGURE 4.31 Infill panels with (a) small-sized good-quality bricks or concrete blocks, with cracks in joints (vertical loading transmitted to foundation), and (b) large and/or poor-quality bricks or concrete blocks, with diagonal cracks (vertical loading produces sliding forces).

FIGURE 4.32 Typical apartment house with an open first story and no shear walls. The floor beams are flexible and the story heights are low.

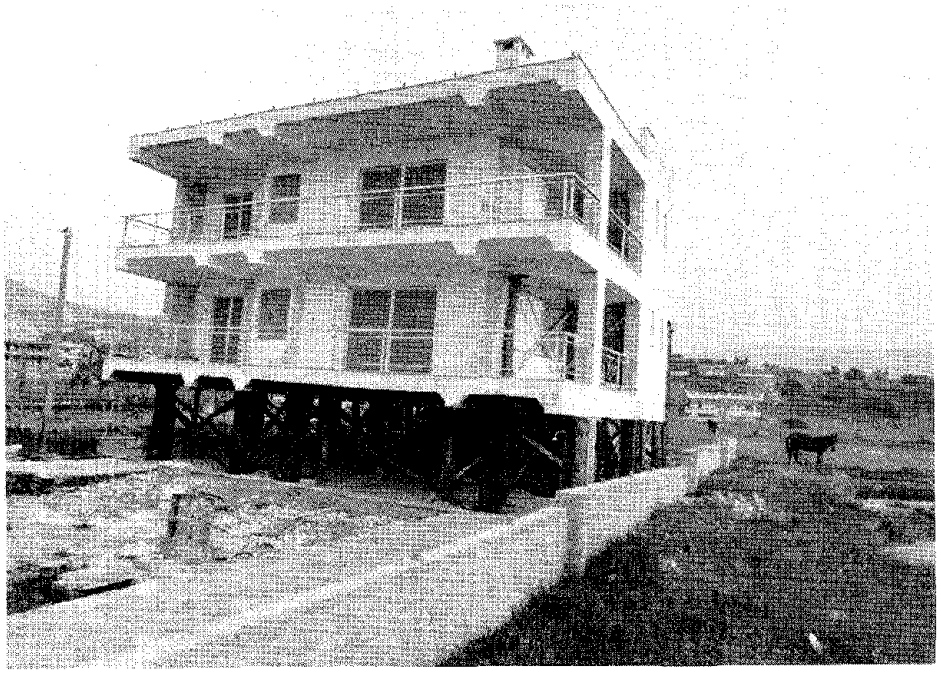

FIGURE 4.33 Modern resort apartment building in Alepohori with open first story. The damage was limited to the lower story. The heavy scaffolding (placed after the earthquake) consists of H-shaped steel beams.

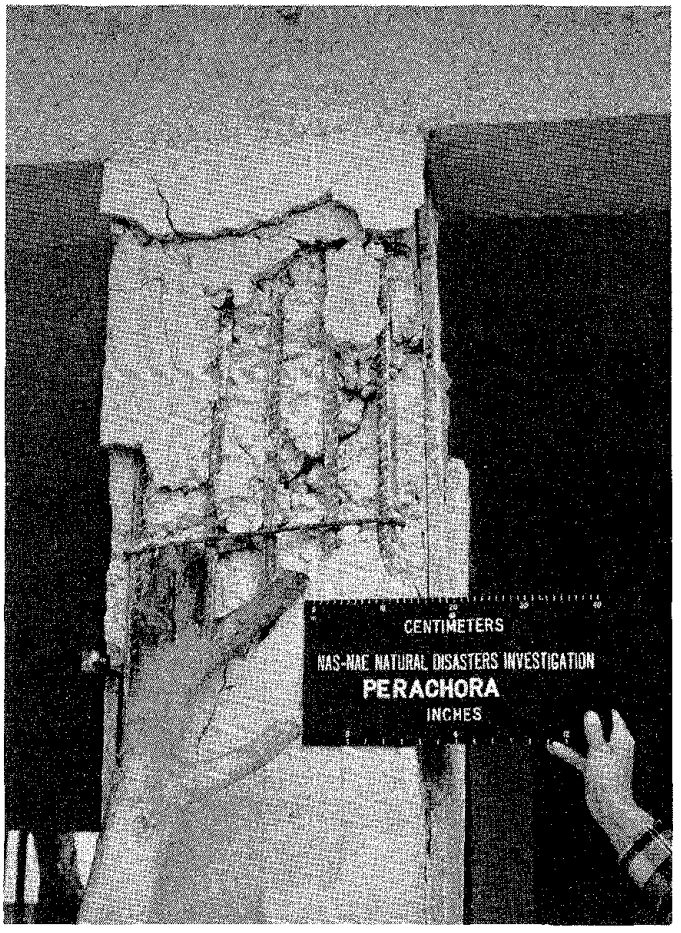

FIGURE 4.34 Column shear failure in first-floor column.

sometimes to the third and upper stories, and to the foundation as well, as shown in Figure 4.35.

Damage to "pilotis" multistory construction was common. Serious damage was observed in Loutraki, Halandri (a suburb northeast of Athens), Kiato, and Anthoupolis (a suburb west of Athens). In some cases apartment buildings with masonry walls extending throughout the height exhibited limited cracking while adjacent buildings with an open first story were heavily damaged. Two- to three-story apartment buildings collapsed or were damaged beyond repair in Pisia, Alepohori, Kineta, Kiato, Plataeae, Erythrae, Thebae, and Corinth, although some nearby stone masonry structures of the same height did not even crack.

As indicated above, the response of structures with a reinforced concrete frame and infill panels was influenced by many factors. For such a structure to be earthquake resistant requires sound design and good construction techniques (Figure 4.36). The construction of buildings with a flexible reinforced concrete frame demands quality design, detailing, and execution. The cost of such construction will

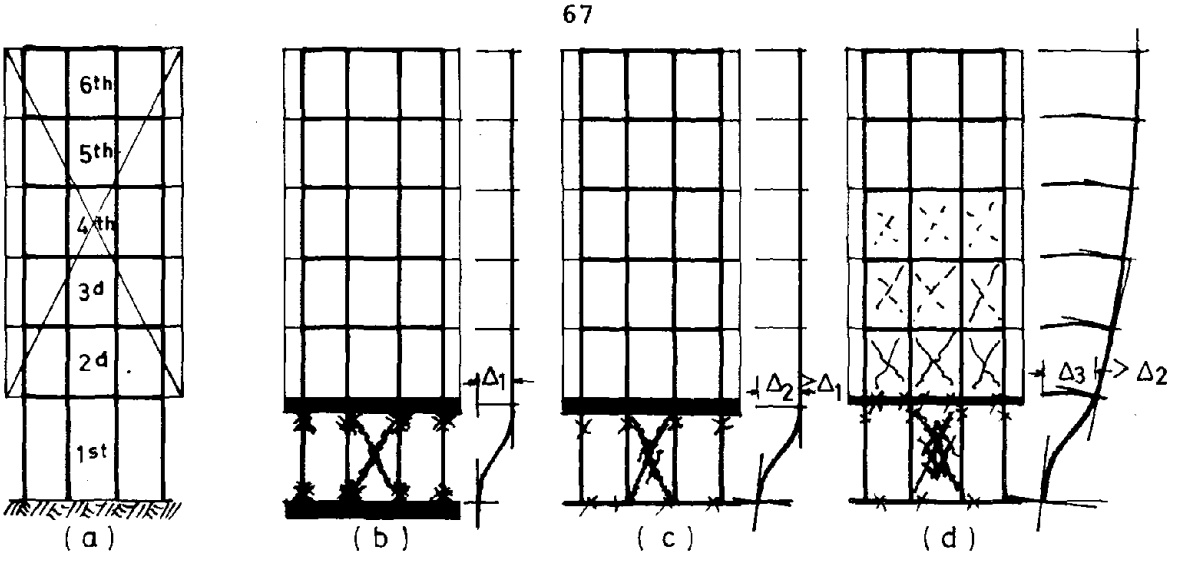

FIGURE 4.35 Typical deformation damage pattern of structures with flexible reinforced concrete frame, masonry infill panels, and an open first story: (a) elevation view; (b) strong top and bottom beams, with extended damages in the first story only; (c) strong top and weak bottom beams, with more damage in nonstructural elements and concrete walls, less damage in top parts of the columns of the first story only, and damage in the foundation; and (d) weak top and bottom beams, with more damage in nonstructural elements and concrete walls than in case (c), less damage in columns than in case (c), and extension of damage in upper stories.

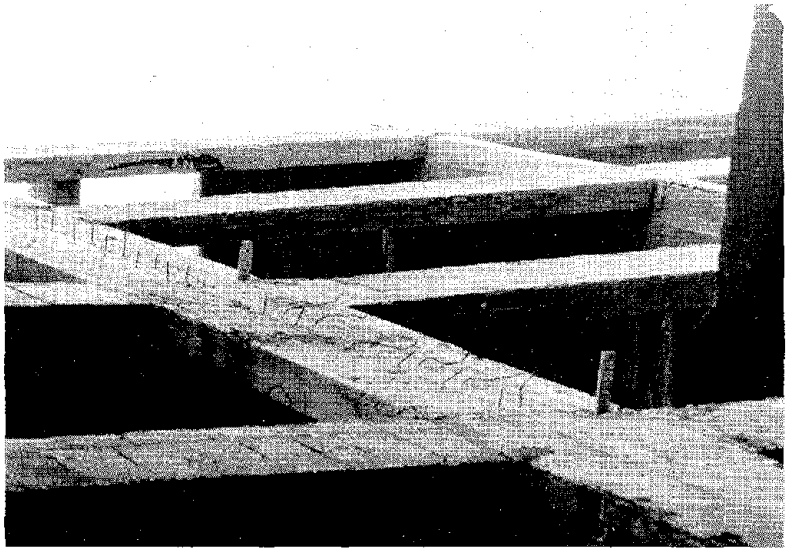

FIGURE 4.36 Poor construction quality in reinforced concrete frame. The columns run from lower right to upper left. The beams are roughly horizontal in this photograph.

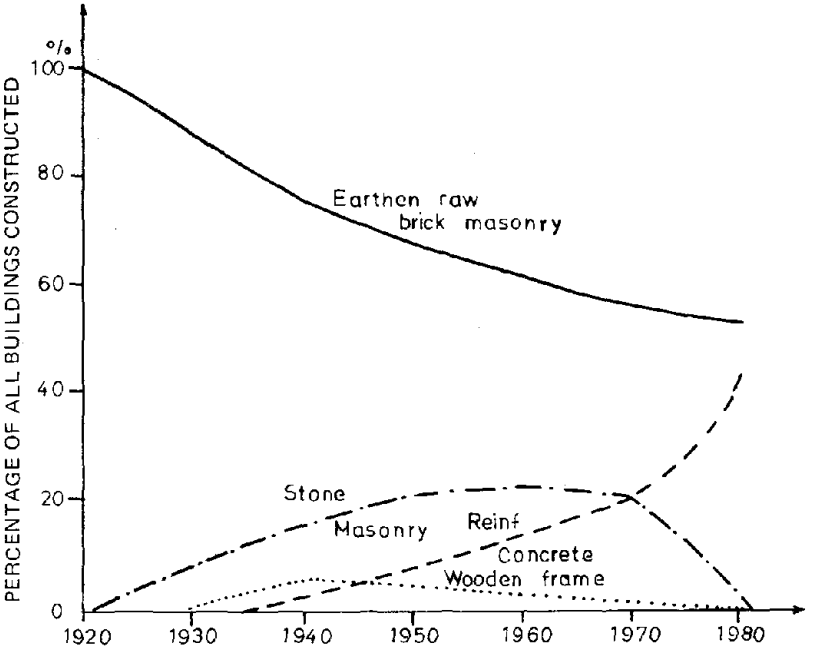

FIGURE 4.37 Statistics for the city of Kiato of various types of buildings since 1920.

likely be higher than that for a rigid structure. It should be noted that in these earthquakes rigid structures generally performed better than did flexible structures, even when the quality of the rigid construction was inferior to that of the flexible structures.

BUILDING TRENDS

The number of earthen and stone masonry buildings is diminishing with time. Priority is being given to structures with a reinforced concrete frame with infill panels. The results of a limited survey in the city of Kiato are presented in Figure 4.37. The percentage of buildings with reinforced concrete frames is rapidly increasing. With reconstruction following the 1981 earthquakes, 80 percent of the buildings in Kiato will have reinforced concrete frames.

5

OBSERVATIONS OF DAMAGE

The February-March 1981 earthquake damage was concentrated primarily in the towns and villages located around the eastern end of the Gulf of Corinth (Figure 1.2). Some damage was observed along the coast of the Saronic Gulf west of Athens. Several villages between the Gulf of Corinth and Thebae were devastated by the March 4 event.

Prior to describing the damage by locality, some general comments may serve to provide background or reasons why some types of damage were observed in many structures. Four general categories may be identified, but specific damage may be the result of a combination of more than one effect. Many examples of the behavior of structures are given in Chapter 4.

1. Concept or Synthesis of the Whole Structure and Interaction Between Adjacent Structures

- o Hammering between adjacent buildings due to inadequate free space between them (primarily local damage) (Figures 4.20 and 4.21).
- o A domino effect produced by collapse or heavy damage of adjacent buildings.
- o Inconsistency between the deformability of a structure and its materials and connections (Figure 4.32).
- o Flat slab reinforced concrete construction without shear walls or stiffening elements (Figures 4.17, 4.18, and 4.19).
- o Lack of redundancy in the framing system.
- o Drastic change in the plan area, especially in penthouses (Figure 4.15).
- o Eccentricity between center of torsion and center of mass due to geometry of structural system.

2. Influence of Secondary Systems and Interaction with the Framing Systems

- o Action of infill walls with the adjacent vertical or horizontal elements of the framing system (Figures 4.10, 4.11, 4.12).

o Creation of stiffer stories than the adjacent ones with the construction of many infill walls.

o Creation of short columns by infills or panels of partial story height.

o Eccentricities in the plan due to infill walls.

3. Design Detailing and Quality of Construction

o Inadequate dimensions of cross sections of the members of the framing system, beams, columns, walls, connections, etc.

o Inadequate number and/or size of longitudinal or transverse reinforcing bars in members or joints (Figures 4.27 and 4.34).

o Poor quality of materials and workmanship (Figures 4.24 and 4.25).

o Poor installation techniques for utilities (Figure 4.28).

o Improper formation of construction joints in concreting, in extending the reinforcing bars, or in changing the shape and diameter of reinforcement (Figures 4.24 and 4.26).

4. Severity and Direction of Ground Motion

The fourth category should not be considered alone, since the response of a structure is a combination of the characteristics of the structure and of the ground motion.

GULF OF CORINTH

The Gulf of Corinth is bordered by a beautiful coastline with numerous resort towns that are visited in season by the population of nearby Athens. Loutraki and Corinth are the largest towns located at the southeastern end of the gulf near the mouth of the Corinth Canal. Corinth is a regional business and commercial center as well as a seaport. Loutraki is a seaside resort on the shores of the Gulf of Corinth at the foot of the Gherania Mountains. The city has grown as a seasonal resort, with numerous high-rise (6- to 10-story) apartment buildings and resort hotels situated along the seashore. The residential homes are scattered behind the city on a gradual slope up to the mountains behind.

The last strong earthquake in the area occurred in 1928 (with a magnitude of 6.2+), but smaller quakes have occurred periodically. Historically, many earthquakes have devastated Corinth (see Appendix A). A great earthquake in 1858 destroyed ancient Corinth, and the present town was established on the coast 6 km northwest of the site of the ancient city. Loutraki reportedly was also damaged in this earthquake.

As reported by the government, damage from the February 24 and 25, 1981, earthquakes in the Corinth Prefecture was 375 buildings regarded as ready to collapse or destroyed. In Loutraki 197 buildings were reported destroyed or dangerous, and in Corinth 189 buildings were so reported.

LOUTRAKI

The mostly heavily damaged part of the city of Loutraki was along the southern seashore, which constitutes about one third of the total shore length of the town. Most of the damages were observed within the triangle ABC in Figure 5.1. There were two total collapses (the Contis Hotel, marked 1; the Apollo Hotel, marked 3), one partial collapse (the block of flats Segas, marked 2), and other heavily damaged structures. The area within the triangle ABC is a new section of the city mostly built after 1960. This area was recently included into the official town plan. The city extends to the east, to the north, and then to the northwest of the triangle ABC. Damage decreased rapidly with distance from the coast.

Andronopoulos (1982) gives a brief description of the geological conditions:

> Under the surface soil layer (0.5-1.5 m) we meet loose fluvial or torrent deposits with a varying depth (between 4-40 m). They are

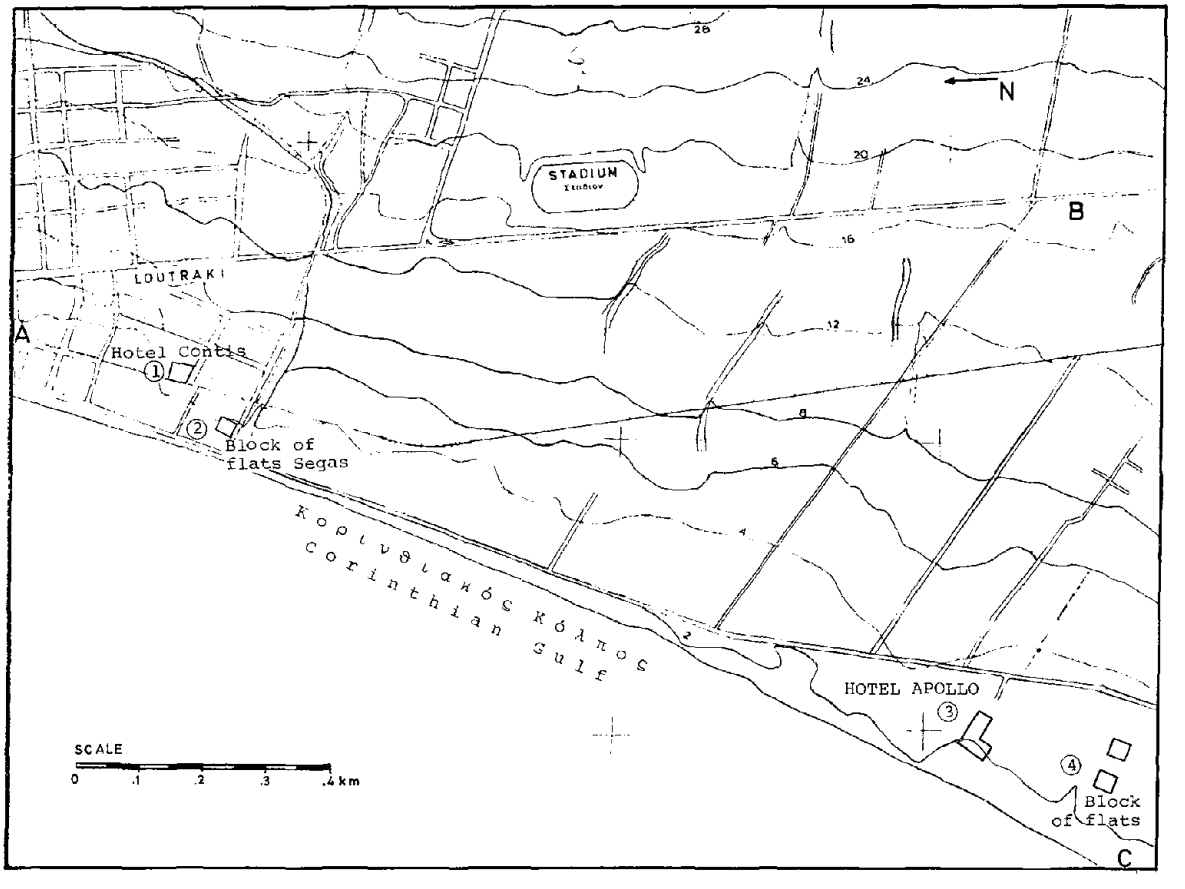

FIGURE 5.1 Topographic diagram of the south part of Loutraki.

marked by a rapid variation--lateral and vertical--of the lithologic composition and granulometry as well as of the depth of the formation.

They are composed of silty clay, sand, and debris from solid, consistent rocks (limestone, shale, etc.).

Under these deposits we find a bedding of immature clays and marls. The depth where they are first met depends on the thickness of the above-mentioned cover by the various deposits. At some positions they are found at a depth of just a few meters (e.g., 4 m at the area of Contis Hotel, 6-7 m at the area of Apollo Hotel). These conclusions are based on the interpretation of some geophysical tests and on the general knowledge of the geology of the area. There are not (as there should be) any data from drillings to help the evaluation of the results of the geophysical tests.

We may conclude that the ground of foundation at the Contis Hotel must consist of layers 2-3 m thick of loose, coarse material, while at the Apollo Hotel the layers of the same material are a little thicker (3-4 m). These loose deposits with their relatively small thickness lay over the immature marls which have a completely different behavior and response.

Figure 5.2 shows a collapsed five-story building known as the Segas block of flats. The first-story columns punched through or collapsed (Figure 5.3). The upper four stories are relatively intact except on the south side, where lower columns failed and allowed the upper floors to collapse. This structure is described in greater detail in Chapter 6.

Another new apartment building in the same region, shown in Figure 5.4, suffered damage to the wide columns in the first story. This building was constructed in the "pilotis" scheme with the lowest floor relatively free of partitions; in the floors above, the concrete frame was infilled with very stiff unreinforced masonry walls. The wide column shown in Figure 5.5 was stiffer than adjacent columns and attracted a greater portion of the lateral force, which resulted in the shear cracking shown.

Figure 5.6 shows the Contis Hotel, which collapsed in the central part of the city. The structure consisted of slab and beam construction, and the failure of the columns caused a total collapse of the building. The columns contained smooth reinforcing bars and widely spaced wire ties. The Apollo Hotel south of Loutraki was a large eight-story resort hotel that totally collapsed (Figure 5.7). The destruction was so complete that the structural system could not be easily identified. It appeared to be a reinforced concrete frame with infill walls. Both hotel failures are described in more detail in Chapter 6.

Along the seashore, damage to quays was observed. Figure 5.8 indicates the substantial settlement that occurred.

FIGURE 5.2 Partially collapsed five-story block of flats "Segas" in Loutraki. (Note temporary tent shelters in foreground.)

FIGURE 5.3 Failure of first-story columns.

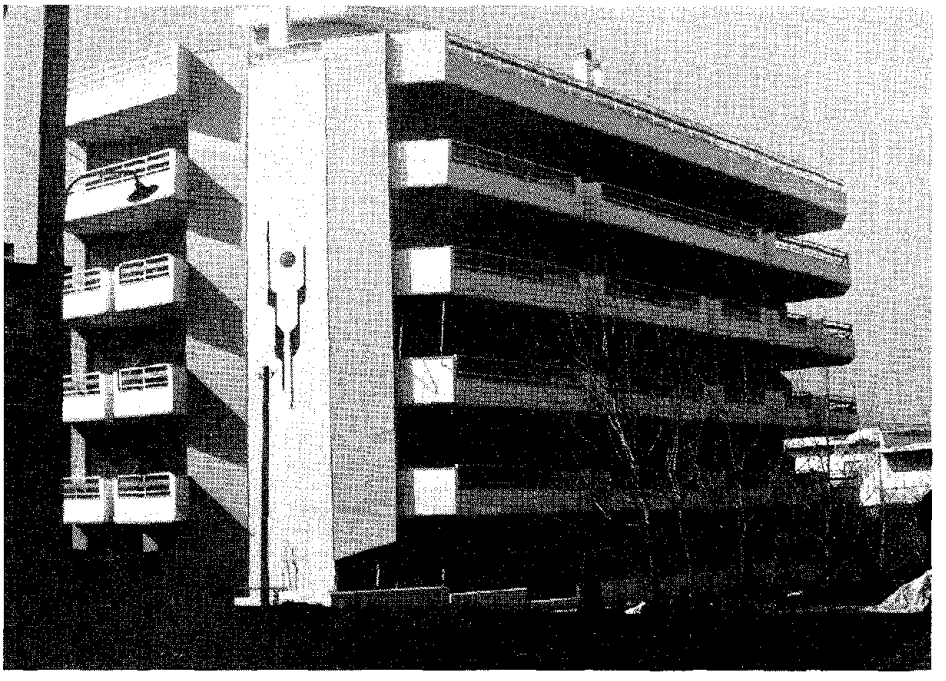

FIGURE 5.4 New apartment building with "pilotis" construction in Loutraki.

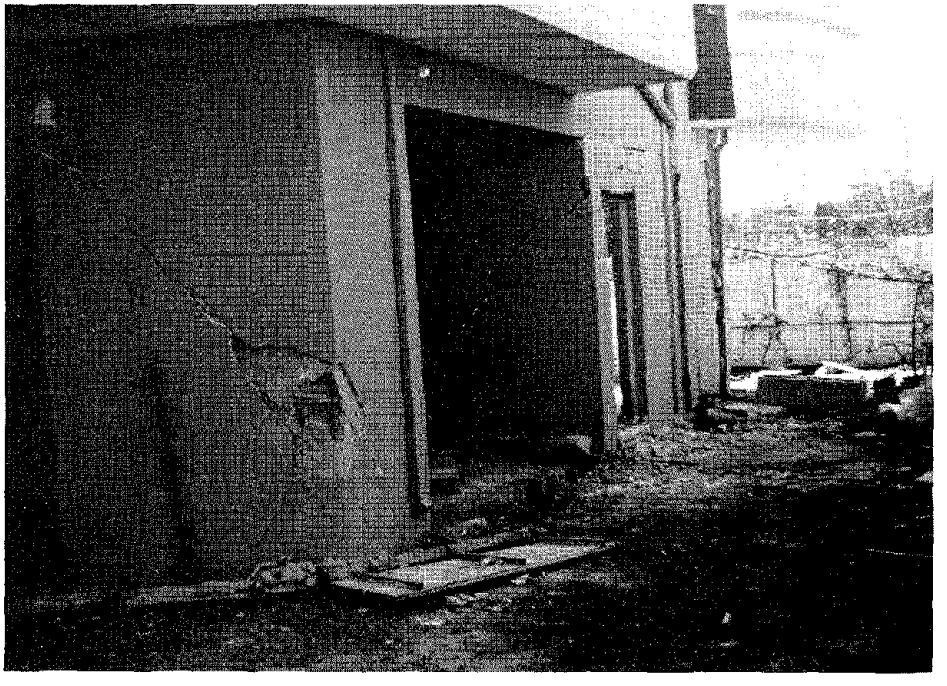

FIGURE 5.5 Failed wide column.

FIGURE 5.6 Collapse of Contis Hotel in Loutraki.

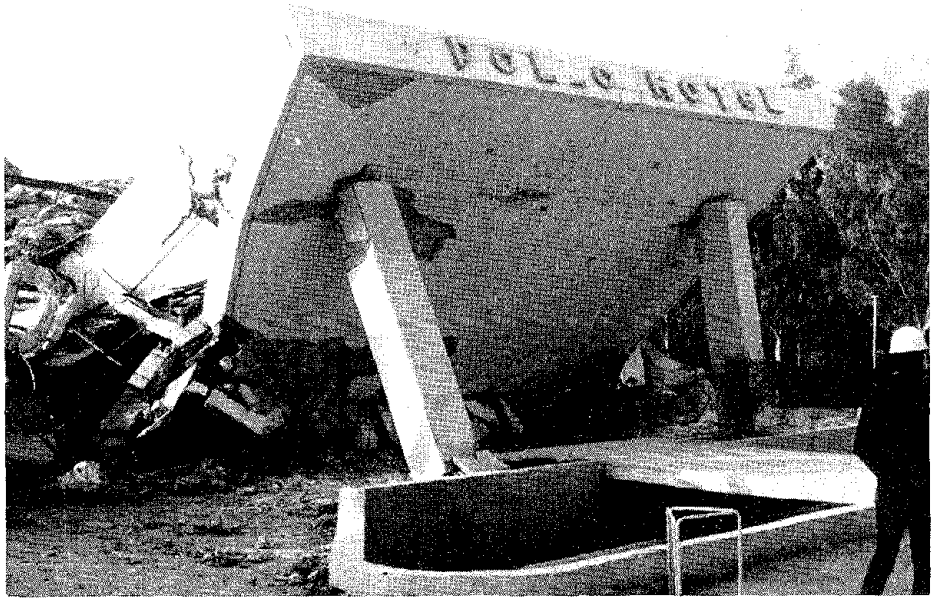

FIGURE 5.7 Collapse of Apollo Hotel in Loutraki.

FIGURE 5.8 Quay wall in Loutraki. The earthen embankment has settled quite substantially.

PERAHORA AND SHINOS

Above Loutraki in a small plain in the mountains is the village of Perahora. Of the approximately 500 houses in the village, 150 collapsed. Only three or four people were killed. The typical older houses were constructed of stone and mud with thick walls and tile roofs over wood framing. The collapse of many of these buildings was almost total, as shown in Figure 5.9. Damage to a three-story reinforced concrete frame house is shown in Figure 5.10. The structure was built on a hillside with the footing at the back, so that it functions as the axis of rotation. Figure 5.11 shows the complete collapse of a reinforced concrete house in the village of Shinos, which is near Perahora. Figure 5.12 shows three identical structures located near the seashore. Damage was least to the structure nearest the sea while the one farthest from the sea collapsed (Figure 5.13).

FIGURE 5.9 Stone houses in Perahora.

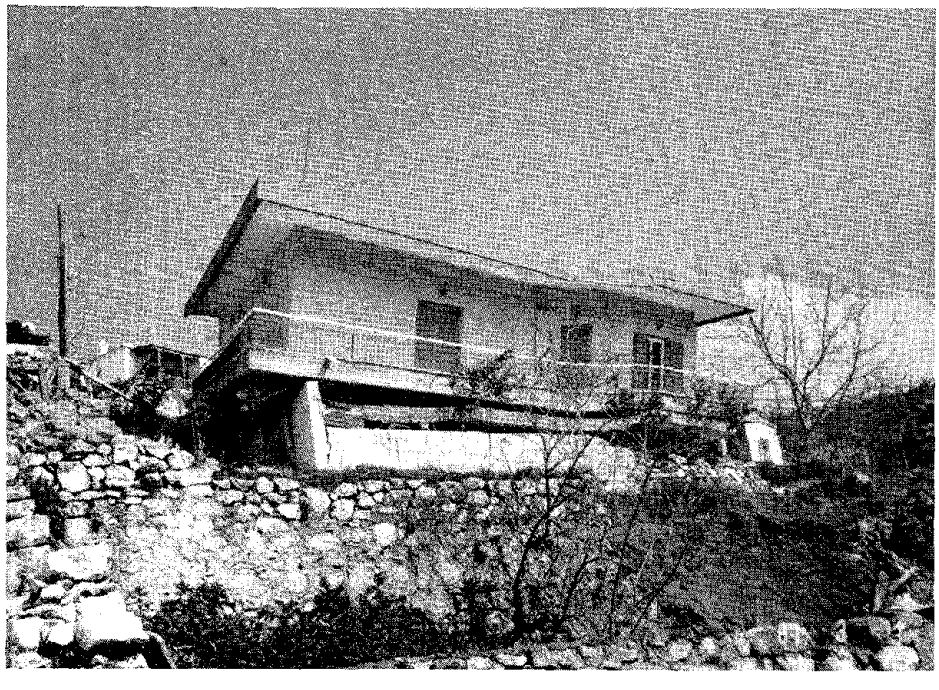

FIGURE 5.10 Damage to a three-story house built on sloping ground in Perahora. The retaining wall at the back of the house, which acts as a footing, functioned as the axis of rotation.

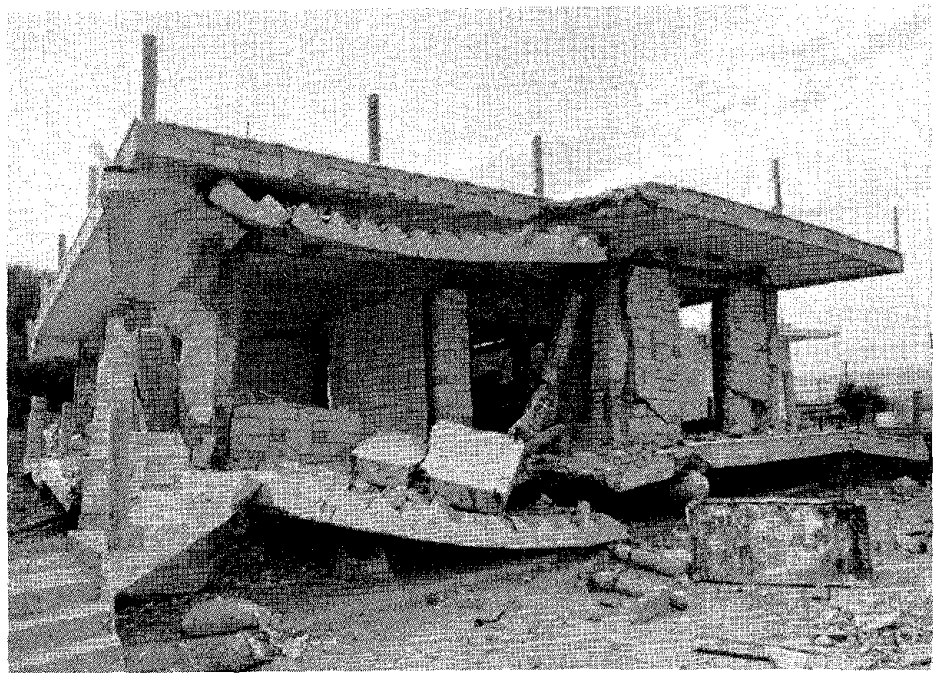

FIGURE 5.11 A two-story building in Shinos.

FIGURE 5.12 Three identical two-story buildings in Alepohori showed quite different behavior. The degree of damage increases from left to right. The left building is closer to the sea--no more than 60 m away--and suffered little damage to its first story. The third building collapsed totally (see Figure 5.13).

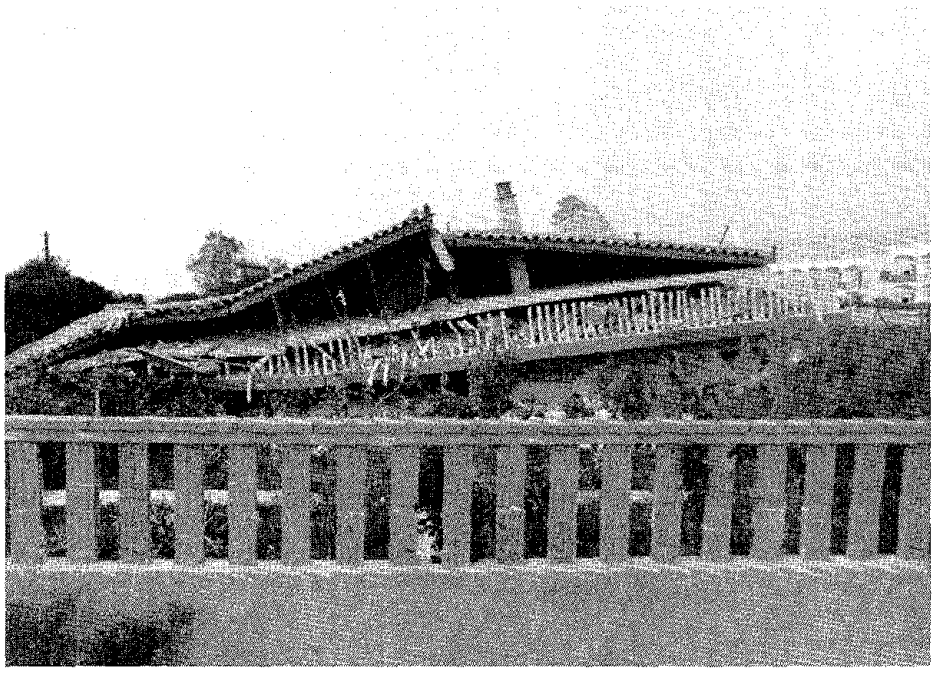

FIGURE 5.13 One building, identical to the others shown in Figure 5.12, collapsed totally.

CORINTH CANAL

Between Loutraki and Corinth the highway crosses the Corinth Canal, which was built in 1893. The canal is 6,400 m long and only 24.6 m wide at sea level. The steep walls rise more than 80 m with an 80° slope. Numerous fault breaks can be seen in the walls of the canal (Figure 5.14). In some of the breaks, small relative motions were observed at the ground surface, which caused some damage to pavements and farm structures. Three bridges cross the canal. One is a railway bridge (Figure 5.15) and the other two are highway bridges. The construction of the railway and one of the highway bridges was completed in 1948. The second highway bridge was constructed about eight years ago. Some of the piers of the hinged supports of the railway bridge on the side toward Beotia cracked, with some minor fault breaks in the rock strata below (Figure 5.16). The older highway bridge suffered some damage to the main load-carrying system near the hinged support on the side toward Beotia. Some deformation, slip, and failure of the rivets were observed, and the heads of most of the rivets near the supports were loosened (Figures 5.17 and 5.18)

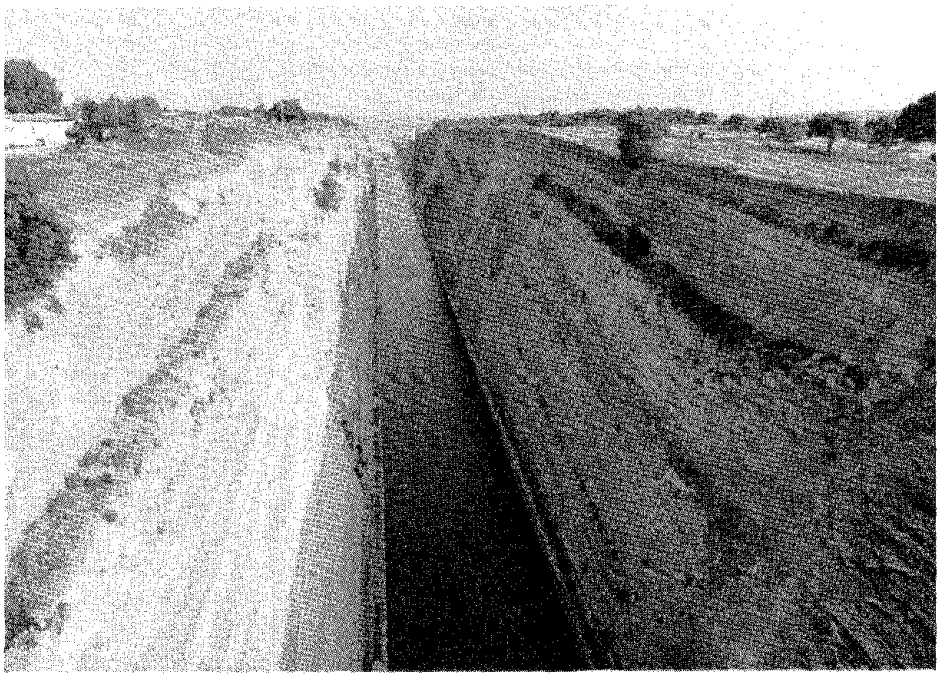

FIGURE 5.14 Corinth canal looking east from the road bridge. Note the descending beddings. At each change of elevation there is a fault.

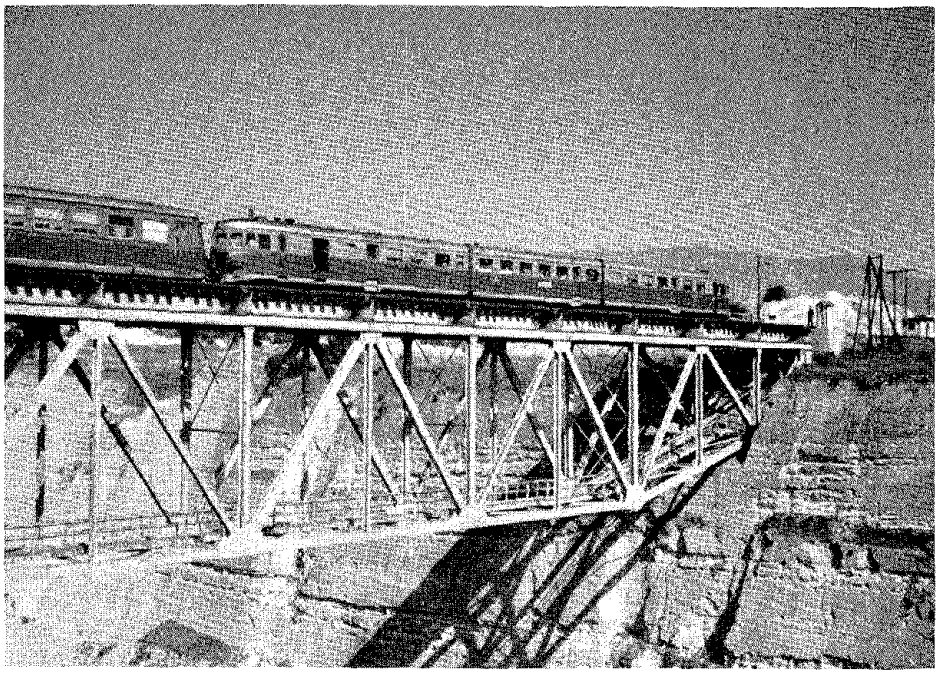

FIGURE 5.15 The railway bridge over the Corinth Canal was out of service for a few days after the earthquake for inspection.

FIGURE 5.16 A witness of glass to check the relative motion of the various minor faults in the Corinth Canal. This shows a breaking below the pier of the railway bridge on the Beotia side. The glass broke during the aftershocks.

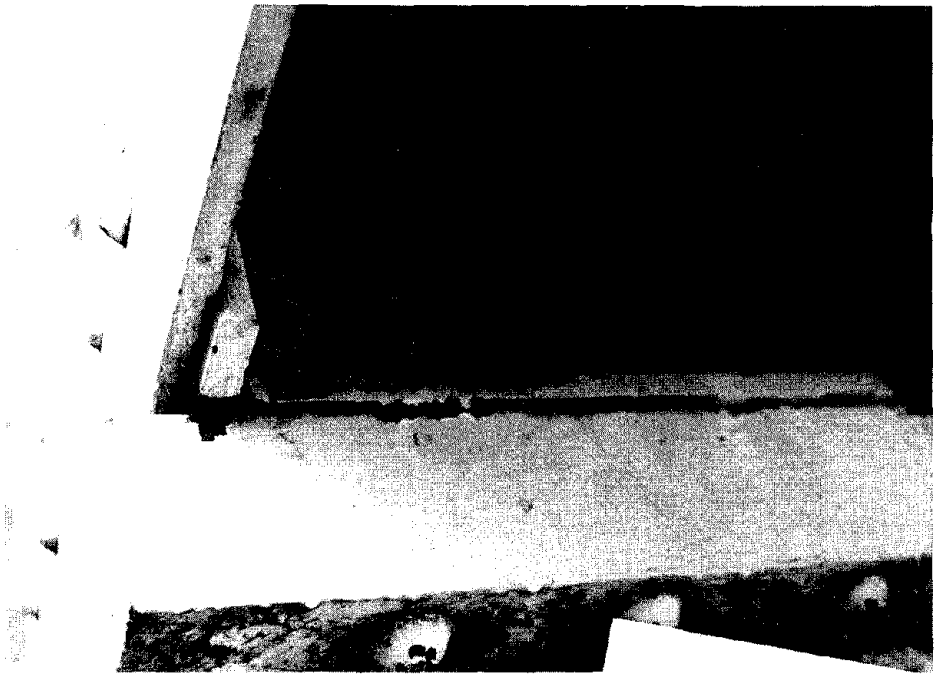

FIGURE 5.17 The hinged support of the old road bridge over the Corinth Canal at the Beotia side. Some deformations were observed.

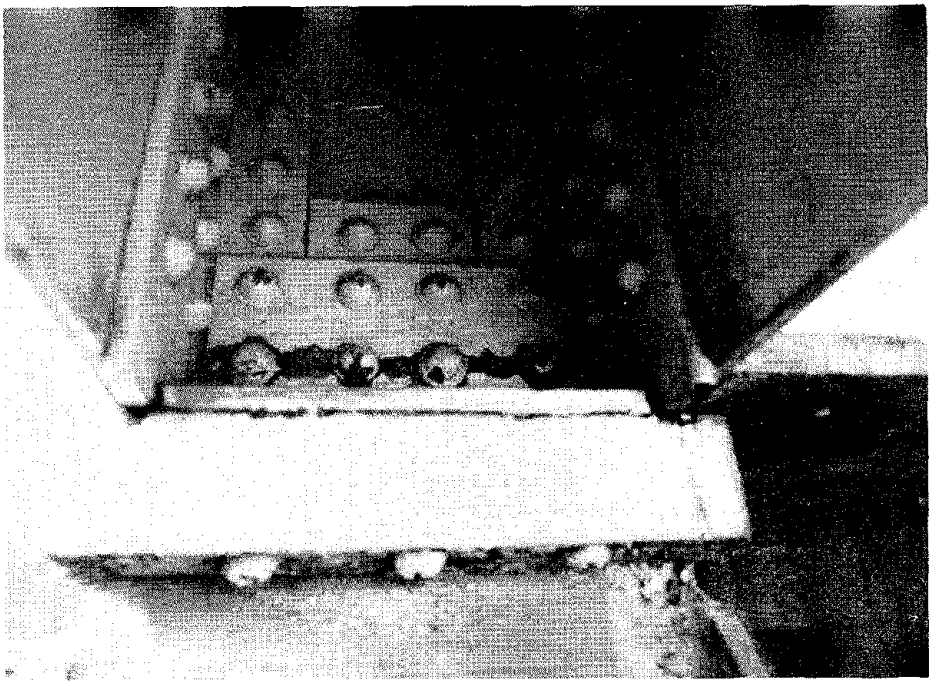

FIGURE 5.18 At the hinged support of the old road bridge over the Corinth Canal, two or three rivets that were connecting the support with the main girder broke in shear. Some tension was also observed in the L-shaped stiffening members.

CORINTH, VRAHATI, AND KIATO

The present town of Corinth is situated on the coast and has a small port facility. The town is a seasonal resort with numerous 6- to 10-story apartment buildings and resort hotels. The damage to the modern town consisted of nonstructural damage to unreinforced tile and masonry infill walls in the concrete frame buildings. The building shown in Figure 5.19 exhibits no apparent distress, but inspection of the interior revealed numerous cracks in the infilled masonry walls (shown in Figure 5.20).

West of Corinth several buildings were reported collapsed in the towns of Vrahati and Kiato along the coast. When the first-story columns failed in the three-story house shown in Figure 5.21, occupants "rode" the building down. The construction had a concrete frame with smooth reinforcing bars and widely spaced wire ties. The upper two floors had infilled masonry walls that made them very stiff and heavy. The lower story was relatively free of walls and thus flexible. It should be noted that in addition to the destroyed dwellings, many residents lost their business or trade as well. The uninhabited first stories of many residences served as stores, shops, or open space. In many villages farmers and tradesmen lost tools and equipment when the first floor of their homes collapsed. Older buildings with stone and mud walls suffered heavy damage to the walls, as shown in Figure 5.22.

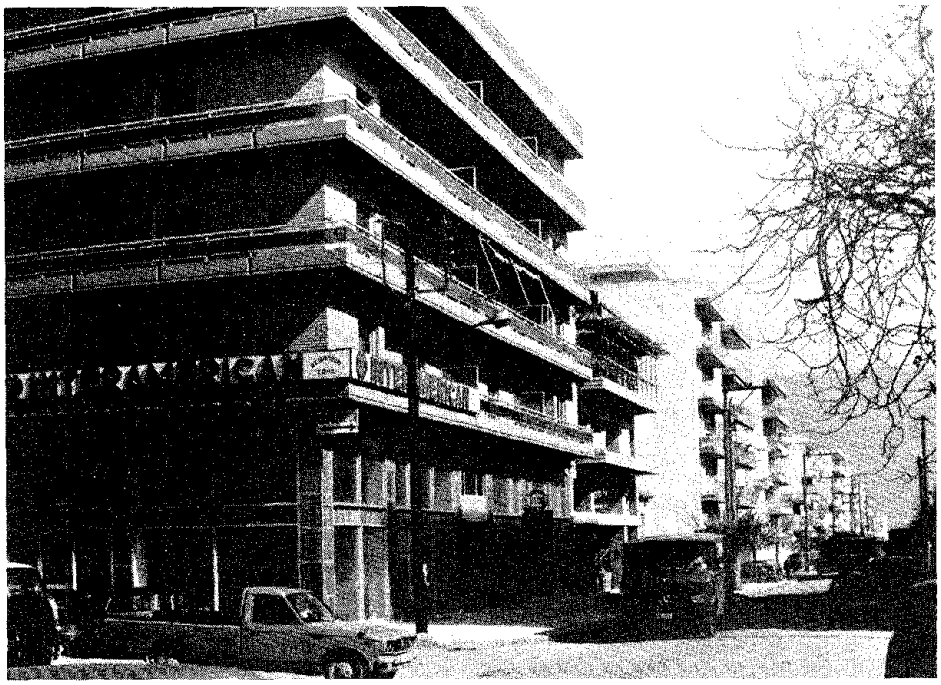

FIGURE 5.19 Office buildings in Corinth.

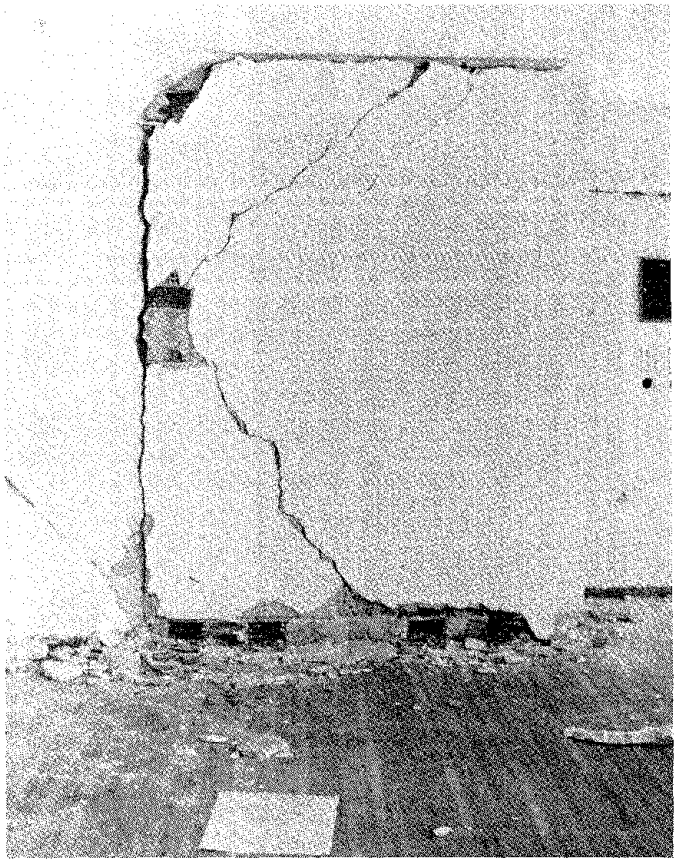

FIGURE 5.20 Infill wall damage.

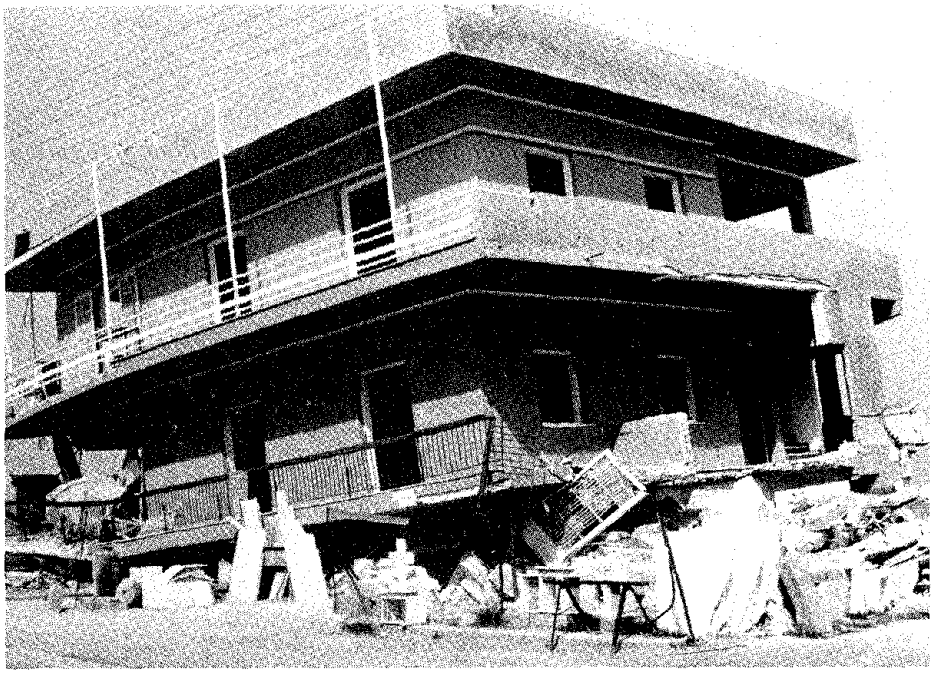

FIGURE 5.21 Collapse of three-story house in Kiato. (Lower floor was stone mason's shop.)

FIGURE 5.22 Older stone wall buildings in Vrahati.

In contrast, a very large church in the same area had no damage even to the very elaborate masonry arches and facade shown in Figure 5.23. The jetty in Kiato settled considerably during the earthquakes, with differential settlements of as much as 20 to 30 cm (Figures 5.24 and 5.25).

The most dramatic collapse occurred at the site of a nearly completed hotel constructed on the coast. Although the hotel was not open, it was virtually finished, with drapes and interior finishing completed. About two thirds of the hotel collapsed, as indicated by the rubble and "pancaked" floors in Figure 5.26. One remaining wing of the hotel is shown behind the pile of rubble in Figure 5.27. The building was constructed as a beam and slab building with masonry infill walls primarily above the first floor. The wing still standing showed signs of considerable lateral motion, with horizontal cracks in the infill walls and cracks in the joints of the concrete frames. The first floor was permanently distorted several inches and posed a dangerous problem in future aftershocks. The bodies of three caretakers were removed from the rubble. Details of this structure are discussed in Chapter 6. It is interesting to note that a small abandoned adobe structure across the road from the hotel showed no evidence of damage due to the earthquake. Other stone and earthen structures in the area also performed well (Figures 5.28 and 5.29).

KINETA AND MEGARA

Between Athens and the Corinth Canal the resort town of Kineta lies between the highway and the coast. The Kineta Bungalows is a cluster of one- and two-story cottages located near the highway about 100 yards from the beach. One of the two-story bungalows collapsed, as shown in Figure 5.30. All bungalows consisted of concrete frames with pumice-concrete block infilled walls. The frames were very light and had no detailing for ductility. It was interesting to observe that none of the other bungalows collapsed even though all were in close proximity (Figure 5.31) and were of identical construction with similar or identical plans. Several bungalows were damaged, as shown in Figure 5.32, and others showed no damage. The map in Figure 5.33 shows a layout of the bungalows.

Nearby a four- or five-story hotel collapsed (Figure 5.34). The concrete frame had smooth reinforcing bars and widely spaced wire ties. The lack of ductility and apparent lack of strength (Figure 5.35) caused the failure of all the columns and stacking of the floors and roof. A view across the roof (Figure 5.36) shows column stubs projecting up for future stories planned for the hotel. The house in the background was undamaged.

A large ceramics factory building near Isthmia collapsed, as shown in Figures 5.37 and 5.38. The factory structure consisted of a three-span concrete frame in the short direction and solid walls with long slotted windows in the long direction of the building. The short piers between the windows apparently failed and caused the progressive

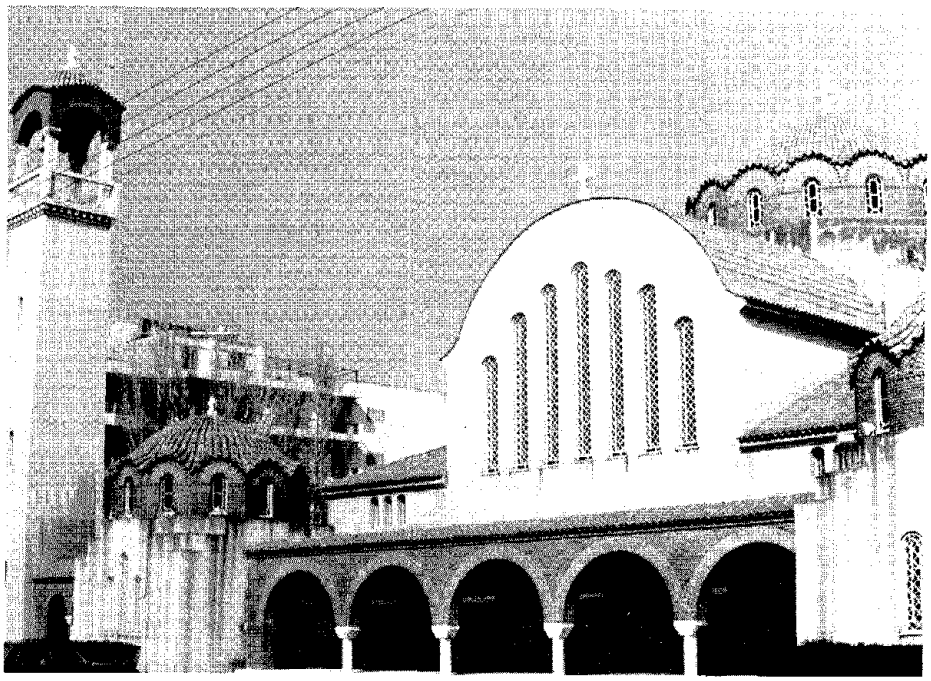

FIGURE 5.23 Undamaged church in Kiato.

FIGURE 5.24 Jetty in Kiato. Differential settlements and rotations of the concrete blocks were observed.

FIGURE 5.25 Jetty in Kiato. The expansion joints between the concrete blocks have been damaged. Note the differential settlement of about 20 to 30 cm.

FIGURE 5.26 Collapse of nearly completed hotel in Vrahati.

FIGURE 5.27 Portion of hotel standing (an expansion joint separated the sections).

FIGURE 5.28 Some well-maintained earthen buildings in the area, including this one in Kiato, suffered no damage.

FIGURE 5.29 Many earthen buildings are about 100 years old. They have experienced two to three earthquakes as strong as the present ones and only needed the plaster surface repaired (although the repairs were not always done).

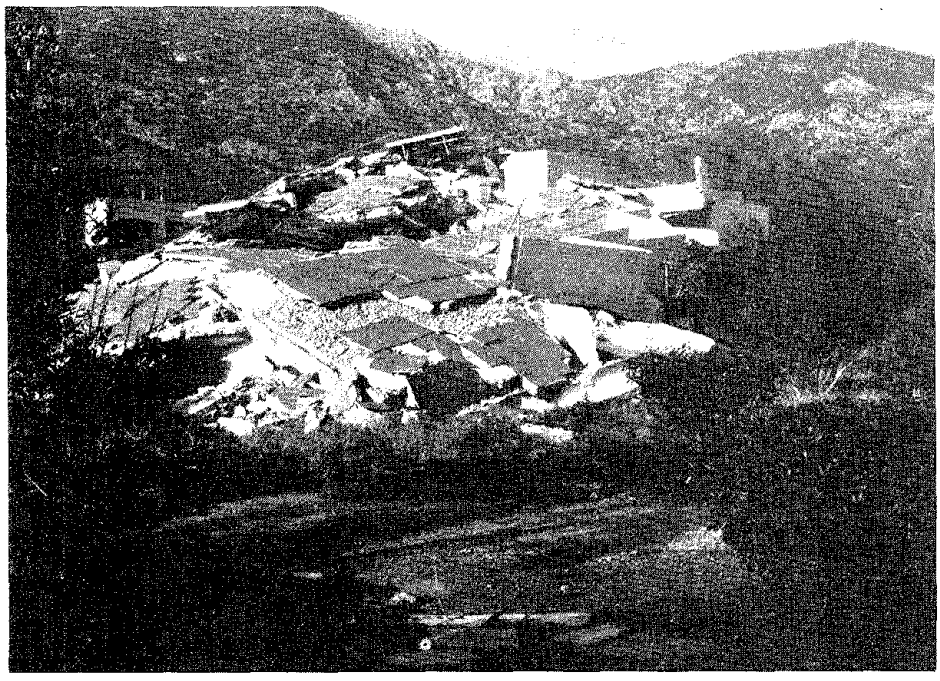

FIGURE 5.30 Collapse of Kineta bungalows.

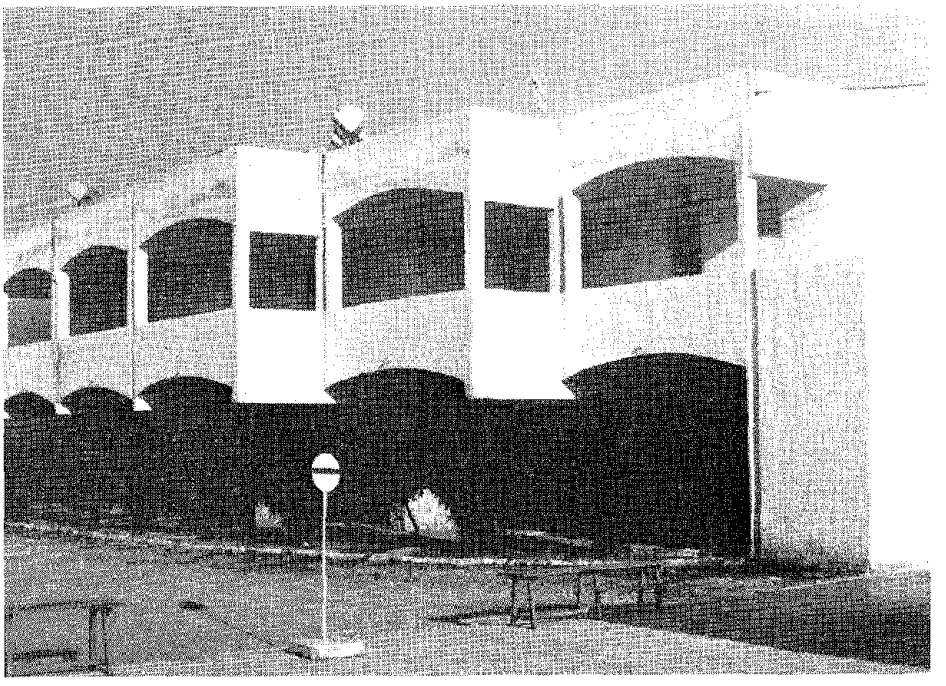

FIGURE 5.31 Undamaged bungalows.

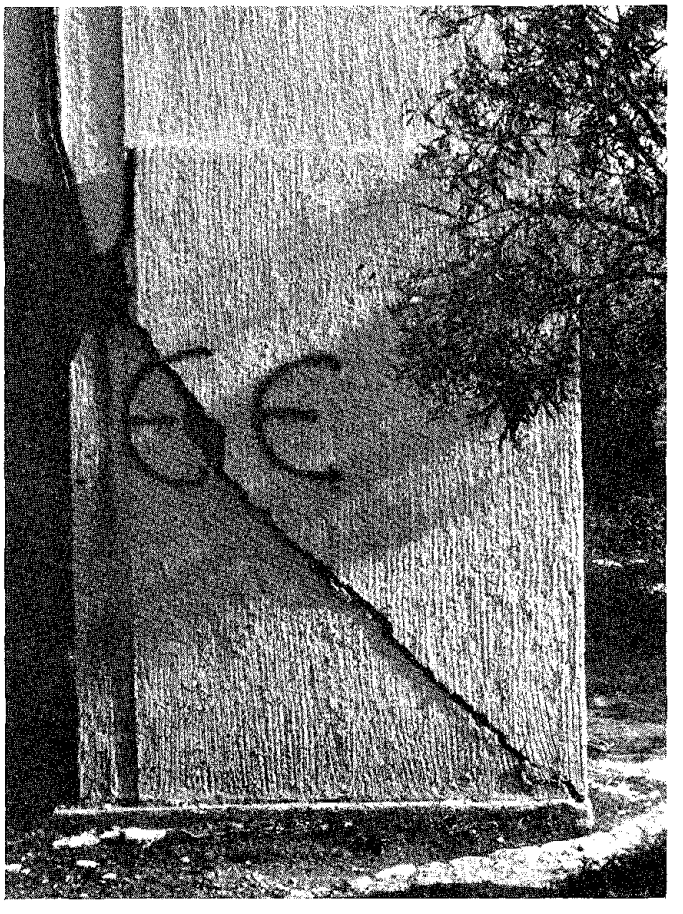

FIGURE 5.32 Damage to bungalows. EE is a designation by government officials for buildings not to be occupied.

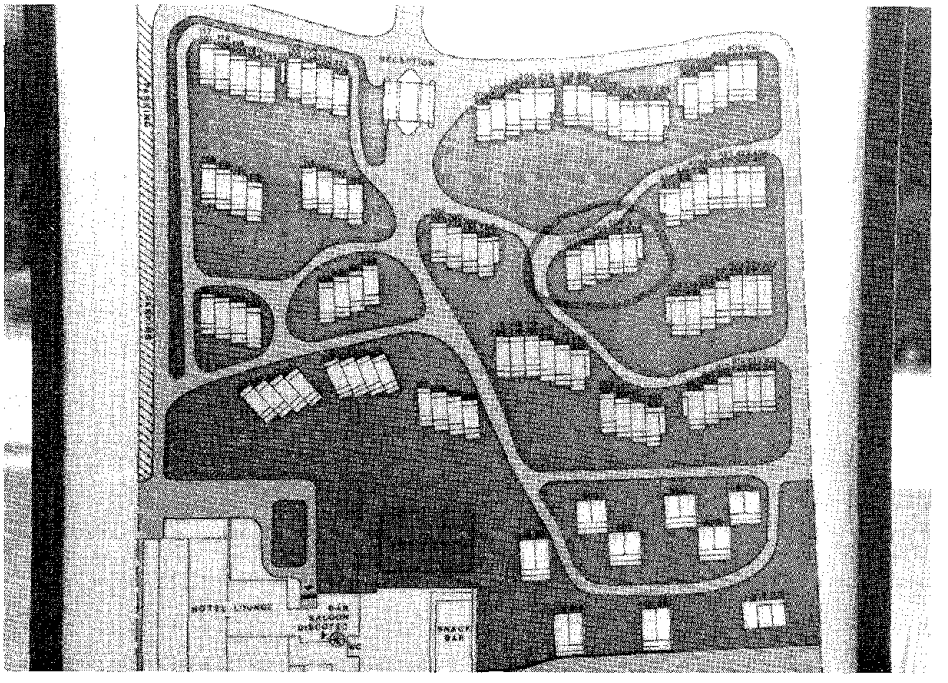

FIGURE 5.33 Map of bungalow development (circled units collapsed).

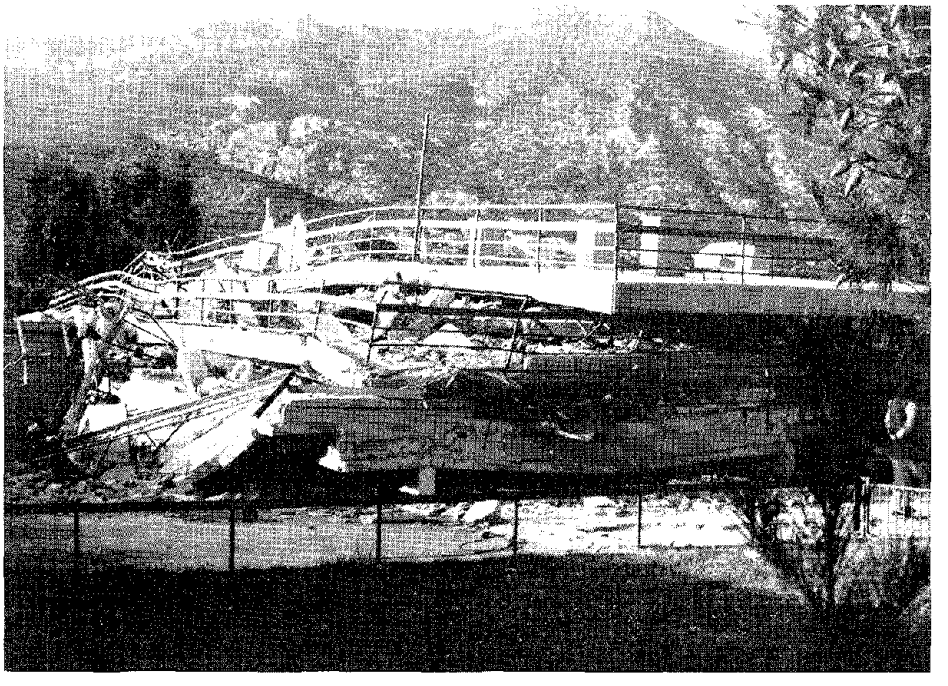

FIGURE 5.34 Collapsed hotel in Kineta.

FIGURE 5.35 Detail of the collapsed hotel in Kineta. Note the slip of the hook and necking of the longitudinal bar (arrow).

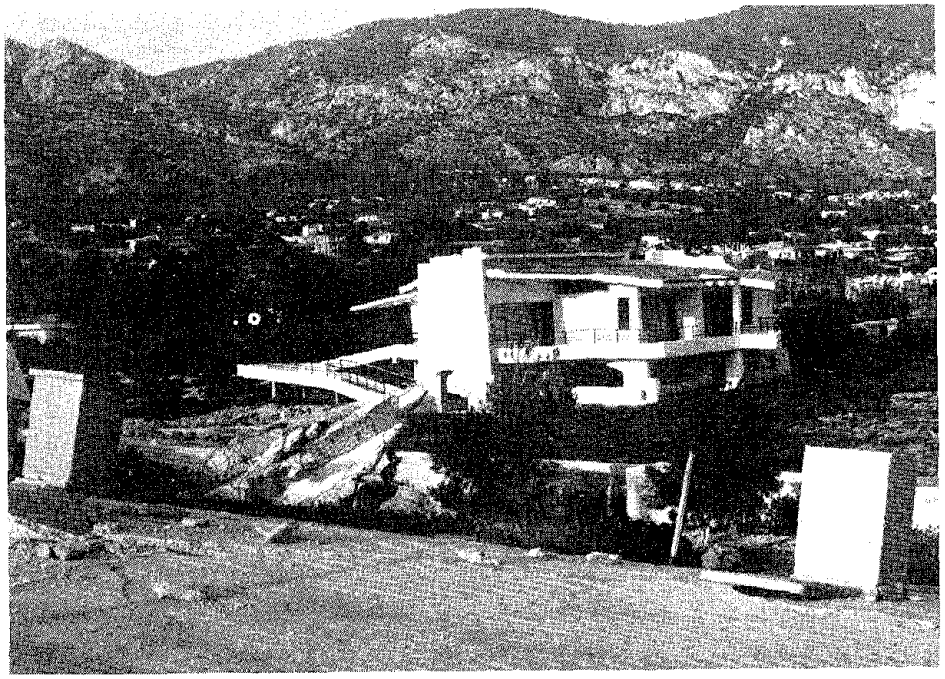

FIGURE 5.36 Column stubs on roof of Kineta hotel to accommodate future expansion. Home in background was undamaged.

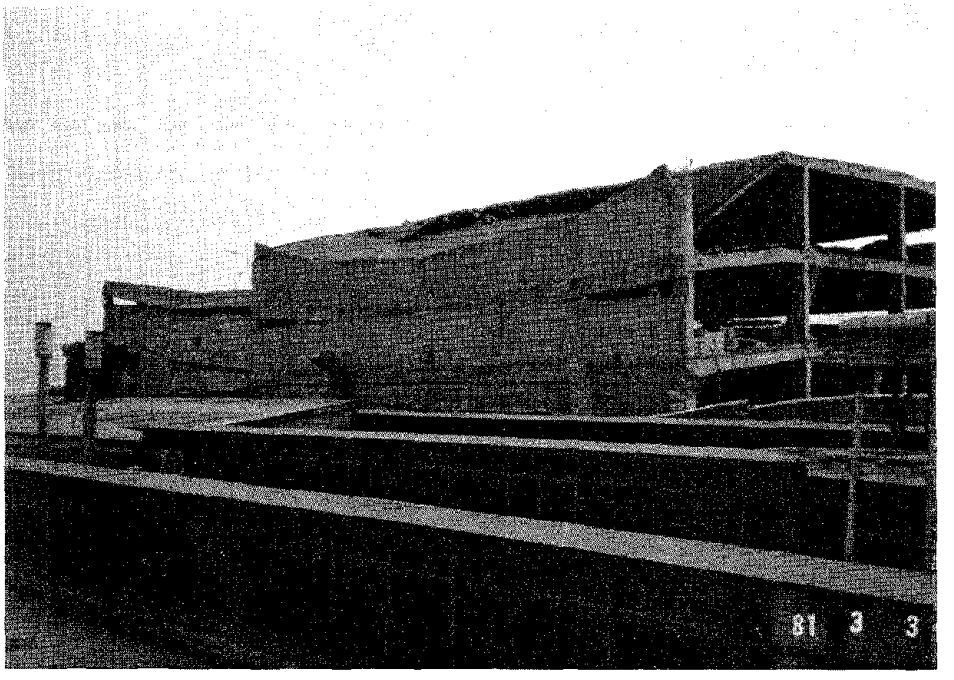

FIGURE 5.37 Ceramic factory near Isthmia (side view).

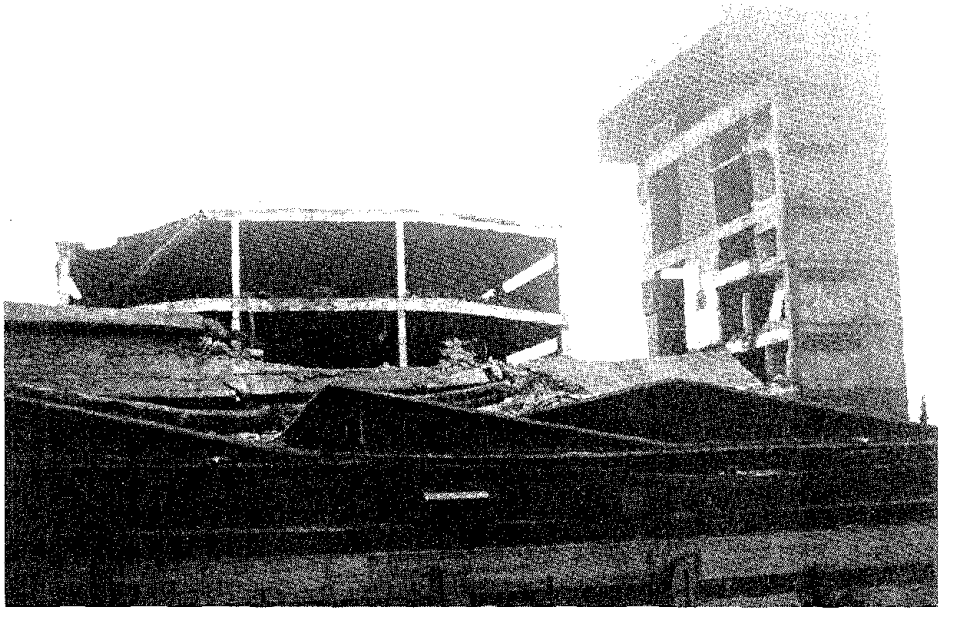

FIGURE 5.38 Ceramic factory near Isthmia (front view, with elevator shaft on right).

failure of the building. Note the slope of the floor and roof in the outer spans. After columns at lower levels collapsed, the upper floors settled a distance equivalent to the window height.

The town of Megara is a regional agricultural and commercial center. The town suffered considerable damage in the events of February 24 and 25. Structures around the town square were already being repaired when additional damage was produced by the earthquake of March 4. The general construction techniques are described in Chapter 4, and some examples can be seen in Figures 4.17, 4.18, and 4.19. A grain alcohol processing plant in Megara lost the top 3 m of a tall masonry chimney. Empty steel storage tanks showed considerable movement at their bases but no permanent damage (Figure 5.39). The main distilling building was a three-story masonry structure with a cast-in-place roof and no interior intermediate floors. It was severely damaged but was not vacated.

Elsewhere along the coast, there were a number of refinery and heavy industrial facilities that suffered very little damage. The only damage observed was to anchors to footings and to diagonal steel ties (Figures 5.40 and 5.41).

PLATAEAE AND KAPARELI

Northwest of Athens and northeast of the Gulf of Corinth, the farming villages of Plataeae and Kapareli were devastated by the March 4 earthquake. The village of Plataeae lies at the end of the Kapareli fault described previously. The village can be seen in Figure 5.42. Virtually every dwelling in the village suffered some damage, and many collapsed. Here, as in Perahora, the homes on hillsides had entries to the living quarters at ground level but the first floor was supported on columns on the other three sides. As a result, the stiff upper floor rotated about the edge supported at ground level and produced very large deformations in the outermost columns, sometimes leading to collapse of the entire structure (Figures 5.43 and 5.44). The cathedral in the village was nearly destroyed. Although the main facade does not appear to be heavily damaged, a side view indicates that the structure is near collapse (Figures 5.45 and 5.46). The village of Kapareli was also heavily damaged, with residents reporting nearly continuous ground movement during the day following the March 4 event. Nearly the entire population of Plataeae and Kapareli was evacuated to tent housing. Lesser damage from this event was reported in Thebae to the northeast.

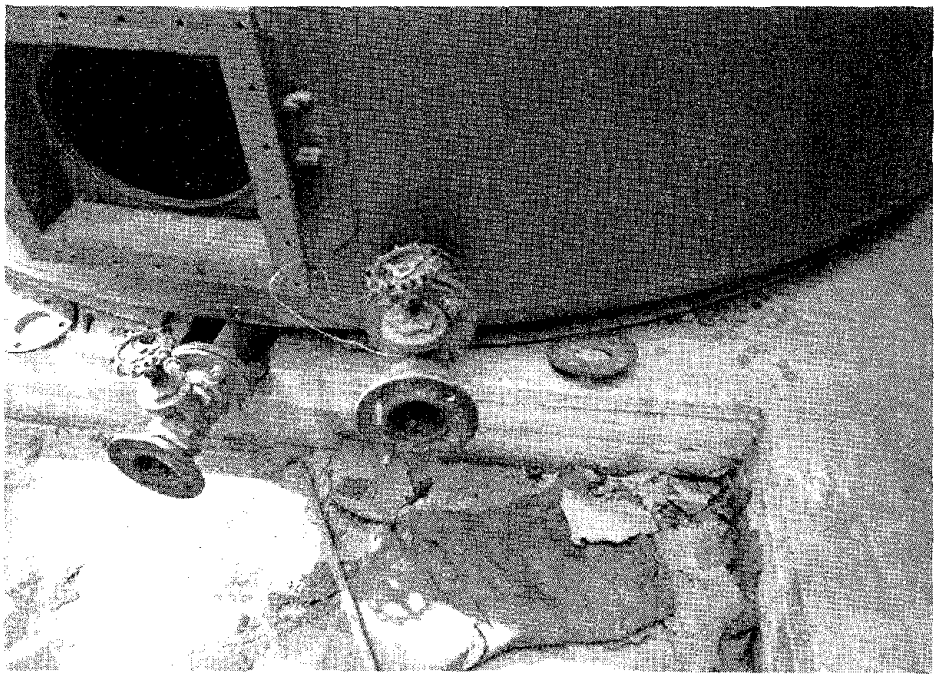

FIGURE 5.39 Winery tank in Megara. The tank tilted a little and was displaced about 3 to 4 cm. The tank overrode the steel washer.

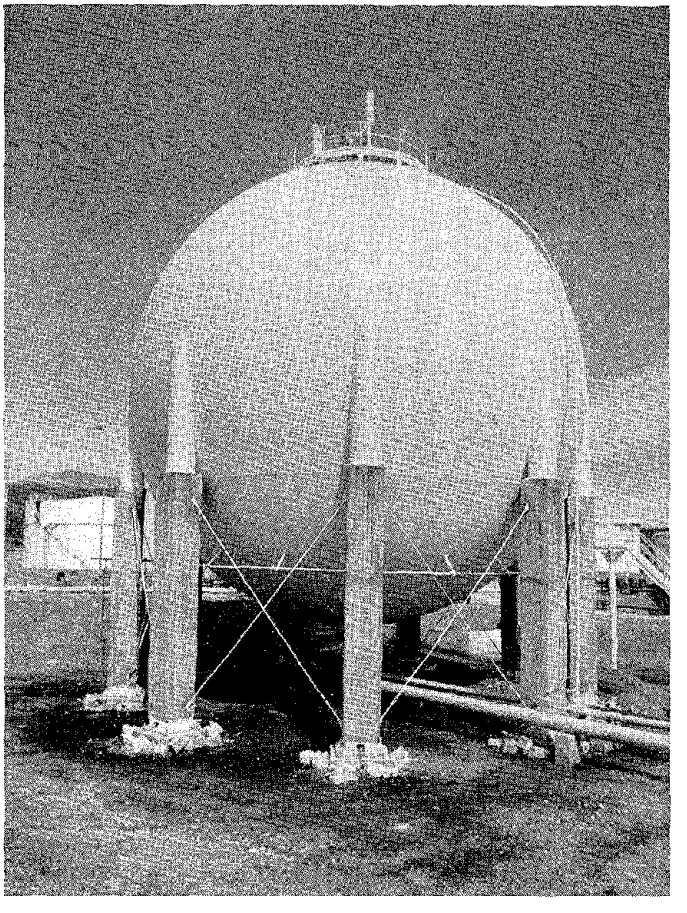

FIGURE 5.40 A huge liquid gas storage tank at the "Motor Oil" refinery suffered limited damage in the anchors of footings and the diagonal tension bars.

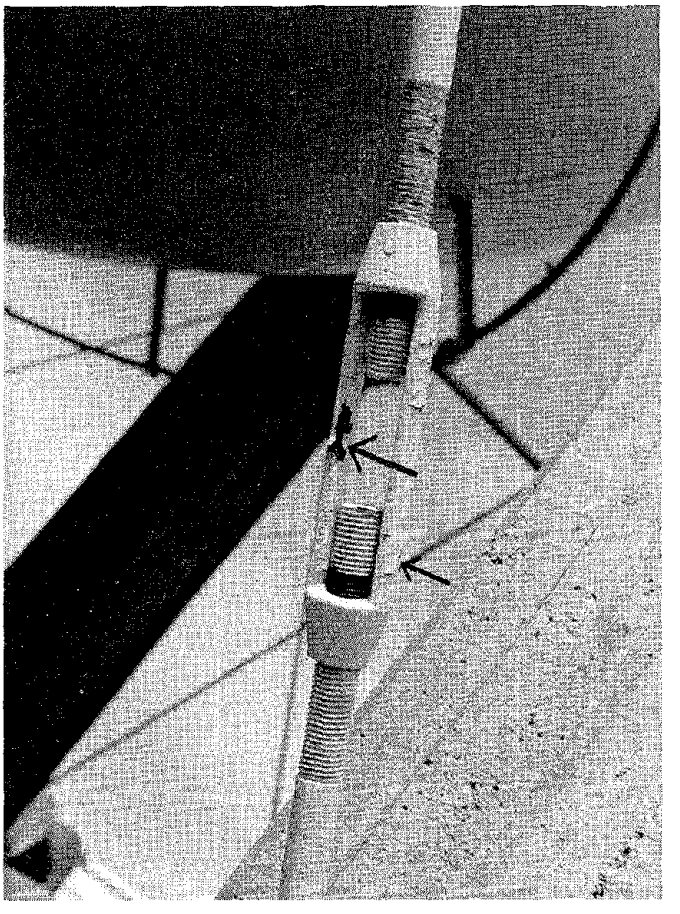

FIGURE 5.41 The diagonal tension bars of the liquid gas storage tank at the "Motor Oil" refinery extended beyond their elastic limit and stressed some bolts (see arrows).

FIGURE 5.42 Village of Plataeae at end of Kapareli fault.

FIGURE 5.43 Damaged home in Plataeae.

FIGURE 5.44 Building collapse on bus in Plataeae.

FIGURE 5.45 Cathedral in Plataeae.

FIGURE 5.46 Cathedral in Plataeae.

ATHENS

The modern city of Athens is a sprawling metropolis that extends from the port of Piraeus northward about 12 km. The area (900 km^2) has a population in excess of 3,000,000. All possible types of construction can be found in Athens, from the ancient ruins of the Acropolis and the old stone and mud buildings of the city that grew up around the Acropolis to modern high-rise (ductile concrete moment-resisting frame) office buildings. A panorama of the city, as in Figure 5.47, shows that the majority of the buildings are four- to eight-story apartment buildings constructed of concrete frames with infilled walls. According to government estimates, an estimated 10,000 buildings were damaged in the Athens area and 600 buildings were vacated. Many residents moved out of their damaged dwellings into temporary tent houses in parks and vacant land, as shown in Figure 5.48.

The Parthenon temple atop the Acropolis (Figures 5.49) suffered some significant cracks, but none of the huge stones was dislodged. The superintendent of the Acropolis reported that in addition to causing the cracks in the Parthenon, the earthquake shattered 50 of the 5,000 priceless vases in the Erechtheum and 10 others in the Acropolis museum. Because of its historic significance, a more detailed description of damage to the Parthenon is given in Chapter 6.

The historic Athens Cathedral suffered numerous cracks over the arches, and masses had to be discontinued until the damage could be repaired. None of the parapets or ornamentation shown in Figure 5.50 was damaged. The cathedral was built 140 years ago and had not been seriously damaged in previous earthquakes. It has been reported that in the 1894 earthquake, when all the surrounding buildings collapsed, the cathedral was the only building not damaged.

Recently constructed high-rise office buildings designed to have ductile moment-resisting frames were reported to have performed without any problems. A new apartment building (Figure 5.51) in a suburb of Athens suffered severe damage to some of its first-story columns. Above the first story the building had extensive masonry partitions. The building was of typical "pilotis" construction with wide and thin columns oriented primarily on one of the major building axes. The column shown in Figure 5.52 was the only one oriented longitudinally on the front face of the building, and it had to carry about half of the total building shear in the longitudinal direction. The overloaded column failed in shear.

FIGURE 5.47 Athens.

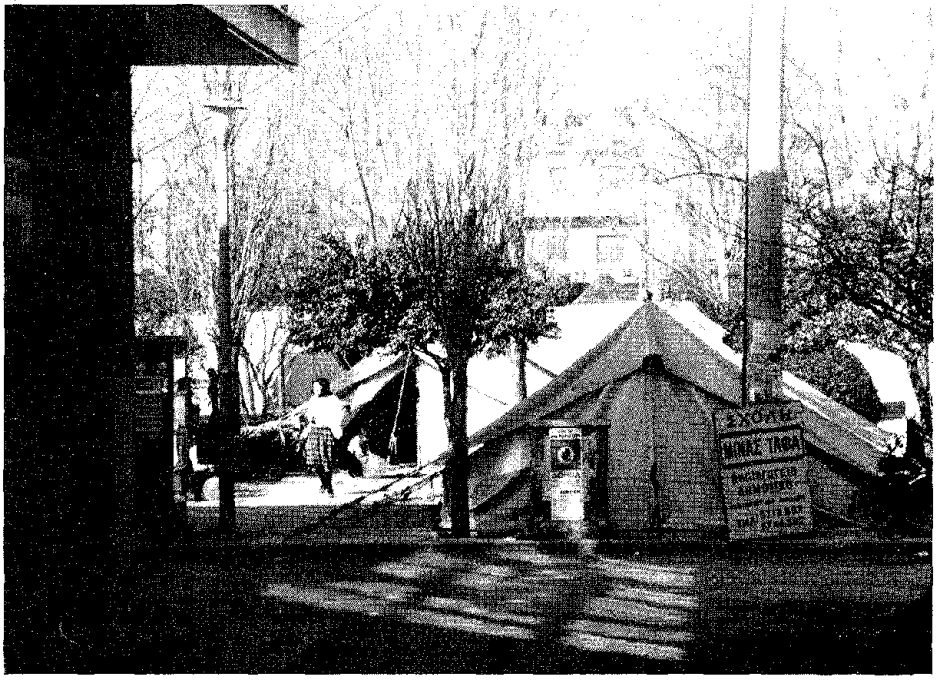

FIGURE 5.48 Temporary tent housing in Athens.

FIGURE 5.49 Parthenon on the Acropolis in Athens.

FIGURE 5.50 Athens Cathedral.

FIGURE 5.51 New apartment building in Athens (Anthoupolis region).

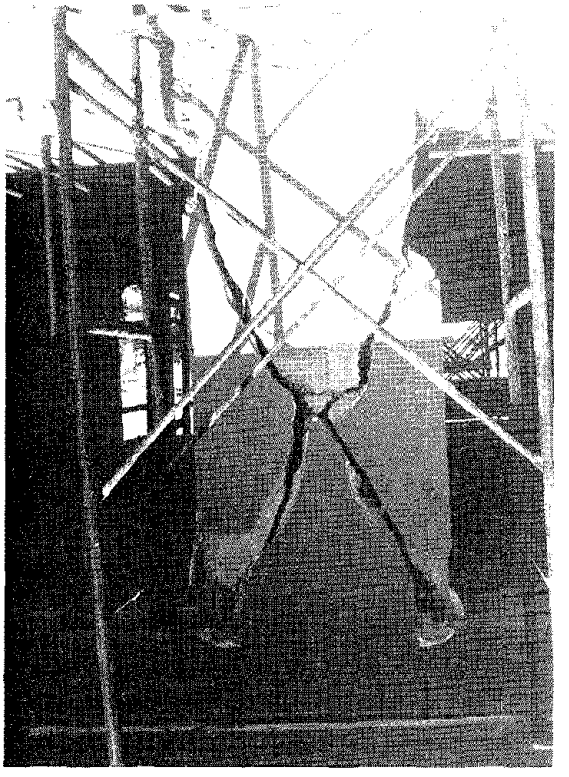

FIGURE 5.52 Heavily damaged stiff column at corner of apartment building shown in Figure 5.51.

6

DETAILS OF SELECTED DAMAGED OR DESTROYED STRUCTURES

A number of modern structures were heavily damaged or destroyed during the February-March 1981 earthquakes. These structures are a source of information that may be useful in developing future design or detailing requirements. Some structures, however, may warrant more detailed studies to correlate analytical techniques with observed patterns of response and failure.

At the end of this chapter we briefly describe the effects of the February-March 1981 events on the Parthenon. The Parthenon is a unique structure of historical interest, and we felt that it merited special mention.

VIP'S HOSTEL

The Vip's Hostel in Perahora is a modern three-story structure that suffered heavy damage. It is founded on fractured hard rock. A site investigation discovered no permanent relative movement between the various rock formations on which the structure is founded.

The framing system is simple, as shown in Figure 6.1. To drain the roof, plastic tubes are embedded into the outside corners of each of the four corner columns (Figure 6.1d). The quality of construction is good. In the x direction the building is structurally symmetric (Figure 6.1a); in the y direction the shear wall SW_1 introduces a very small eccentricity. The second story has some brick partitions, while the first story and, especially, the third story have a number of brick walls. The walls produce a stiffness discontinuity in the second story.

For architectural reasons the northern part of the building was built around a natural rock outcropping that penetrates to the second story, as shown in Figures 6.1, 6.2, and 6.3. The north end of the floor slab for the second floor was cast on this rock. A part of the rock extends through the second floor (Figure 6.3). This rock produces an eccentricity in lateral resistance that may have initiated the destruction.

Long cantilevers are also present all around the building. The cantilevers (spandrels) support the heavy vertical parapets on their free ends (see Figure 6.2), which are faced with thick marble panels. The long heavy cantilevers created large torsional moments about the

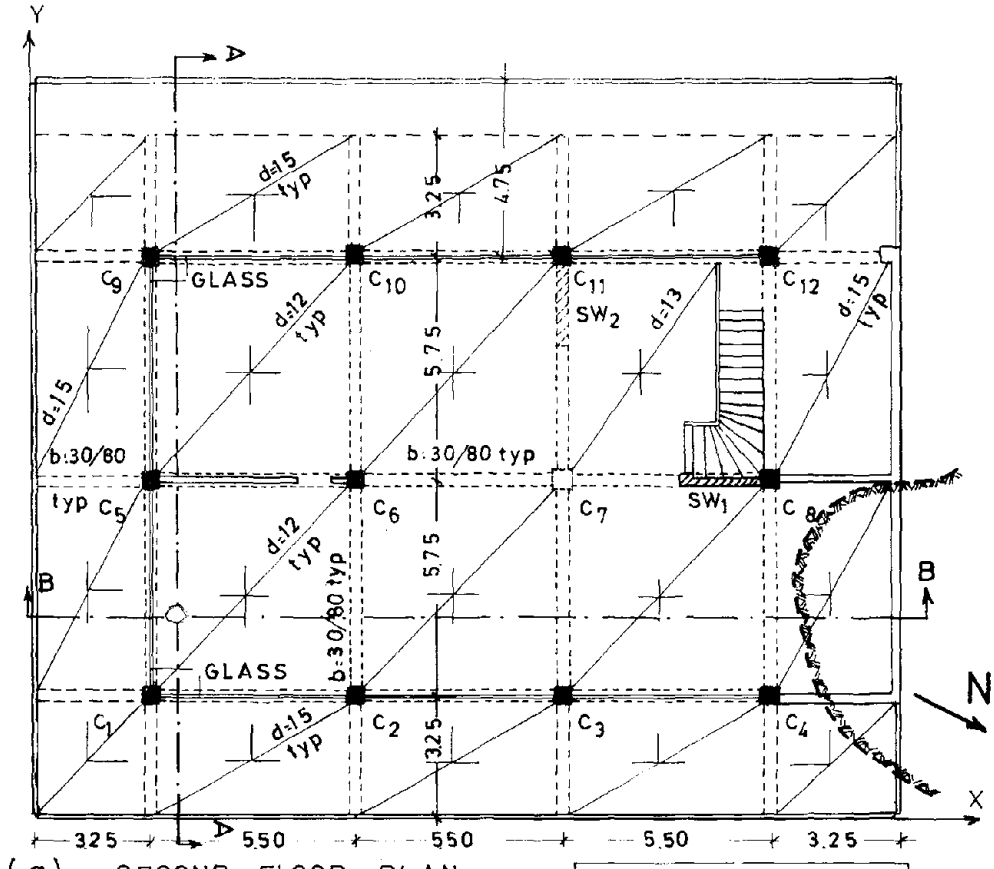

(a) SECOND FLOOR PLAN

TYPICAL COL. DIM.
FIRST FL.: 50/50
SECOND FL.: 45/45
THIRD FL.: 40/40

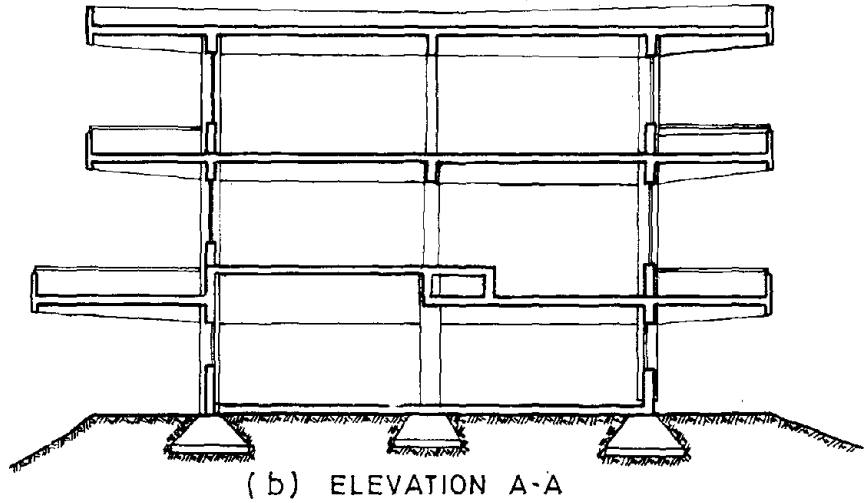

(b) ELEVATION A-A

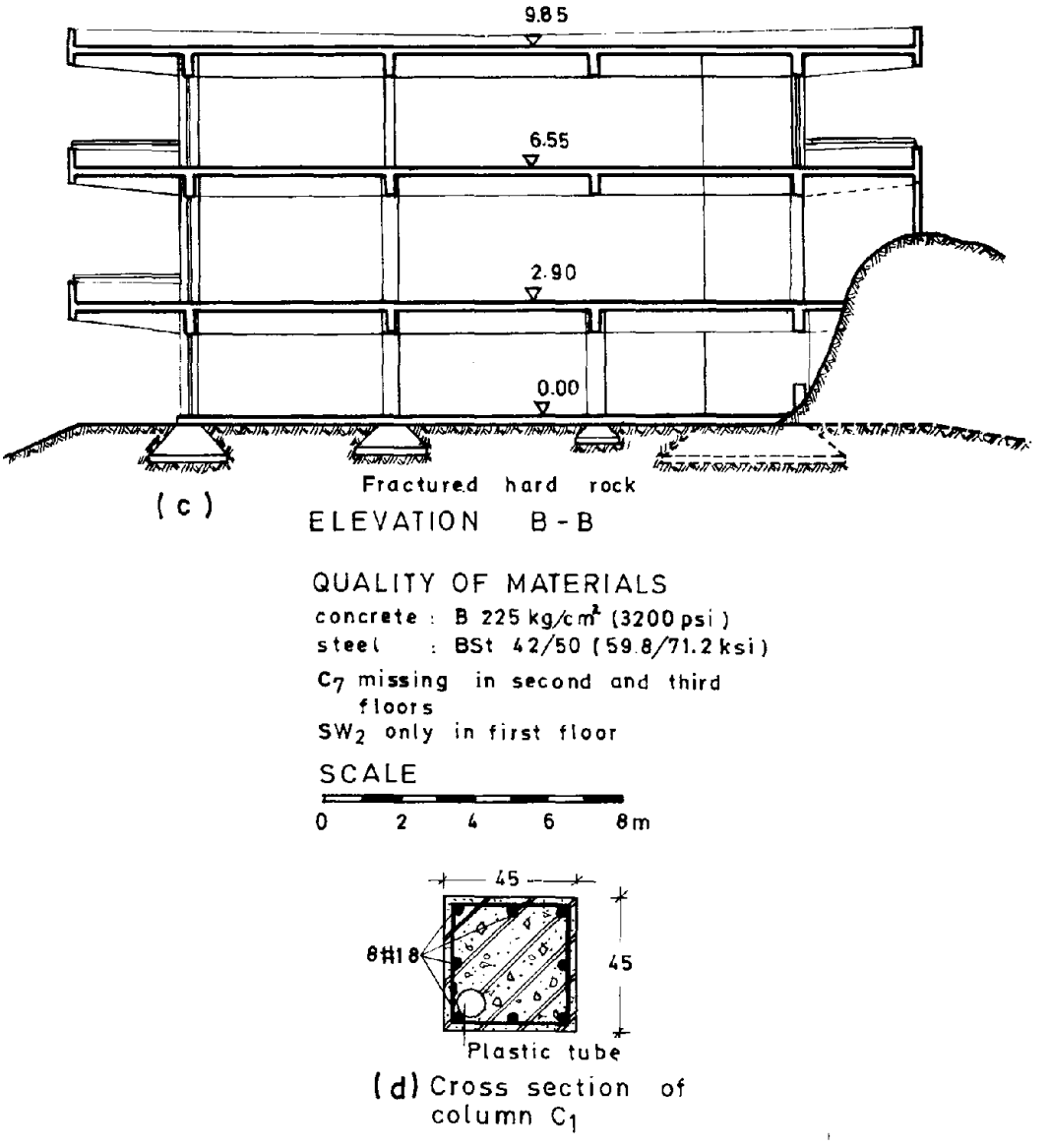

FIGURE 6.1 Vip's Hostel in Perahora. General drawings.

centroid of lateral resistance (the rock outcropping). Damping was low because there were few partitions and vertical elements.

Damage was concentrated in the south end of the building's second story, as shown in Figures 6.4 and 6.5. Figures 6.5 and 6.6 show the large lateral deformations and shortening of columns c_1 and c_5, which deformed horizontally about 40 cm at their bottom ends. Column c_9 shortened about 70 cm at the second level, as shown in the sketch of Figure 6.7.

The columns located the greatest distance from the center of torsion deformed horizontally the greatest amount and probably experienced several repetitions of deformation. The top and bottom parts of the columns formed hinges and subsequently failed in shear or by crushing.

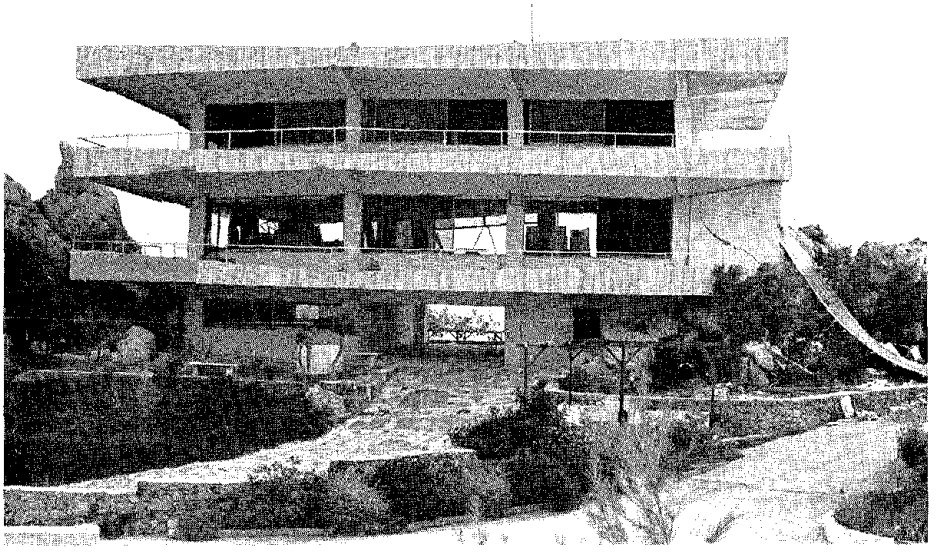

FIGURE 6.2 Vip's Hostel in Perahora. Northeast view of the building soon after the earthquake.

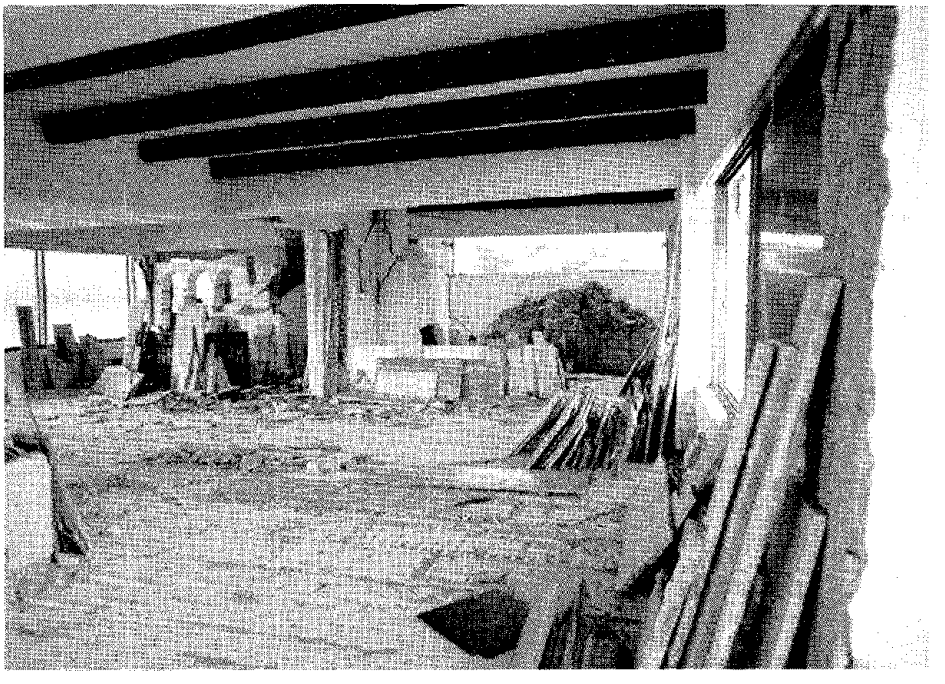

FIGURE 6.3 Vip's Hostel in Perahora. The natural rock outcrops over the second story in the far northwestern side and northern corner of the building.

FIGURE 6.4 Vip's Hostel in Perahora. This view from the south shows part of the damaged columns in the second story. The arrow shows the large deformation of the ceiling. There are no ties in the column-to-beam connection (c_9).

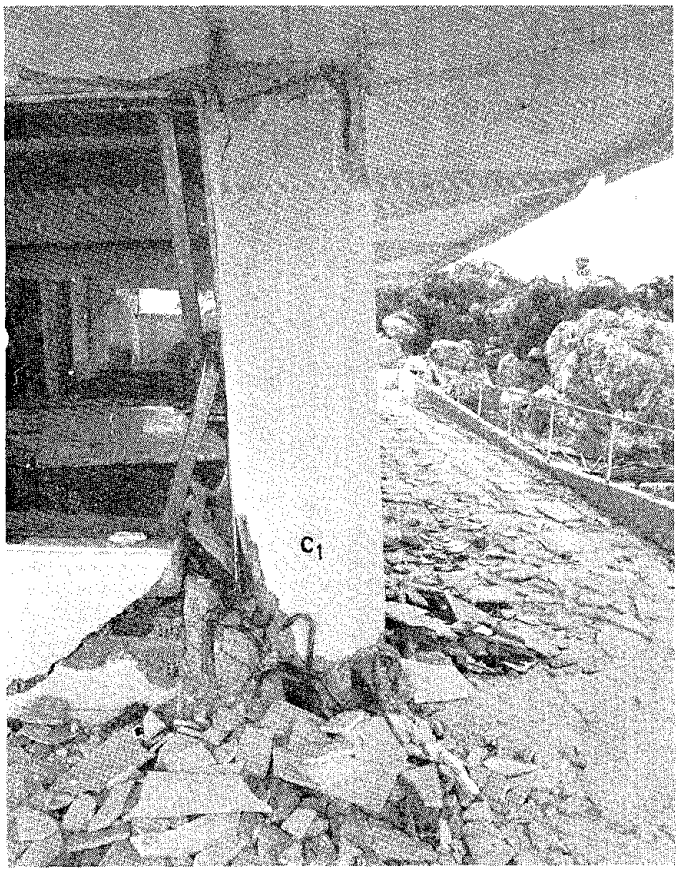

FIGURE 6.5 Vip's Hostel in Perahora. Column c_1 on the second story, viewed from the southeast.

FIGURE 6.6 Vip's Hostel in Perahora. Column c_5 on the second story, viewed from the southeast.

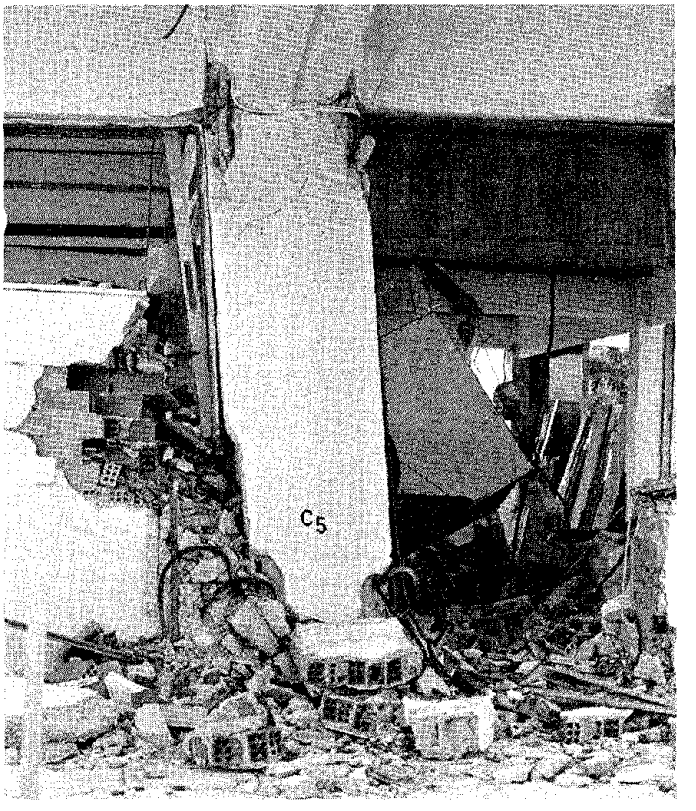

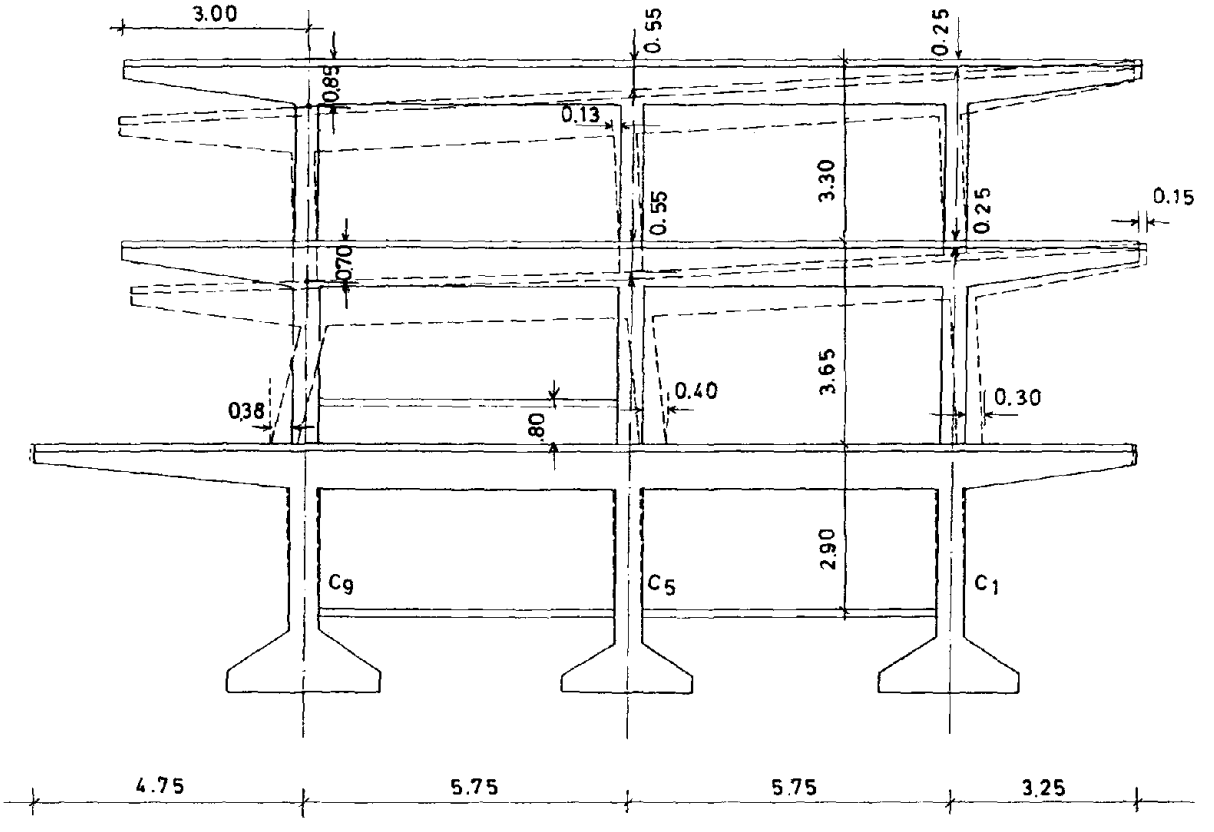

FIGURE 6.7 Vip's Hostel in Perahora. Deformation of the south-eastern elevation of the building.

CONTIS HOTEL

The Contis Hotel in Loutraki was a seven-story reinforced concrete frame structure that collapsed totally, as shown in Figures 6.8 and 6.9a. The site is about 150 m from the sea in the middle of the city (number 1 in Figure 5.1). Construction started in 1966 and was completed in 1972. The building was constructed in four stages because of various extensions and additions to the original building. The first permit, issued in 1966, refers to the construction of the lower three stories and includes provision for adding two stories in the future. Four stories were subsequently added, as shown in Figure 6.9b. The foundation plan is shown in Figure 6.10. As can be seen, the structure was quite irregular in plan. The footings were connected by tie beams at the grade level (Figures 6.11 and 6.12). However, many of the beams had large openings at the columns to accommodate utility lines.

According to witnesses, the collapse started from the third story toward the small southwest face of the structure. The building likely underwent some torsional deformation, rotating about the inside corner of the structure. Damage to the adjacent structures is indicated in Figures 6.9 and 6.13. These adjacent buildings were seriously damaged and had to be demolished.

GALAXY HOTEL

The Galaxy Hotel in Vrahati was a modern reinforced concrete frame structure with hollow brick partitions. The building was divided into three sections by two expansion joints (see Figures 6.14 and 6.15) having a width of about 2 to 3 cm. The two lower stories of sections I and II contained a restaurant and reception areas. The height of the two lower stories was 50 percent greater than that of section III, as shown in Figure 6.14. In section III many brick wall partitions (with thicknesses of 18 cm) were in place from the ground level to the top of the structure. Sections I and II had no partitions in the lower two stories (see Figure 6.15), while in the upper stories the partitions were hollow bricks with a thickness of 8 cm. Table 6.1 gives the dimensions of the first story columns.

Construction of the framing system started near the end of 1969 and continued without serious delays until the end of 1971, when all of the framing system and some brick walls were completed. Construction slowed from 1971 to 1974, and from 1974 to 1979 the site was completely abandoned. After 1979 work started again and the hotel was scheduled to open for the summer of 1981. Figures 6.16 and 6.17 show views of the hotel during construction.

The site is about 80 m south of the seashore on a flat area. The soil at the site is aggraded material of recent (Holocene) origins. Cotzias and Stamatopoulos (1969) carried out a geotechnical investigation and laboratory tests of the site in February 1969, before the framing system was begun. Two boreholes, BH_1 (near the northwest corner) and BH_2 (near the northeast corner), were drilled, as shown in Figure 6.14. Table 6.2 summarizes the in situ tests and laboratory findings. The recommended pressure on the foundation soil under full

FIGURE 6.8 Contis Hotel in Loutraki. Southwest view one week after collapse. Photograph courtesy A. Manis.

load was set at 0.12 MPa (2,500 lb/ft^2) after the soil investigation. Where a raft foundation was used (see Figures 6.14b and 6.14d), this was lowered to 0.06 MPa (1,250 lb/ft^2). The original surface of the ground sloped gradually toward section III, as shown in Figure 6.14b. A small marsh developed in the area where section III was to be constructed. To remove the mud, the excavation was deepened about 30 cm for the foundation of section III.

The owner was a civil engineer who designed and personally supervised the construction. The quality of the construction was good.

The epicenter of the February 24 earthquake was about 25 km northeast of the hotel, and the hypocentral line was inclined about 40^o with respect to the site. Witnesses of the hotel's collapse provided the following information.

- The two sections of the hotel collapsed after the main shock on February 24.
- People eating in a nearby restaurant some tens of meters east of the hotel said that the dining tables appeared to be jumping vertically from the ground during the earthquake; some of the tables broke.
- An artesian well some tens of meters northwest of the hotel started producing three times more water than before the earthquake. This production gradually diminished and returned to normal in four days.
- The jetty directly in front of the hotel (Figure 6.18) subsided quite a few centimeters, and part of it rotated a few degrees. About 40 m east of the jetty's end a strong whirlpool was observed for two days after the earthquake.

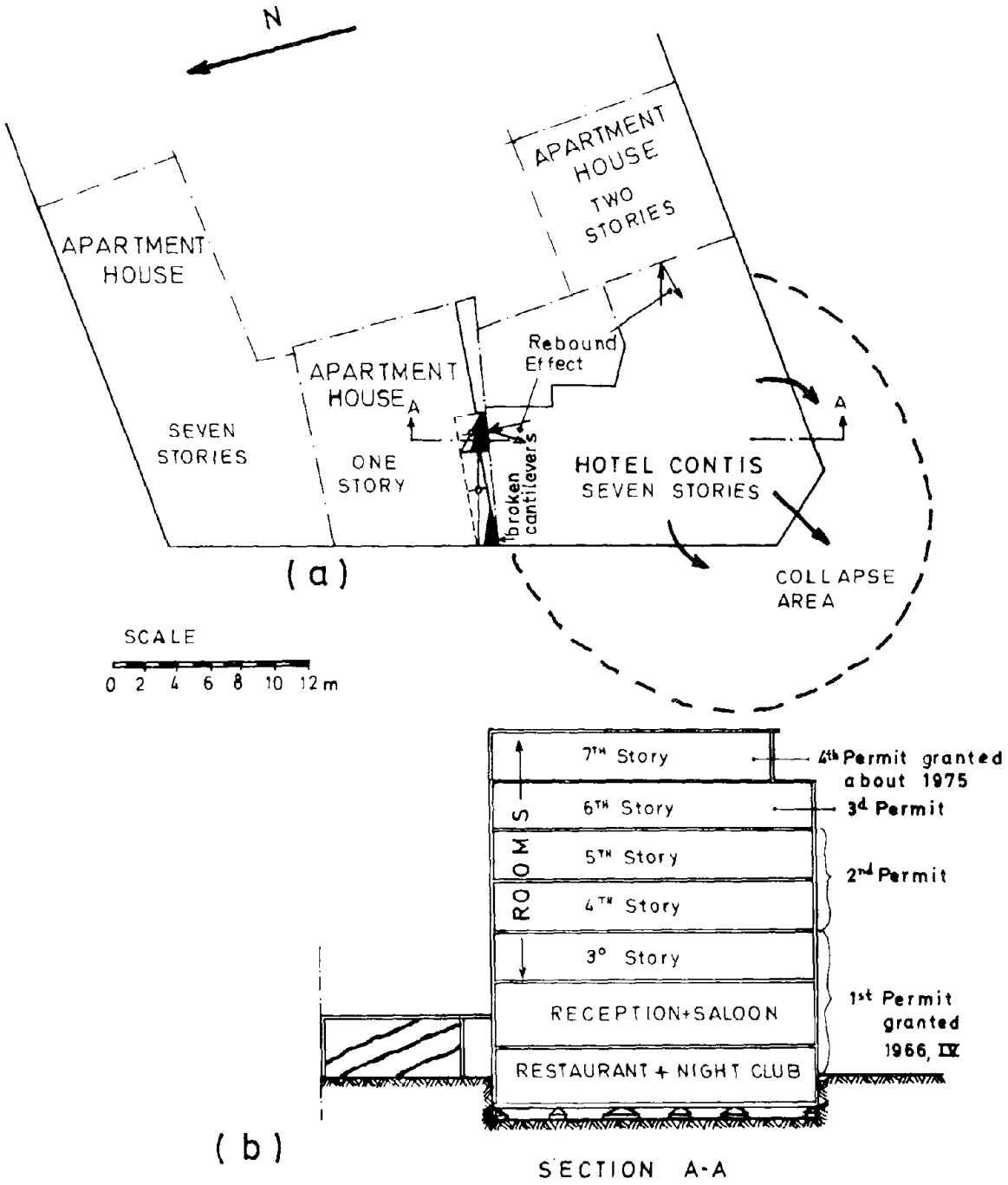

FIGURE 6.9 Contis Hotel in Loutraki. Plan and section of the building.

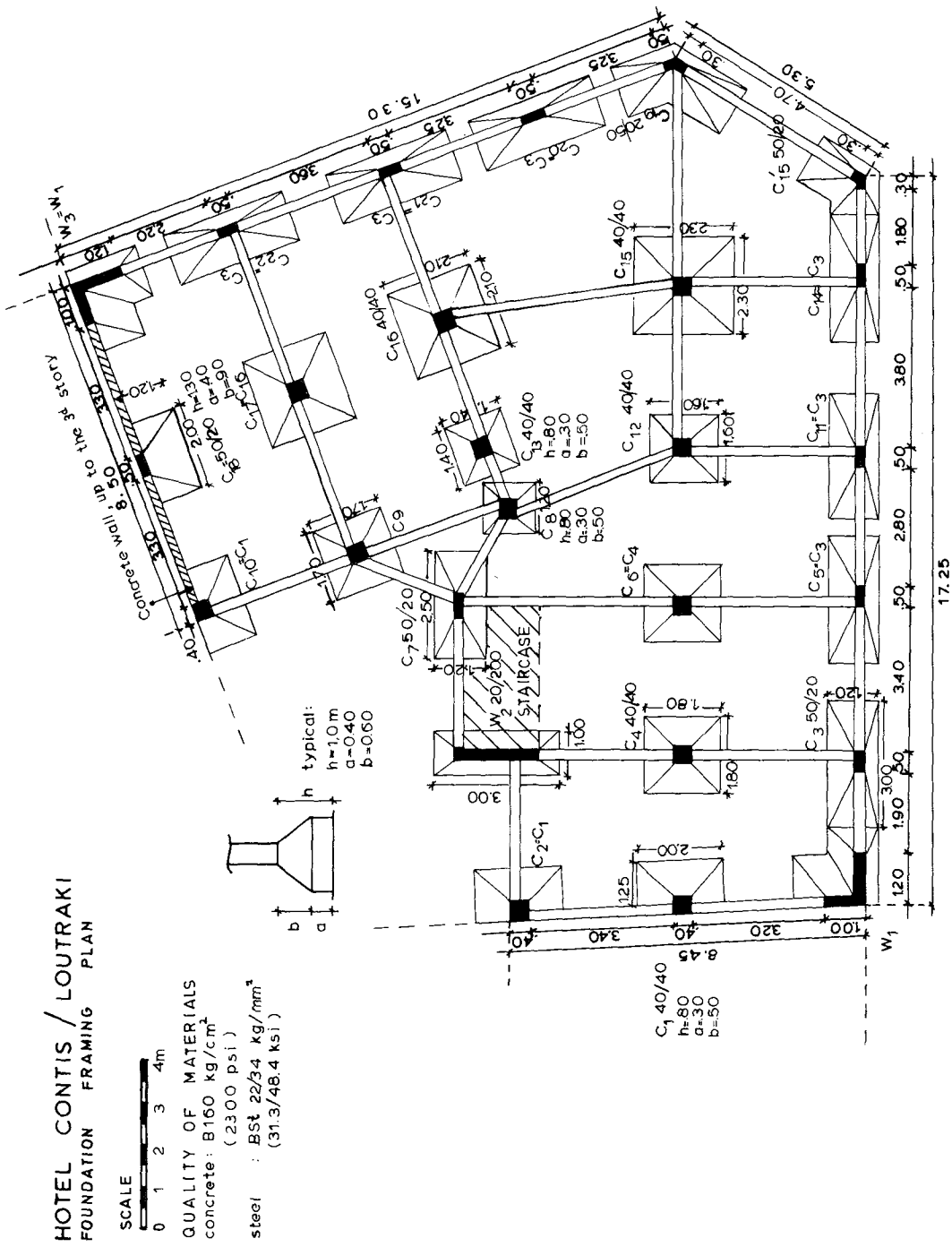

FIGURE 6.10 Contis Hotel in Loutraki. Foundation framing plan.

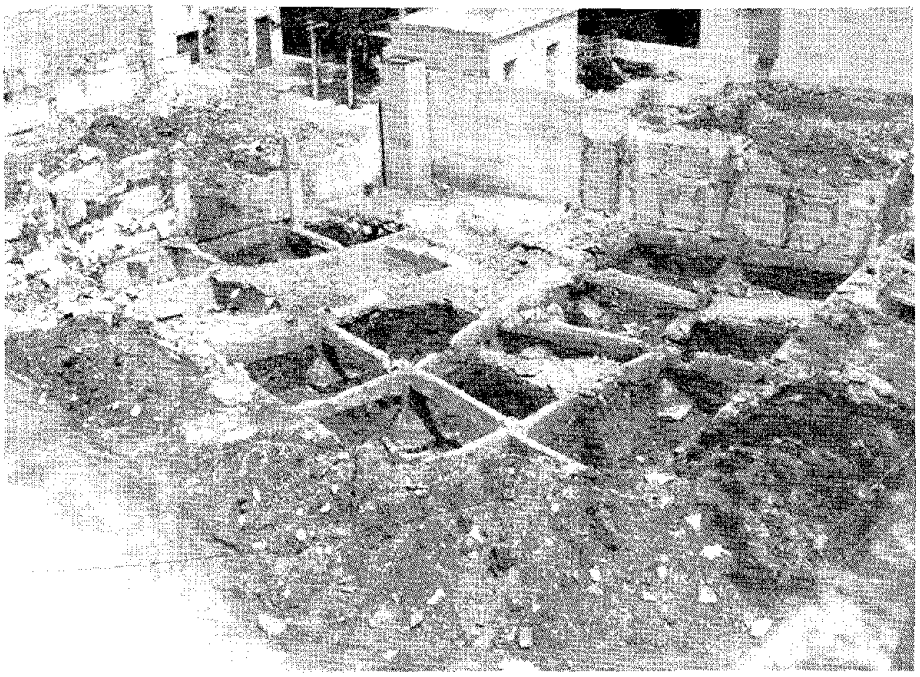

FIGURE 6.11 Contis Hotel in Loutraki. General southwest view of the foundation after removal of the debris. The tie beams are 15 by 40 cm.

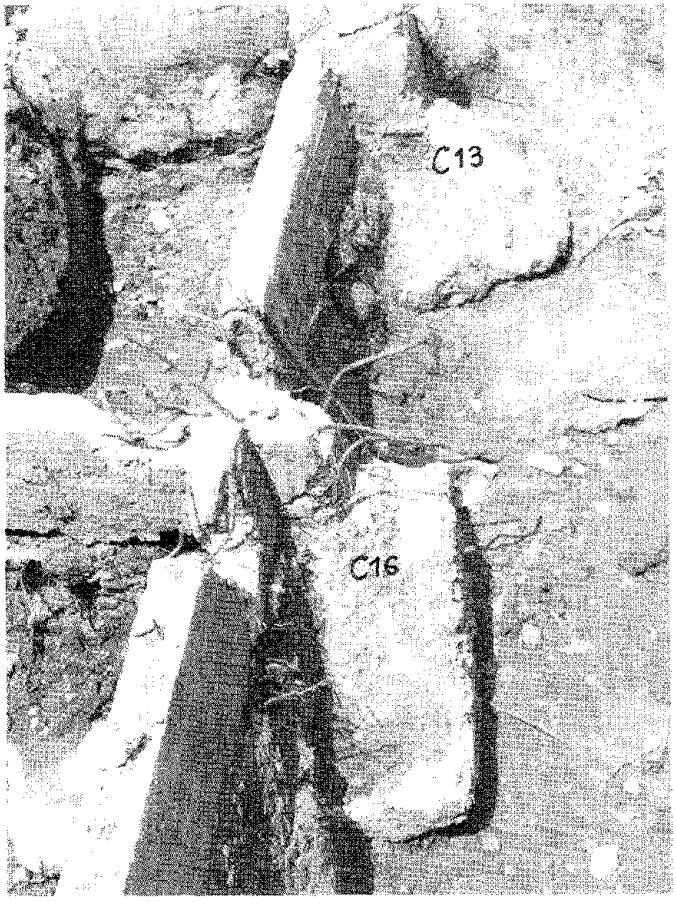

FIGURE 6.12 Contis Hotel in Loutraki. Most of the tie beams around the columns are discontinued to accommodate wastewater pipes.

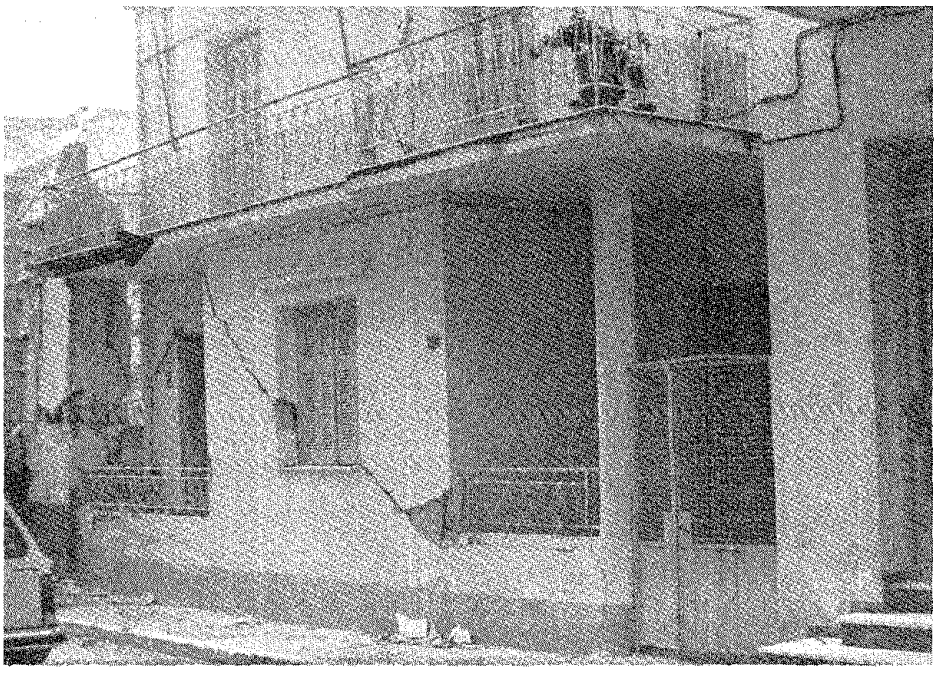

FIGURE 6.13 Contis Hotel in Loutraki. South view. A two-story building was located adjacent to the hotel. The arrow shows the excessive forces transmitted to this structure by the hotel during the rebound. Photograph courtesy A. Manis.

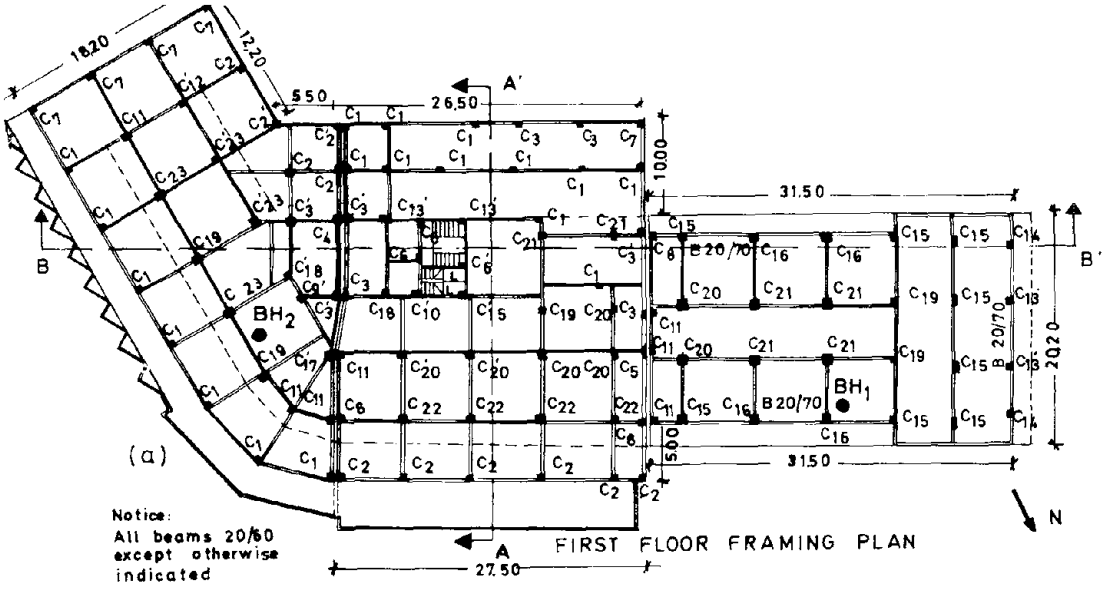

FIGURE 6.14 Galaxy Hotel in Vrahati. The first floor framing plan and two elevations. Sections I and II collapsed.

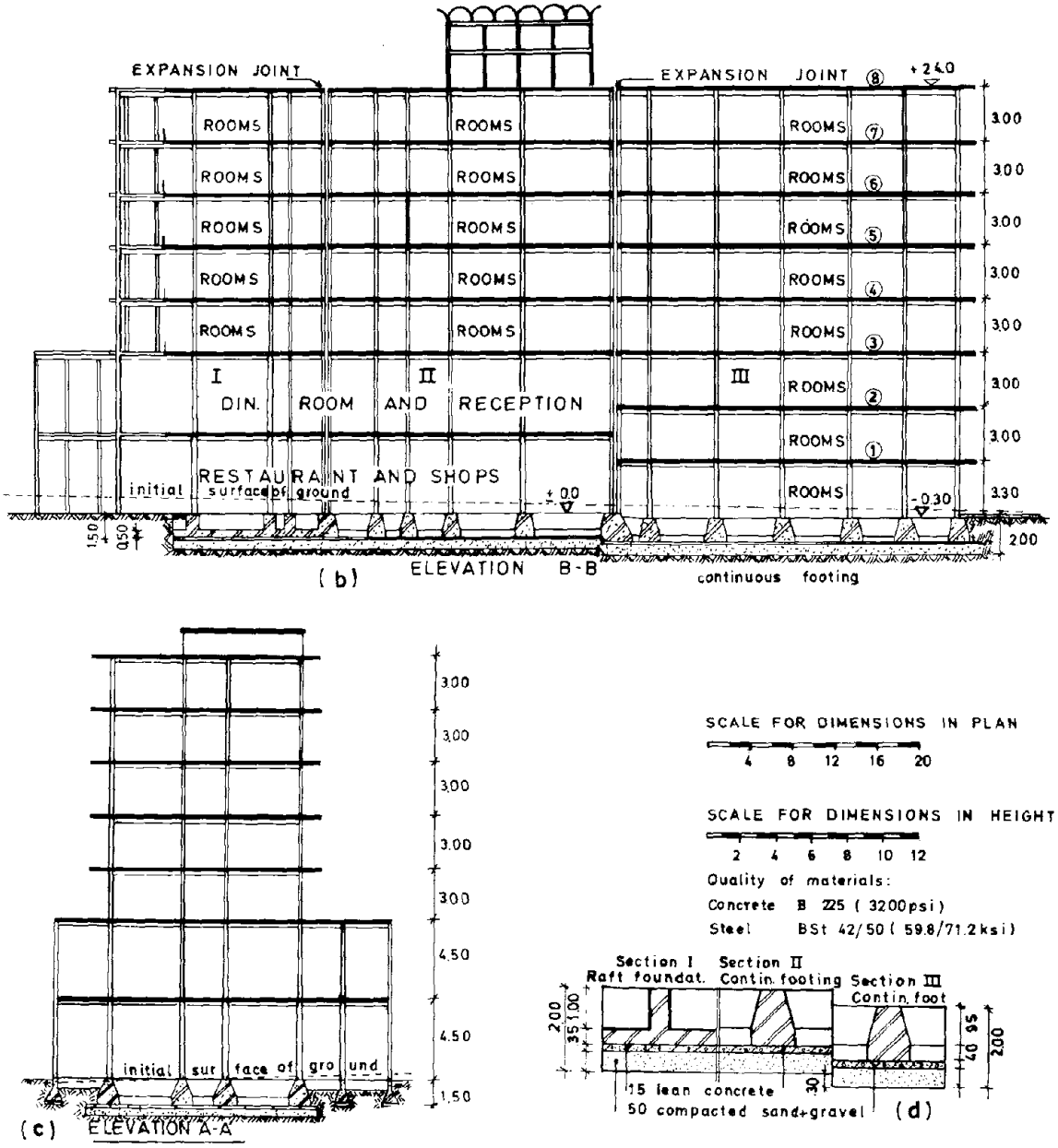

FIGURE 6.14 (Continued) Galaxy Hotel in Vrahati. The first floor framing plan and two elevations. Sections I and II collapsed.

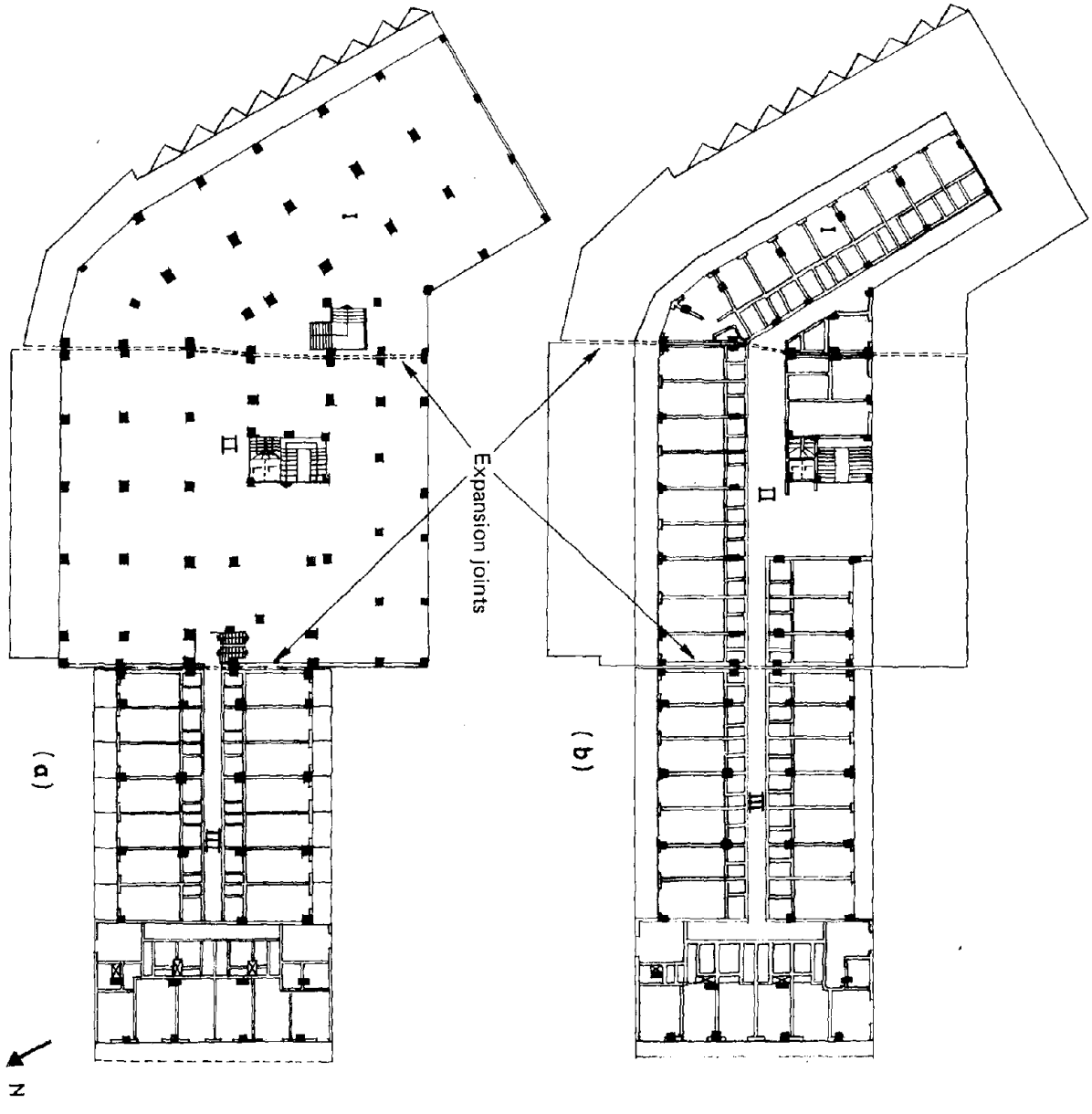

FIGURE 6.15 Galaxy Hotel in Vrahati. General architectural plans: (a) first floor, (b) typical floor.

TABLE 1 Dimensions of the Columns of the First Story

Symbol	Dimens. X/Y (cm)	Reinforcement No, Dia(mm)	Symbol	Dimens. X/Y (cm)	Reinforcement No, Dia(mm)
C_1	30/30	4 #20	C_{13}	40/60	10 #20
C_2	30/35	4 #20	C_{14}	40/65	10 #20
C_3	30/40	4 #20	C_{15}	40/70	10 #20
C_4	30/45	6 #20	C_{16}	40/75	10 #20
C_5	30/50	6 #20	C_{17}	45/55	12 #20
C_6	30/60	6 #20	C_{18}	50/50	14 #20
C_7	35/35	4 #20	C_{19}	50/60	18 #20
C_8	35/40	6 #20	C_{20}	50/70	18 #20
C_9	35/45	6 #20	C_{21}	50/80	22 #20
C_{10}	35/50	6 #20	C_{22}	60/60	18 #20
C_{11}	40/40	6 #20	C_{23}	60/70	20 #20
C_{12}	40/50	6 #20			

The same symbol with a dash, means same dimensions but in the Y/X direction respectively.

FIGURE 6.16 Galaxy Hotel in Vrahati. Northeast view of the hotel during construction.

FIGURE 6.17 Galaxy Hotel in Vrahati. North view of the hotel during construction.

TABLE 2 Summary of Borehole Test Results

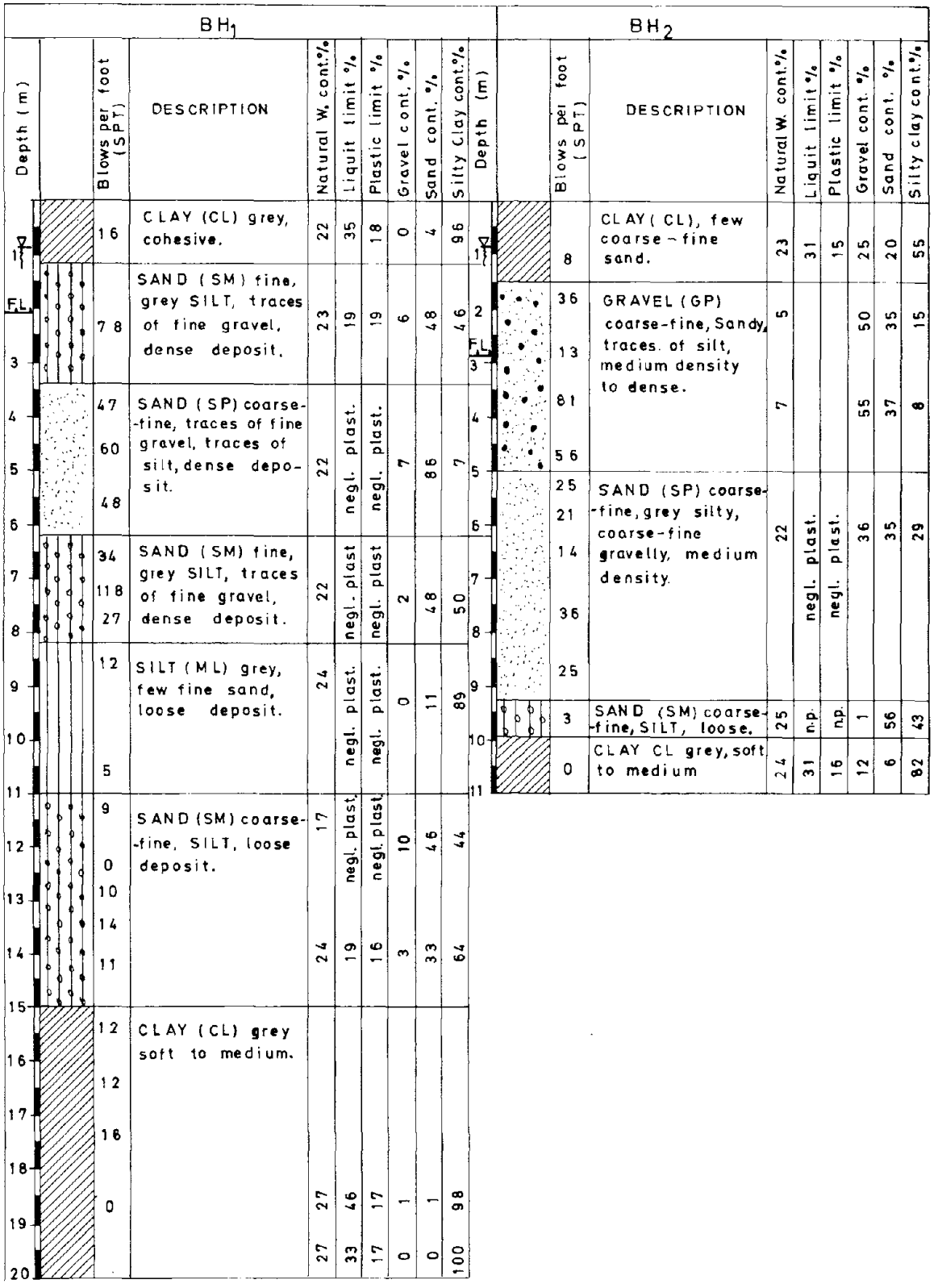

BH1

Depth (m)	Blows per foot (SPT)	DESCRIPTION	Natural W. cont.%	Liquit limit %	Plastic limit %	Gravel cont. %	Sand cont. %	Silty Clay cont.%
1	16	CLAY (CL) grey, cohesive.	22	35	18	0	4	96
FL 3	7 8	SAND (SM) fine, grey SILT, traces of fine gravel, dense deposit.	23	19	19	6	48	46
4	47	SAND (SP) coarse-fine, traces of fine gravel, traces of silt, dense deposit.	22	negl. plast.	negl. plast.	7	86	7
5	60							
6	48							
7	34	SAND (SM) fine, grey SILT, traces of fine gravel, dense deposit.	22	negl. plast	negl. plast	2	48	50
8	118 27							
9	12	SILT (ML) grey, few fine sand, loose deposit.	24	negl. plast.	negl. plast.	0	11	89
10								
11	5							
12	9	SAND (SM) coarse-fine, SILT, loose deposit.	17	negl. plast.	negl. plast.	10	46	44
13	0 10							
14	14		24	19	16	3	33	64
15	11							
16	12	CLAY (CL) grey soft to medium.	27	33	17	0	0	100
17	12							
18	16							
19	0		27	46	17	1	1	98
20								

BH2

Depth (m)	Blows per foot (SPT)	DESCRIPTION	Natural W. cont.%	Liquit limit %	Plastic limit %	Gravel cont. %	Sand cont. %	Silty clay cont.%
1	8	CLAY (CL), few coarse - fine sand.	23	31	15	25	20	55
2 FL 3	36	GRAVEL (GP) coarse-fine, Sandy, traces of silt, medium density to dense.	5			50	35	15
4	13 81		7			55	37	8
5	56							
6	25 21	SAND (SP) coarse-fine, grey silty, coarse-fine gravelly, medium density.	22	negl. plast.	negl. plast.	36	35	29
7	14							
8	36							
9	25							
10	3	SAND (SM) coarse-fine, SILT, loose.	25	n.p.	n.p.	1	56	43
11	0	CLAY CL grey, soft to medium	24	31	16	12	6	82

Sections I and II of the hotel collapsed almost inside the plan of the building, as seen in Figures 6.19 and 6.20. The two-story southern wall and the west and east parts of the ground floor are still standing. The wall between sections II and III can be seen in Figure 6.21. Figure 6.22 shows the search for victims in the rubble.

In section III thicker brick walls throughout the height of the structure resulted in a relatively stiffer and stronger structural system than in sections I and II, enabling section III to survive the earthquake (Figure 6.23). The appearance of the walls in section III is shown in Figures 6.24 and 6.25. The collapse did not extend to the ground floors in section I and II except at the curved east corner (Figure 6.14a), where the most severe collapse was observed.

Without further investigation it is not possible to determine the mechanism that triggered the collapse, although there are several possible explanations.

1. Because the sections were separated by expansion joints and because the sections had different stiffnesses due to the change in story height and partitions, it is possible that there was a hammering effect between sections. There was little evidence of such action between sections II and III. The expansion joint between sections I and II, which were oriented at about a 60° offset, was irregular and could have transferred lateral forces normal and parallel to the joint as the sections deformed. The damage in section III (Figures 6.24 and 6.25) indicates that there was deformation along both axes of the structure. The largest deformations, however, were roughly in a north-south direction, the short direction of the structure. Maximum deformations in all three sections were probably largest in the short directions.

2. The hollow brick walls increased the stiffness of the structure, and in sections I and II there was an abrupt change of stiffness above the second story. As a result, according to Carydis and Ermopoulos (1975), the member forces may increase locally by a factor of about 2.5 at the top of the second story. Such large forces would likely exceed the lateral capacity of the framing system, especially in the vicinity of the east corner.

3. The vertical acceleration and displacement may have been quite large. The beams and slabs of the diaphragm between the second and third story may have been overstressed, since most of the vertical loads above that level would have been transferred to this floor through the walls. The horizontal framing system of the third floor was the same as that of the floors above. The cross section of the beams was typically 20 by 60 cm. It is possible that, with high gravity loading coupled with high vertical acceleration, the floor system failed in shear.

4. The influence of local site conditions may have been quite large. According to Richart, Hall, and Woods (1970), under a building groundwater forms an inclined piezometric surface that for the "reflection and refraction of waves has a behavior similar to the effects of inclined layers." This inclined layer should be thought of as harder, since its P wave velocity, V_p, is about 1,500 m/s. Between this inclined layer and the surface of the ground a wedge is formed that increases the seismic intensity.

FIGURE 6.18 Galaxy Hotel in Vrahati. North view of the hotel after the earthquake. The remaining part of section III is shown in Figure 6.14a and 6.14b.

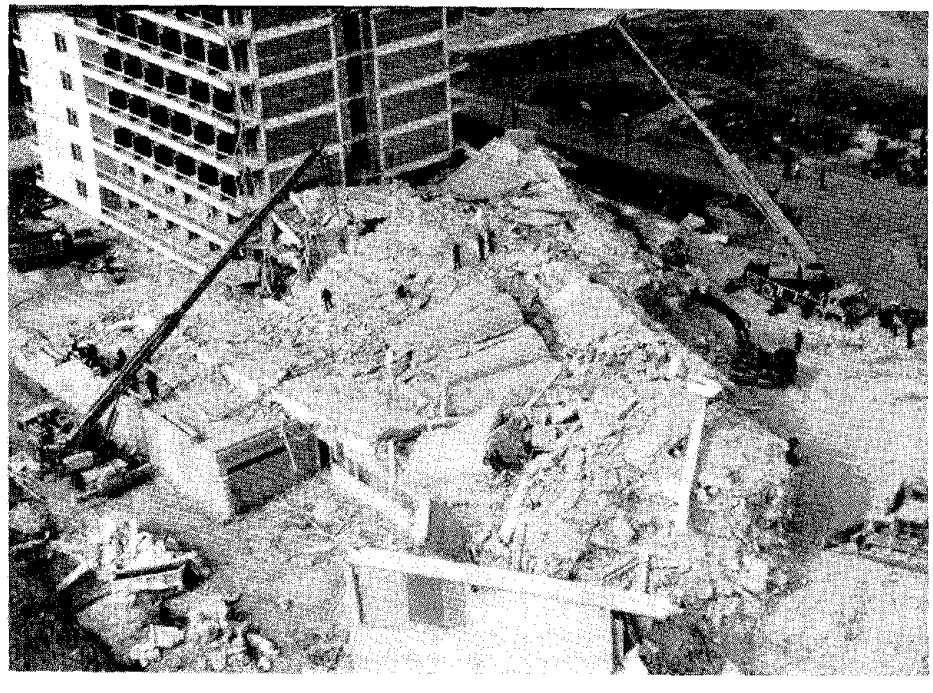

FIGURE 6.19 Galaxy Hotel in Vrahati. Aerial view from the south of the collapsed sections I and II (see Figure 6.14) a few days after the earthquake. Photograph courtesy Tachydromos magazine.

FIGURE 6.20 Galaxy Hotel in Vrahati. View from the east one day after the earthquake and collapse. Photograph courtesy N. Floros.

FIGURE 6.21 Galaxy Hotel in Vrahati. North side of the expansion joint between sections II and III.

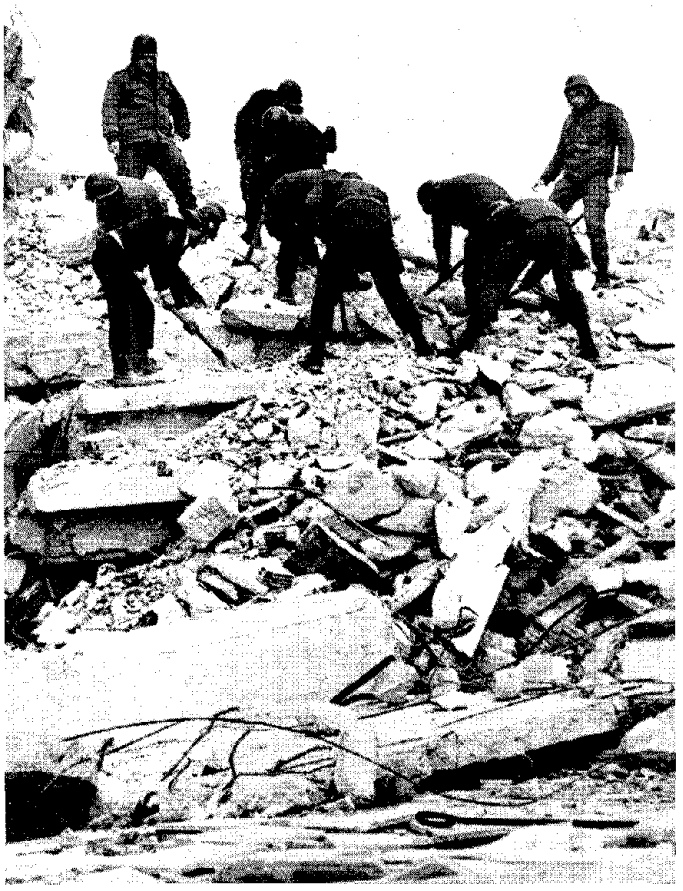

FIGURE 6.22 Galaxy Hotel in Vrahati. Search for the three victims. Photograph courtesy the Synergatici.

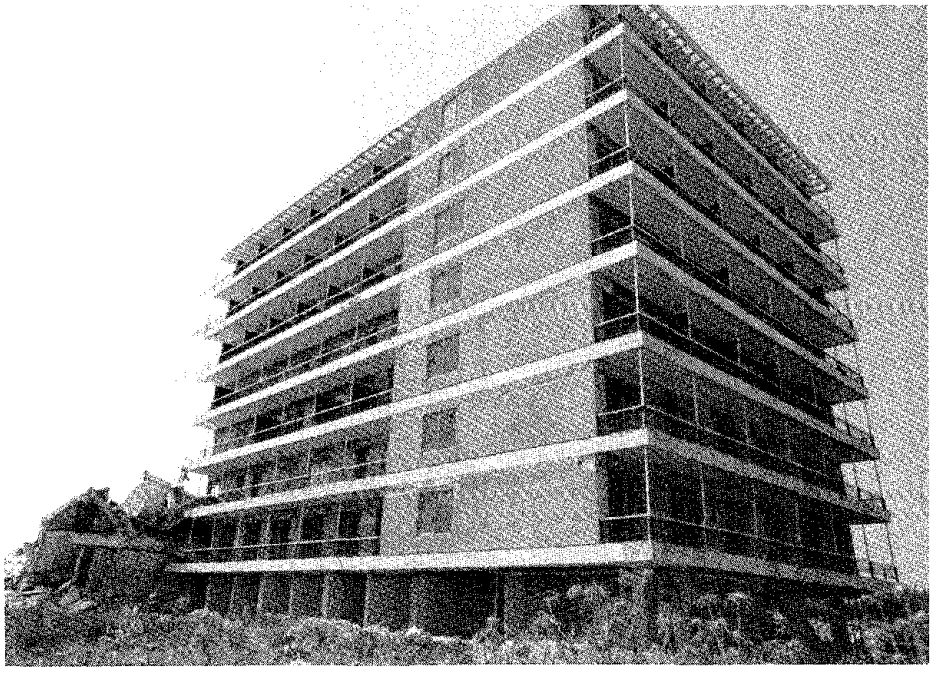

FIGURE 6.23 Galaxy Hotel in Vrahati. North view of section III. Columns and walls in the first floor were heavily damaged.

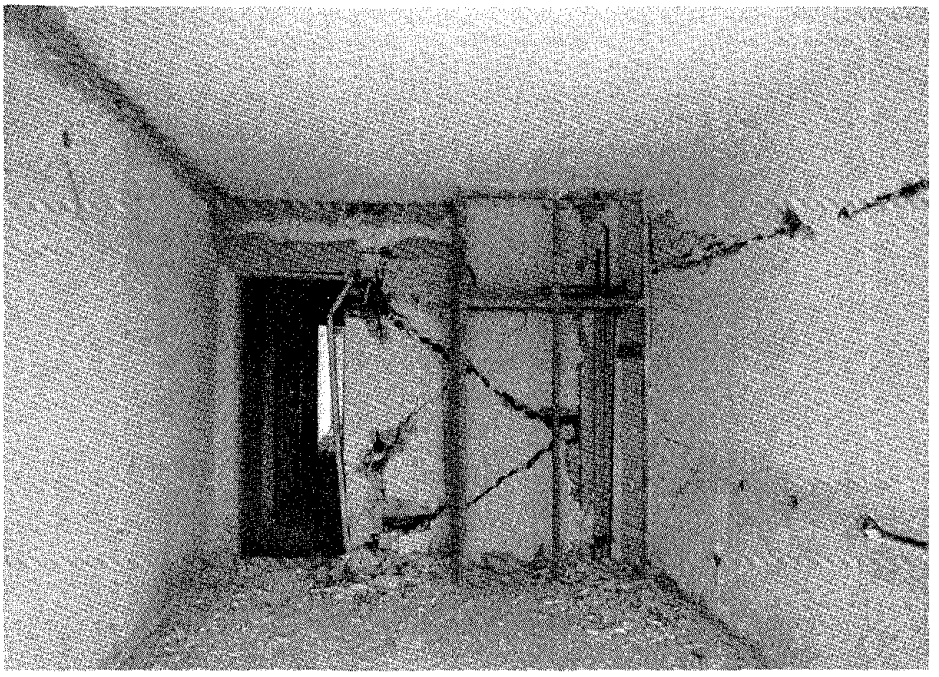

FIGURE 6.24 Galaxy Hotel in Vrahati. Inside view of a room in the second story of section III. The front brick wall extends along the long axis of section III (northwest to southeast).

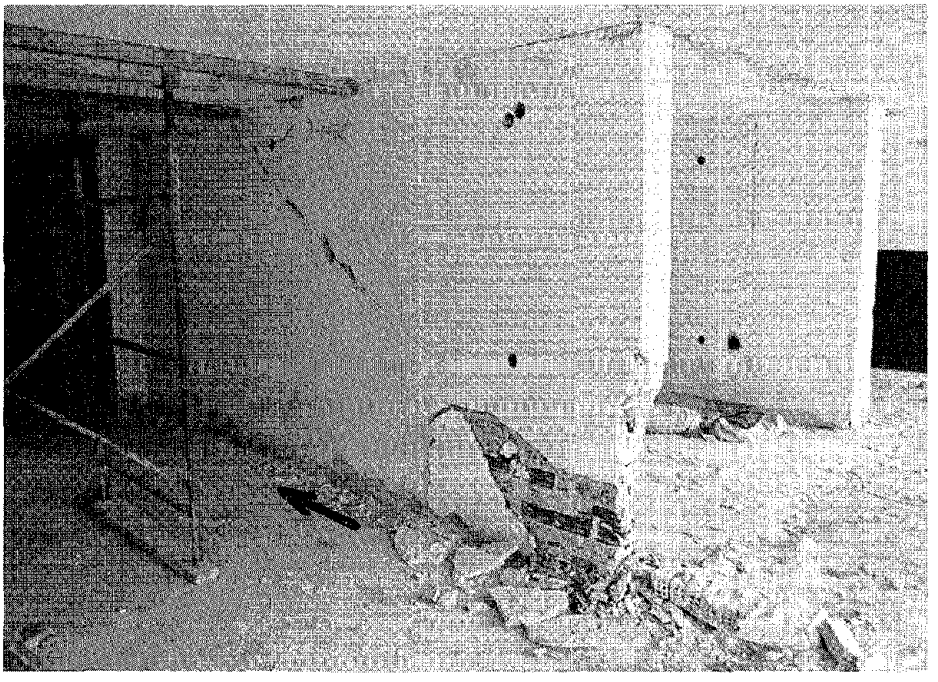

FIGURE 6.25 Galaxy Hotel in Vrahati. West view of the first story. The cracked walls are directed southwest to northeast.

The foundation level of section III was at a depth of about -2.20 m from the initial ground surface. Borehole 1 (see Table 6.2) shows fine sand and gray silt with traces of fine gravel (dense deposit) at that depth. Sections I and II were founded at a depth of about -2.80 m. From borehole 2 the foundation soil was coarse to fine gravel, sandy with traces of silt, and medium dense to dense. BH_1 had a denser deposit with more silt and thinner layers than did BH_2, which was loose, had more gravel, and produced thicker layers. The foundation soil of sections I and II could have been more mobile than that of section III. In any case, the alluvial soils were clearly quite variable.

5. Before arriving at any general conclusion, it must be noted that a collapse results from the combination of many factors. The hotel's foundation lay under the level of the water table. Due to the presence of water, the pore pressure during the earthquake was tremendously increased. Raft foundations on porous material directly receive the pore pressure front of P waves in the vertical direction, as shown schematically in Figure 6.26. Such foundations combined with low soil pressures may be unsuitable in cases where direct water pressure can be applied. For isolated footings the overpressure may be relieved, as indicated in Figure 6.26b.

In the case of the Galaxy Hotel, the different soil conditions and changes in pore water pressure during the earthquake may have changed the response of the structure's different sections.

After considering the different possibilities, it seems most likely that the failure of the Galaxy Hotel was produced by abrupt changes in stiffness--both vertically and horizontally--in the different sections of the structure and by a structural layout (L-shaped) that led to differences in the response of the hotel's sections to ground motion. The long flexible columns at the first and second levels of sections I and II could not sustain the large deformations caused by the earthquake. While it is interesting to speculate on the influence of the site's soil conditions, it should be noted that the Galaxy Hotel was the only multistory structure in the area and the only structure heavily damaged.

Because soil and structural details are available, some additional study of the Galaxy Hotel is warranted.

APOLLO HOTEL

The Apollo Hotel in Loutraki was a modern reinforced concrete structure. It was located about 1,500 m southwest of the Contis Hotel and about 80 m from the sea (the number 3 in Figure 5.1 shows its location). The structure collapsed totally.

The building had nine floors and 271 rooms. Views of the hotel prior to the collapse are given in Figures 6.27, 6.28, and 6.29. A row of columns along the west side of the hotel, shown in Figure 6.30, did not collapse. Figure 6.30 shows a general view of the site after the earthquake. Since no drawings are available, it is not possible to make

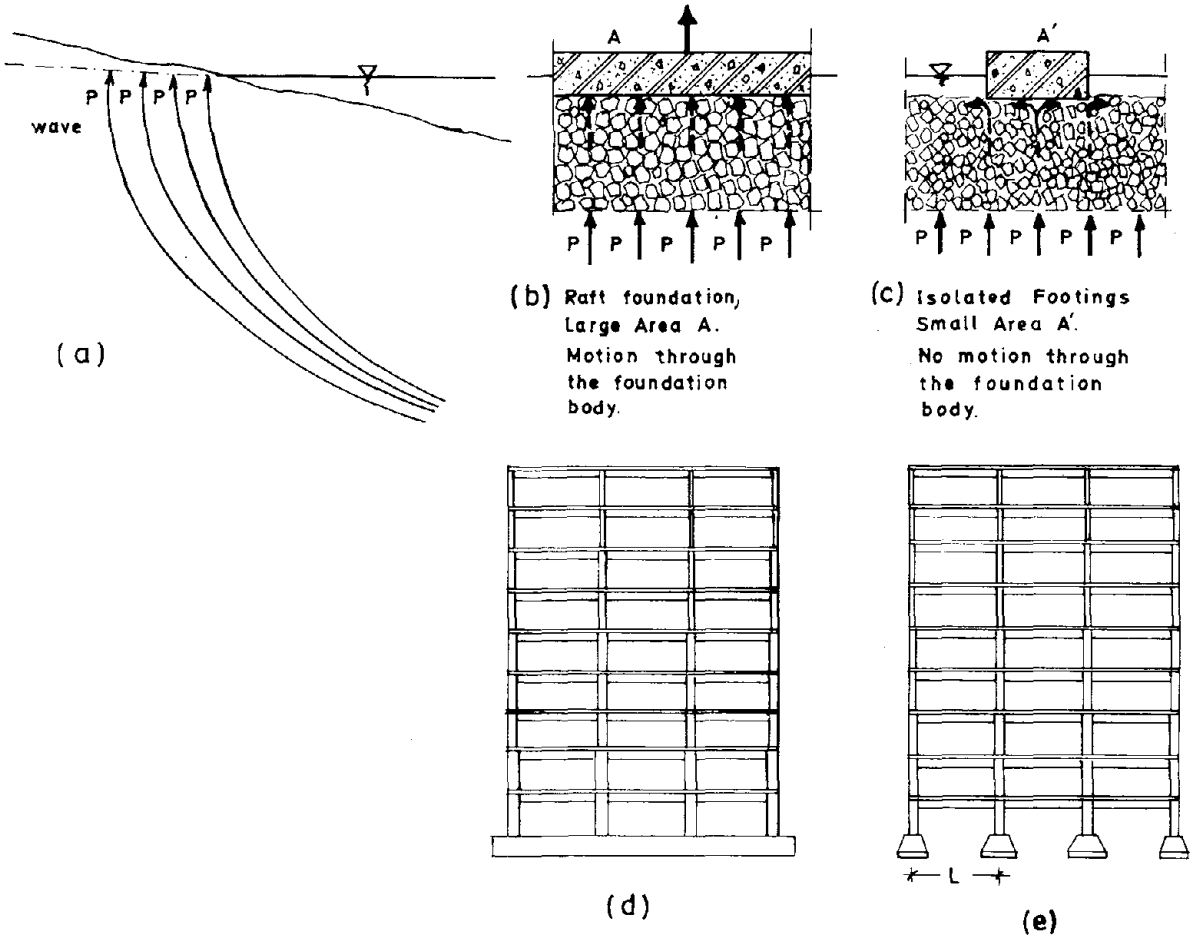

FIGURE 6.26 Incident P wave fronts (a) may disturb a foundation over porous submerged soil material (b) or they may not disturb it (c). In all cases the extra dynamic vertical pressure of the porous material should be added to the existing static pressure due to the structure. Case (d) gives a small static pressure, which is less favorable than in case (e), which gives a higher static pressure, depending on the dimensions of the footings.

any specific comments about the reasons for the collapse. However, some general observations may be helpful.

o Above the first floor the columns became "shear walls," as shown in Figure 6.31.

o No transverse beams were provided perpendicular to the plane of the "walls."

o The slabs were supported directly by the "walls" and on beams in the plane of the "walls," as shown in Figures 6.32 and 6.33.

o The slab reinforcement was a 6-mm-mesh wire that pulled out or fractured, as shown in Figure 6.33.

o The slabs were sheared from the columns (probably in a progressive manner) and collapsed in a nearly vertical direction, as indicated by the "pancaked" layers of floors.

FIGURE 6.27 Apollo Hotel in Loutraki. View from the southeast before the earthquake.

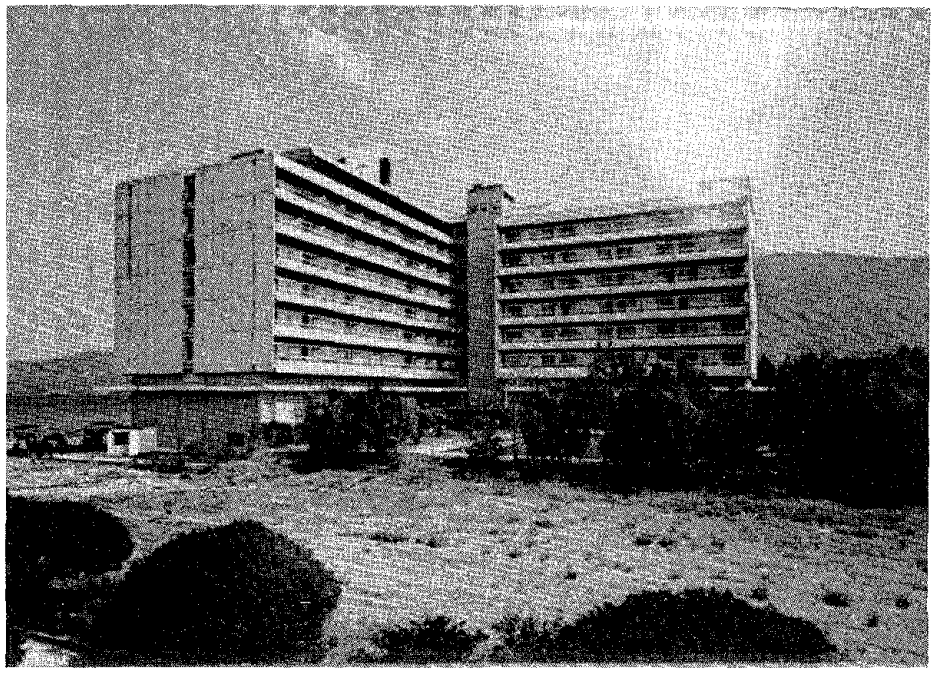

FIGURE 6.28 Apollo Hotel in Loutraki. View from the south before the earthquake.

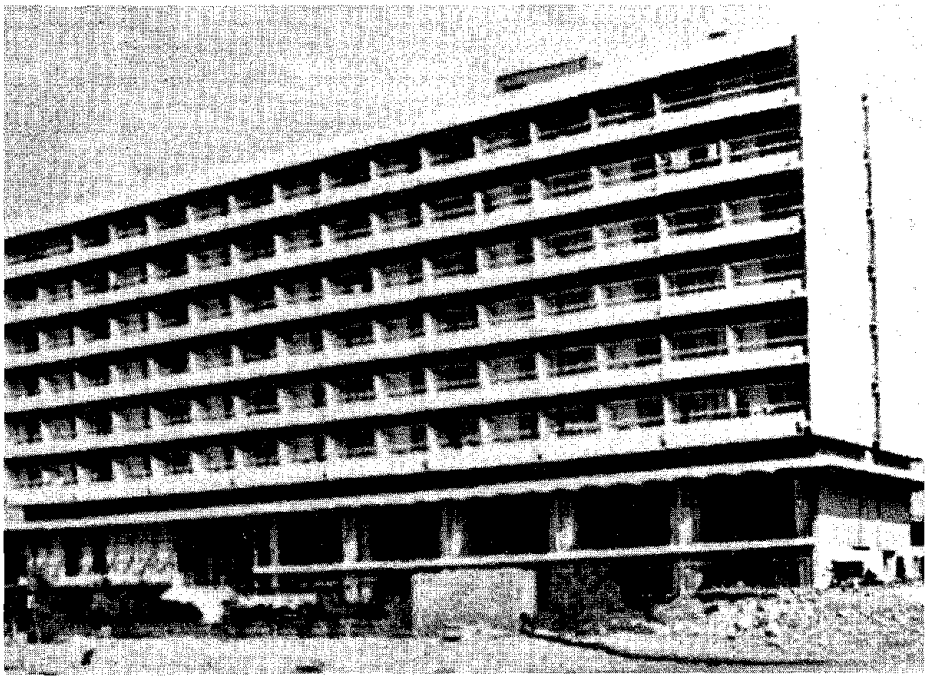

FIGURE 6.29 Apollo Hotel in Loutraki. View from the sea on the west side.

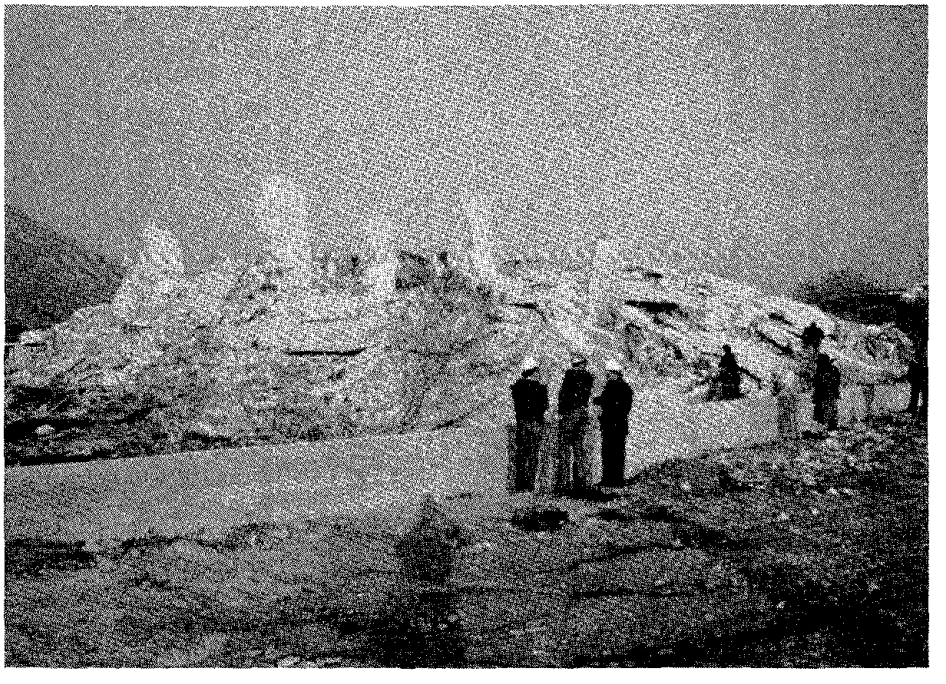

FIGURE 6.30 Apollo Hotel in Loutraki. View from the southwest (showing the same facade as in Figure 6.29).

FIGURE 6.31 Apollo Hotel in Loutraki. The columns of the west wing, here seen from the west side, were still standing after the earthquake.

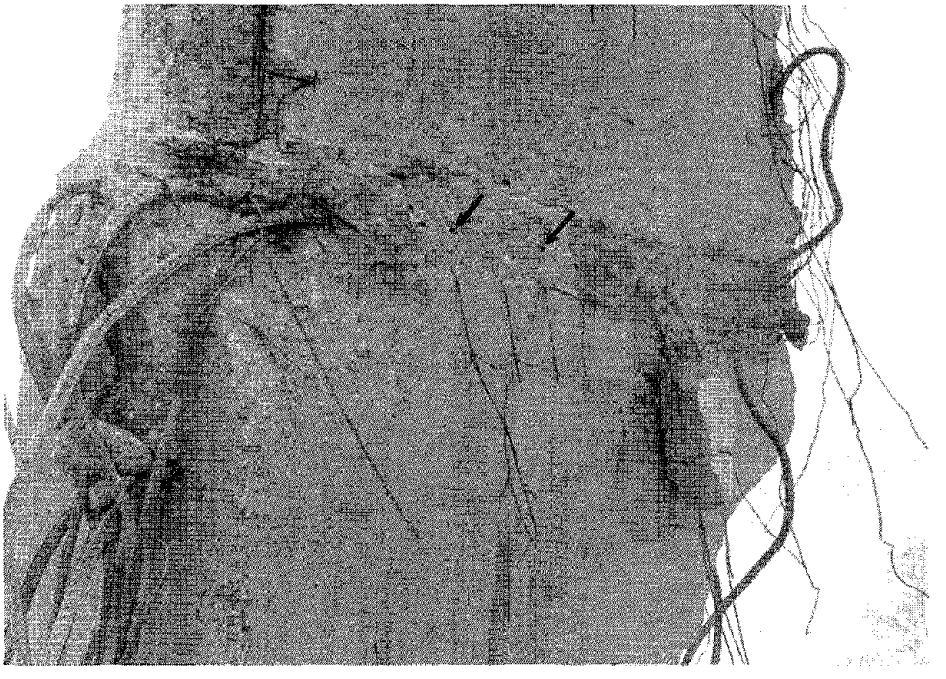

FIGURE 6.32 Apollo Hotel in Loutraki. Detail of the joint between shear wall and horizontal diaphragm. Note the slip of the horizontal reinforcing mesh wires of the slabs from the walls (arrows).

FIGURE 6.33 Apollo Hotel in Loutraki. The slabs sheared away from the column walls and came down one on top of the other.

BLOCK OF FLATS SEGAS

The Block of Flats Segas was a five-story reinforced concrete structure. The building partially collapsed after the earthquake on February 25. It is located no more than 100 m from the seashore (number 2 in Figure 5.1).

Construction started about the beginning of 1974. Figures 6.34 and 6.35 give some general structural details. The building had an open and rather weak first story that "disappeared" when the upper levels collapsed onto the first level (Figures 6.36, 6.37, and 6.38). A low wall, constructed as a kind of retaining wall, formed short columns in the open first story around the periphery of the structure. Heavy beams supported the first floor, as shown in Figures 6.39 and 6.40. The structure above the first story was stiff due to the presence of brick partition walls. Columns c_1, c_7, and c_{15} collapsed and the adjacent slabs ruptured (see Figures 6.34 and 6.36). The rupture of the slabs was due to the complete absence of reinforcement parallel to the edge at column c_{15}. It is interesting to note that corner column c_{21} did not collapse, as did column c_1. Some of the columns penetrated the slabs, as can be seen for column c_6 in Figure 6.41.

The framing system caused some columns to have little bending resistance at floor levels. For example, columns c_7, c_{15}, c_{20}, and c_{12} had no beams normal to their edges or to the weak direction of bending. The column failures indicated a general lack of sufficient lateral reinforcement near the ends and in the joints (Figures 6.38, 6.39, and 6.40).

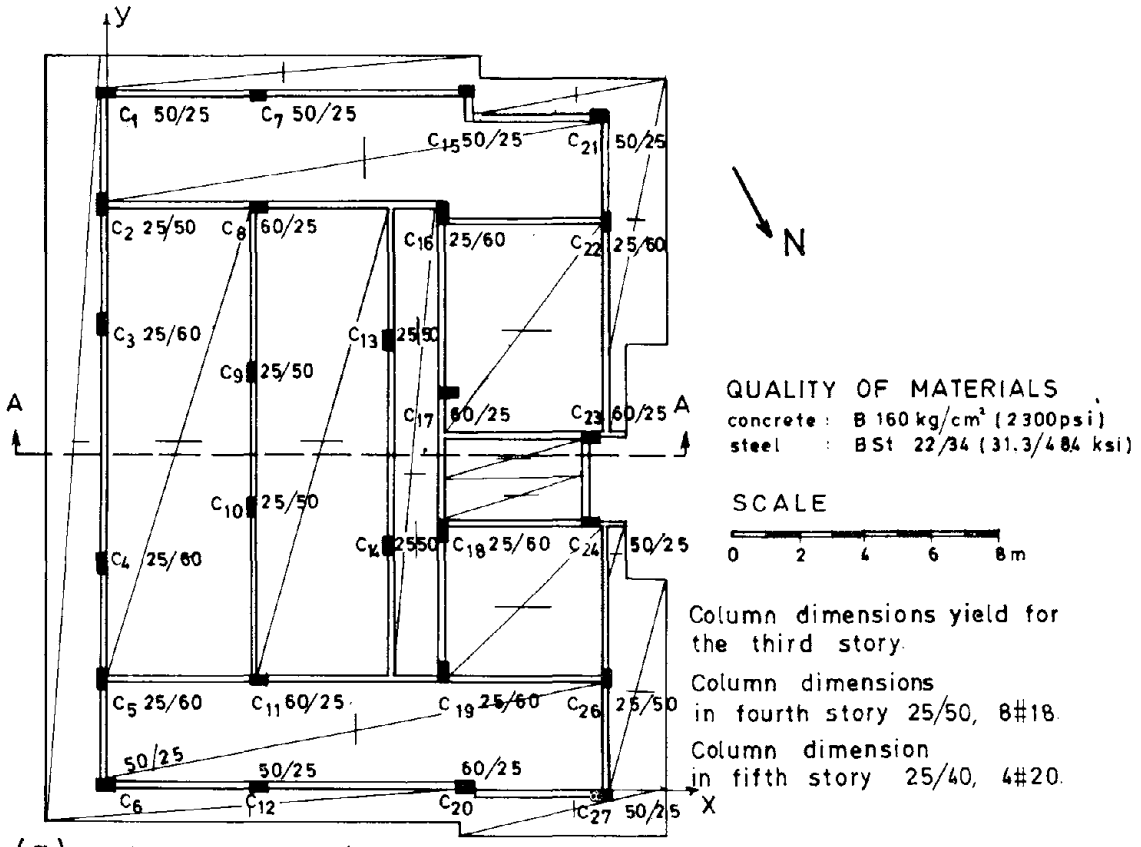

(a) Typical floor framing plan.

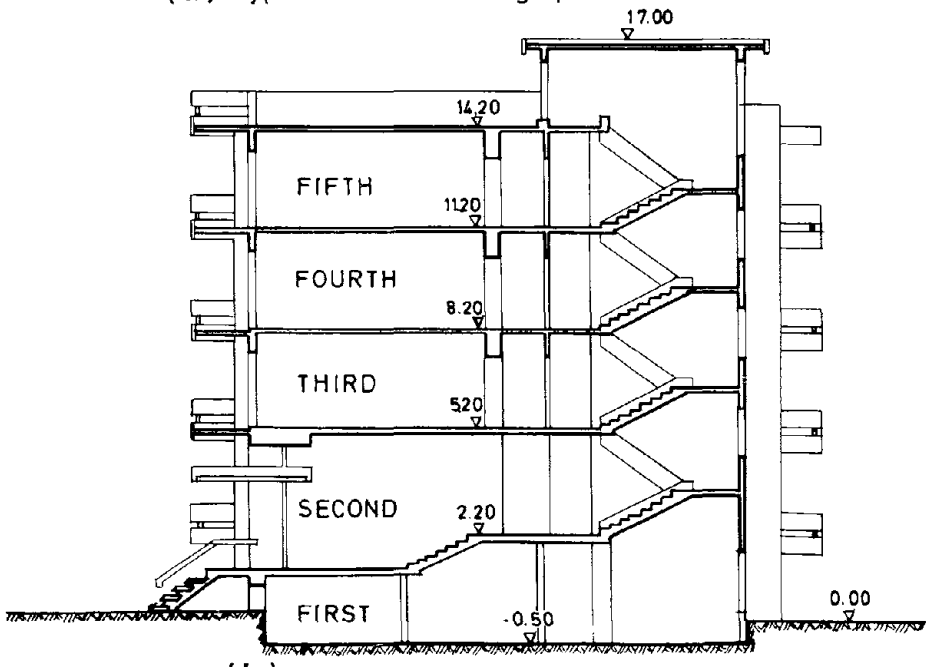

(b) Elevation A-A

FIGURE 6.34 Block of Flats Segas in Loutraki. Typical floor framing plan and elevation.

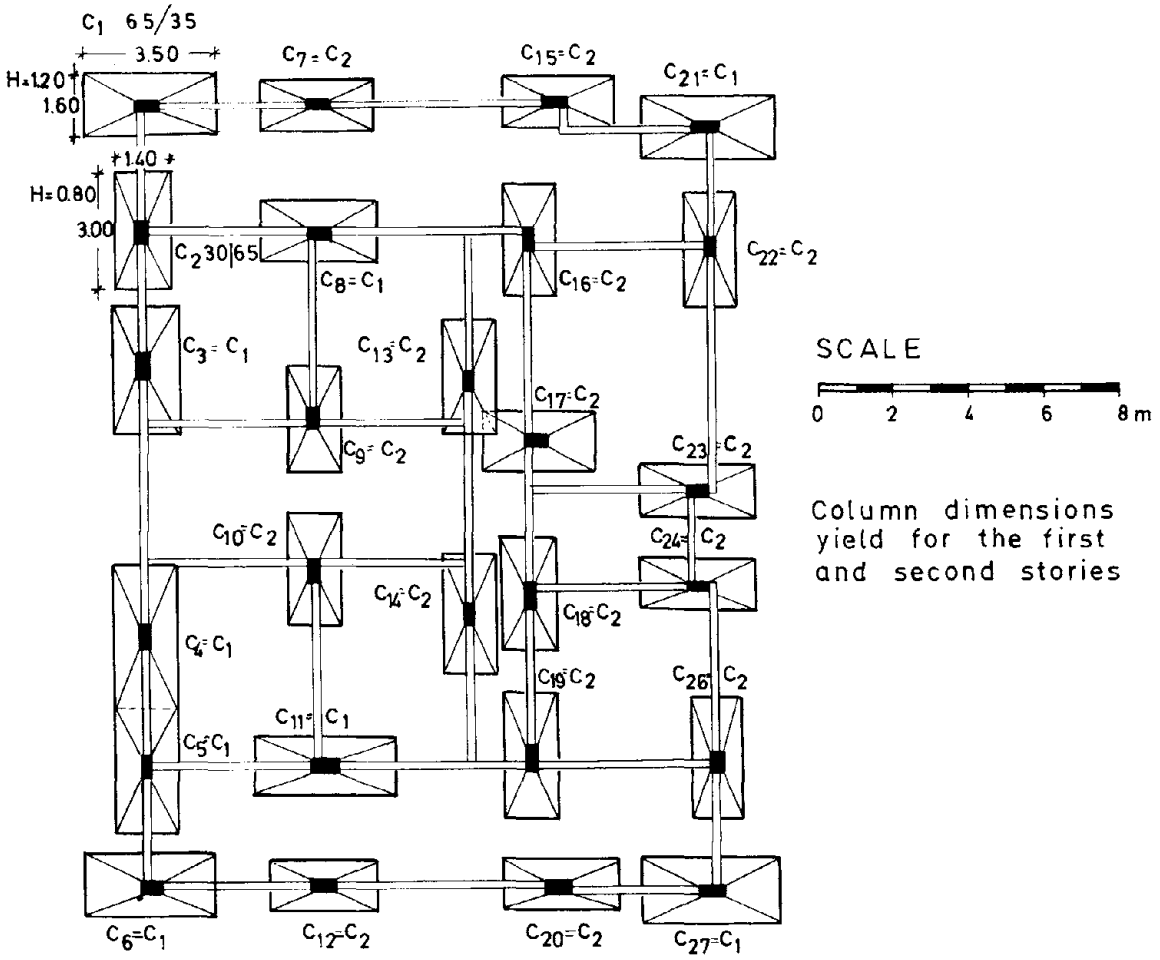

FIGURE 6.35 Block of Flats Segas in Loutraki. Foundation framing plan.

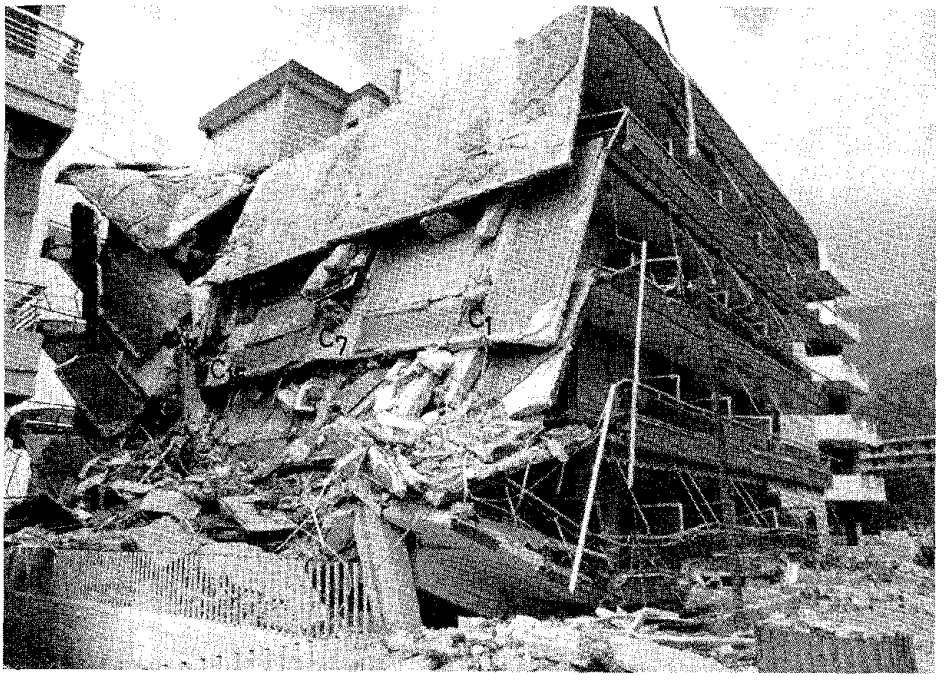

FIGURE 6.36 Block of Flats Segas in Loutraki. The structure from the southeast.

FIGURE 6.37 Block of Flats Segas in Loutraki. The structure from the west.

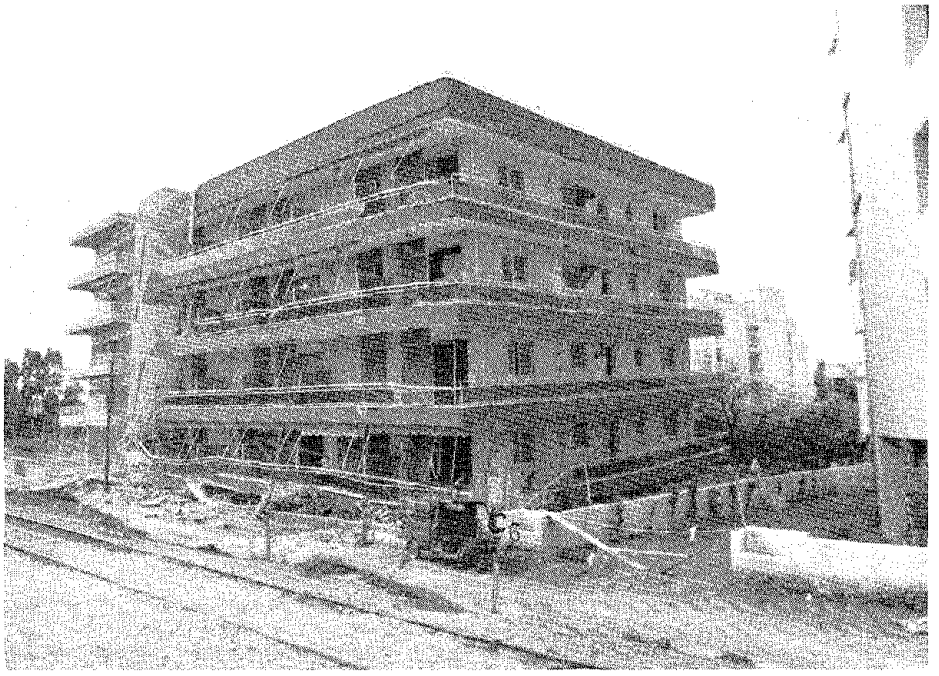

FIGURE 6.38 Block of Flats Segas in Loutraki. The structure from the northeast.

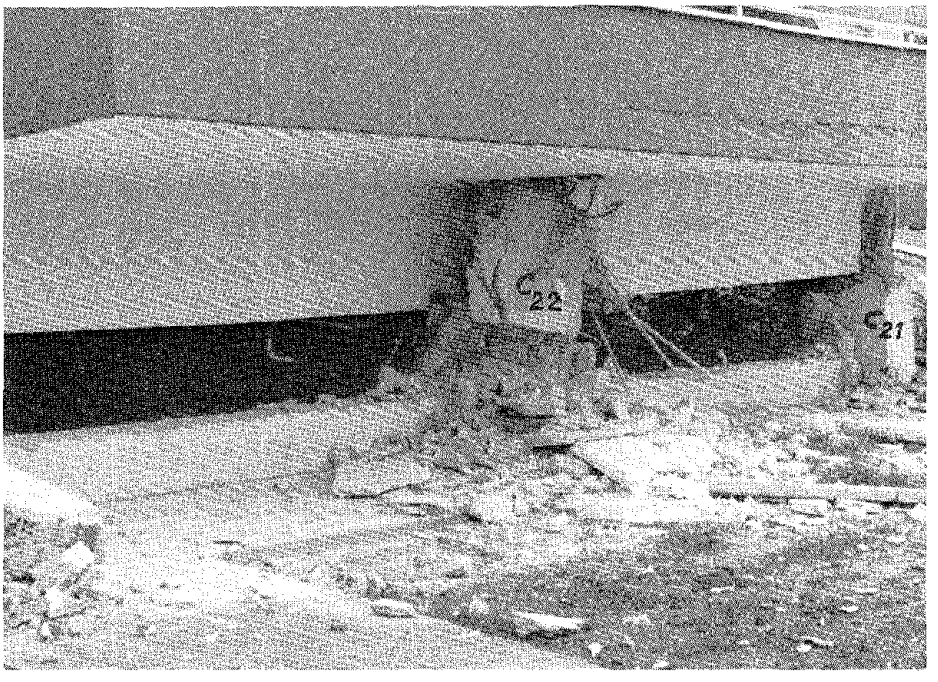

FIGURE 6.39 Block of Flats Segas in Loutraki. Columns c_{22} and c_{21} viewed from the north.

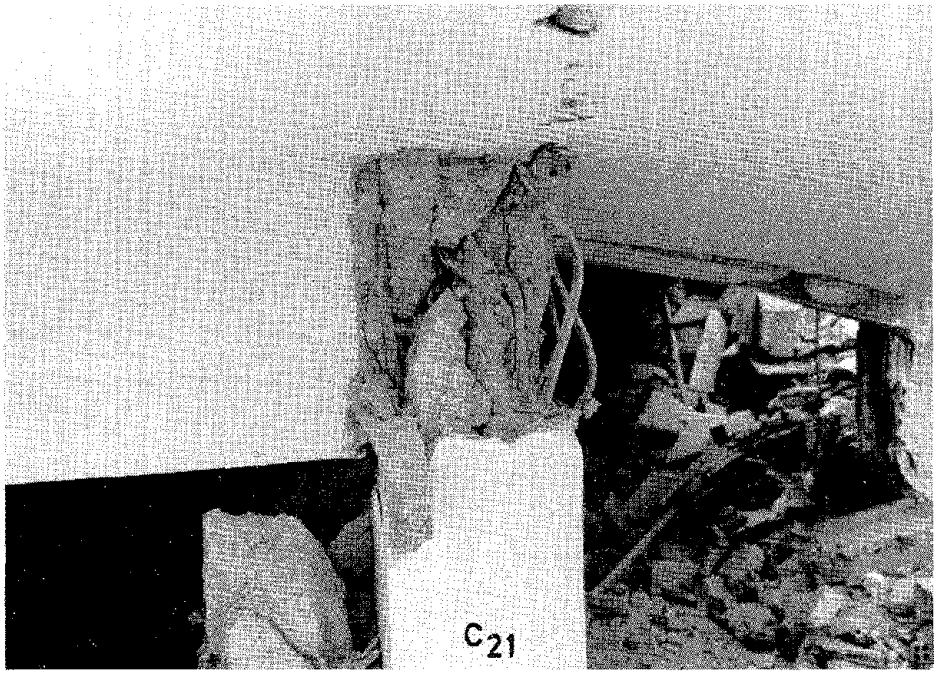

FIGURE 6.40 Block of Flats Segas in Loutraki. As shown by column c_{21}, there is no tie within the height of the column-to-beam connection.

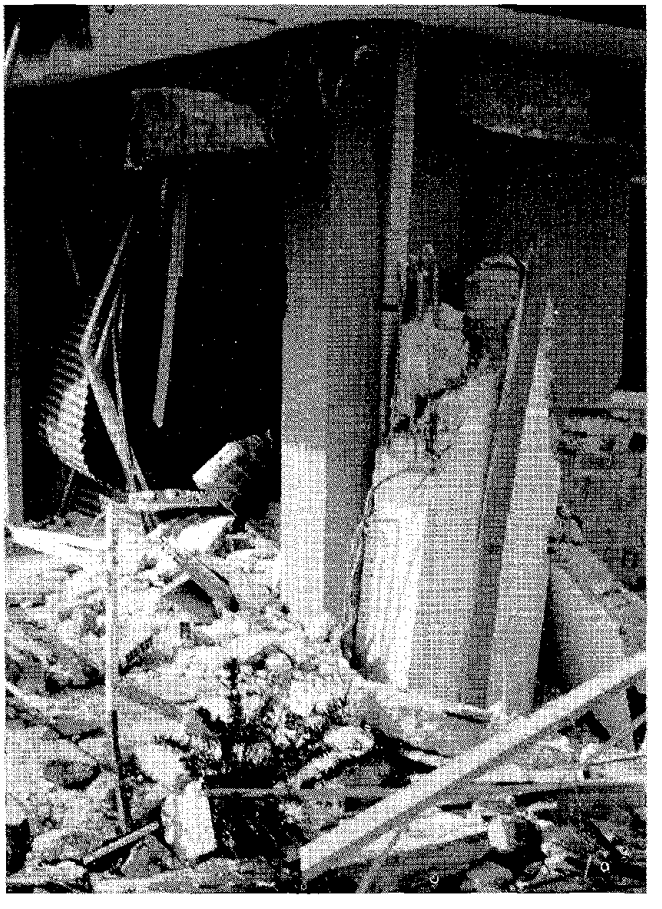

FIGURE 6.41 Block of Flats Segas in Loutraki. Column c_6, shown here, penetrated the slab.

PARTHENON OF ATHENS

Because of historical interest in the Parthenon, we briefly describe the damage produced by the 1981 earthquakes. Figure 6.42 shows the present condition of the monument.

Andronopoulos and Koukis (1976) have given a brief description of the foundation geology. The monument is founded on two different soils. Limestones are under the northern part, and earthfill is under the southern part. The boundary between these two is approximately line AB in Figure 6.42. The Acropolis hill of Athens (Figure 6.43) consists in its upper part (between elevations 118 and 156 m) of upper cretaceous limestones, usually thick, platy, and in places very fractured, with obvious karst and erosion features. The limestone beds, with a maximum thickness of about 40 m, cover formations of the Athens schist series (sandstones, marls, and argillaceous schists) at the base of the hill. Near the contact of these two systems, which is, according to different opinions, normal or tectonic, the poor existing hanging aquifer is discharged regularly by three small springs, with a discharge of 0.5 to 1 liter per minute during the dry season.

The earthquake produced relatively small permanent displacements in almost all parts of the monument. The northern part of the monument displaced westward, while the southern part displaced eastward.

The most severe displacements and damage were observed at the east side (see Figure 6.44), where many marble chips fell. The scaffolding shown in Figures 6.44 and 6.45 was erected immediately after the earthquake to prevent further dislocations of the head beams near the corners. The east top beam at the north end displaced westward about 4 cm in relation to the ground. This total displacement is the sum of smaller displacements almost equally distributed among the 10 or 11 rigid blocks that make up each pillar.

The west side suffered much smaller displacements, which were concentrated near the bottom end of the pillars. This difference in the deformation of the pillars between the east and west sides may result from the east side having no horizontal connections between the inside and outside pillars (Figures 6.42 and 6.45), while the west side has more horizontal supports along the span (Figures 6.46 and 6.47). Under these conditions the east side shows more "bending" deformation, while the west side shows more "shear" deformation. Because the east side has no connection at the top perpendicular to the front face, the pillars form free-standing cantilevers.

The pillars around the corners of the monument rotated, as shown schematically in Figure 6.42. The biggest rotation was observed in the northeast corner pillar, which underwent extensive spalling at the lower end (Figures 6.48 and 6.49). Less rotation was observed at the southeast corner pillar (Figures 6.50 and 6.51), and very little rotation was seen at the southwest and northwest corner pillars.

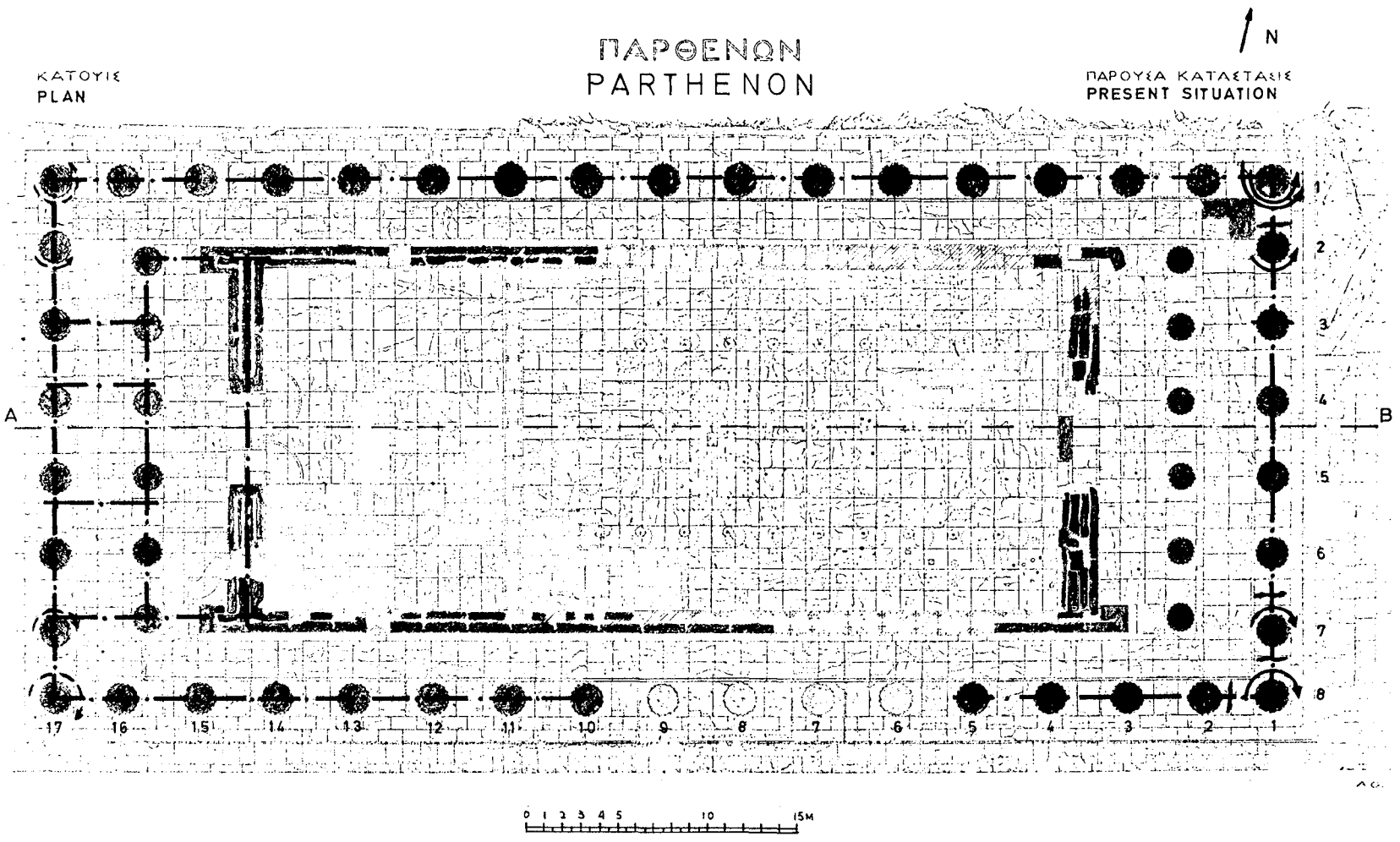

FIGURE 6.42 Present condition of the Parthenon. The arcs with arrows indicate rotations of the top in relation to the bottom. The lines indicate cracks of the head beams after the recent earthquakes. The dotted and dashed lines indicate horizontal beams at the top. Source: Orlandos (1976).

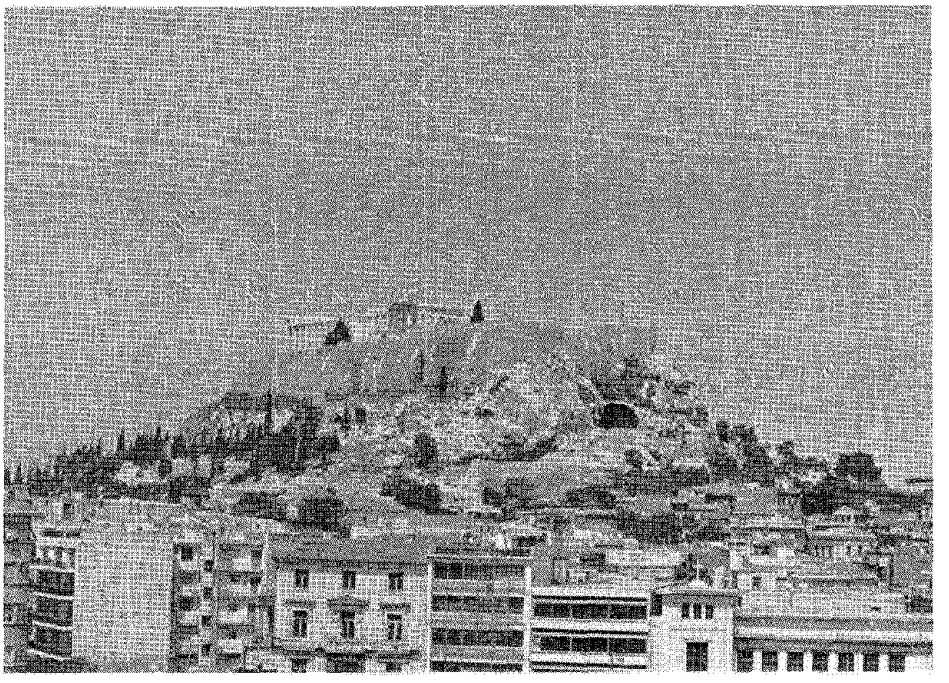

FIGURE 6.43 East view of the Parthenon on the Acropolis hill.

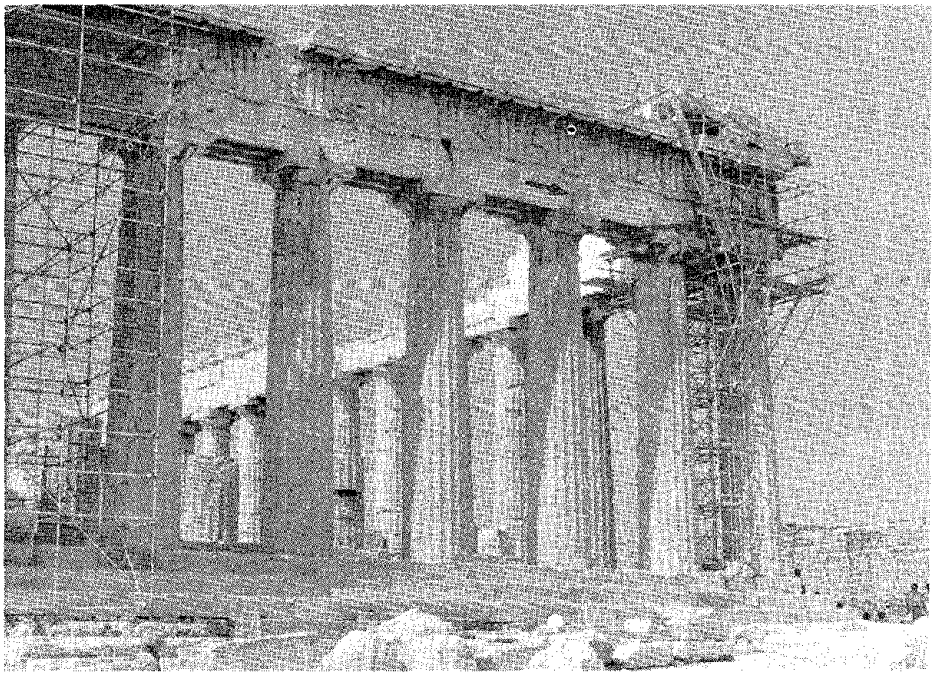

FIGURE 6.44 East view of the Parthenon. The arrow indicates a large crack in the head beam over the third pillar. There are also large cracks in the head beam between the first and second pillars.

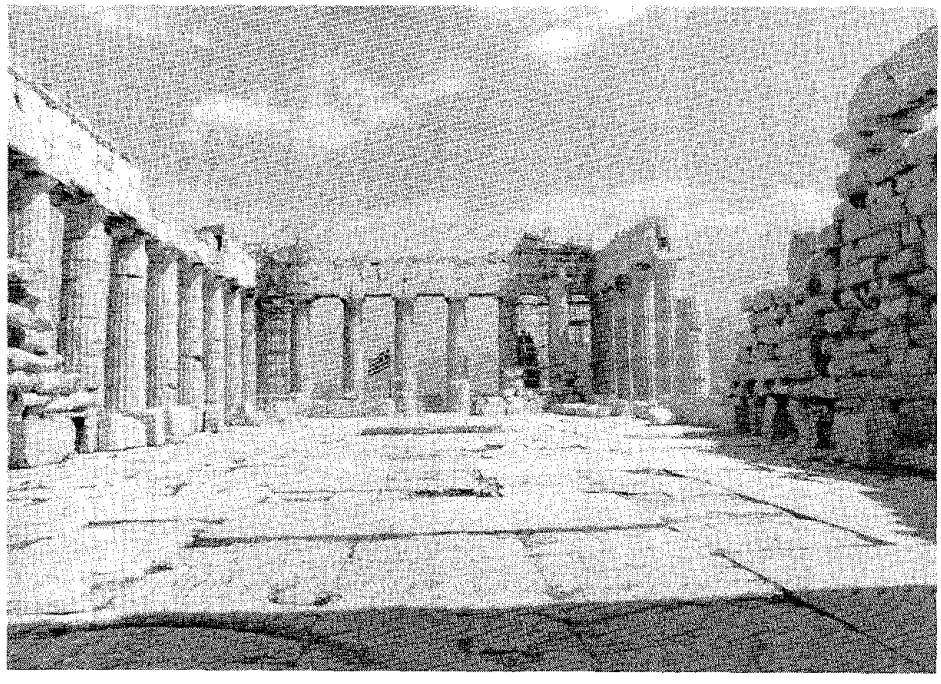

FIGURE 6.45 East side of the Parthenon viewed from the inside. The head beam is supported horizontally only at its two ends. The most damage was concentrated around these two points. Source: Dontas (1981).

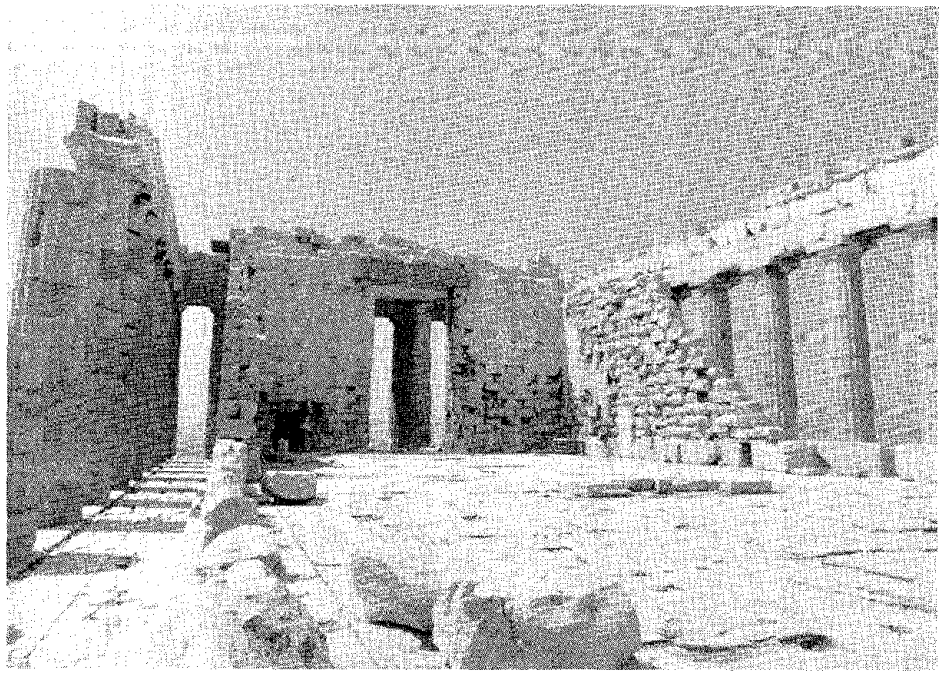

FIGURE 6.46 West side of the Parthenon viewed from the inside. The head beam in the back is connected horizontally by short beams to the inside construction (see Figure 6.42). Source: Dontas (1981).

FIGURE 6.47 West view of the Parthenon as it stands now, after the earthquakes. The north and west sides are the best preserved and were least damaged by the recent earthquakes. Source: Dontas (1981).

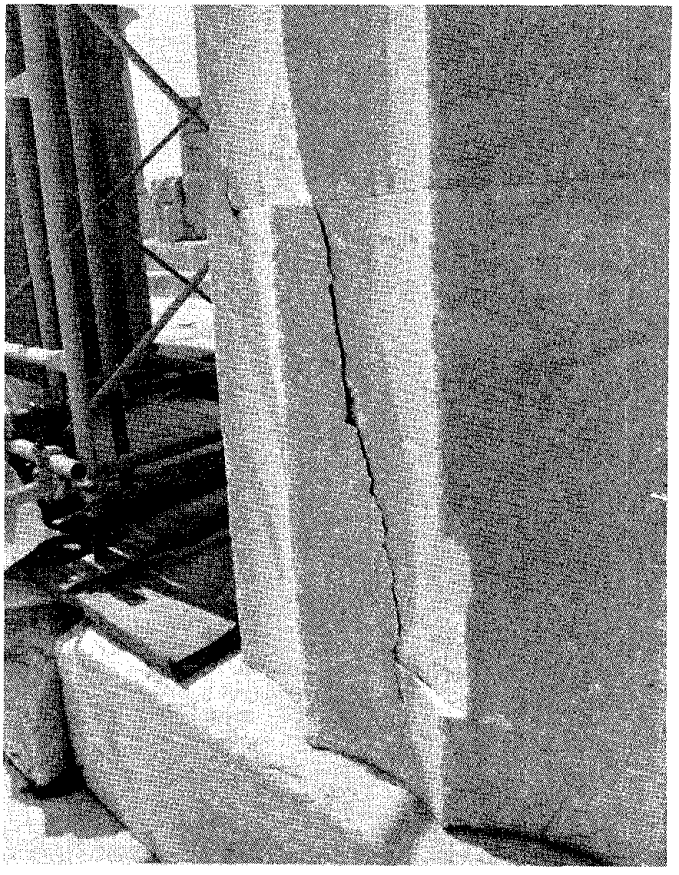

FIGURE 6.48 Pillar at the northeast corner of the Parthenon. The pillar rotated anticlockwise, which displaced its top periphery by about 5 cm. Source: Dontas (1981).

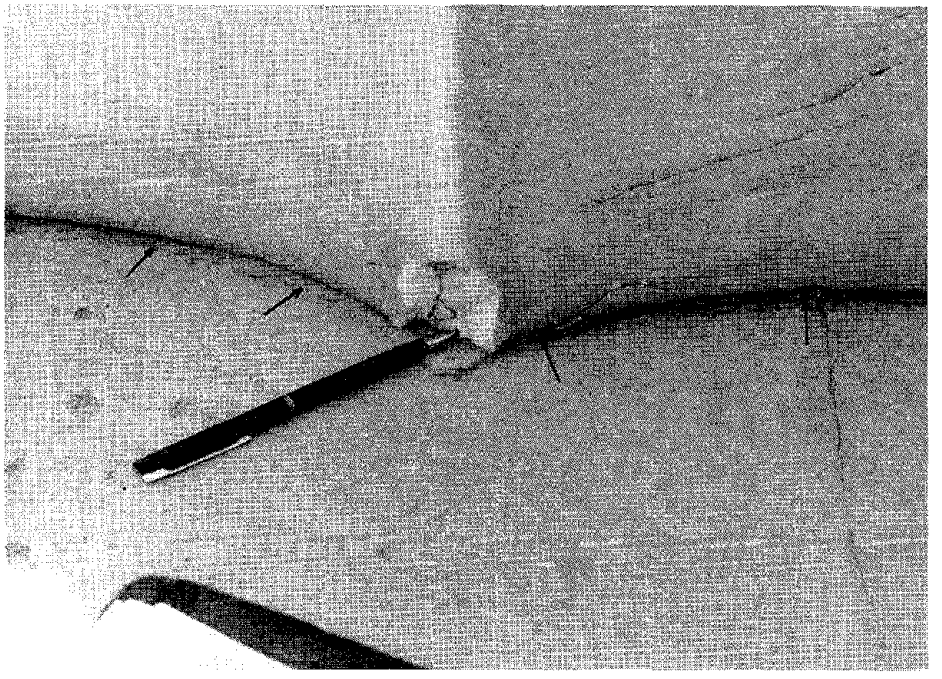

FIGURE 6.49 Lowest part of the pillar at the northeast corner of the Parthenon. This shows typical breaking of the edge of the pillar. An anticlockwise rotation and displacement of about 1-2 cm to the west was observed. Source: Dontas (1981).

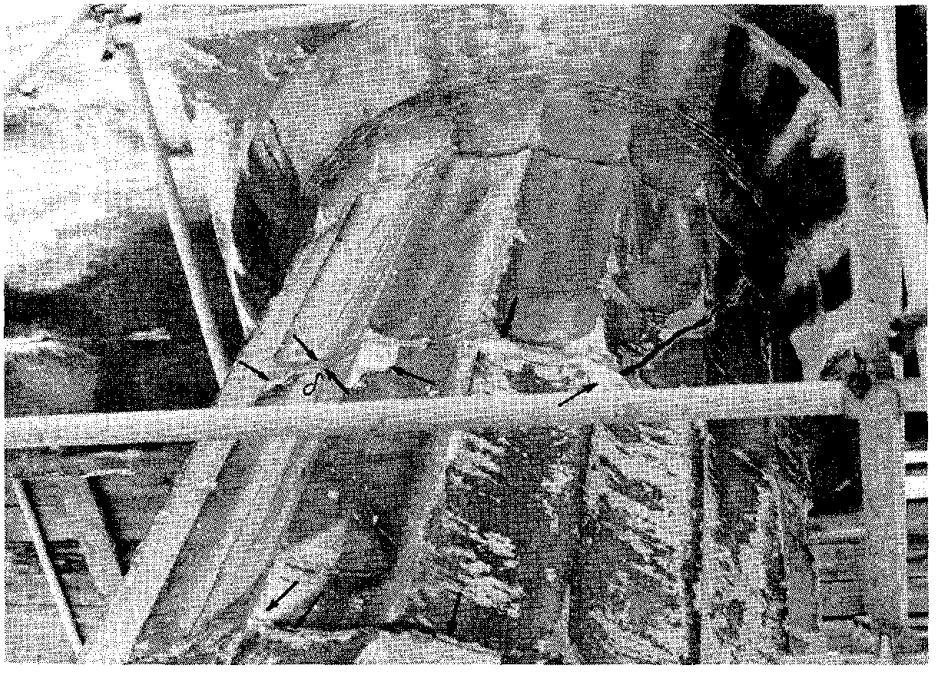

FIGURE 6.50 Upper part of the seventh pillar on the east side of the Parthenon. Arrows show spalling due to recent earthquakes. Source: Dontas (1981).

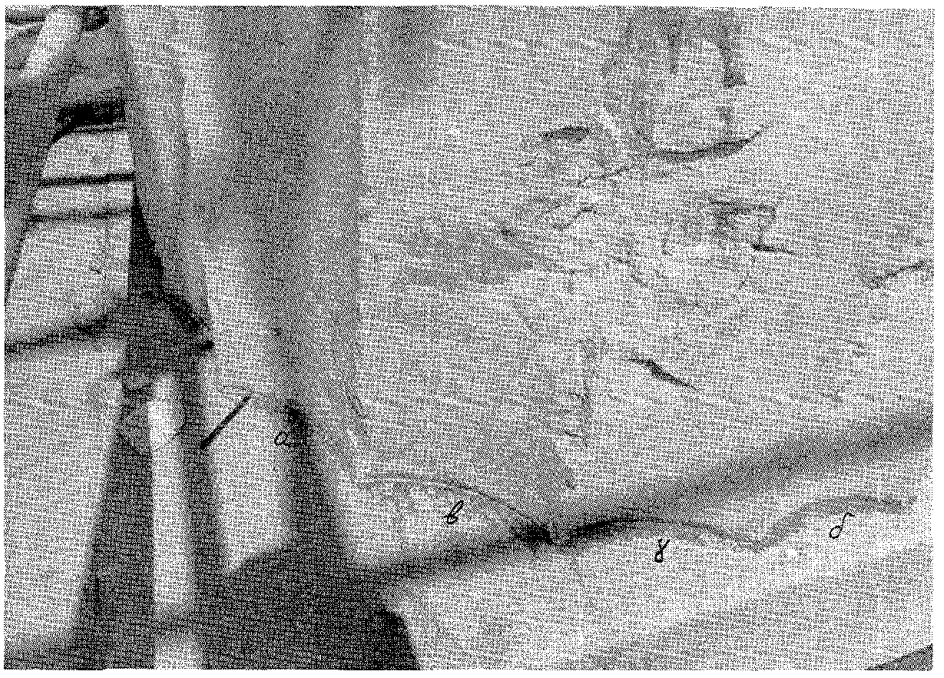

FIGURE 6.51 Lower part of the pillar at the southeast corner of the Parthenon. A clockwise rotation and displacement of the pillar to the east of about 1-2 cm was observed. Some fallen marble chips may be seen. Source: Dontas (1981).

APPENDIX A

SEISMIC HISTORY OF CENTRAL GREECE

In the following table the seismic activity of the major area is translated from Galanopoulos (1955).

Before 600 B.C.		Destruction of Delfi.
421 B.C.	Winter	Earthquakes in Beotia.
373 B.C.		Strong earthquake at the southern side of the Gulf of Corinth caused complete destruction of the city of Voura and sinking under the sea of the city of Elike, including all of its 2-km-long beach. The tsunami caused the sinking of 10 naval ships.
227 (or 222) B.C.		Destruction of Sikyon.
A.D. 23		Destruction of Egio (50 km west-northwest of Xylokastro).
A.D. 77	June 10	Destruction of Corinth. Many deaths.
A.D. 551		Destruction of eight cities due to earthquake on northern shore of the Gulf of Corinth.
1641	June 1	Earthquake in Attica with heavy damage to buildings in Athens. Slide of some rocks of the Athens Acropolis.
1748	May 14	Destruction of Egio, completed by tsunami after earthquake.

1805	November 16-17	Strong earthquake in Attica with serious damage in Athens and the Parthenon.
1817	August 23	Strong earthquake followed by tsunami caused complete destruction of Egio.
1821	January 9	Tsunami caused various damage along beaches of the Gulf of Corinth.
1837	March 20	Earthquake caused damage in Egina.
1853	August 18	Strong earthquake destroyed many houses and churches in Thebae.
1858	February 21	Strong earthquake destroyed the old city of Corinth and caused some deaths.
1861	December 26	Strong earthquake with large tsunami hit the western part of the Gulf of Corinth between Xylokastro and Egio, causing four deaths. On the shore it caused the settlement of a strip with an area of 15,000,000 m^2, several fissures, and a fault 13 km long and 2 m wide.
1866	March 2	Strong earthquake caused 20 deaths and serious damage in Avlon and the surrounding area.
1870	August 1	Earthquake with ground surface disturbances and rock slides occurred in the northern Gulf of Corinth, mainly affecting Itea, Hrysso, and Delfi.
1873	July 25	Earthquake caused damage in Epidauros.
1874	January 17	Earthquake caused damage in Athens and its Acropolis.
1876	July 26	Strong earthquake caused fissures and rock slides, destroyed some houses, and caused damage to others in Nemea.

1914	October 17	Serious earthquake (magnitude 6) completely destroyed 20 houses in Thebae and rendered practically all the other houses in the city uninhabitable.
1928	April 22	Strong earthquake (magnitude 6.25) destroyed Corinth. Of the approximately 2,000 houses in the new city of Corinth, only a few suffered minor damage; many collapsed wholly or partly and many were rendered uninhabitable. The earthquake caused 20 deaths and 30 serious injuries.
1931	January 4	Strong earthquake (magnitude between 5.5 and 6) caused damage in Corinth, Isthmia, Xylokastro, and Nemea.
1934	March 22	Strong earthquake caused the collapse of one house and serious damage to eight houses in Egio.
1938	July 20	Serious earthquake (magnitude 6.25) caused considerable damage in Oropos, Skala Oropou, and Malakasa. On September 15 a serious aftershock caused collapse of some walls and new damage to houses.
1953	June 13	Strong earthquake (magnitude 5.75) caused the collapse of 14 houses, serious damage to 105 houses, and light damage to 84 houses in Xylokastro.
1953	September 5	Strong earthquake (magnitude 6) caused serious damages in six villages of the area of Isthmia. Fifty-three houses were reportedly completely destroyed, 175 had serious damage, and 223 had light damage.
1954	April 17	Strong earthquake (magnitude 5.75) caused severe damage in the villages between Corinth and Kiato.

APPENDIX B

DESCRIPTION OF THE EXISTING GREEK CODE FOR ASEISMIC STRUCTURES

HISTORICAL BACKGROUND

The existing Greek code for aseismic construction was introduced in June 1959. It is obligatory for all structures erected in Greece regardless of their use and location. This code is still in use without any change.*

For the area affected by the recent earthquakes, provisions for aseismic structures were instituted on November 1, 1928, after the great earthquakes that struck the region on April 22 of that year. Various ameliorations and additions were made to the provisions of this code in 1931, 1935, 1941, 1947, and 1954. The code was later applied to other Greek regions suffering strong earthquakes.

The code of 1931 consists of 27 articles grouped into six chapters. In Chapter A the field of application of the code is mentioned--masonry, wood, steel, and reinforced or unreinforced concrete--and a horizontal seismic coefficient equal to 10 percent of gravity is generally applied. In Chapter B the design of buildings with uniform load carrying systems is described. Various general rules for the composition of the load carrying system are given. Some rules refer to the partitions. A restriction of two stories and one basement, or of a total height of the building above ground level of 8.5 m, is set. All cases of the above-mentioned materials used for load carrying systems are described. In Chapter C the design of buildings with nonuniform load carrying systems is described, with similar details as in Chapter B. For masonry the thickness and quality of the walls are prescribed for each level, as well as the minimum distances between openings and the end of the walls. In Chapter D the repairs of buildings (and of various members in the buildings) due to earthquake damages are described according to the structural system and material. The underlying logic for the repair and reinforcement is presented. In Chapter E general provisions are set, for example, foundation soil,

*International Association of Earthquake Engineering, Earthquake Resistant Regulation--A World List, 1980, International Association of Earthquake Engineering, Tokyo, Japan, pp. 256-267.

suitable systems for foundations, maintenance of buildings. In Chapter F some town planning restrictions and the responsibilities for the efficient application of the code are given.

FORMAT OF CURRENT SEISMIC CODE

Five to six years before 1959 the "new" code was circulated as informal recommendations for all of Greece. The new code consists of 16 articles that reflect the existing older codes, as well as the experience gained after the many major earthquakes that have struck Greece. However, some of the structures erected recently go beyond the provisions of this code. For example, before 1959 no architectural needs for an open and/or high first story were apparent. Partitions were continuous down to the ground floor level, while the openings, in general, were in most cases rather small. The quality of concrete and of structural technology was quite low. All of the above contribute to rather stiff structures. The behavior of ductile frames was not very well understood at that time.

The previous codes, starting in 1931, recommended that repairs of buildings should tend toward stiffer structures with the use of reinforced concrete walls. The existing code recommends, in terms of general design concepts, the use of reinforced concrete walls. In other articles the need for a seismic design of ordinary structures is exempted if the structures are symmetrical and if adequate shear walls are used in both directions. If the required walls are missing, or if the construction is asymmetrical, the code states that the columns and beams should "function as frames" in order to withstand horizontal seismic loads.

The code specifies the level of required design detailing according to the kind of structure. It also mentions the design seismic loads, the methodology for the analysis, and the allowable stresses in the structure and soil. The code deals with masonry (artificial or natural stone and brick walls) and reinforced or unreinforced concrete as load carrying systems. Attention is paid to details of the nonbearing partitions.

SEISMIC ZONES AND DESIGN FORCES

The country is divided into three zones of seismicity according to the distribution of observed damage in the past: weak (I), moderate (II), and strong (III), as shown in Figure B.1. There are four soil categories, with the erection of permanent structures permitted only in the first three. The soil categories are of low (a), of medium (b), and of high (c) seismic risk, and the fourth category (d), "great seismic risk," includes nonhomogeneous or loose soils on steep slopes or areas above caves. The corresponding seismic coefficients (ε) take the following values, independent of the type of structure.

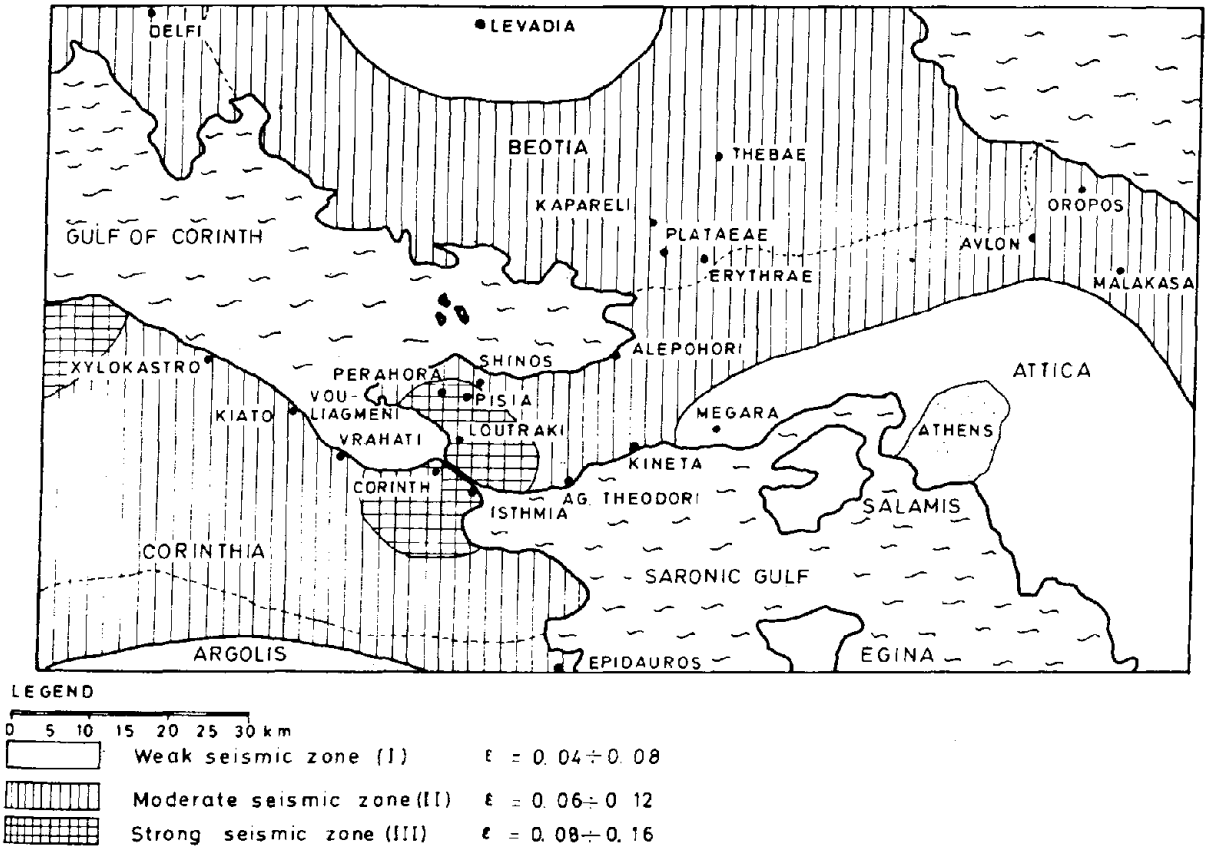

FIGURE B.1 Seismic zones of the affected area according to the existing code.

Seismic Coefficient (ε)

Seismicity Zones	Soil Category (a)	(b)	(c)
I	0.04	0.06	0.08
II	0.06	0.08	0.12
III	0.08	0.12	0.16

The seismic coefficient for horizontal forces is unchanged throughout the height of the structure. Forces in the vertical direction must be considered only in special cases (e.g., cantilevers, concentrated loads, vault or shell structures) for which the relevant seismic coefficient is tripled.

STRUCTURAL REQUIREMENTS: FRAMES AND SHEAR WALLS, ALLOWABLE STRESSES

The forces in the structural elements may be calculated according to the stiffness of the element and its position in the plan, taking into consideration the geometric eccentricity between the center of gravity and the center of rigidity (the torsional effect). In addition, the structural elements on the perimeter of the building are designed to form a frame that must withstand horizontal loads equal to the vertical load multiplied by half of the applied horizontal seismic coefficient, but not less than 0.06. Corner columns should be checked in biaxial bending. Shear walls should end in columns or other walls.

The corner columns should have, as a minimum, rectangular dimensions of 30 x 30 cm at the top three stories, with an addition to each side of 5 cm for every three lower stories. The minimum longitudinal reinforcement is four 20-mm bars. The minimum percentage of the reinforcement is 8 percent for inner columns and 10 percent for corner columns.

For ordinary structures an exemption from the need for aseismic design is permitted in areas of seismicity I and II, where the seismic coefficient is less than 0.08, provided that the following conditions are met: (1) the distance between two successive supporting elements is no more than 6.5 m and the story height is no more than 5.5 m, (2) the sum of the cross sections in both directions of the shear walls (a wall is considered as such if it is longer than 1.20 m) in a certain level is at least 1/500 (for $0.04 < \varepsilon < 0.08$) or 1/800 ($\varepsilon = 0.04$) of the sum of the floor areas that are above that level, (3) there is coincidence between the center of gravity and the center of rigidity, and (4) the walls are extended throughout the height of the structure and the thickness of each wall is not less than 0.20 m or 1/25 of the story height.

Numerous guidelines are given in the code for the seismic design of one- and two-story masonry structures. In the present code the "allowable stresses" are approximately equal to the corresponding yield stress divided by 1.75. For the most adverse combination of vertical static loads and seismic loads, an increase of the allowable stresses by 20 percent is allowed for the structural materials, while a 50 percent increase is allowed for the foundation soil, irrespective of its quality.

FOUNDATIONS

Tie beams in foundations are required unless grid beams or raft foundations are used. Tie beams should form panels with a maximum dimension of 10 m. The lateral seismic pressure for earth-retaining structures is $2\varepsilon(G + P)$, where G is the dead load and P is the moving load. The lateral seismic pressure used in cases of hydrostatic pressure (whenever such a pressure must be considered) is also a multiple of 2ε.

REFERENCES

Andronopoulos, B. (1982) Personal communication based on geophysical data from A. Stavrou, Institute of Geological and Mining Engineering (IGME).

Andronopoulos, B., and Koukis, G. (1976) "Engineering Geology Study in the Acropolis Area--Athens," IGME, Eng. Geol. Invest., Vol 1.

Carydis, P., Drakopoulos, J., and Taflambas, J. (1981) "Analyses of February 24 and 25, 1981, Earthquakes," Scientific Papers of the National Technical University, Faculty of Civil Engineering, Athens.

Carydis, P., and Ermopoulos, J. (1975) "Influence of the Discontinuity Along the Height of Multistory Frames on Their Dynamic and Seismic Response," Hellenic Conference on Tall Buildings, Part A, Technical Chamber of Greece, Athens.

Carydis, P. G., and Sbokos, J. S. (1978) Seismic Engineering Data Report, Greek Records, 1972-1977, USGS Open-File Report 78-1022, U.S. Geological Survey, Reston, Virginia.

Cotzias, P., and Stamatopoulos, P. (1969) Report on the Condition of Foundation of the Hotel in Vrahati, A Geotechnical and Foundation Engineering Investigation, Athens.

Dontas, G. (1981) Personal communication about the earthquake damages of the Acropolis of Athens.

Galanopoulos, A. G. (1955) "Historical Seismicity of Greece," The Geological Annals of Greece, Laboratory for Geology and Paleontology of the Athens University, Athens, pp. 83-121 (in Greek).

Hudson, D. E. (1979) Reading and Interpreting Strong Motion Accelerograms, Earthquake Engineering Research Institute, Berkeley, California.

National Observatory of Athens (1975) Bulletin of the National Observatory of Athens, October, Seismological Institute.

Nigam, N. C., and Jennings, P. C. (1968) Digital Calculation of Response Spectra from Strong-Motion Earthquake Records, Earthquake Engineering Research Institute, Berkeley, California.

Orlandos, A. (1976) The Architecture of the Parthenon, Pub. No. 86, Archeological Society of Athens, Athens.

Richart, F. E., Jr., Hall, J. R., and Woods, R. D. (1970) Vibrations of Soils and Foundations, Prentice-Hall, Englewood Cliffs, New Jersey.

Tocher, D. (1956) Earthquake Intensity and Magnitude Scales, AGI Data Sheet 47a, American Geological Institute, Falls Church, Virginia.

BRIEF BIOGRAPHIES OF STUDY TEAM MEMBERS

GREGG E. BRANDOW is a structural engineer with the firm of Brandow & Johnston Associates in Los Angeles, California. He received his B.S. in Civil Engineering from the University of Southern California in 1967, his M.S. in Civil Engineering from Stanford University in 1968, and his Ph.D. in Civil Engineering from Stanford University in 1971. A registered Civil Engineer and Structural Engineer, he has had experience in the structural design of major high-rise office buildings, hospitals, and other public and private buildings. He has participated in investigations of the 1971 San Fernando earthquake, the 1976 Guatemala earthquake, the 1979 El Centro earthquake, and the 1981 Greek earthquakes. Since 1971 he has served as an adjunct assistant professor in the Department of Civil Engineering at the University of Southern California, teaching classes in computer applications, plastic design, and timber design. He is a member of the Structural Engineer's Association of Southern California, the American Society of Civil Engineers, and the Earthquake Engineering Research Institute.

PANAYOTIS G. CARYDIS is Professor of Earthquake Engineering at the National Technical University of Athens, Greece. He received his M.S. in Civil Engineering from the Technical University of Athens and his Ph.D. in Engineering from the same university in 1968. He followed the advanced course in engineering of the International Institute of Seismology and Earthquake Engineering in Tokyo from 1968 to 1970. He has actively participated in the UNESCO project "Survey of the Seismicity of the Balkan Region," 1970-1976, and has been a member of the coordinating committee for the UNESCO project "Earthquake Risk Reduction in the Balkan Region" since 1980. He has participated in many earthquake reconnaissance missions in Greece and abroad, including Tokachi-Oki in 1968, San Fernando in 1971, Bucharest in 1977, and El Asnam in 1980. He is the designer of numerous factories, blocks of flats, auditoriums, and high-rise buildings. He is a member of the Technical Chamber of Greece, the Earthquake Engineering Research Institute, the American Society of Civil Engineers, and the American Concrete Institute.

JAMES O. JIRSA is Stanley P. Finch Professor of Civil Engineering at the University of Texas at Austin. He received his B.S. in Civil Engineering from the University of Nebraska in 1960, his M.S. in 1962

from the University of Illinois, and his Ph.D. from the University of Illinois in 1963. A registered professional engineer in Texas, he specializes in the design and behavior of reinforced concrete structures. He is a member of the American Concrete Institute and past chairman of their Committee on Joints and Connections in Monolithic Concrete Structures, a member of the Comite Euro-International du Beton Task Group on Seismic Design, a member of the American Society of Civil Engineers and past Chairman of their Structures Division Committee on Concrete and Masonry Structures, and a member of the Earthquake Engineering Research Institute. He has received several awards, including the Walter L. Huber Research Prize for 1978 from the American Society of Civil Engineers and the Raymond C. Reese Structural Research Award in 1979 from the American Concrete Institute.

NORMAN R. TILFORD is Chief Geologist for Ebasco Services in Greensboro, North Carolina, and Associate Professor of Engineering Geology at Texas A&M University in College Station. He received his B.S. in Geology from Arizona State University in 1958 and his M.S. in Geology from the same university in 1966. At Texas A&M University he teaches courses in site selection for critical facilities and advanced engineering geology and carries out research in neotectonics. A registered professional geologist in seven states, he has participated in siting investigations, design exploration, supervision of foundation construction, and as a reviewer for over 30 major projects, including one of the world's largest zoned rock fill dams in Keban, Turkey. He commonly participates in the Federal Energy Regulatory Commission's licensing and review process. He is National Secretary of the Association of Engineering Geologists and past chairman of their Nuclear Energy Committee, President of the Carolina Section of the International Association of Engineering Geologists, and a member of the American Institute of Professional Geologists, the U.S. Committee on Large Dams, and the Earthquake Engineering Research Institute.

Copies available from sources given in footnotes a, b, and c.

EARTHQUAKES

[a]The Great Alaska Earthquake of 1964

Biology, 0-309-01604-5/1971, 287 pp.
Engineering, 0-309-01606-1/1973, 1198 pp.
Geology, 0-309-01601-0/1971, 834 pp.
Human Ecology, 0-309-01607-X/1970, 510 pp.
Hydrology, 0-309-01603-7/1968, 446 pp.
Oceanography and Coastal Engineering, 0-309-01605-3/1972, 556 pp.
[a,c]Seismology and Geodesy, 0-309-01602-9/1972, 598 pp., PB 212 981.
Summary and Recommendations, 0-309-01608-8/1973, 291 pp.

[c]Engineering Report on the Caracas Earthquake of 29 July 1967 (1968) by M. A. Sozen, P. C. Jennings, R. B. Matthiesen, G. W. Housner, and N. M. Newmark, 233 pp., PB 180 548.

[c]The Western Sicily Earthquake of 1968 (1969) by J. Eugene Haas and Robert S, Ayre, 70 pp., PB 188 475.

[b,c]The Gediz, Turkey, Earthquake of 1970 (1970) by Joseph Penzien and Robert D. Hanson, 88 pp., PB 193 919.

[b,c]Destructive Earthquakes in Burdur and Bingol Turkey, May 1971 (1975) by W. O. Keightley, 89 pp., PB 82 224 007 (A05).

---

[a]Available from National Academy Press, 2101 Constitution Avenue, N.W., Washington, D.C. 20418.

[b]Available from Committee on Natural Disasters, National Academy of Sciences, 2101 Constitution Avenue, N.W., Washington, D.C. 20418.

[c]Available from National Technical Information Service, 5285 Port Royal Road, Springfield, Virginia 22161.

b,c<u>The San Fernando Earthquake of February 9, 1971</u> (March 22, 1971) by a Joint Panel on San Fernando Earthquake, Clarence Allen, Chairman, 31 pp., PB 82 224 262 (A03).

b,c<u>The Engineering Aspects of the QIR Earthquake of April 10, 1972 in Southern Iran</u> (1973) by R. Razani and K. L. Lee, 160 pp., PB 223 599.

b,c<u>Engineering Report on the Managua Earthquake of 23 December 1972</u> (1975) by M. A. Sozen and R. B. Matthiesen, 122 pp., PB 293 557 (A06).

c<u>The Honomu, Hawaii, Earthquake</u> (1977) by N. Nielson, A. Furumoto, W. Lum, and B. Morril, 95 pp., PB 293 025 (A05).

b,c<u>Engineering Report on the Muradiye-Caldiran, Turkey, Earthquake of 24 November 1976</u> (1978) by P. Gulkan, A. Gurpinar, M. Celebi, E. Arpat, and S. Gencoglu, 67 pp., PB 82 225 020 (A04).

b,c<u>Earthquake in Romania March 4, 1977</u>, An Engineering Report, National Research Council and Earthquake Engineering Research Institute (1980) by Glen V. Berg, Bruce A. Bolt, Mete A. Sozen, and Christopher Rojahn, 39 pp., PB 82 163 114 (A04).

b,c<u>Earthquake in Campania-Basilicata, Italy, November 23, 1980</u>, A Reconnaissance Report, National Research Council and Earthquake Engineering Research Institute (1981) by James L. Stratta, Luis E. Escalante, Ellis L. Krinitzsky, and Ugo Morelli, 100 pp., PB 82 162 967 (A06).

FLOODS

b,c<u>Flood of July 1976 in Big Thompson Canyon, Colorado</u> (1978) by D. Simons, J. Nelson, E. Reiter and R. Barkau, 96 pp., PB 82 223 959 (A05).

b,c<u>Storms, Floods, and Debris Flows in Southern California and Arizona--1978 and 1980</u>, Proceedings of a Symposium, September 17-18, 1980, National Research Council and California Institute of Technology (1982) by Norman H. Brooks et al., 487 pp., PB 82 224 239 (A21).

b,c<u>Storms, Floods, and Debris Flows in Southern California and Arizona--1978 and 1980</u>, Overview and Summary of a Symposium, September 17-18, 1980, National Research Council and California Institute of Technology (1982) by Norman H. Brooks, 47 pp., PB 82 224 221 (A04).

b,c<u>The Austin, Texas, Flood of May 24-25, 1981</u> (1982) by Walter L. Moore, Earl Cook, Robert S. Gooch, and Carl F. Nordin, Jr., 54 pp.

DAM FAILURES

b,c<u>Failure of Dam No. 3 on the Middle Fork of Buffalo Creek Near Saunders, West Virginia, on February 26, 1972</u> (1972) by R. Seals, W. Marr, Jr., and T. W. Lambe, 33 pp., PB 82 223 918 (A03).

[b,c]Reconnaissance Report on the Failure of Kelly Barnes Lake Dam, Toccoa Falls, Georgia (1978) by G. Sowers, 22 pp., PB 82 223 975 (A02).

LANDSLIDES

[b,c]Landslide of April 25, 1974, on the Mantaro River, Peru (1975) by L. Lee and J. Duncan, 79 pp., PB 297 287 (A05).

[c]The Landslide at Tuve, near Goteborg, Sweden, on November 30, 1977 (1980) by J. M. Duncan, G. Lefebvre, and P. Lade, 25 pp., PB 82 233 693.

WINDSTORMS

[c]Lubbock Storm of May 11, 1970 (1970) by J. Neils Thompson, Ernest W. Kiesling, Joseph L. Goldman, Kishor C. Mehta, John Wittman, Jr., and Franklin B. Johnson, 81 pp., PB 198 377.

[c]Engineering Aspects of the Tornadoes of April 3-4, 1974 (1975) by K. Mehta, J. Minor, J. McDonald, B. Manning, J. Abernathy, and U. Koehler, 124 pp., PB 252 419.

[b,c]The Kalamazoo Tornado of May 13, 1980 (1981) by Kishor C. Mehta, James R. McDonald, Richard C. Marshall, James J. Abernathy, and Deryl Boggs, 54 pp., PB 82 162 454 (A04).

EARTHQUAKE ENGINEERING RESEARCH INSTITUTE PUBLICATIONS

Available, except as noted, from the Earthquake Engineering Research Institute, 2620 Telegraph Avenue, Berkeley, California 94704.

1. Earthquake and Blast Effects on Structures, Proceedings of a symposium held in Los Angeles, California, 1952, 322 pp.*

2. First World Conference on Earthquake Engineering, Proceedings of a conference held in Berkeley, California, 1956, 536 pp.

3. Bibliography of Effects of Soil Conditions on Earthquake Damage by C. Martin Duke, 1958. 47 pp.**

4. Earthquake and Fire by Donald F. Moran et al., 1959, 15 pp.

5. Earthquakes: Construction Inspection by Harry W. Bolin et al., 1959, 20 pp.**

6. Translations in Earthquake Engineering by K. V. Steinbrugge et al., 1969, 150 pp.**

7. Earthquake Damage Survey Guide, 1964, 20 pp.*

8. State-of-the-Art Symposium, Earthquake Engineering of Buildings, Abstracts of Papers, February 5-6, 1968, S. B. Barnes, Chairman.**

9. Peru Earthquake of May 31, 1970, Preliminary Report by J. L. Stratta et al., 1970, 55 pp.*

10. Bibliography of Earthquake Engineering by Edward P. Hollis, 1971, 247 pp.

*Available from University Microfilm, Inc., 300 North Zeeb Road, Anne Arbor, Michigan 48106.

**Out of print.

11. Investigations of the San Fernando Earthquake, Program and Abstracts of Papers, National Conference on Earthquake Engineering, February 2-9, 1972, R. B. Matthiesen, Chairman.

12. Managua, Nicaragua, Earthquake of December 23, 1972, Reconnaissance Report, by J. F. Meehan et al., May 1973, 214 pp.

13. Proceedings of the Managua Earthquake Conference, November 29, 30, 1973, Christopher Rojahn, Chairman, 2 volumes, 975 pp.**

14. Report on the San Fernando Earthquake of February 9, 1971, Performed by EERI for NOAA, Donald F. Moran, Chairman.**

15. Peru Earthquake of October, 1974, Reconnaissance Report, by D. F. Moran et al., 1975, 85 pp.

16. Proceedings of the First US National Conference on Earthquake Engineering, June 18-20, 1975, 661 pp.

17. The Oroville Earthquake by J. F. Meehan et al., EERI Newsletter, Vol 9:5B, September, 1975.**

18. The Lice, Turkey, Earthquake of September 6, 1975 by Peter Yanev, EERI Newsletter, Vol 9:6B, November, 1975.**

19. The Island of Hawaii Earthquake of November 29, 1975 by C. Rojahn et al., EERI Newsletter, Vol 10:1B, February, 1976.

20. The Guatemala Earthquake of February 4, 1976, A Preliminary Report, by D. F. Moran et al., EERI Newsletter, Vol 10:2B, May, 1976.**

21 6th World Conference on Earthquake Engineering, Programme and Author Index, New Delhi, January, 1977, 34 pp.

22. Earthquake in Romania, March 4, 1977, EERI Newsletter, Vol 11:3B, May, 1977, 85 pp.

23. Learning from Earthquakes, 1977 Planning Guide, 41 pp.**

24. Learning from Earthquakes, 1977 Planning and Field Guides, 200 pp.

25. Mindanao, Philippines, Earthquake, August 17, 1976 by J. L. Stratta et al., August, 1977, 106 pp.

26. Engineering Features of the Santa Barbara Earthquake of August 13, 1978 by Miller and Felszeghy, 1978.

27. Miyagi-Ken-Oki, Japan, Earthquake, June 18, 1978, Peter Yanev, Editor, 1978, 165 pp.

28. Proceedings of the Second US National Conference on Earthquake Engineering, August 22-24, 1979, 1168 pp.

29. Reading and Interpreting Strong Motion Accelerograms, a monograph by D. E. Hudson, 1979.

30. Potential Utilization of the NASA/George C. Marshall Space Flight Center in Earthquake Engineering Research, R. E. Scholl, Editor, December, 1979, available from NASA.

31. Friuli, Italy, Earthquakes of 1976 by James L. Stratta and Loring A. Wyllie, Jr., 1980, 97 pp.

32. Thessaloniki, Greece, Earthquake, June 20, 1978, J. A. Blume and Mary Stauduhar, Editors, 1980, 86 pp.

33. Learning from Earthquakes, Project Report, 1973-1979, 1980.

34. Imperial County, California, Earthquake, October 15, 1979, Gregg Brandow, Coordinator, David J. Leeds, Editor, 1980, 200 pp.

35. Greenville (Diablo-Livermore) Earthquakes of January, 1980, EERI Newsletter, Vol 14:2, March, 1980, 70 pp.

36. Northern Kentucky Earthquake of July 27, 1980 by R. D. Hanson et al., September, 1980, 105 pp.

37. The 1976 Tangshan, China, Earthquake, Papers presented at the 2nd US National Conference on Earthquake Engineering held at Stanford University August 22-24, 1979, Introduction by James M. Gere and Haresh C. Shah, March, 1980.

38. Results of the Information Exchange in Earthquake Research Between the United States and the People's Republic of China (August 20 to September 15, 1979), Indentification of Mutual Research Needs and Priorities, October, 1980.

39. Montenegro, Yugoslavia, Earthquake, April 15, 1979, Reconnaissance Report, D. Anicic, G. Berz, D. Boore, J. Bouwkamp, U. Hakenbeck, R. McGuire, J. Sims, and G. Wieczorek, Contributors, R. B. Matthiesen, Coordinator, Arline Leeds, Editor, November, 1980.

40. El-Asnam, Algeria, Earthquake, October 10, 1980, and Trinidad-Offshore California Earthquake, November 8, 1980, EERI Newsletter, Vol 15, No 1, Part B, January, 1981, 113 pp.

41. Introduction to Dynamics of Structures, a monograph by A. K. Chopra, 1981.

42. Mexico Earthquakes: Oaxaca--November 29, 1978; Guerrero--March 14, 1979, Reconnaissance Report, by Nicholas Forell and Joseph Nicoletti, October, 1980, 89 pp.

43. Earthquake in Campania-Basilicata, Italy, November 23, 1980, Architectural and Planning Aspects by Henry J. Lagorio and George C. Mader, 1981, 103 pp.

44. EERI Delegation to the People's Republic of China (September 19 to October 6, 1980), Roger E. Scholl, Editor, 1982, 120 pp.

45. Earthquake Spectra and Design, a monograph by Nathan M. Newmark and William J. Hall, 1982.

46. Mexicali Valley Earthquake of 9 June 1980 by John Anderson, EERI Newsletter, Vol 16, No. 3, May, 1982, 33 pp.

47. Highway Structure Damage Caused by the Trinidad-Offshore, California, Earthquake of November 8, 1980, Report sponsored by Federal Highway Administration, 1982, 26 pp.

48. The Role of Architects and Planners in Post-Earthquake Studies, Proceedings of a colloquium, February 23 and 24, 1982, 26 pp.

Also available: Soil and Structure Response to Earthquakes, a videotaped lecture series, by H. B. Seed, A. K. Chopra, P. C. Jennings, and A. S. Veletsos.